Ingenieurfakultät Bau Geo Umwelt

Engineering Risk Analysis Group

Bayesian network models for wildfire risk estimation

in the Mediterranean basin

Panagiota Papakosta

To Monika and Brigitte

and to my mother Gioula…of course

Abstract

Wildfires are common in geographic areas where the climate is sufficiently moist for vegetation growth but also features extended dry hot periods. Besides climate, human interventions either on purpose or by accident also play an important role in the occurrence of wildfires. Although wildfire incidents have always accompanied vegetation growth, there is an increase in the severity of wildfires during the past three decades with severe impacts on vegetation, animals, crops, human lives and properties. Record temperatures occurring during recent summer periods (Southeast Australia 2009, Russia 2010, South California 2014) lead to extreme wildfire events that were associated with huge socio-economical costs. In addition, scenarios of global warming suggest that wildfires will become more frequent and more intense in the future.

The above stress the need for efficient wildfire risk predictive models to support the planning of precautionary, preventive and mitigating measures (e.g. danger communication, evacuation preparedness, dead fuel clearing activities, firefighting infrastructure, property insurance). In order to quantify wildfire risk, the predictive model must include models for fire occurrence, fire behavior and fire effects. Due to the randomness inherent in the wildfire process and because the modeling is subject to uncertainty in all three stages (occurrence, behavior, damages), fire risk prediction is ideally carried out in a probabilistic format. Available data and expert knowledge should be incorporated for parameter learning. Moreover, the applications need to deal with (partly incomplete) data from various sources.

The aim of this thesis is to introduce a daily fire risk prediction model in the meso-scale and to produce daily fire risk maps. The modeling is carried out with Bayesian Networks (BN). BN are graphical probabilistic models that can effectively represent complex processes with multiple random variables, their interdependencies and the associated uncertainties.

A probabilistic spatio-temporal BN model for fire risk prediction is presented, which predicts daily fire risk on houses and vegetated areas in the meso-scale (1 km² spatial resolution). The BN model consists of three parts:

- The fire occurrence model, which involves as predictive variables weather conditions (expressed by the Fire Weather Index - FWI), land cover types, population and road density. It predicts the probability of a fire occurring daily in each 1km² and is based on the results of a Poisson regression analysis
- The fire size model, triggered by the occurrence model, which includes the influence of actual and past weather conditions, fire behavior indices and topography.
- The damage model, which predicts the expected losses relevant to houses and vegetated areas conditional on fire hazard.

Vulnerability (resistance capacity) and exposure (values at risk) indicators are used to quantify the damage, which also depends on the fire suppression efficiency. The final outputs of the model are the expected house damage costs (the risk to houses) and the restoration costs for the vegetation (the risk to vegetated areas). The BN model is exemplarily established and predictions are made for study areas in Greece, Cyprus and France. The conditional probability distributions of the BN variables are populated with data for different time periods, regression model results and expert knowledge. The BN models are coupled with a GIS for both parameter learning and output

mapping. Data from 2010 for Cyprus and from 2003 and 2010 for South France are used as verification datasets. The predictions are compared with actual losses for selected fire periods. The results are shown in daily maps with 1 km² spatial resolution.

Acknowledgements

Contents

Abstract

Acknowledgements

Contents

1 Introduction

Wildfires are common in geographic areas where the climate is sufficiently moist for vegetation growth but also features extended dry hot periods. These areas include the Mediterranean basin, Southeast Australia, Central and Southern California, or South Africa. Long periods of drought and hot temperatures combined with strong winds and unmanaged biomass, make such areas naturally fire-prone. Besides climate, human interventions also play an important role in the occurrence of wildfires. Humans have used fire for their interests throughout history and the result is observable in the mosaic landscapes of the Mediterranean. The regeneration of pastures, land use change, suppression of natural vegetation to implement crops, land clearing activities or revenge are all human motives that caused and still cause wildfires (Leone *et al.* 2009).

Although wildfire incidents have always accompanied vegetation growth, statistical evidence suggests an increase in the severity of wildfires during the past three decades (FAO 2001, JRC 2006). In the Mediterranean, long periods of high above-average temperatures and draught, especially in the summer months, have produced large fires with severe impacts on vegetation, animals, crops, human lives and properties. Record temperatures occurring during recent summer periods (Southeast Australia 2009, Russia 2010) lead to extreme wildfire events that were associated with huge socio-economical costs. In addition, scenarios of global warming suggest that wildfires will become more frequent and more intense in the future (Wotton *et al.* 2003;Flannigan *et al.* 2005;MunichRE 2010).

The prediction of the occurrence and extend of fire incidents and their effects is of great importance. Fire risk prediction is essential for the planning of precautionary, preventive and mitigating measures. Property insurance as a precautionary measure in high fire risk areas, although often not acceptable measure by the residents, who refuse to share fire management costs (e.g. Cortner *et al.* 1990), can reduce monetary fire losses and reinforce the resilience capacity of communities. Fuel treatment activities (e.g. thinning, prescribed fires) as preventive measures can be effective in modifying fire behavior and as a result fire losses (e.g. Shang *et al.* 2004;Stephens and Moghaddas 2005;Penman *et al.* 2013a;Penman *et al.* 2014). Fire danger communication, evacuation preparedness, and preparation of residents to defend property as preventive measures

can be essential for life and property safety (e.g. Penman *et al.* 2013b). Finally, fire crew allocation, time of response and efficiency to mitigate fire events are critical measures for fire containment and life and property safety (e.g. Plucinski *et al.* 2012). All the above demand effective fire risk assessment in order to identify in good time fire danger and location vulnerability. The temporal and spatial resolution of the assessment depends on the measure. While insurance, danger communication and evacuation measures are implemented in the meso-scale, fuel treatment and ground fire crew allocation are measures implemented in the micro-scale (< 1km²). Temporal resolution also varies from seasonal (evacuation and fire protection plans) to daily (fire danger communication, crew allocation, prescribed burning).

When modeling wildfires, it is commonly distinguished between the ignition and the behavior (including the spread) of the wildfires. Here, the occurrence of wildfires, is defined as the event that a fire has ignited and has spread to an extent that it is registered. Therefore, to model the occurrence of a fire it is necessary to consider factors leading to ignition as well as its initial spread. Due to the random nature of fire occurrences and behavior and the uncertainties in the influencing factors, such a prediction should ideally be probabilistic. Various probabilistic models are proposed in the literature concerning fire occurrence and the resulting burnt area, but limited research has been reported on modeling possible effects. In addition, research on wildfire occurrence and behavior addresses the questions on when, where and why wildfires are triggered and grow. The answer to these questions requires understanding of the interrelations among biotic and abiotic factors and multidisciplinary approaches are thus needed for modeling fire risk. The interdisciplinary approach to natural hazard risk modeling can be supported efficiently by Bayesian networks (BN). Based on acyclic graphs, BN enable to model the probabilistic dependence among a large number of variables influencing the risk. The causalities expressed by the arcs between the variables make BN not only convenient for graphical communication of the interrelations between the influencing factors (qualitative part), but also include, through conditional probability tables, a quantitative probabilistic model (Jensen and Nielsen 2007). In other words, the graphical representation of the dependence structure among stochastic variables makes it easy to understand intuitively and facilitates the consistent modeling of complex problems involving many variables. For these reasons, BN are increasingly applied for risk assessment of natural hazards, e.g. for rock-fall hazards (Straub 2005), avalanches (Grêt-Regamey and Straub 2006), tsunamis (Blaser *et al.* 2009) earthquakes (Bayraktarli *et al.* 2005;Bensi 2010;Kuehn *et al.* 2011), landslides (Song *et al.* 2012), volcanoes (Aspinall *et al.* 2003) and wildfires (Dlamini 2009).

1.1   Research objectives

The objective of this thesis is to create a probabilistic tool for the prediction of fire risk in the meso-scale. In particular, the thesis aims to:

- develop a probabilistic fire occurrence model that includes as influencing variables both weather conditions and human involvement to account for ignitions related to humans and improve the currently used fire danger models
- develop a probabilistic fire size model that takes into account weather conditions, topography and vegetation types, deals with the problem of non-observable variables and gives predictions on the resulting burnt area

- develop a fire effects model to houses and vegetation that introduces vulnerability and exposure indicators for the quantification of effects in the meso-scale
- combine the above models to a fire risk model that connects the probability of the occurrence of a wildfire hazard with the resulting effects
- apply the proposed models for study areas in the Mediterranean basin, with real data of various sources and expert knowledge
- couple the BN with a Geographic Information System (GIS) for parameter learning and for illustration of the prediction results with maps of high spatial and temporal resolution

The model of fire occurrences aims to evaluate the probability of fire occurrence and will be part of the fire danger model. The latest will also include the fire size model, resulting to the prediction of the burnt area, determining thereby the resulting size of the fire. The fire danger model aims to represent the probability of occurrence of a fire hazard in the overall fire risk model. The effects model aims to model the vulnerability of house portfolios and vegetation types and to quantify the exposure of the items at risk. This model quantifies the effects caused by the predicted fire hazard event. The application of the model to areas of the Mediterranean basin with similar fire regime characteristics allows the calibration of the model for similar areas and the validation of the predictions for selected data sets. In order to manage data from various sources and to enable fire risk mapping, GIS is utilized, which coupled with the proposed BN serves the purpose of model parameter learning and output mapping.

1.2 Thesis outline

The thesis consists of nine chapters and four Appendices.

The second chapter "Fires" introduces the reader into the definition of fire risk, the phenomenon of fire, the Canadian Forest Fire Weather Index System (CFFWIS) as widely used in present fire danger predictive systems (equations for CFFWIS calculation provided in Appendix I), factors influencing damages to houses and vegetation and fires specifically occurring in the Mediterranean basin.

The third chapter "Modelling methods" discusses the methods used in the thesis. It describes the concept of Bayesian networks (BN) and the dependencies between the random variables. The coupling types between BN and Geographic Information System (GIS) found in the literature are introduced and the chosen coupling between GIS and BN is shown in more detail; in this coupling the input of the GIS is used for parameter estimation of the BN, and then the output of the BN is given as input to the GIS to map the resulting risk. The Poisson regression method, used in this thesis to model fire occurrences is introduced, together with the maximum likelihood estimation method used to define the coefficients of the regression equation. The Akaike Information Criterion and the ROC curves used as diagnostics are described. In addition, the interpolation method of weather observations and the specifics of the calculation of the components of the CFFWIS are shown.

The fourth chapter "Study areas" gives a detailed overview on the chosen areas to which the models are applied, the data used and their sources. The study areas of this thesis are the islands Rhodes (Greece) and Cyprus and South France. This chapter together with Appendix II includes preliminary data analysis of fire occurrences, resulting burnt area and registered losses.

The fifth chapter "Fire occurrence model" introduces the reader to the models developed to predict fire occurrence and their performance. The best model is chosen to make predictions for a validation time period of the study areas and the first maps of the predicted fire occurrence rate in the meso-scale are demonstrated.

The sixth chapter "Fire size model" gives an insight to the prediction of the resulting burnt area, once a fire has occurred. The proposed model takes under account the initial spread conditions, the recent weather conditions and the topography and accounts also for non-observable variables. The predictive ability of the model is studied and the results of the predicted burnt area on specific days in the study area are shown in maps.

The seventh chapter "Fire effects model" introduces two models which estimate expected damage cost to houses and vegetation respectively, for given fire characteristics. The effect estimation is facilitated by BNs, which allow modeling the damage cost of wildfires in the meso-scale with respect to different hazard characteristics and include vulnerability and exposure indicators. After the application of the model to the study areas expected house damage cost and vegetation damage cost maps are presented.

The eighth chapter "Fire risk model" introduces the fire risk model, which results as a compound of the three previously described models (fire occurrence model, fire size model, fire effects model). The fire risk model is applied to the study areas and the accumulated daily risk for a verification dataset is presented. Fire risk maps of selected days demonstrate the predictions. Sensitivity analysis and additional maps are included in Appendix III.

The ninth chapter "Conclusion" summarizes the main outputs of the thesis, discusses critical issues of the modelling process and offers insight for future work.

Finally, the author's publications related to and made during the present PhD research work are listed in Appendix IV.

2 Wildfires

2.1 Fire risk

Wildfires cause severe damages to built and natural environment. In order to enhance the resilience of the communities threatened by fires, it is essential to develop efficient fire risk predictive systems. The quantification of fire risk can support both preventive and mitigating measures for fire control. Thus, it is an essential task in order to control fire damages.

In this work fire risk is estimated as a function of occurrence probability and effects. Wildfire effects are a function of vulnerability and exposure of the affected biotic and abiotic systems (e.g. human properties, infrastructure, soil and air quality). Vulnerability describes the degree of expected damage as a function of hazard intensity (UNDRO 1991;Thywissen 2006). Exposure refers to the items at risk, such as house density. Risk is thus the intersection between hazard, vulnerability and exposure. The general conceptual framework to quantify disaster risk is shown in Figure 2.1. A fire disaster can be expressed by the fire hazard, characterized by the occurrence and the hazard severity, the vulnerability of the affected assets (social, economic, environmental) and the presence of the assets (e.g. people, houses, infrastructure, public buildings such as schools, hospitals).
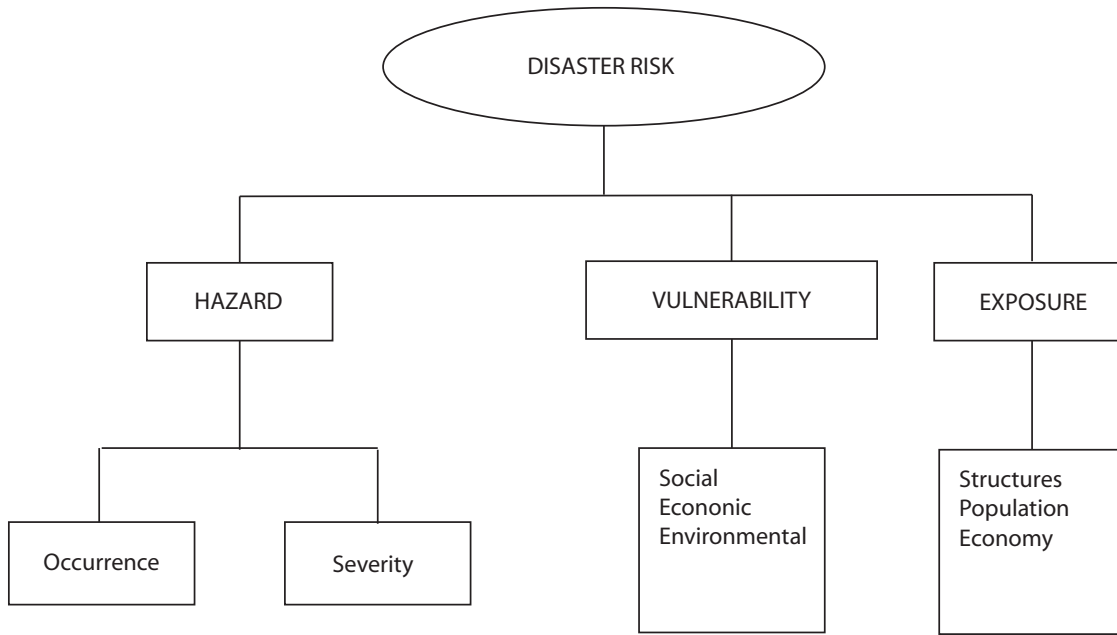
Figure 2.1: The conceptual framework of disaster risk

Risk is the expected consequences of wildfires and can be formulated as a function of the hazard H, the resulting damages D and the consequences C as,

$$R = \mathrm{E}_{H,D}[C] = \int_H p(H) \int_D p(D|H)C(D,H)dD \, dH \qquad (2.1)$$

$\mathrm{E}_{H,D}$ denotes the expected value with respect to H and D. $p(\mathrm{D}|\mathrm{H})$ is the probability of damage D conditional on the hazard H, i.e. it describes the vulnerability, and $C(\mathrm{D},\mathrm{H})$ is the cost as a function of damage and hazard. The inner integral in Eq. (2.1) describes the expected consequences for given hazard:

$$\mathrm{E}_D[C \mid H] = \int_D p(D|H) \, C(D,H)dD \qquad (2.2)$$

Consequences are a thus function of damage and cost:

$$R = f(D|H,C) \qquad (2.3)$$

Figure 2.2 shows graphically the risk assessment in the form of a 2D matrix, where the horizontal axis refers to the probability of hazard occurrence and the vertical axis to the possible consequences. The risk results from the multiplication of the scores of the states of the probability of hazard occurrence and of the states of consequences. The risk is then classified in extreme (red), high (orange), medium (yellow), low (light green) and very low (dark green) based on the resulting scores.

Consequences	Probability of Hazard				
	almost certainly will occur (5)	good chance to occur (4)	likely to occur (3)	unlikely to occur (2)	extremely unlikelyto occur (1)
Disastrous (5)	25	20	15	10	5
Critical (4)	20	16	12	8	4
Serious (3)	15	12	9	6	3
Significant (2)	10	8	6	4	2
Minor (1)	5	4	3	2	1

Risk	Extreme	High	Moderate	Low	Very Low

Figure 2.2: Risk assessment matrix

There are multiple criteria to classify consequences. Consequences can be classified based on their ability to be measured by market values as either tangible (e.g. house damage) or intangible (e.g. cultural heritage losses). Consequences can furthermore be classified according to whether they are direct (e.g. house damage) or indirect (e.g. erosion on slopes following the destruction of a stabilizing forest). Tangible direct damages can be measured by the costs of repairing or replacing damaged items, whereas intangible direct damages may be measured in terms of number of affected items (Paul 2011).

In the contrary to the above introduced definitions of risk, which will be used throughout this thesis, one can find very different approaches concerning fire risk in the literature. Previous studies have attempted to quantify fire risk using satellite images and GIS to identify influencing variables and then fire risk is given as a linear function of weighted variables (e.g. Jaiswal *et al.* 2002) or as a result of multicriteria evaluation technique (e.g. Chuvieco *et al.* 2010). Moreover, many

publications use the term fire risk to express fire hazard and do not take into account the potential consequences (e.g. Beringer 2000, Haight *et al.* 2004, He *et al.* 2004, Shang *et al.* 2004, Amatulli *et al.* 2006, Hernandez-Leal *et al.* 2006, Moriondo *et al.* 2006, Carmel *et al.* 2009, Catry *et al.* 2009). In this thesis the term fire risk will express the result from both the probability of hazard and its consequences based on the definitions given above. Fire danger will be expressed indices influenced by weather conditions (see later Section 2.3). To give an insight into the problematic of the fire hazard and the resulting consequences the paragraphs following will introduce the phenomenon and types of fire, the use of weather indices to describe fire danger related to fuel moisture and the damages to houses and vegetation. The chapter will end with information on the fire phenomenon in the Mediterranean basin, areas of which will be used later on as study areas for the application of models (Chapter 4).

2.2 Fire hazard

This chapter is based on Van Wagtendonk (2006). Fire hazard is the physical phenomenon of a fire occurring and spreading. The severity of a fire hazard can be described by the resulting burnt area, the fire spread rate and the fire intensity. Based on the burnt vegetation, fire can be classified in different types.

2.2.1 Fire as a physical process

Fire is a natural process and in order for combustion to occur, heat, fuel and oxygen must be present. These three elements form the so called fire triangle (Figure 2.3) and fire control measures aim to break the link among them. To do so, they aim to reduce the fuels or the amount of oxygen or lower the temperature of the fuel.
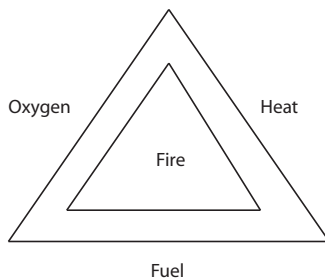
Figure 2.3: The fire triangle

Fire burns the accumulated debris, when decomposition is unable to keep up with the deposited material, and organic debris begins to accumulate. Combustion is an oxidation process, it combines materials which contain hydrocarbons with oxygen and produce carbon dioxide, water and energy. Heat of combustion is the energy resulting by this reaction. The combustion equation is as follows,

$$4C_6H_9O_4 + 25O_2 \rightarrow 18H_2O + 24CO_2 + 5{,}264{,}729 \; kJ \qquad (2.4)$$
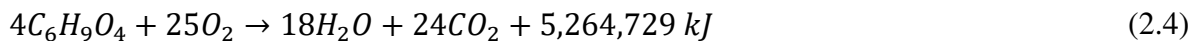
Combustion takes place in three phases: preheating, gaseous and smoldering (Figure 2.4). In the preheating phase, fuels ahead of the fire are heated, water evaporates from the fuel, and gases are partially distilled. The gaseous phase starts with ignition as gases continue to be destilled, active burning begins and an active flaming front develops. Ignition occurs in four stages: contact to receptive fuel, moisture in fuel is driven off, temperature of fuel raised to the point of pyrolysis, gases heated to ignition temperature. During the smoldering phase, charcoal and other unburned material, which remain after the flaming phase, continue to burn leaving a small amount of residual ash.
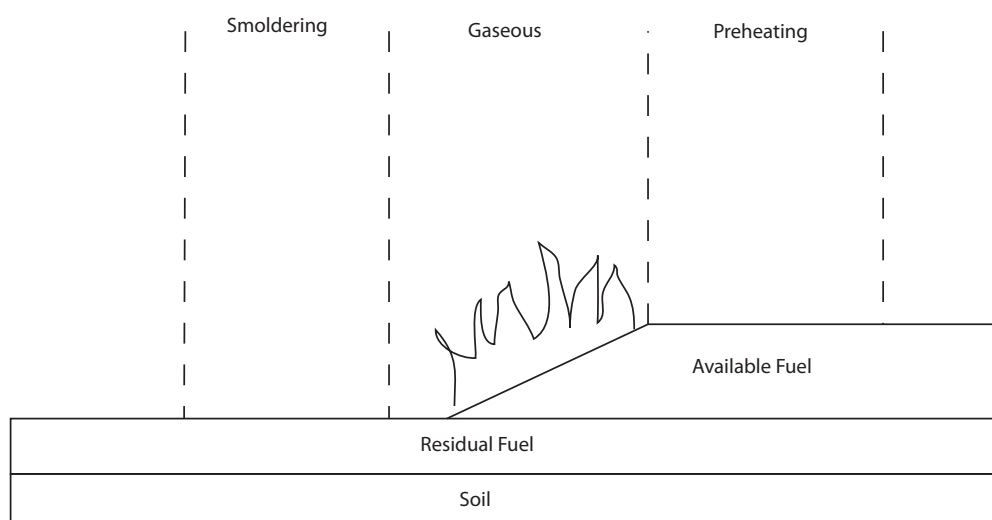
Figure 2.4: The three phases of combustion (Van Wagtendonk 2006)

Not every combustion leads to a fire hazard. Whether a combustion will spread to become a fire event that needs to be suppressed (fire hazard) or will extinguish on its own, depends on the available fuel and the weather conditions. After a fire occurs, fire behaviour is primary determined by moisture contained in the proportion of a fuel particle. The interaction of a fuel particle with the ambient moisture depends on its size or its depth in the organic layer (duff). The size classes used to categorize fuels are the fuel moisture timelag classes (Table 2.1). Timelag is defined as the amount of time necessary for a fuel component to reach 63% of its equilibrium moisture content at a given temperature and relative humidity. One-hour timelag fuels react to hourly changes in relative humidity and include dead herbaceous plants and small branchwood as well as the uppermost litter on the forest floor. 10-hour timelag fuels reflect the day-to-day changes in moisture. Moisture trends from days to weeks are reflected by 100-hour fuels, whereas 1000-hour fuels reflect seasonal changes in moisture.

Table 2.1: Moisture timelag classes and corresponding woody fuel size and duff fuel depth classes (Van Wagtendonk 2006)

Timelag class	Time period	Woody fuel size class (cm)	Duff fuel depth class (cm)
1-hour	Hourly	0.00-0.64	0.00-0.64
10-hour	Daily	0.64-2.54	0.64-1.91
100-hour	Weekly	2.54-7.64	1.91-10.16
1,000-hour	Seasonally	7.62-22.86	10.16+

Apart from fuel moisture, weather conditions are primarily influencing fire behaviour. Fire weather conditions include air temperature, atmospheric moisture, wind speed and direction, and precipitation. Air temperature influences the amount of heat necessary to evaporate fuel moisture and raise fuel temperature. Relative humidity influences the exchange of water vapour between air and dead fuels. Relative humidity is defined as the ratio between the actual and the maximum amount of humidity at any particular temperature and pressure. The winds carry away the moisture in the air, dry the fuels and supply oxygen. Winds also carry embers from torching trees, creating new fire hotspots in front of the fire. They can change the direction that a fire moves (flaming front turns to fire back and vice versa, see later Section 2.2.3 Fire characteristics) and turbulent wind conditions can create fire whirls, making fire difficult to suppress. Precipitation influences directly fuel moisture. The influence of weather conditions on fuel moisture and initial fire behaviour will be discussed in more detail in Section 2.3.

2.2.2   Types of fires

Fires can be classified in different types. The type of fire is defined by the fuel consumption and the method of spread (Table 2.2). Ground fires burn the ground fuel and include slow-moving smoldering fires. Surface fires burn litter and woody fuels of the surface with an active flaming front. Passive crown fires burn fuels of the surface and individual trees. Active crown fires burn in the canopies together with surface fires. Independent crown fires burn only in the canopies. In Table 2.2 fuel types with similar characteristics are grouped into fuel models. Fuel models determine fire behaviour. The main fuel models are tree canopy fuels (understory and overstory fuel), shrub fuels, low vegetation fuels (grasses, sedges), woody fuels (sound logs, rotten logs, snags, stumps), litter fuels and ground fuels. Fire severity, thus the loss or change of organic matter aboveground and belowground (Keeley 2009), is higher for active crown fires, since these affect both surface and tree canopy fuels.

Table 2.2: Fire types, fuel model and fuel categories (Van Wagtendonk 2006)

Fire type	Fuel model	Fuel category
Ground	Ground fuel	Duff, peat, basal accumulation, animal middens
Surface	Litter fuel Woody fuel	Litter, linches, moss Sound wood, rotten wood, piles and jackpots, stumps
Passive Crown	Shrub Low vegetation Litter fuel Woody fuel	Shrubs, needle drape Grasses and sedges, forbs Litter, lichens, moss sound wood, rotten wood, piles and jackpots, stumps
Active Crown	Shrub Low vegetation Tree canopy Litter fuel	Shrubs, needle drape Grasses and sedges, forbs Canopy, snags, ladders Litter, linches, moss

	Woody fuel	Sound wood, rotten wood, piles and jackpots, stumps
Independent Crown	Shrub Low vegetation Tree canopy	Shrubs, needle drape Grasses and sedges, forbs Canopy, snags, ladders

2.2.3 Fire characteristics

The geometry of a fire can be modelled as an ellipse, whose one side is the flaming front and the opposite the fire back. The flaming front is the area at the front of a fire and is described by the flame depth (Figure 2.5), fire intensity and fire spread rate.

Fire intensity describes the physical combustion process of energy release from organic matter (Keeley *et al.* 2012). It is the energy release of the fire front per unit length. Byram's definition of fireline intensity I (kWm^{-1}) used in the literature, is as follows (Byram 1959),

$$I = HWR \tag{2.5}$$

wherein H is the heat of combustion (kJ kg^{-1} of fuel), W is the consumed fuel (kgm^{-2}) and R is the rate of fire spread (ms^{-1}). Rate of spread is the speed that the fire front moves forward and is defined in measures of distance per unit of time. Often flame length is used to replace fire intensity due to their significant relationship in forest and shrubland ecosystems (Keeley *et al.* 2012).
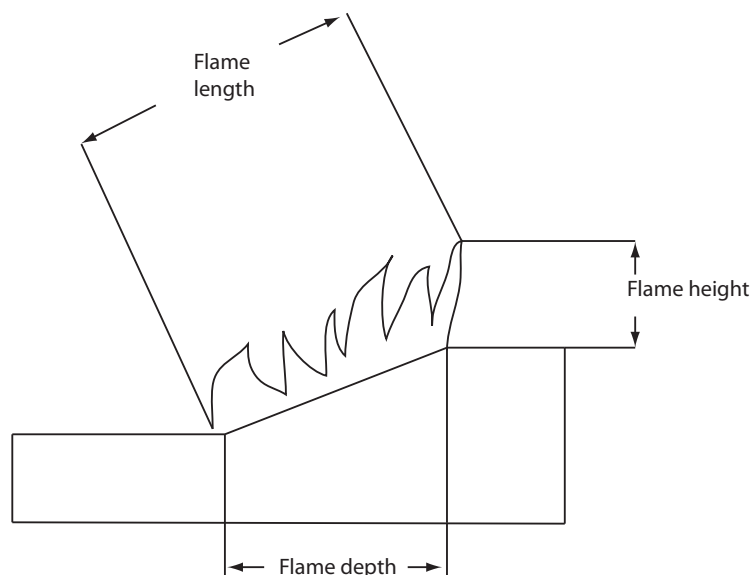
Figure 2.5: Flame dimensions of the fire front of a fire (Van Wagtendonk 2006)

2.3   The Canadian Forest Fire Weather Index System

As already mentioned, weather plays an important role in both the ignition potential but also in the spread of fire. High temperatures and low humidity favour the drying of the litter and woody fuels of the surface, which can be thus more easily ignited. Strong winds reinforce flame length and fire spread rate, accelerate fine fuel drying process and carry burning particles (embers) to long distance in front of the active fire front, creating new hot spots. Quantifying fire weather conditions is an important step in the quantification of daily fire risk.

For the quantification of weather influence on fuels, there are several (fire danger rating) systems used worldwide, developed based on empirical studies and adapted to local conditions (e.g. fuel types, day length). Fire danger rating systems are used to evaluate the influence of the weather on fuel moisture and the potential of (initial) fire spread, once an ignition takes place. One of the most used fire danger rating systems worldwide is the Canadian Forest Fire Weather Index System (CFFWIS) (Lawson and Armitage 2008). CFFWIS is one of the principal subsystems of the Canadian Forest Fire Danger Rating System (CFFDRS) (Figure 2.6), which encompasses both predictive fire occurrence and fire behavior systems. The overall system (CFFDRS) aims to quantify the forest fire danger with input weather conditions, fuel types, topography and ignition cause, whether the subsystem (CFFWIS) focuses on the influence of weather conditions on the fuel moisture.
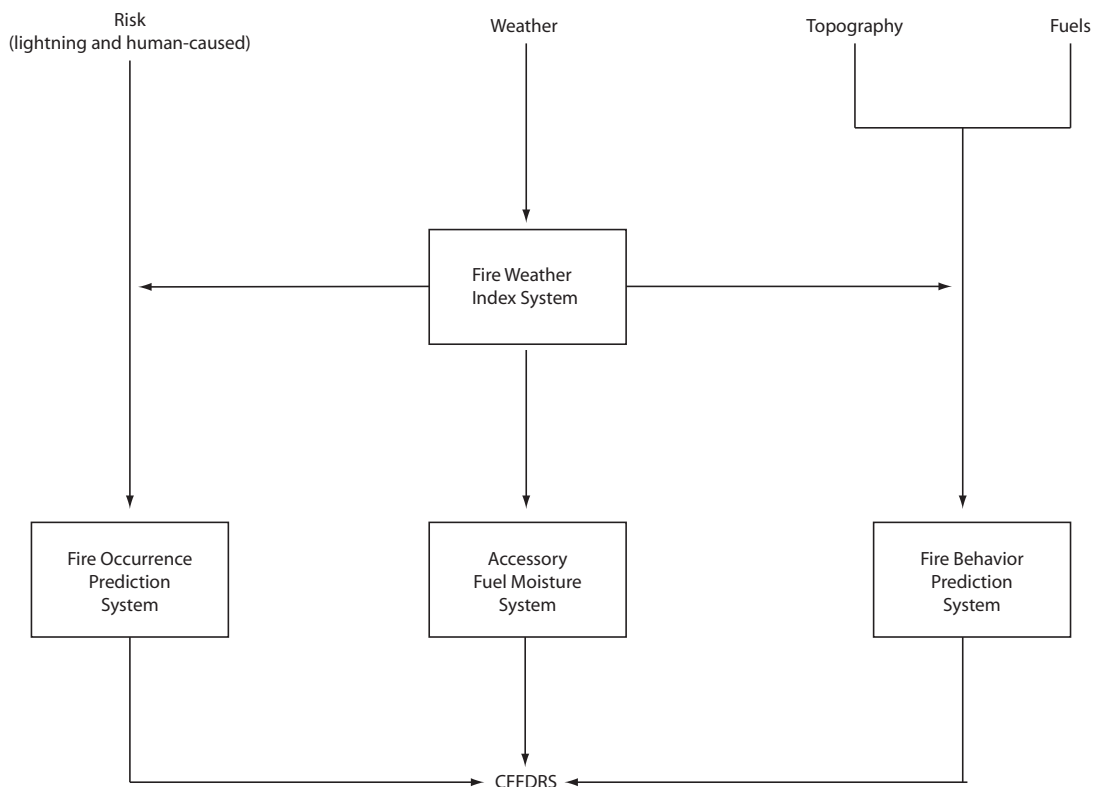
Figure 2.6: Structure of the Canadian Forest Fire Danger Rating System (CFFDRS) (Lawson and Armitage 2008)

CFFWIS's main components are three fuel moisture codes and three fire behavior indices (Figure 2.7). These components provide numeric ratings of relative potential for wildland fire. The system takes as input easily observed weather elements such as rain accumulated over 24h, temperature, wind speed and relative humidity. The latest three weather parameters are measured at noon (12 o'clock).

The Fine Fuel Moisture Code (FFMC) rates the moisture content of litter and other fine fuels. It expresses the interaction of the fine fuel particles (nominal depth 1.2 cm) with the ambient moisture and is related to 2/3-hour timelag class. FFMC is an indicator of the relative ease of ignition and flammability of fine fuels. It takes as input rain, temperature, wind speed, relative humidity and the value of the FFMC of the last day.

The Duff Moisture Code (DMC) rates the moisture content of deep, compact organic layers. It is an indicator of seasonal drought effects on forest fuels (nominal depth 7 cm) and the amount of smoldering in deep duff layers and large logs (relates to 15-hour timelag class). It takes as input rain, temperature, relative humidity and the value of DMC of the last day.

The Drought Code (DC) rates the moisture content of deep, compact organic layers. It is an indicator of seasonal drought effects on forest fuels (nominal depth 18 cm) and the amount of smoldering in deep duff layers, and is related to 53-hour timelag class. It takes as input rain and temperature and the value of DC of the last day.

The Initial Spread Index (ISI) rates the expected rate of fire spread. It combines the effect of wind speed and FFMC and does not take under account the fuel. It takes as input wind speed and FFMC.

The Buildup Index (BUI) rates the total amount of fuel available for combustion. It combines the DMC and the DC.

The Fire Weather Index (FWI) represents the intensity of a spreading fire as energy output rate per length of fire front. It combines ISI and BUI.
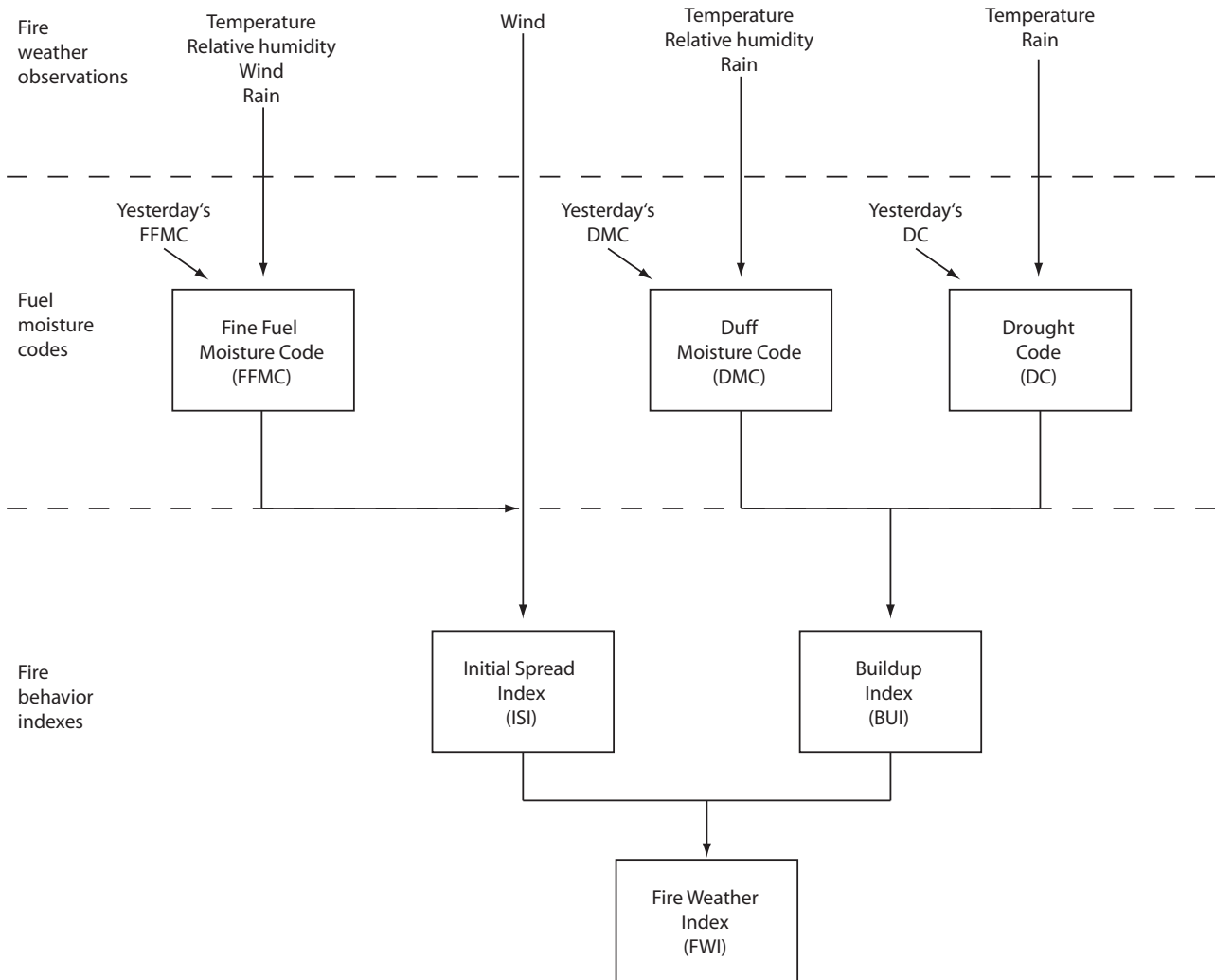
Figure 2.7: Structure of the Canadian Forest Fire Weather Index System (Service 1984, Lawson and Armitage 2008)

In the calculation of all three fuel moisture codes, first the amount of rain in the past 24 h is evaluated and then the appropriate degree of drying is taken under account (Figure 2.8). The thresholds of rain are for FFMC, r>0.5mm, for DMC, r>1.5mm and for DC, r > 2.8mm. The equations for the calculation of the CFFWIS are given in Appendix I. The starting values for the calculation of the three moisture codes are FFMC = 85, DMC = 6 and DC = 15. The system does not allow missing observations, so blank spaces of weather observations must be completed.
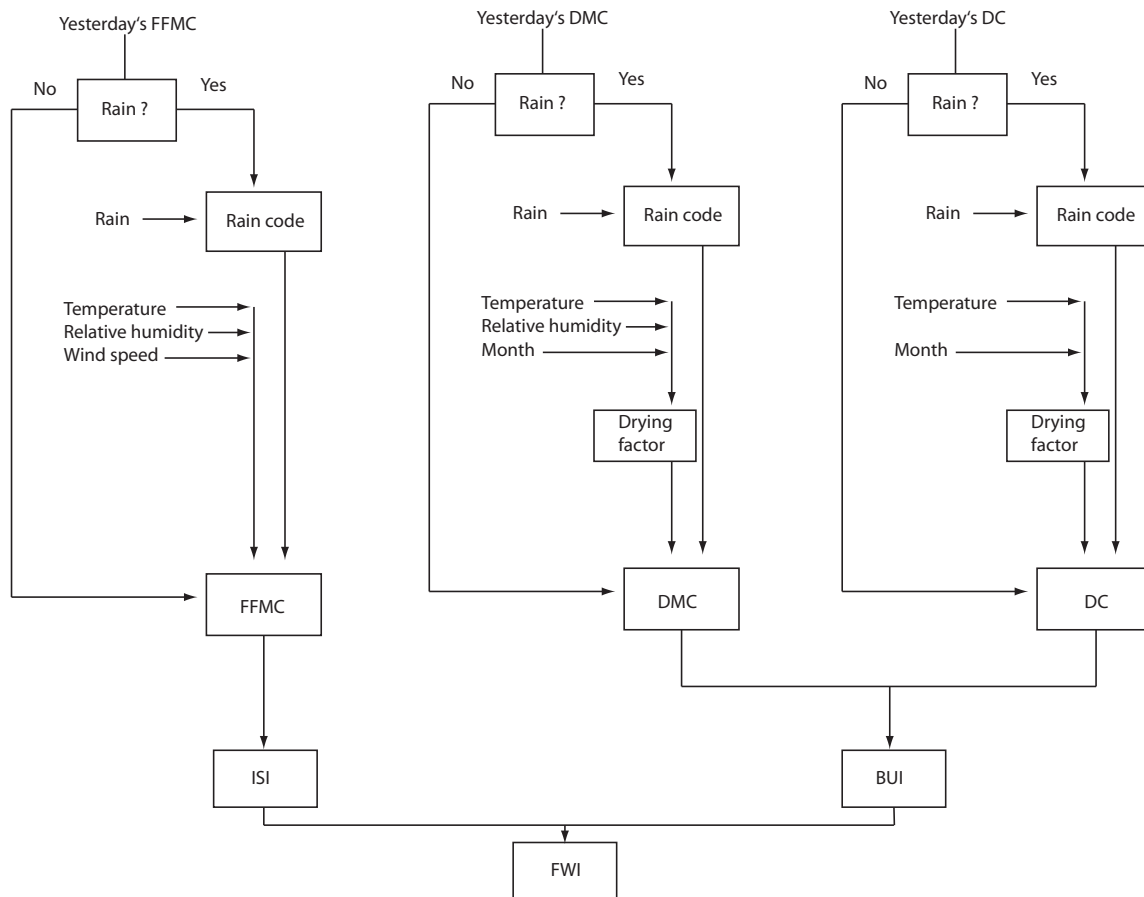
Figure 2.8: Schematic diagram for calculating the six standard components of the Canadian Forest Fire Weather Index System (Lawson and Armitage 2008) (see Appendix for the algorithm of the system)

Although created for Canada, the CFFWIS is adopted by many other countries. The Joint Research Center of the European Union is using currently the CFFWIS to evaluate fire danger in Europe. The system is called European Forest Fire System (EFFIS) and produces daily maps of the six components of the CFFWIS with 10 km² spatial resolution. An example of those maps is shown in Figure 2.9. Based on the values of the mapped component of the CFFWIS fire danger is classified in six classes (Very low, Low, Moderate, High, Very high, Extreme). The countries of the Mediterranean basin are the ones, where the highest values of FWI are registered. This classification of fire danger, which is the widely used instrument of the European Union, takes into account only weather conditions and neglects other fire occurrence and spread influencing parameters, such as population, land cover types or topography. It can be therefore assumed, that a system taking into account also additional parameters can model fire danger more accurately.
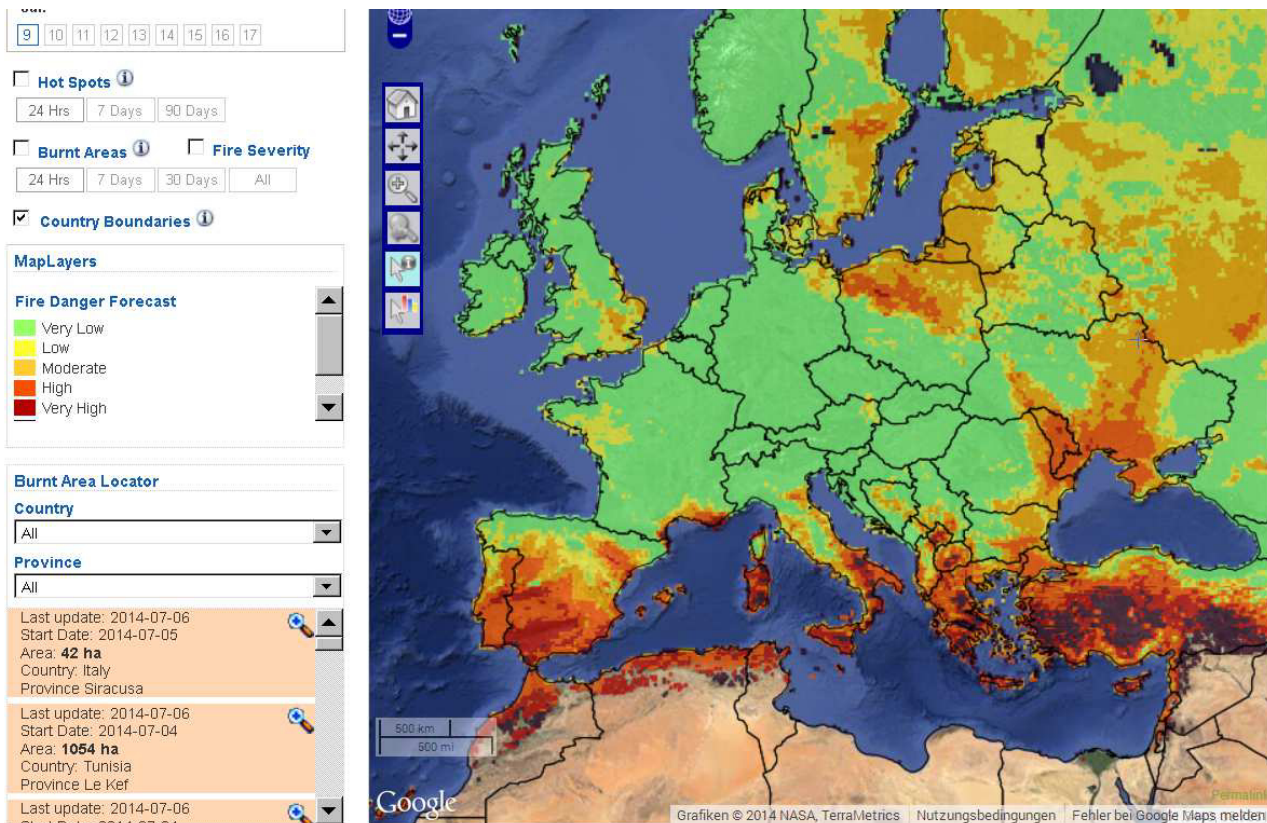
Figure 2.9: FWI on the 9th July 2014 in Europe with 10 km² spatial resolution (European Forest Fire Information System) (retrieved on 09.07.14)

The EFFIS is the official operational fire danger predictive instrument of the EU and as a result the system that the local governments of the EU states refer to, to evaluate daily fire danger. It can be therefore of great importance to evaluate the predictive ability of the FWI to identify fire danger in Europe. Since FWI takes under account only weather conditions and knowing that most fires in Europe are ignited by humans (as discussed later in Section 2.5 Fires in the Mediterranean basin) it can be assumed that FWI alone cannot accurately predict fire occurrence in Southern Europe and that other factors, such as land cover types or population density should be included in the prediction. This is further discussed in Chapter 5. Nevertheless, some countries of South Europe use additionally other fire danger indicators, which combine daily weather conditions with past recent weather. Some of the methods used in France, Italy, Portugal and Spain can be found in Viegas *et al.* (1999).

2.4   Fire effects

Fires cause severe damages to the built and natural environment. Among others they cause life losses and injuries, house losses, infrastructure damages, agricultural production losses and forest biodiversity losses. As an example the damaging fires in Greece in August 2007 resulted in 84 life losses, 1000 houses totally destroyed and 2700 km² of burnt forests, olive groves and farmland (http://en.wikipedia.org/wiki/2007_Greek_forest_fires). The focus of this work relating to fire

effects is the house losses and the damages to vegetated areas (both natural vegetation and agricultural areas). These fire effects are influenced by both natural and anthropogenic factors.

The main factors influencing the resulting house effects are the presence and intensity of fire, the flammability of the exposed objects and the suppression effectiveness. Interrelations of the influencing factors are present (e.g. fire characteristics and flammability of houses influence the result of fire suppression). In more detail, the factors influencing losses are fire characteristics (flame length, fire intensity, spread rate, burning ember density), house design and construction materials, the surroundings of the house (defensible space, distance from forest, fuel accumulation) and fire suppression effectiveness (Blanchi *et al.* 2010;Gibbons *et al.* 2012).

Houses usually either survive a fire or get totally destroyed (Cohen 2000;Blong 2003). Since combustion requires all three fire triangle elements (fuel, heat, oxygen) (as shown in Figure 2.3), a house will also ignite, if all requirements occur. Fire impact may include direct contact of the flames, radiant heat flux from nearby flames and airborne embers/firebrands (Cohen 2000;Koo *et al.* 2010;Mell *et al.* 2010). Radiant heat from an intense fire can cause house ignitions within a 40m distance from the flame or even more (Cohen 2000;Cohen 2004). Gibbons *et al.* (2012) showed that a reduction (from 90% to 5%) of trees and shrubs cover within 40m of houses could potentially reduce house loss by an average of 43%. In spot fire phenomena generated firebrand from torching trees (sometimes lofted by fire whirls occurring in large-scale forest fires) can be transported by strong winds to long distances typically up to 3 km (Albini 1979;Koo *et al.* 2010) and can result to ignitions in landing positions. Moreover, Syphard *et al.* (2012) proved that property loss is more likely to occur when structures were surrounded by wildland vegetation rather than by urban areas.

The characteristics of a building structure and its immediate surroundings influence the probability of ignition and therefore survival (Cohen 2000). Structure flammability depends on exterior construction materials (e.g. roof type and roof material influencing the ignition by firebrands (Koo *et al.* 2010;Gibbons *et al.* 2012) and construction design (e.g. number, size and characteristics of openings)). Homes should not be considered simply as potential victims of wildland fire, but also as potential participants in the continuation of the fire in their location (Cohen 2000). Therefore, building density is also included in studies of house losses due to wildfires (Gibbons *et al.* 2012). Poor firefighter access may explain why housing clusters with fewer roads were more vulnerable. However, it has been documented in numerous cases that homes with low ignitability can survive high intensity wildland fires, whereas highly ignitable homes can be destroyed during lower intensity fires (Cohen 2000).

Apart from house damages, also vegetation damages will be addressed in this study. Although fires favor the re-sprouting of some fire resistant species (Pausas 1997), when repeated fire events occur, the vegetation fails to regenerate naturally due to the enlargement of fire scars on the trees that consequently leads to tree loss. Fires burn the outer bark, the inner bark and the wood of the bole (Show and Kotok 1924). When no new reopening takes place, the wound will heal completely with new wood that comes from the edges of the inner bark and a scar will remain, able to define the date of the fire event. A fire can either create scars to the trees or burn them down. When a fire occurs and reaches the base of a tree, the tree will burn down if there are previous scars present. For e.g. in the California pine forests, the presence of older scars is the primary influential factor of the overall loss and the rate of spread, the amount of flammable material, the fire intensity are all secondary factors. Thus, the process of damage from a fire gathers momentum with each succeeding fire and ends up to the loss of the individual tree or the stand. The oldest trees burn down as a result of repeating fire events, which reduces the quality and the volume of a forest. Direct loss of merchantable timber occurs, since the burned volume includes the clear grades of lumber, the highest quality material of the tree. Moreover, direct heat killing occurs, when a fire has

reached the crowns of the trees and has burned up the foliage completely, or a surface fire has reached such intense heat that the foliage and buds are killed without being consumed. The most important factors in heat killing is the amount of inflammable material on the forest floor, such as litter and duff and the amount of brush under the timber stand. Topography influences also the damage, since fires travel uphill and the upper standing timber bears the burn of the increased fire intensity of the flames. Climatic conditions influence the resulting damage to the timber. Dry and windy conditions favor fire spread and the consumption of the forest floor. Additionally, in spring and early summer, when the forest is actively growing, it is more probable that the timber is damaged by a fire, than in late summer or autumn, when the protected winter buds have been formed. Lastly the density of the forest stand influences the damage. Dense, closed stand of timber with uninterrupted canopy favors the development of crown fires, which lead to higher damages.

2.5   Fires in the Mediterranean basin

As discussed above, the ignition and behavior of a fire, as well the resulting effects depend mainly on the local conditions (e.g. local vegetation, weather, construction types). On account of this, no model can predict at the same time fire risk in European pine forests, the Amazon rainforest and the African savannas. Therefore models should be adapted to the characteristics of each biotope and human infrastructure. This thesis focuses on areas with Mediterranean type climate regions (MTC) and the study areas chosen are located in the Mediterranean basin (Chapter 4).

MTC regions are fire prone areas and experience fire events every year. These regions have climatic conditions similar to the Mediterranean basin (Keeley *et al.* 2012). The Mediterranean type climate is the result of global circulation patterns, that generate a summer high pressure cell of dry sinking air that blocks incoming summer storms on the western sides of continents concentrated between 32° and 38° N or S latitude. MTC regions are defined by long summer drought and winter rainfall with mild temperatures. These landscapes are highly fire prone, because of the fact that wet winters favour fuel accumulation and dry summer periods favour fuel drought. There are five MTC regions in the world. These are the Mediterranean basin, California, Central Chile, Cape Province in South Africa, Southwest and South Australia. The dominant vegetation types in MTC are shrublands, which are typically evergreens with broad or small, stiff and sclerophyllous leaves on woody stems.

The Mediterranean basin, which is the largest MTC region, includes portions of the countries Portugal, Spain, France, Italy, Greece, Turkey, Morocco, Algeria and Tunisia (Figure 2.10). The dominant vegetation types are evergreen broadleaf maquis shrublands, which transit in arid sites to a lower growing drought-deciduous spiny formation known as phrygana (Greek) or tomillares (Spanish). Shrublands are dominated by evergreen sclerophyllous-leaved shrubs that re-sprout after fire. In the northern side of the Basin, forests are dominated by *Pinus halepensis*, which typically burn in high intensity crown fires. In the eastern side of the basin these are replaced by *Pinus brutia*. The long history of human civilization has led to a high landscape fragmentation level in the Mediterranean basin and as a result natural pine stands and plantations are often difficult to differentiate.

The fires in the Mediterranean are spread by fire weather winds that occur in the summer period. Fire weather winds, thus katabatic foehn (dry downslope) winds flowing from high pressure ridge to low pressure have different names in the Mediterranean, such as mistral in France and meltemia in Greece. These winds develop from synoptic weather conditions where interior high pressure cells

are juxtaposed with low pressure troughs at the coastal side of mountains. These foehn winds are related to extreme fire weather due to their ability to produce severe burning conditions known as firestorms.

Fires are ignited both by nature and humans. Lightning is the natural source of fires. However, lightning does not correspond to the major fire inducing parameter in the MTC areas, since the lightning strikes occur mainly during winter storms that seldom contribute to fires. It is humans that mainly cause fire ignitions in MTC regions. Most fires in the Mediterranean basin are started by people, either on purpose (e.g. arson) or by accident (e.g. campfire, agricultural activities). The reason for this is the high population density of the coastal areas. Current landscapes of the Mediterranean are a result of long history land use and comprise mosaics of natural vegetation, agricultural land, old fields and urban areas. Fire has been used historically by humans for hunting, food gathering, deforestation, agricultural purposes, domestic grazing (pasture improvement) and wars (Leone *et al.* 2009). As a result the Mediterranean landscapes are strongly shaped by humans and fire has played an important role on achieving this. Due to the high landscape fragmentation burnt areas are relatively small in the Mediterranean compared to other MTC regions.

Generally - with the exception of natural parks, which allow fires induced by lightning to burn naturally (Parsons *et al.* 1986) - humans aim to prevent and control fire events, thus to conduct fire management. Among the preventive fire management measures also applied in the Mediterranean basin are fuel clearing, thinning, fire breaks, prescribed burning, monitoring and prediction. Among mitigation measures are fire suppression and prescribed burning. Unfortunately, much effort is given mainly in mitigation measures (fire suppression equipment) and less in preventive measures, which are less expensive and can contribute to successful fire management.

Figure 2.10: Active fire map of the Mediterranean basin (11 June 2014) (FIRMS Web Fire Mapper, NASA) (retrieved on 11.06.14)

Table 2.3 and Table 2.4 show statistics on fire occurrence and resulting burnt area in several countries of the Mediterranean basin for 1980-2010. Among the countries Portugal has the highest amount of fire occurrences and France the highest resulting burnt area. Figure 2.11 and Figure 2.12 show the distribution of the fire occurrences and burnt area (ha) respectively among the countries of South Europe for 2010.

Table 2.3: Number of fires in South Europe (1980-2010) (JRC 2011)

Number of fires	Portugal	Spain	France	Italy	Greece	Total
2010	22,026	11,475	3,900	4,884	1,052	43,584
% of total(1980-2010)	37 %	30 %	10 %	20 %	3 %	100 %
Average 1980-1989	7,381	9,515	4,910	11,575	1,264	34,645
Average 1990-1999	22,250	18,152	5,538	11,164	1,748	58,851
Average 2000-2010	24,684	17,736	4,360	7,043	1,636	55,458
Average 1980-2010	18,317	15,218	4,917	9,834	1,552	49,838
Total (1980-2010)	567,831	471,760	152,431	304,861	48,110	1,544,993

Table 2.4: Burnt area (ha) in South Europe (1980-2010) (JRC 2011)

Burnt areas (ha)	Portugal	Spain	France	Italy	Greece	Total
2010	133,090	54,770	10,300	46,537	8,967	253,664
% of total(1980-2010)	23 %	37 %	6 %	24 %	10 %	100 %
Average 1980-1989	73,484	244,788	39,157	147,150	52,417	556,995
Average 1990-1999	102,203	161,319	22,735	118,573	44,108	448,938
Average 2000-2010	148,555	118,833	21,247	80,483	45,577	414,695
Average 1980-2010	109,386	173,169	27,504	114,276	47,309	471,644
Total (1980-2010)	3,390,976	5,386,227	852,632	3,542,542	1,466,591	14,620,968

Fire occurrences in South Europe (2010)
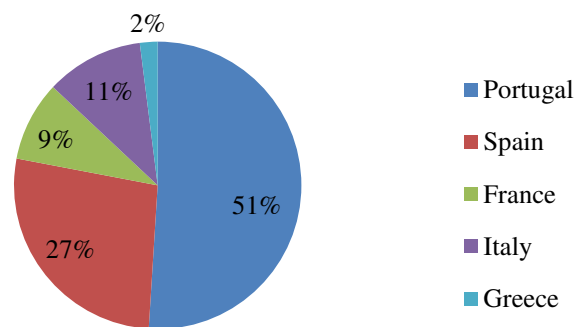
Figure 2.11: Fire occurrences (%) in South Europe (2010) (JRC 2011)

Burnt area in South Europe (2010)
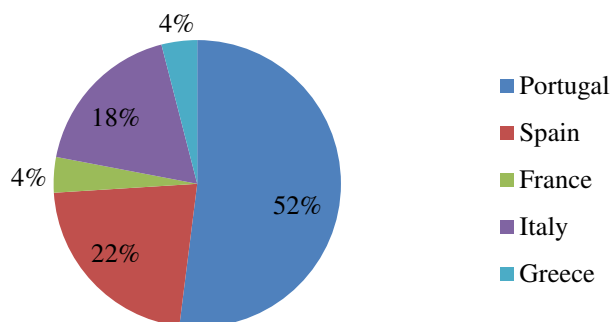
Figure 2.12: Burnt area (%) in South Europe (2010) (JRC 2011)

2.6   Summary

Chapter 2 introduces the reader into the definition of fire risk, the phenomenon of fire, the Canadian Fire Weather Index System, the factors influencing damages and the fires in the Mediterranean basin. The fire risk assessment matrix (Section 2.1) shows a simple case of risk calculation, as a product of scores between the probability of hazard and the consequences. Combustion is closely related to what in common is understood by fire. Combustion is an oxidation process that produces among others energy. Combustion takes place in three stages: preheating, gaseous and smoldering. In the gaseous stage active burning takes place. The fuels can be categorized with their moisture timelag classes, which depends on their size and the depth of the organic layer where they are. Fire types can be classified based on the vegetation they burn. Ground fires burn the ground fuel. Surface fires burn litter and woody fuels of the surface. Passive crown fires burn on the surface and individual trees. Active crown fires burn in the canopies together with surface fires. Independent crown fires burn only in the canopies. As a rule of thumb, crown fires are more destructive than surface fires. Basic fire characteristics are the flame length, the fire intensity and fire spread.

   In Europe, daily fire danger evaluation is currently done by the Joint Research Center of the European Union with the Canadian Forest Fire Weather Index System (CFFWIS). CFFWIS rates how weather conditions influence fuel moisture and initial spread. The system consists of six components, three fuel moisture codes and three fire behavior indices. Its final product is the Fire Weather Index, which represents the intensity of a spreading fire as energy output rate per length of fire front. However, this instrument takes into account only weather parameters and neglects other influencing factors, such as population, land cover types or topography. The inclusion of additional influencing parameters would model more accurately the complexity of the fire occurrence and fire behavior phenomenon. The main factors influencing the resulting house losses are the exposure of the items to fire effects, the item flammability and the suppression effectiveness. Timber loss is influenced by the amount of inflammable material on the forest floor, topography and forest density. Mediterranean climate type regions such as the Mediterranean basin are affected every year by wildfires. The main characteristic of these areas are the wet mild winters and the long summer droughts accompanied by strong winds. Shrubland is the dominant vegetation type, which re-sprouts after fire. The Mediterranean basin has a mosaic shaped landscape, in which fires result in relatively small burnt areas due to its high fragmentation. Fire management measures include fuel reduction, fire breaks, prescribed burning and fire suppression. Although fire preventing measures could be less expensive and reduce fire risk, most efforts focus on fire suppression and less on measures such as fuel reduction, monitoring and prescribed burning.

3 Modelling methods

The research on wildfire risk addresses the questions on when, where and why wildfires are triggered and how they spread and which are their consequences. Understanding of the interrelations among biotic and abiotic factors for the modelling of these mechanisms, the employment of various data from different sources and the need for the visualization of the results are all reasons for which multidisciplinary approaches are needed for modelling fire risk. The interdisciplinary approach to natural hazard risk modelling can be supported efficiently by Bayesian networks (BN). Based on acyclic graphs, BN enable to model the probabilistic dependence among a large number of variables influencing the risk. The causalities expressed by the arcs between the variables make BN not only convenient for graphical communication of the interrelations between the influencing factors (qualitative part), but also include, through conditional probability tables, a quantitative probabilistic model (Jensen and Nielsen 2007). In other words, the graphical representation of the dependence structure among stochastic variables makes it easy to understand intuitively and facilitates the consistent modelling of complex problems involving many variables. For these reasons, BN are increasingly applied for risk assessment of natural hazards, e.g. for rock-fall hazards (Straub 2005), avalanches (Grêt-Regamey and Straub 2006), tsunamis (Blaser *et al.* 2009) and earthquakes (Bayraktarli *et al.* 2005;Bensi 2010;Kuehn *et al.* 2011) and wildfires (Dlamini 2009).

3.1 Modelling with Bayesian Networks

Bayesian Networks (BN) are directed acyclic graphs and consist of nodes, arcs and probability tables attached to the nodes (Jensen and Nielsen 2007). In a discrete BN considered here, each node represents a discrete random variable, whose sample space consists of a finite set of mutually exclusive states. The arcs describe the assumed dependence structure among the random variables.

A conditional probability table (CPT) is attached to each of the nodes, defining the probability distribution of the variable conditional on its parents. If we consider a BN with discrete random variables $\mathbf{X} = [X_1, \ldots, X_n]$, then the full (joint) probabilistic model of these variables is the joint Probability Mass Function (PMF), $p(\mathbf{x}) = p(x_1, \ldots, x_n)$, which can be specified with the help of the chain rule:

$$p(\mathbf{x}) = p(x_n|x_{n-1}, \ldots, x_1)p(x_{n-1}|x_{n-2}, \ldots, x_1) \ldots p(x_2|x_1)p(x_1) \tag{3.1}$$

By making use of the independence assumptions encoded in the graphical structure of the BN, this chain rule reduces to:

$$p(\mathbf{x}) = \prod_{i=1}^{n} p(x_i|pa(x_i)) \tag{3.2}$$

wherein $pa(x_i)$ are realizations of the parents of X_i. In words, the joint probability mass function (PMF) of all random variables in the BN is simply the product of the conditional PMFs of each individual random variable given its parents. Therefore, the graphical structure of the BN, together with the conditional PMFs $\Pr(x_i|pa(x_i))$, are sufficient for specifying the full (joint) probabilistic model of $\mathbf{X} = [X_1, \ldots, X_n]$. A simple BN with three nodes is shown in Figure 3.1. Based on Eq. 3.1 the joint PMF of the model is

$$p(\mathbf{x}) = p(x_3|x_2, x_1)p(x_2|x_1)p(x_1) \tag{3.3}$$

wherein $p(x_2|x_1)$ reduces to $p(x_2)$, since the variables X_2 and X_1 are d-separated, meaning that knowing the state of variable X_2 does not influence the probability of X_1 being in any of its states and vice versa. Therefore Eq. 3.3 reduces to:

$$p(\mathbf{x}) = p(x_3|x_2, x_1)p(x_2)p(x_1) \tag{3.4}$$

which corresponds to Eq. 3.2.

Inference in the BN model is performed through updating. When one or several variables are observed or fixed, this information (evidence $\mathbf{e}$) is propagated through the network and the joint prior probability of all nodes is updated to its posterior. The posterior joint probability of a set of variables $\mathbf{y}$ in the network given the evidence $\mathbf{e}$ is:

$$p(\mathbf{y}|\mathbf{e}) = \frac{p(\mathbf{y}, \mathbf{e})}{p(\mathbf{e})} \tag{3.5}$$

In the example of Figure 3.1, when evidence is given on variable X_2 the joint posterior probability of all nodes is:

$$p(\mathbf{x}|X_2 = i) = \frac{p(\mathbf{x}, X_2 = i)}{p(X_2 = i)} \tag{3.6}$$

which becomes:

$$p(\mathbf{x}|X_2 = i) = \frac{p(X_2 = i|\mathbf{x})p(\mathbf{x})}{p(X_2 = i)} \tag{3.7}$$

with respect to Eq. 3.4:

$$p(\mathbf{x}|X_2 = i) = \frac{p(X_2 = i|x_1, x_3)p(x_3|x_2, x_1)p(x_2)p(x_1)}{p(X_2 = i)} \tag{3.8}$$

and since X_1 and X_2 are d-separated:

$$p(\mathbf{x}|X_2 = i) = \frac{p(X_2 = i|x_3)p(x_3|x_2, x_1)p(x_2)p(x_1)}{p(X_2 = i)} \tag{3.9}$$

finally:

$$p(\mathbf{x}|X_2 = i) = \frac{p(X_2 = i|x_3)p(x_3|x_2, x_1)p(x_2)p(x_1)}{p(X_2 = i|x_3)p(x_3) + p(X_2 = i|x_1)p(x_1)} \tag{3.10}$$
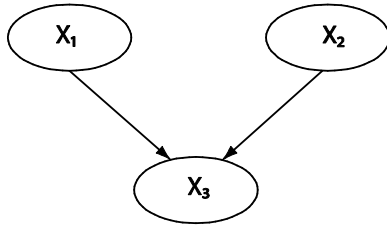
Figure 3.1: A simple Bayesian Network. X_1 and X_2 are the parents of X_3, and X_3 is the child of X_1 and X_2.

In the context of wildfire risk assessment, the advantage of the BN is not its computational effectiveness but that it facilitates the combination of information and models from various sources in a single model. This means, that nodes with different data sources (e.g. slope from a Digital Elevation Model, precipitation observations from a weather station, population density from census data, street density from a street map) and additional expert knowledge (e.g. home roof made of wood ignites easier than one out of roof tiles) can be all incorporated in the same model.

Three BN are constructed in this thesis to model fire risk. The first model describes fire occurrence, the second fire size and the third fire consequences. The models are described in detail in Chapter 5 – Chapter 7. The fire occurrence model is shown in Figure 3.2. The variables *FWI, Land cover, population density* and *street density* are the parent nodes of the variable *Occurrence rate*, and some (e.g. FWI) have causal influence on the *Occurrence rate*. The variable *Occurrence rate* is the child node of these variables. *Fire occurrence* is the child variable of the node *Occurrence rate*. In BN the arcs can express causality, thus the direction of the arc can show causal direction but this is not necessary. Although it is generally advisable to model causality in the BN among others for better communication of the model, it is not strictly necessary that the arcs of the model follow a causal interpretation (Kjaerulff and Madsen 2013). Later on, in Chapter 6, this becomes obvious with the interconnections between non-observable variables and the resulting burnt area.
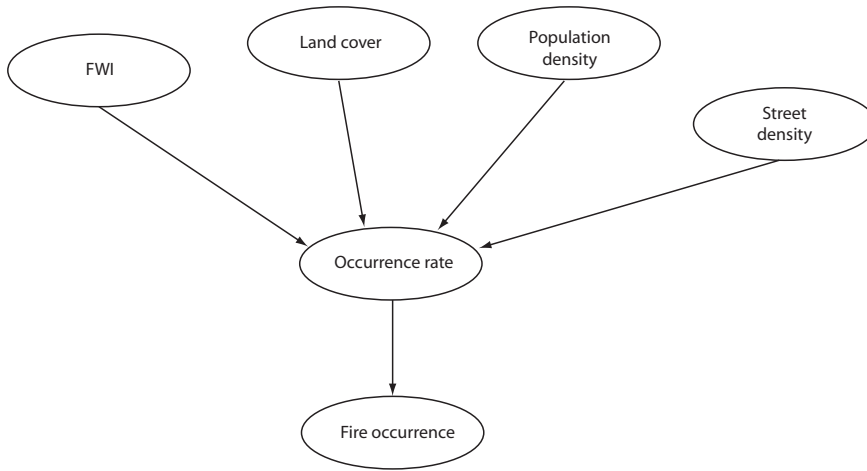
Figure 3.2: Bayesian Network modeling fire occurrences

There can be three types of connections between the nodes in a BN: serial, diverging and converging connection (Kjaerulff and Madsen 2013). The type of connection influences the flow of information in the BN. In a serial connection ($X \rightarrow Y \rightarrow Z$), evidence on X will affect the belief about the state of Z and vice versa, unless the state of Y is known. In a diverging connection ($X \leftarrow Y \rightarrow Z$), evidence on X will affect the belief about the state of Z and vice versa, unless the state of Y is known. In a converging connection ($X \rightarrow Y \leftarrow Z$), information may only be transmitted, when the state of Y is known.

In the example of Figure 3.2, the variables *FWI, Land cover, Population density* and *Street density* have a converging connection to the variable *Occurrence rate*. The variables expressing the influence of weather conditions, land use type and human presence were chosen to account for easily understandable proxies, for which data are readily available. Later on in this thesis, this scheme is used for different case studies in the Mediterranean - all three with similar fire occurrence rate, although influencing factors usually vary geographically. This assumption serves this study's aim to present a methodology applicable on similar areas without the need for major readjustment.

Each of these factors has a serial connection to the variable *Fire occurrence*. This means that evidence on one of the variables *FWI, Land cover, Population density* and *Street density* will not affect the belief about the state of the others, unless evidence is given on *Occurrence rate*. When evidence is given on the variable *Occurrence rate*, then no evidence can be transmitted from the variables *FWI, Land cover, Population density* and *Street density* to the variable Fire occurrence. The parent nodes *FWI*, *Land cover*, *Population density* and *Street density* are thus independent from the child variable *Fire occurrence* (i.e. they are d-separated). The parent nodes are then dependent to each other (i.e. d-connected), meaning that information may be transmitted, if evidence is given to one of it to the other parents.

If the parent nodes have each two possible states, then for the node *Occurrence rate* we need to specify $2^4 = 16$ conditional probability distributions, one for each combination of possible states of the four parent variables. The probability distributions appear in the conditional probability table attached to the node *Occurrence rate*. Assuming the following probability tables:

FWI (States)	Pr (State)
high	0.8
low	0.2

Land cover (States)	Pr (State)
urban	0.6
rural	0.4

Population density [People/km²] (States)	Pr (States)
0-100	0.9
100-1000	0.1

Street density [km/km²] (States)	Pr (States)
0-5	0.7
5-15	0.3

Here, the states of the variables and the attached probabilities are fictional and serve the demonstration of the application of Total Probability Theorem on the proposed BN structure. When such a model is applied on case study areas, the states of continuous variables such as FWI or population/street density can be defined by using appropriate discretization methods (e.g. Zwirglmaier *et al.* 2013).

The (half) conditional probability table of the node *Occurrence rate* can be as follows:

	FWI: high								*FWI*: low
	Land cover: urban				*Land cover*: rural				…
	Pop: 0-100		*Pop*: 100-1000		*Pop*: 0-100		*Pop*: 100-1000		…
Occur. rate	*Street*: 0-5	*Street*: 5-15	*Street*: 0-5	*Street*: 5-15	*Street*: 0-5	*Street*: 5-15	*Street*: 0-5	*Street*: 5-15	…
low	0.999	0.998	0.997	0.996	0.995	0.994	0.993	0.992	…
high	0.001	0.002	0.003	0.004	0.005	0.006	0.007	0.008	…

When evidence is given on *FWI*, *Land cover* and *Population density* then the probability of the *Occurrence rate* being in the first state (low) can be calculated as follows:

$$
\begin{aligned}
\Pr(Occ.rate &= \text{low}|FWI = \text{high}, Land\ cover = \text{urban}, Pop = 0-100) \\
&= \Pr(Occ.rate = \text{low}|FWI = \text{high}, Land\ cover = \text{urban}, Pop \\
&= 0-100, Street \\
&= 0-5) \cdot \Pr(Street = 0-5) + \Pr(Occ.rate = \text{low}|FWI \\
&= \text{high}, Land\ cover = \text{urban}, Pop = 0-100, Street \\
&= 5-15) \cdot \Pr(Street = 5-15)
\end{aligned}
\tag{3.11}
$$

$$
\begin{aligned}
\Pr(Occ.rate &= \text{low}|FWI = \text{high}, Land\ cover = \text{urban}, Pop = 0-100) \\
&= 0.999 \cdot 0.7 + 0.998 \cdot 0.3 = 0.9987
\end{aligned}
\tag{3.12}
$$

and given evidence only on *FWI* and *Land cover*,

$\text{Pr}(Occ.rate = \text{low}|FWI = \text{high}, Landcover = \text{urban})$
$$= 0.999 \cdot 0.7 \cdot 0.9 + 0.998 \cdot 0.3 \cdot 0.9 + 0.997 \cdot 0.7 \cdot 0.1 + 0.996 \cdot 0.3 \qquad (3.13)$$
$$\cdot \, 0.1 = 0.9985$$

Now, when fixing the value of *Occurrence rate* = low, then using Bayes' rule we can get the probability of a cause when its effect is observed (statistical inference), as

$\text{Pr}(FWI = high|Occ.rate = low)$
$$= \frac{\text{Pr}(Occ.rate = low|FWI = high) \cdot \text{Pr}(FWI = high)}{\text{Pr}(Occ.rate = low)} \qquad (3.14)$$

The above gave an insight into the concept of BN, the interconnections between the variables and the calculation of the prior and posterior joint probability distributions of the model. Efficient algorithms for performing these computations exist, which are implemented in software such as GeNIe (Decision Systems Laboratory 2013) or Hugin (HUGIN EXPERT 2012).

3.1.1   EM algorithm

Constructing a BN model is done, first by defining the structure of the directed acyclic graph and then populating the CPTs of the nodes. When the BN model is structured based on expert knowledge, it is possible to populate the conditional probability tables of the variables (parameter estimation) based on observations. The process is straightforward when all variables are observed, as this is achieved as a result of frequency counting.

In case of missing values, parameter estimation can be performed with the Expectation-Maximization (EM) algorithm (Kjaerulff and Madsen 2013). Thus, when one of the variables is a hidden variable, meaning there are no data for the parameter estimation (i.e. variable is non observable), then parameter estimation can be performed by the EM algorithm. This can also be the case, when intermediate non observable variables are included in the modeling, with the aim of reducing the number of parameters of other variables required to specify, or so that modeled causalities can be easier understood and communicated (Chapter 6).

The EM algorithm is performed by iterating two steps; the expectation E step and the maximization M step. In the E step, the expected values of the parameters are computed. In the M step, the parameter likelihood is maximized, using the expected values as if they were observed values. The iteration is repeated until a criterion is fulfilled. The criterion can be when the difference of two consecutive iterations is less than or equal to the numerical value of a log-likelihood threshold times the log-likelihood. Thus, when the relative difference between the log-likelihood for two successive iterations becomes less than a tolerance, which must be a positive number. Alternatively, an upper limit of the number of iterations can be set.

For a BN with x the observed values, Z the hidden variable and θ the parameters of the model, the ith iteration of the EM algorithm is (Russell and Norvig 2003),

$$\theta^{(i)} = \text{argmax}_\theta \sum_z p\big(Z = z|\text{x}, \theta^{(i-1)}\big)\ln L(\theta|\text{x}, Z = z) \qquad (3.15)$$

The E step corresponds to the summation, which is the expectation of the log likelihood of the completed data with respect to the posterior over the hidden variables given the data $p(Z = z|x, \theta^{(i-1)})$. The M step is the maximization of this expected log likelihood.

3.2 Coupling of Bayesian Networks with GIS

For BN that involve geographic features, spatial information can be used to define the conditional probability tables of the nodes, or the result of BN can be then spatially mapped. Georeferenced spatial information is often managed in Geographic Information Systems (GIS). Coupling of the BN with the GIS can facilitate the parameter learning and the mapping process. Thus once coupled, the GIS can inform the BN and so can the BN inform the GIS (Johnson *et al.* 2012).

In published literature there are four types of coupling documented (Figure 3.3). GIS as input in the BN (a), GIS as input in the BN and BN result as input in the GIS (b), complex interactions between BN and GIS (c) and BN and GIS within a larger framework (d). In the first type (a) the GIS layers are used as inputs for some BN nodes. In the second type (b) GIS layers are used as inputs for some BN nodes and the spatially referenced output of the BN is visualized in the GIS. In the third type (c), the integration approach uses BNs to combine informative layers from the GIS for each pixel/area to account for uncertainty. In the fourth type (d), BN and GIS model different factors in a larger descriptive system.
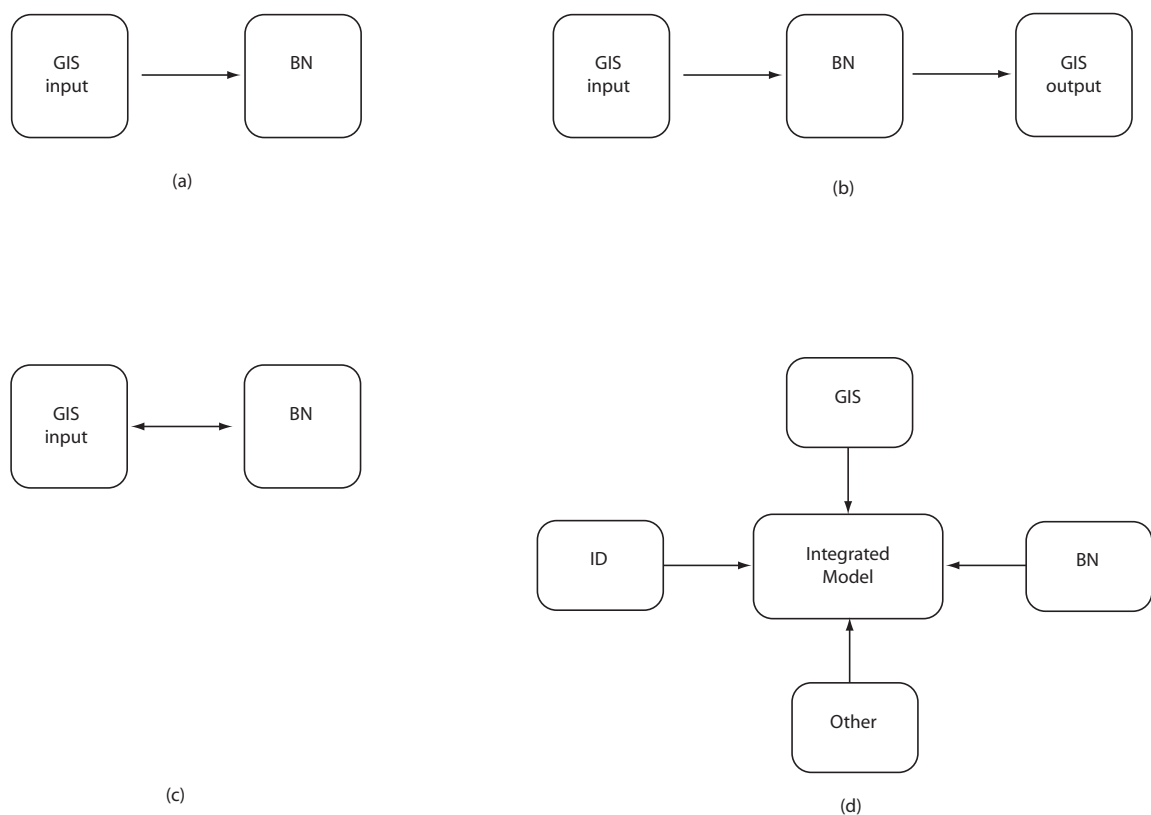
Figure 3.3: Types of BN and GIS coupling (Johnson *et al.* 2012)

In this thesis the coupling resembles the second type (b). It is a loose coupling between the systems , where the two components BN and GIS are used together but the modeller has to interact with both models (Scherb 2014) (Figure 3.4).
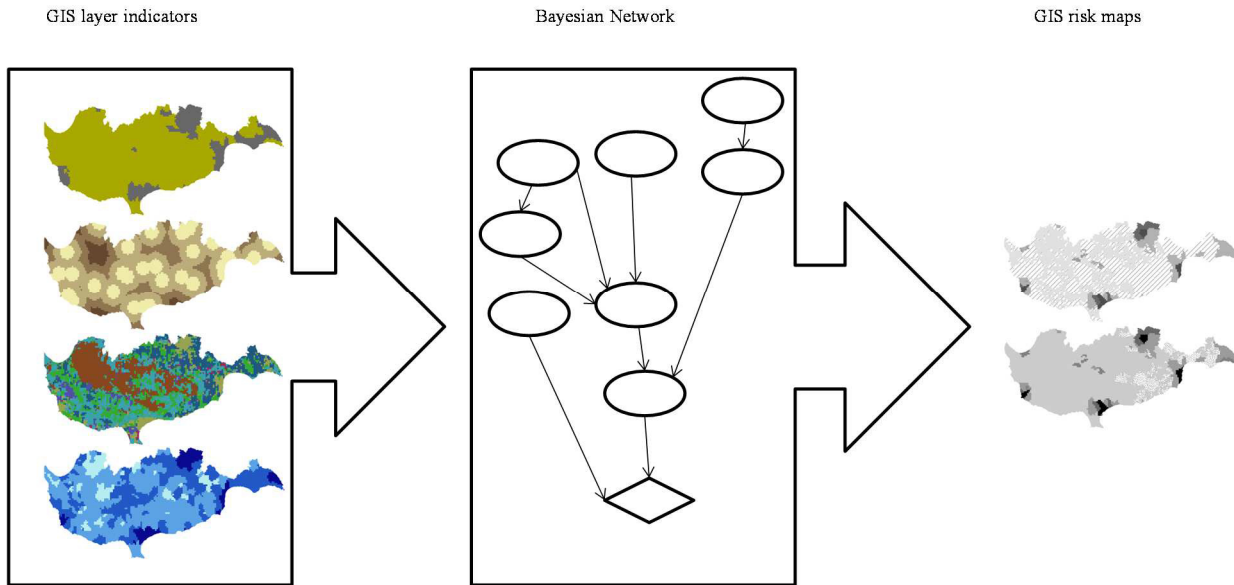
Figure 3.4: Loose coupling between GIS and Bayesian network

The parameters of the BN model are trained with information managed in a GIS database (Figure 3.5). Thus, the conditional probability tables (CPT) of the random variables are learned from the attribute tables of the GIS layers. After the learning process, the BN model can be applied to new spatial-temporal datasets for prediction, or model evaluation purpose. The new dataset is initiated as evidence on the parentless BN nodes and the target nodes are updated via inference based on the trained CPTs as explained in Section 3.1. The output of these calculations is the probability of fire occurrence, of resulting burnt area, or of fire risk. The evidence propagation is conducted as batch propagation within the BN software shell.
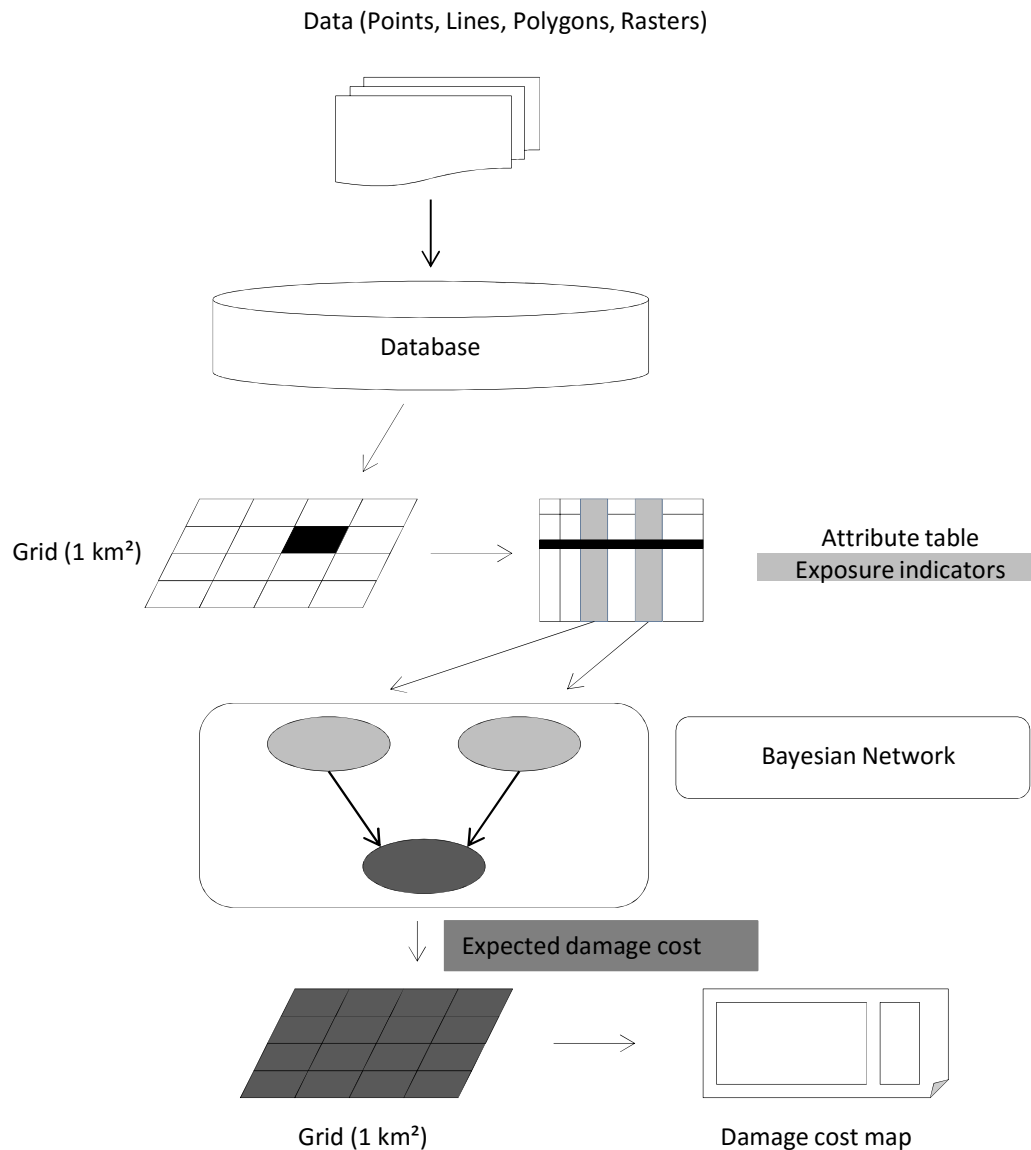
Figure 3.5: Batch propagation from dataset from and result input in the Geodatabase

3.3   Poisson regression

The task of probabilistic prediction, often breaks down to the task, in which a set of observations of random variables is available and the aim is to predict one of the random variables, while knowing the value of the others. For solving this task, most studies operate regression analysis.

Regression is a parametric method aiming to describe the functional relationship between dependent variables and an independent variable (McKillup and Dyar 2010). Regression gives an equation for a line or surface, which is the best fit through a set of data points.

The problem of fire occurrence prediction, with the observable influencing variables and the lack of physical models, is often approached with regression analysis. Different types of regression

have been widely used in the literature to model fire occurrences, including Poisson models (e.g. Cunningham and Martell 1973;Mandallaz and Ye 1997;Syphard *et al.* 2008), logistic regression (e.g. de Vasconcelos *et al.* 2001;Preisler *et al.* 2004;Kalabokidis *et al.* 2007;Syphard *et al.* 2008;Chuvieco 2009;Arndt *et al.* 2013) and multiple regression (e.g. Sebastián-López *et al.* 2008;Oliveira *et al.* 2012), to name only some.

Here, fire occurrence events are modeled as a Poisson process and the occurrence modeling is made with Poisson regression. Poisson regression assumes that the dependent variable (i.e. fire occurrence) follows the Poisson distribution and that the logarithm of its expected value (i.e. the fire occurrence rate) can be modeled as linear function of independent variables. In these models temporal and spatial discretization is needed. This means that the fires occur in a certain time and space step. The fire occurrence rate expresses the number of events per time and space step.

Poisson distribution assumes independence among events for given rate. Therefore here it is assumed that fires occur randomly in space and time. The conditional probability of observing n events given λ is thus

$$\Pr(N = n | \lambda) = \frac{(\lambda\alpha)^n}{n!} \exp(-\lambda\alpha), \qquad n = 0,1,2,\dots \tag{3.16}$$

wherein λ is the mean occurrence rate, α is the area and $N \in 0,1,2,\dots$ is the number of events. Observations of N are used to estimate λ based on Eq. (3.16).

The response variable is the number of events N, which – following the previous – is a random variable described by the Poisson distribution with rate λ. This motivates the use of the generalized linear model of the Poisson regression for estimating λ (Mandallaz and Ye 1997). The rate λ is related to the explanatory variables $\mathbf{x} = [x_1; \dots; x_k]$ by means of the link function

$$\log(\lambda) = \beta_0 + \beta_1 x_1 + \beta_2 x_2 + \cdots + \beta_k x_k = \mathbf{x}^T \boldsymbol{\beta}. \tag{3.17}$$

$\boldsymbol{\beta} = [\beta_0, \dots, \beta_k]$ is the vector of regression coefficients. This link function ensures that λ is a non-negative real number. The mean occurrence rate is then given as

$$\lambda = \exp(\mathbf{x}^T \boldsymbol{\beta}) = \exp(\beta_0) \exp(\beta_1 x_1) \exp(\beta_2 x_2) \dots \exp(\beta_k x_k). \tag{3.18}$$

Changing one of the explanatory variables from x_i to $x_i + \Delta x$, while keeping all other fixed, leads to a relative change in λ of

$$\begin{aligned} \left(\frac{\Delta\lambda}{\lambda}\right)_i &= \frac{\exp(\beta_0)\exp(\beta_1 x_1)\dots\exp(\beta_i x_i + \Delta x)\dots\exp(\beta_k x_k) - \exp(\mathbf{x}^T\boldsymbol{\beta})}{\exp(\mathbf{x}^T\boldsymbol{\beta})} \\ &= \exp(\beta_i \Delta x) - 1. \end{aligned} \tag{3.19}$$

In the numerical investigations, several models are examined, which differ in the selection of the explanatory variables $\mathbf{x}$. These are selected from a set of variables describing land cover, human population density, road density and components of the CFFWIS.

3.3.1 Maximum likelihood estimation

In order to determine the parameters of a statistical model Maximum likelihood estimation (MLE) can be used. Here it is applied to determine the coefficients $\boldsymbol{\beta}$. For the Poisson regression model, the likelihood function follows from Eq. (3.15) as

$$
\begin{aligned}
L(\boldsymbol{\beta}|\mathbf{n}) &= \prod_{i=1}^{m_d}\prod_{j=1}^{m_a} \Pr\left(N_{ij} = n_{ij}\big|\lambda(\boldsymbol{\beta}, \mathbf{x}_{ij})\right) \\
&= \prod_{i=1}^{m_d}\prod_{j=1}^{m_a} \frac{\left(\lambda(\boldsymbol{\beta}, \mathbf{x}_{ij})\right)^{n_{ij}}}{n_{ij}!} \exp\left(-\lambda(\boldsymbol{\beta}, \mathbf{x}_{ij})\right).
\end{aligned}
\tag{3.20}
$$

m_d is the number of days with observations and m_a is the number of spatial units with observations. n_{ij} is the number of fires observed on day i in area j; $\mathbf{x}_{ij}$ are the values of the explanatory variables on day i in area j.

The MLE is found as the value of $\boldsymbol{\beta}$ that maximizes $L(\boldsymbol{\beta}|\mathbf{n})$:

$$
\boldsymbol{\beta}_{MLE} = \operatorname{argmax} L(\boldsymbol{\beta}|\mathbf{n}). \tag{3.21}
$$

No analytical solution to this optimization problem exists. Numerical optimization must be applied. For this purpose, it is convenient to express the optimization problem in terms of the log-likelihood instead:

$$
\begin{aligned}
\boldsymbol{\beta}_{MLE} &= \operatorname{argmax} \ln L(\boldsymbol{\beta}|\mathbf{n}) \\
&= \sum_{i=1}^{m_d}\sum_{j=1}^{m_a} n_{ij}\ln\left(\lambda(\boldsymbol{\beta}, \mathbf{x}_{ij})\right) - \ln(n_{ij}!) - \lambda(\boldsymbol{\beta}, \mathbf{x}_{ij}).
\end{aligned}
\tag{3.22}
$$

In the numerical investigations, the simplex search method and the quasi-Newton method are used to solve Eq. (3.22), as implemented in the Matlab functions fminsearch and fminunc.

3.3.2 Diagnostics

In order to evaluate the resulting models different diagnostic methods are used; the Akaike Information Criterion, used to compare models of different complexity based on their likelihood and number of parameters and the receiver operating characteristic (ROC) curves, which evaluate graphically the predictive performance of the models.

3.3.2.1 Akaike Information Criterion

To compare different models, the Akaike Information Criterion (AIC) is employed (Akaike 1974). The AIC allows to compare models of different complexity. It is defined as

$$AIC = -2\ln L(\boldsymbol{\beta}_{MLE}|\mathbf{n}) + 2(k+1),\qquad(3.23)$$

where $\ln L(\boldsymbol{\beta}_{MLE}|\mathbf{n})$ is the maximum log-likelihood and $(k+1)$ is the number of coefficients β_i of the model. The first term in the AIC accounts for the likelihood of the model, the second term punishes the models with more parameters to avoid overfitting.

An additional comparison between models is performed with a verification data set $\mathbf{n}_V$, which is not used for estimating $\boldsymbol{\beta}_{MLE}$. The log-likelihood of $\boldsymbol{\beta}_{MLE}$ calculated with the verification data set $\mathbf{n}_V$, i.e. $\ln L(\boldsymbol{\beta}_{MLE}|\mathbf{n}_V)$, provides an indication of model prediction performance.

3.3.2.2 ROC curves

The receiver operating characteristic (ROC) curves provide an additional measurement of the prediction performance of the models with a binary outcome. In ROC curves it is examined how the model predicts real observations. The predictions vary between true positives (i.e. events that model predicted correctly), true negatives (i.e. non-occurrence model predicted correctly), false positives and false negatives (Table 3.**1**).

Table 3.1: Confusion matrix (contingency table) of a ROC curve

		True condition	
		Positive	Negative
Predicted condition	Positive	True Positive (TP)	False Positive (FP)
	Negative	False Negative (FN)	True Negative (TN)

Sensitivity (True positive rate) is the sum of the TPs divided by all occurred events and reflects the probability of detection. 1-specificity (False positive rate) is the FPs divided by the all non-occurring events and reflects the false alarms.

$$\text{Sensitivity} = \frac{\sum \text{TP}}{\sum \text{TP} + \text{FN}}\qquad(3.24)$$

$$1 - \text{specificity} = \frac{\sum \text{FP}}{\sum \text{FP} + \text{TN}}\qquad(3.25)$$

The percentage of true positives (sensitivity) as a function of the complement percentage false positives (1-specificity) is then plotted as a ROC curve (Marcot 2012). The area under a ROC curve (AUC values) describes the system's ability to predict correctly the occurrence of an event (Mason and Graham 2002). AUC values range [0,1]. 1 denotes no error and 0.5 denotes totally random models (Marcot 2012).

3.4   Weather data interpolation and CFFWIS calculation

As already mentioned in Section 2.3, the calculation of the components of the CFFWIS, which will be used to express the influence of weather on the fuel moisture, requires the input of daily values of weather parameters. In the applications, daily weather observations are taken from different local weather stations. These are then interpolated to the whole study area using Inverse Distance Weighting (IDW) (Shepard 1968). This deterministic interpolation method, which is widely used in meteorology due its relative simplicity, was chosen here because of the limited number of weather stations with available data for the case study areas. Other (stochastic) geostatistic interpolation methods, such as Kriging, might interpolate weather observations more accurately, since they take under account also the spatial correlation between the weather stations. Nevertheless, such methods require a minimum number of about 30 observations in order to give solid correlations in the variogram and therefore are not applied in this thesis. After the interpolation of daily weather parameters with IDW, daily values of the CFFWIS components are calculated for each location based on the interpolated values. The equations for the calculation of the six parameters of the CFFWIS can be found in Appendix I.

3.4.1   Inverse Distance Weighting

The Inverse Distance Weighting method is a two dimensional deterministic interpolation method and is based on the assumption that the smaller the distance to the points with given values, the higher their influence on the interpolated value. The values are therefore weighted according to the distance from their location to the location of the unknown value. If k_i, with $i = 1, ...,4$, the locations with known values $z(k_i)$ and k_0 the location to interpolate, then the interpolated value is given from Eq. (3.22) and Eq. (3.23) with r the influence of values close to the interpolated point.

$$\hat{z}(k_0) = \sum_{i=1}^{4} z(k_i) \frac{d_{io}^{-r}}{\sum_{i=1}^{4} d_{i0}^{-r}} \qquad (3.26)$$

$$d_{i0} = \sqrt{(x_i - x_0)^2 + (y_i - y_0)^2} \qquad (3.27)$$
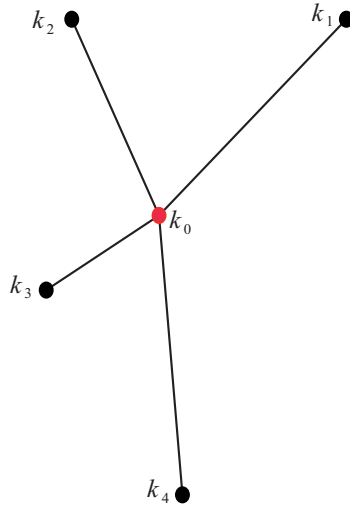
Figure 3.6: Inverse Distance Weighting method

Temperature is additionally adjusted to the altitude based on the normal lapse rate (0.65°C/100m) (Leemans and Cramer 1991) (Figure 3.**7**). At each weather station i, the equivalent temperature at sea level is computed from the measured noon temperature T_{WS} as $T_{0,i} = T_{WS} + 0.0065h_{WS}$, where $h_{WS} = $ altitude of the weather station in [m]. The IDW interpolation is performed using the $T_{0,i}$ values, resulting in a temperature value at sea level T_0. The daily noon value of temperature in the location P, T_P is then computed as $T_P = T_0 - 0.0065h_P$. Here, h_P is the altitude at the location P.
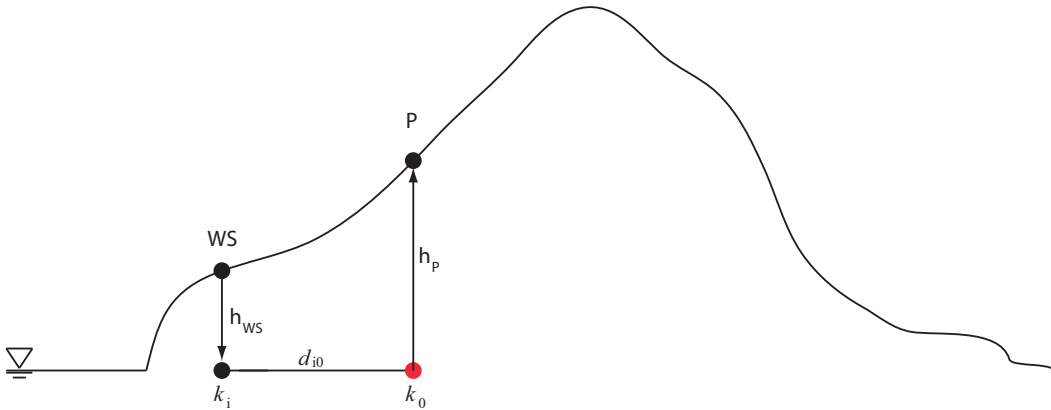
Figure 3.7: Temperature adjustment based on the normal lapse rate

After the weather observations are interpolated, the daily components of the CFFWIS are calculated for each cell of the study area based on the formulation given in Appendix 1. The starting values of the fuel moisture codes for the first day (Jan 1) are the ones proposed in (Canadian Forestry Service 1984), (Lawson and Armitage 2008) (FFMC=85, DMC=6, DC=15). The starting values were reset every year. The calculations were made in Python.

3.5   Summary

Chapter 3 gives an overview of all the methods used in this thesis to model fire risk. The reader is introduced to the concept of BN and to the interrelations between the random variables with the help of simple examples. BN are useful is modeling phenomena with complicated causalities and uncertainties in the values of the variables. In the case of missing values the parameter estimation of the model can be performed with the Expectation-Maximization algorithm. The prior distributions of the random variables of the network can be defined based on real data. In case of spatial or spatio-temporal data managed in a Geographic Information System (GIS), the BN and the GIS can be coupled, to facilitate model parameter learning and result mapping. Different types of BN-GIS coupling are described and focus is placed on the coupling type used in this thesis. Fire occurrence modelling is usually done with regression analysis of empirical data (e.g. Preisler *et al.* 2004;Syphard *et al.* 2008;Oliveira *et al.* 2012). Poisson regression and the parameter estimation method maximum likelihood estimation are here introduced and are both applied later in this thesis. The chapter gives also insight in the diagnostics used in this study, thus the Akaike Information Criterion and the ROC curves. The Akaike Information Criterion compares the resulting models according to their maximum log likelihood and "punishes" the models with the higher number of variables.Weather influence on fire risk is expressed in this thesis directly by weather observations and indirectly by fuel moisture indices. The latest are components of the CFFWIS. The specifics of the calculation of these components and the interpolation method Inverse Distance Weighting method are here described. The latter is used to interpolate the weather observations from the weather stations to the whole study area. The weather parameters wind speed, relative humidity, temperature and precipitation are interpolated according to the inverse distance weighting, where the closer the points to a weather station, the higher the influence of its measurements to the interpolated value. Temperature is also adapted to the elevation based on the normal lapse rate. The daily values of the parameters of the CFFWIS are then calculated from the noon interpolated weather values.

4 Study areas

In this chapter the study areas where the models are applied and tested are introduced. The collected data and their sources are also described. Three study areas (Rhodes, Cyprus and South France) are here presented to introduce the reader to the data that will be used in the applications in the next chapters and to give an insight to the variable selection made further in the thesis. Preliminary data analysis demonstrates the fire occurrence rate and the resulting burnt area in relation to influencing factors. All spatial data are edited and processed with ArcGIS 10. The data analysis presented here can be found also in Papakosta and Straub (2011), Papakosta and Straub (2013), Papakosta *et al.* (2013), Scherb and Öster (2013) and Papakosta and Straub (2015).

4.1 Rhodes

4.1.1 Description

The Greek Mediterranean island of Rhodes has been chosen as a study area, because it represents quite adequately the climate and the mixed land uses of fire-prone Mediterranean regions. Rhodes is located in the south eastern part of the Aegean Sea, its area is 1409 km² and in 2001 the number of permanent residents was 115.334 (Hellenic Statistical Authority). On the administrative level, the island is divided into 43 municipalities. The inner part of the island is mountainous with the highest elevation at 1215 m. The climate of Rhodes is a dry summer subtropical climate (Mediterranean) with wet winter and long dry summer periods and an annual mean temperature of around 22 °C. The natural vegetation consists of evergreen shrubs, genista, pine forests and mixed forests with cypresses. The main agricultural activities on the island are the cultivation of olives and vines. Wildfires are common on Rhodes; as an example wildfires occurring in September 2008 led to a burned area of 122 km² according to recordings of the Greek Fire Service.

4.1.2   Input data

Both spatial and temporal data are used. The elevation of the island is taken from the Advanced Spaceborne Thermal Emission and Reflection radiometer (ASTER) Global Digital Elevation Model (GDEM). ASTER GDEM is a project of the Ministry METI of Japan and NASA. The spatial resolution is 15 meters in the horizontal plane. Three GeoTIFF data sets cover the whole area of the island (ASTGTM_N35EO27, _N36EO27, _N35EO28).

To obtain information on land cover, the 2000 version of Corine Land Cover (CLC) is utilized (European Environment Agency). CLC provides consistent localized geographical information on the land cover of the 12 Member States of the European Community in a scale of 1:100.000. The CLC is the result of the combination of information from different sources, including satellite images, aerial photographs, topographic maps, thematic land cover maps and ground truth surveys (the minimum unit mapping was set at 25 ha (0.25 km²)) and is classified in 44 types. Out of these, only 25 are present on the island. A thematic map with the administrative boarders of municipalities of the island, provided by Agroland SA, is utilized. Demographic data on the population of each municipality in 2001 was obtained from the Hellenic Statistical Authority (Figure 4.1).
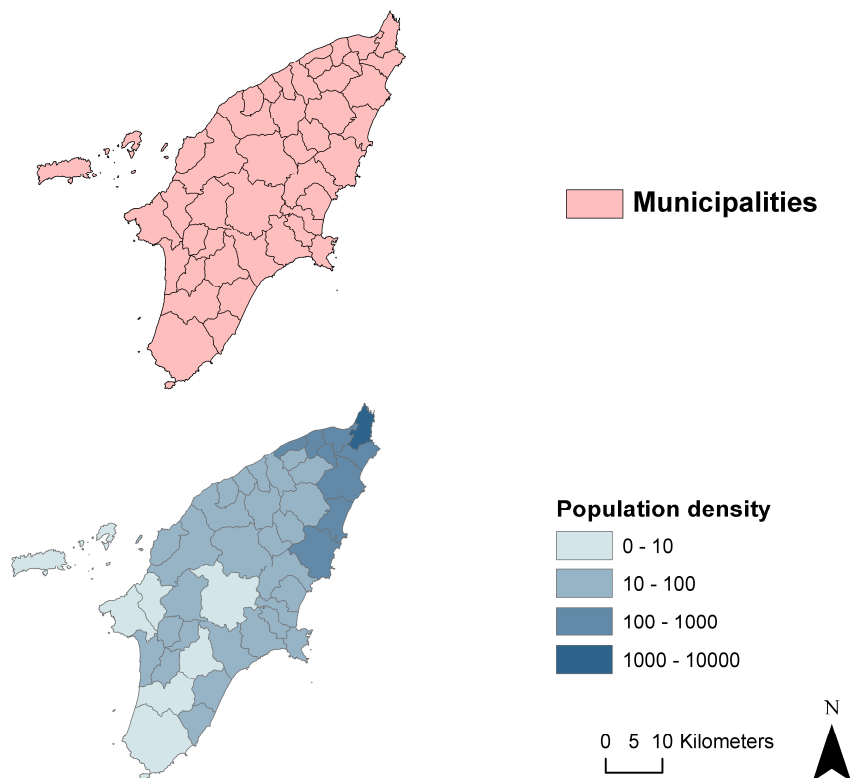
Figure 4.1: Administrative borders (Municipalities) and human population density [Nr. Residents/km²] on Rhodes

Historical data on the occurrences of fires during the period 2000-2009 were obtained by the statistical department of the Greek Fire Service. The data offered information on the date of fire occurrence and the municipality that it occurred. Data related to the mean elevation, land cover classes and area are then extracted for each of the 43 municipalities. Table 4.1 summarizes the data used and their sources.

For the calculation of the components of the CFFWIS, weather data on temperature, relative humidity, wind speed and precipitation for the years 2000-2009 were obtained from the German Weather Service (Deutscher Wetterdienst). The measurements were made at the Greek official weather station at the airport of Rhodes (36°24' N, 28°05' E, 11 m).

Table 4.1: Data types, resolution and sources for Rhodes

Data	Resolution		Source	Additional information
	spatial	temporal		
Digital Elevation Model (DEM)	15m x 15m		ASTER GDEM (Ministry METI Japan & NASA)	3 GeoTIFF data sets
Land cover	250m x 250m		Corine Land cover 2000 (European Environmental Agency)	44 land cover types 1:100,000 (version13)
Admin. borders	municipality		Agroland SA	
Population	municipality		Hellenic Statistical Authority	census 2001
Road network			Open Street Map	
Fire Events	municipality	Date 2000-2009	Greek Fire Service	
Temperature Wind speed Relative humidity Precipitation	Weather Station: Rhodes Airport	3-6hr/Daily 2000-2009 24hr Daily 2000-2009	Deutscher Wetterdienst (DWD)	

4.1.3 Preliminary data analysis

The lack of the exact location of past fire events, as well as the presence of only one weather station in the available data set, limits the preliminary data analysis applied on Rhodes study area to an introductory level. Here, only first analysis of the correlation between components of the CFFWIS (FFMC) and fire occurrences is shown.

Temperature, relative humidity and wind speed are recorded in 3-hour intervals. The daily values at noon are extracted and used as an input for the FFMC calculations. In the case of missing values of relative humidity and wind speed at noon, values from the previous measurement at 09:00 are utilized. In the case of a missing temperature value, the recorded value of the previous day at noon is taken. Since there is only one official weather station on the island, the weather variables at

other locations are inferred from the data obtained at this station. For temperature, the value in each municipality is estimated based on the normal lapse rate of temperature of 0.65°C/100m.

FFMC is found to have only slight influence on the occurrence rate, which is estimated as $8.35 \cdot 10^{-4}$ [Nr.Occurrences/day/km²] for FFMC values in the range of $0-40$ and $8.59 \cdot 10^{-4}$ [Nr. Occurrences/day/km²] for FFMC values in the range of $95-100$. To facilitate the interpretation of this result, Figure 4.2 shows calculated FFMC values for year 2000, together with daily precipitation and the observed number of fires. The FFMC values are generally high, and the only large changes occur during and after rainfall events.

Figure 4.3 shows histograms of FFMC values calculated for days with zero, one or two recorded wildfires. These three conditional histograms and the corresponding conditional means and standard deviations exhibit similar trends, i.e. the FFMC mean value is over 80 independently of fire occurrence. The distribution of FFMC is shifted to the right for Nr. fire occurrences = 0,1,2.
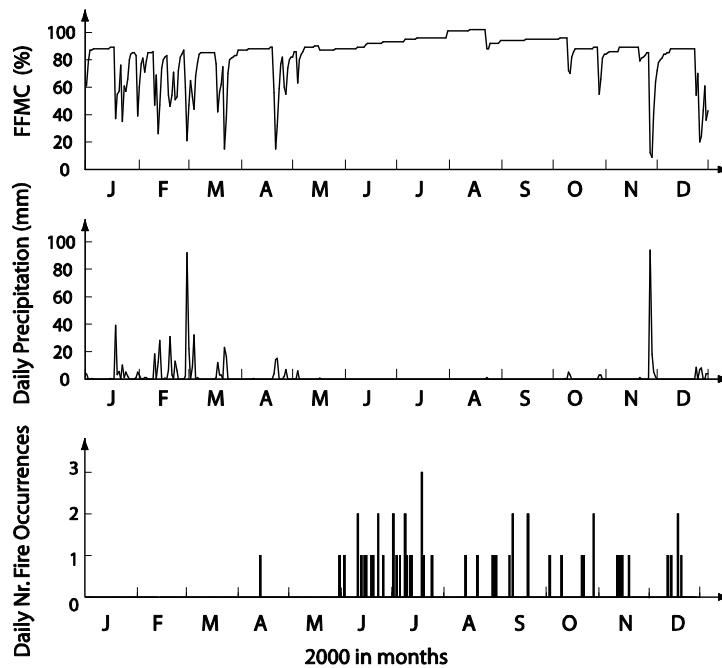
Figure 4.2: FFMC values at a representative municipality, together with observed precipitation at the weather station and total number of wildfire occurrences on Rhodes for year 2000
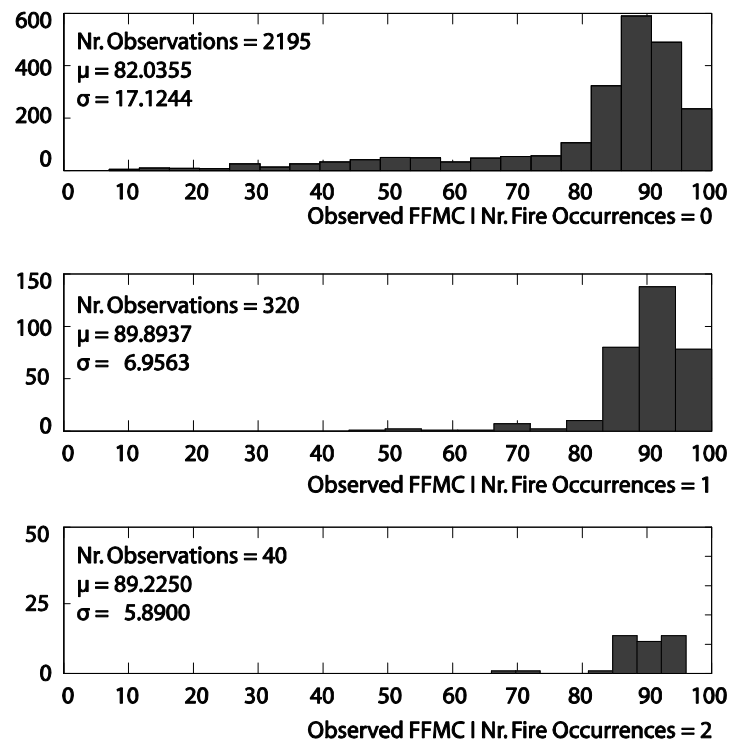
Figure 4.3: Histograms of FFMC for a representative municipality, conditional on the recorded number of fires occurring on Rhodes

4.2 Cyprus

4.2.1 Description

We employ data from the Republic of Cyprus, which is selected due to its representative Eastern Mediterranean climate (short cool winters followed by long hot and dry summers), vegetation and fire history. The maps and data analysis of this study area can be found in Papakosta and Straub (2015). The natural areas on the island are mainly covered by coniferous forests (e.g. *Pinus brutia*), whereas the permanent cultivated areas are dominated by vineyards. The highest peak of the study area is Olympus Mountain of the Troodos Massif (1952 m).

4.2.2 Input data

Figure 4.4a shows the digital elevation model (DEM) of the whole island of Cyprus (ASTER GDEM). The study area is indicated, and the 5 weather stations, whose data is used in the analysis, are marked. Fire data representing all fires suppressed by the state forest agency were provided by

the Department of Forests of Cyprus for the period 2006-2010. Fires of all sizes were recorded, with 10% of recorded fires being less than 0.01 ha.

Figure 4.4b presents the location of all recorded fires in the study area. The total number of recorded fires in this study is 616, which corresponds to a mean annual number of fire occurrences of 123. The mean burnt area [km²] of the fires is 0.17 km² and the standard deviation is 0.92 km². The maximum burnt area recorded in 2006-2010 is 13.62 km² (Figure 4.6b).

Both spatial and temporal data are used. Table 4.2 gives an overview of the utilized data, their spatial and temporal resolution and their sources.

Both spatial and temporal data are managed in a geodatabase. All the spatial and temporal data were attached to a 1km² grid covering the whole area of the case study (6447 grid cells). The population density in each grid cell (people/km²) is determined from the municipality census data (Figure 4.5a). The road density (km/km²) is computed from the actual length of roads in each cell (Figure 4.5b). The land cover type assigned to each cell is the one covering the largest area within that cell (Figure 4.5c). According to Corine land cover (2006), forests and semi-natural areas together with agricultural areas cover the largest part of the study area. The land cover type pastures is included into the Urban-Wetland land covers, since it covered only a small area of the case study (7 km²). The land cover is also classified in urban/rural (Figure 4.7a) based on the population density. This classification influences the types house type, as it will be shown later in Chapter 7. The house type is a portfolio of houses present in km². The houses are divided to single houses, row houses and apartments. The houses are also characterized by the construction type, i.e. the construction materials of the houses. This is also a portfolio of construction types (%) in each km².

4.2.3   Preliminary data analysis

Daily weather observations (extracted from 3hr and 6hr observations) are interpolated using Inverse Distance Weighting (IDW). Daily values of the CFFWIS components are then calculated for each grid cell based on the interpolated values. Temperature is additionally adjusted to the altitude based on the normal lapse rate (0.65°C/100m).

Preliminary analyses of the time series 2006-2010 are shown in Figure 4.9 - Figure 4.16. As there are 616 recorded fires, the average occurrence rate of fires in this period is

$$\frac{\text{Nr. Fires}}{\text{day} \cdot \text{km}^2} = \frac{616}{[(365 \cdot 5) + 2] \cdot 6078} = 5.5 \cdot 10^{-5} \frac{\text{Fires}}{\text{day} \cdot \text{km}^2}.$$

Figure 4.8 displays daily calculated FWI values, daily precipitation and temperature observed at Paphos weather station and the total number of fire occurrences in the entire study area in 2006.

(a)

(b)
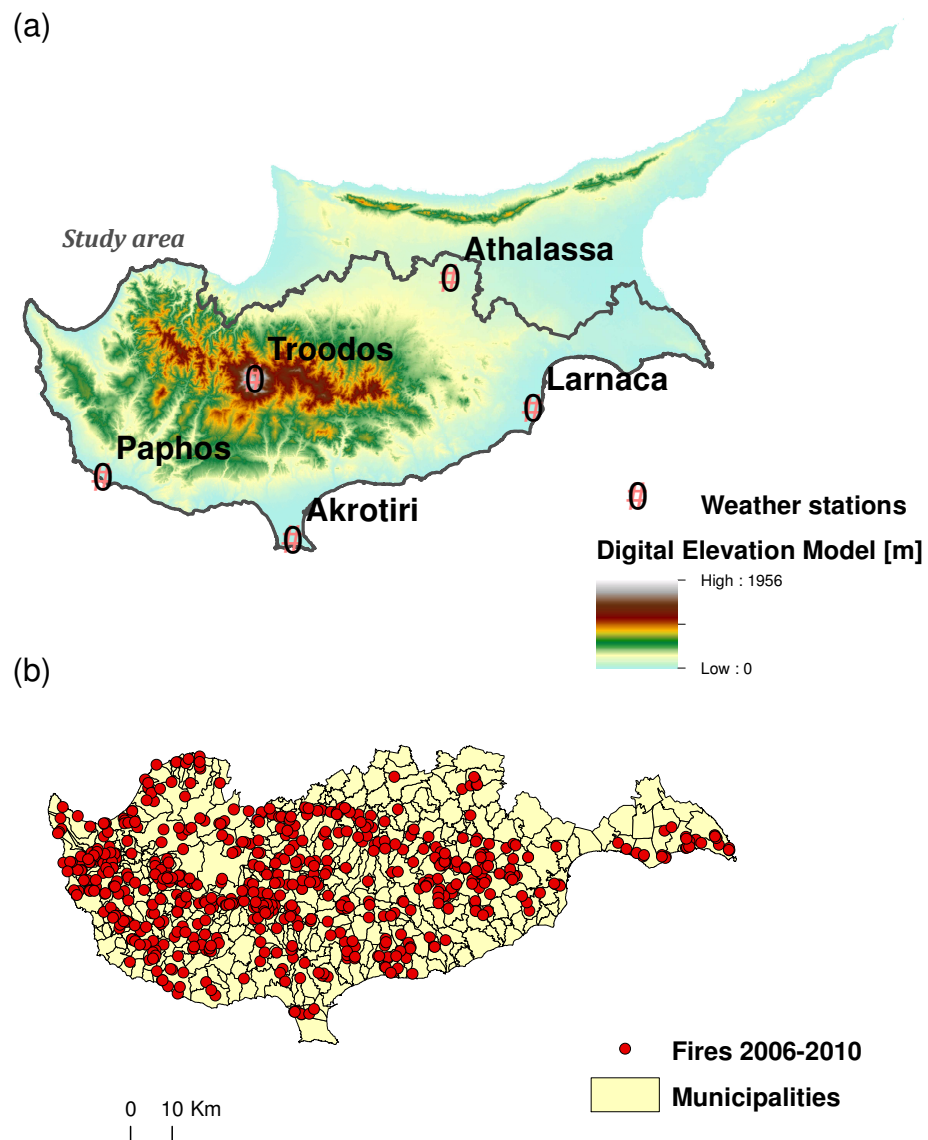
Figure 4.4: (a) ASTER Digital Elevation Model (m) showing the highest peak of the Troodos Massif in white (1956 m) and the included five weather stations on the Republic of Cyprus (included in grey perimeter). (b) Municipality borders of the area of the numerical investigations and registered fire events during 2006-2010 (616 events)

Table 4.2: Data types, resolution and sources for Cyprus

Data	Resolution		Source	Additional information
	spatial	temporal		
Digital Elevation Model (DEM)	15m x 15m		ASTER GDEM (Ministry METI Japan & NASA)	Six GeoTIFF data sets
Land cover	250m x 250m		Corine Land cover 2006 (European Environmental Agency)	44 land cover types 1:100,000 (version13)
Admin. borders	municipality		Statistical Service of Cyprus	
Population	municipality		Statistical Service of Cyprus	census 2011
Road network			Open Street Map	
Fire Events	X,Y burnt area	Date 2006-2010	Department of Forests of Cyprus	
Temperature Wind Speed Relative Humidity Precipitation		3-6hr/ Daily 2006-2010 24hr Daily 2006-2010	Deutscher Wetterdienst (DWD) Cyprus Meteorological Service	Weather Stations: Athalassa, Paphos Airport, Akrotiri RAF, Larnaca Airport, Troodos Square
Fire Stations	address		Fire department Cyprus	29 stations
Houses	municipality		Statistical Service of Cyprus	
House Stock			Statistical Service of Cyprus	single houses row houses apartments % percentage in 1km²
Construction type			Statistical Service of Cyprus	traditional house (stone/mud wall) single brick wall/flat roof house insulated brick/inclined roof % percentage in 1km²
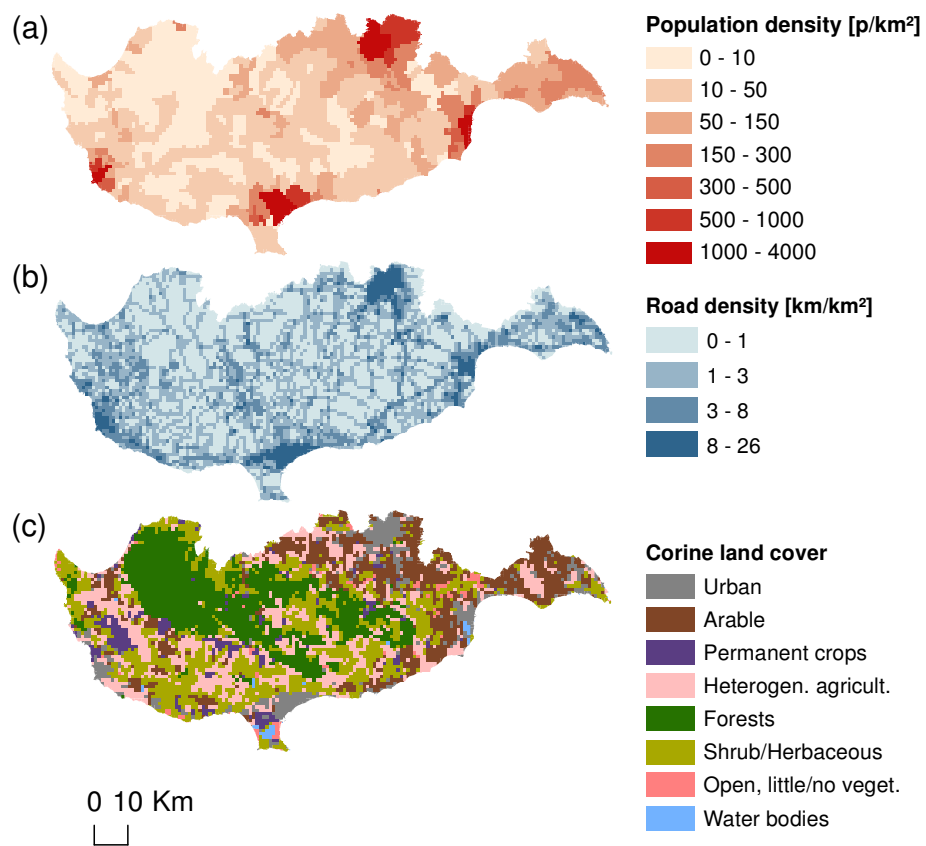
Figure 4.5: Spatial variables of the study area Cyprus: (a) Population density [Nr. people/km²]; (b) Road density [km/km²]; (c) Land cover types
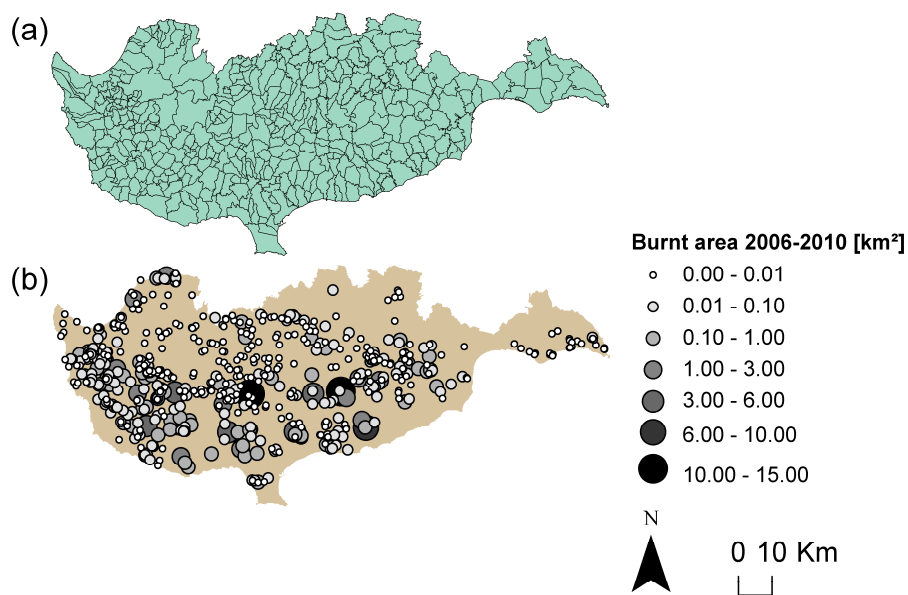
Figure 4.6: (a) Municipalities and (b) Burnt areas [km²] 2006-2010 on Cyprus
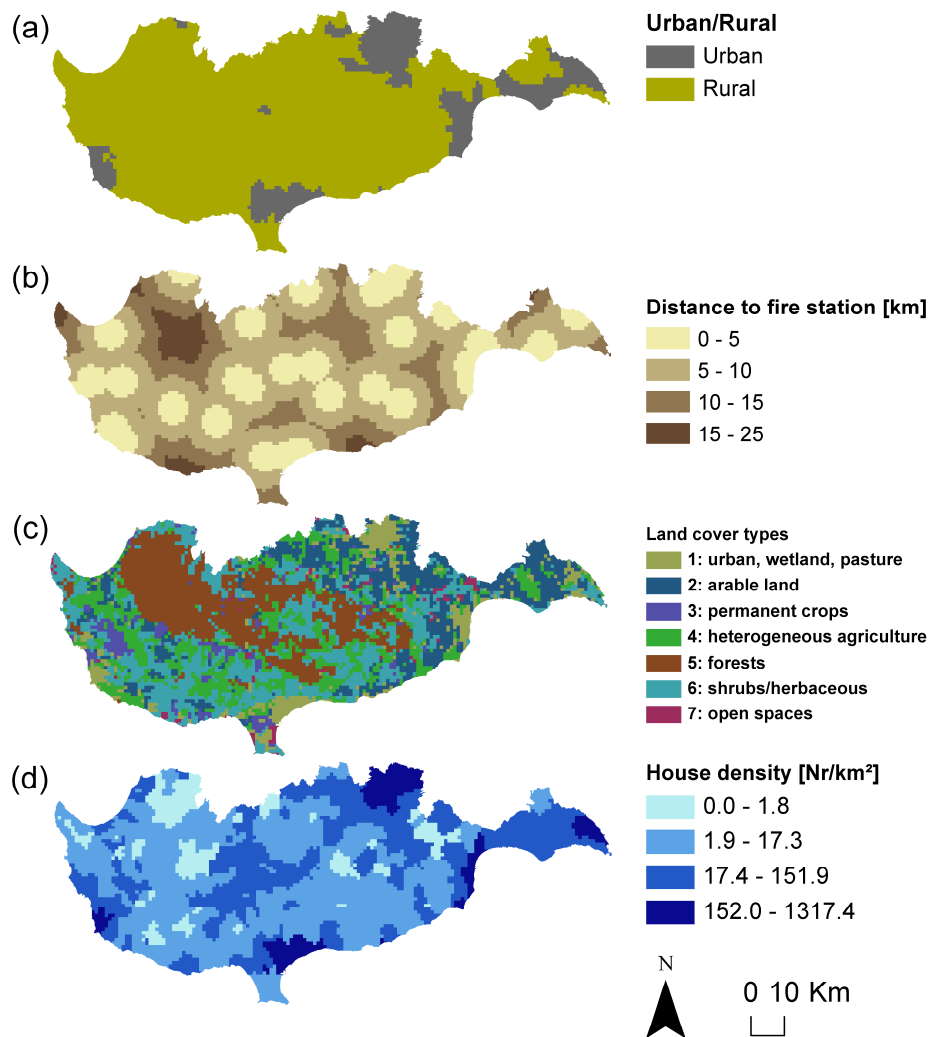
Figure 4.7: (a) Urban/Rural areas; (b) Distance to next fire station [km]; (c) Land cover types; (d) House density [Nr/km²]

Figure 4.9 - Figure 4.12 display histograms of calculated CFFWIS component values conditional on the occurrence of fires on the particular day and location. Figure 4.9 shows FFMC conditional on days with and without fire. The value of FFMC on days and locations with fire occurrences is not significantly different from those without. The FFMC is mainly influenced by precipitation, for this reason it stays high during the dry summer period. ISI (Figure 4.10) and BUI (Figure 4.11) show higher values on days with fires than on days without fire. The conditional histograms in Figure 4.12 show that the FWI on days and locations where fires occurred is higher than on those where none occurred. The mean FWI for days and locations with no fire occurrence is 22.5 and for those with at least one fire occurrence it is 32. These results confirm the potential of ISI, BUI and FWI as explanatory variables in a regression model. However, it is also clear from these results that the components alone have only limited prediction ability. E.g., fires occurred also on days and locations with FWI values close to zero.

Figure 4.13 shows the observed mean occurrence rate of fires as a function of the FWI. As expected, the fire occurrence rate increases with increasing values of FWI. Figure 4.14 shows the observed mean occurrence rate of fires as a function of the population density. There is a clear distinction between rural areas (less than 100 people/km²) and urban areas (more than 100 people/km²). The observed mean occurrence rate of fires for different road density classes is given in Figure 4.15.The occurrence rate increases with road density up to a value in the range of 8 km/km². In areas with road density higher than 8 km/km², the observed rate decreases; these areas are urban areas. Observed mean occurrence rates for different land cover types are shown in Figure 4.16. Among agricultural areas, the highest occurrence rate is found in olive grove areas. Overall, urban areas (U) have the lowest fire occurrence rate. In areas classified as water bodies (W), the observed mean occurrence rate is high, based on 5 registered fires in a 31 km² area. This is due to the approximation introduced by the 1km x 1km grid, which requires assigning a single land cover class to each cell. Fires are frequent in shore areas. Figure 4.17 shows the interpolated weather parameters on a selected day (8th October 2010) on Cyprus.

Figure 4.18 shows the calculated values of the components of CFFWIS on the same day on Cyprus.

Figure 4.19 and Figure 4.20 show the burnt area from each event (2006-2010) versus the weather parameters temperature and wind speed. The figures can be found in Ederle (2013). The scatterplots are shown in both linear and logarithmic scale. Similar plots of relative humidity and precipitation and the calculated components of the CFFWIS (FFMC, DMC, DC, ISI, BUI, FWI) are included in Appendix II. In all plots there is no linear function that can be used to express the relationship between the parameters and the resulting burnt area.

The damages induced by wildfires are very sparsely documented. No information on the losses was found in any administrative level on Cyprus. Nevertheless, the NatCatSERVICE of Munich Re is a database documenting losses from natural hazards worldwide. Two fire periods on Cyprus are documented together with the resulting losses (Table 4.3).
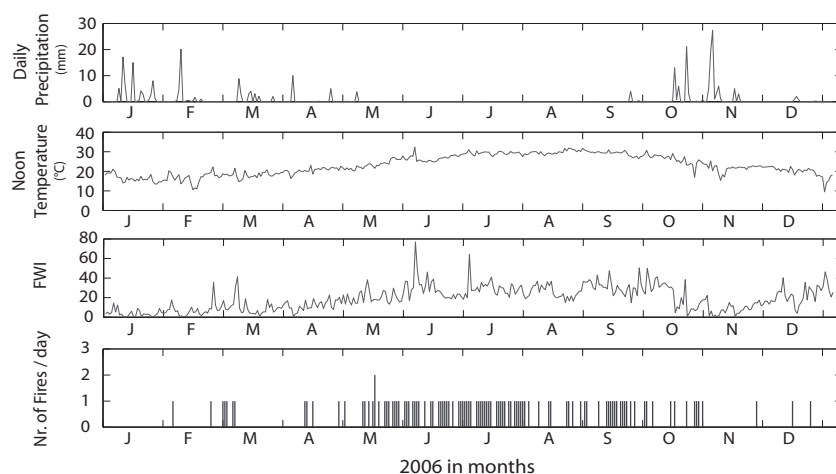
Figure 4.8: Daily values of Fire Weather Index (FWI), precipitation (mm) and noon dry-bulb temperature (° C) at Paphos weather station, and total number of fire occurrences in Cyprus in 2006
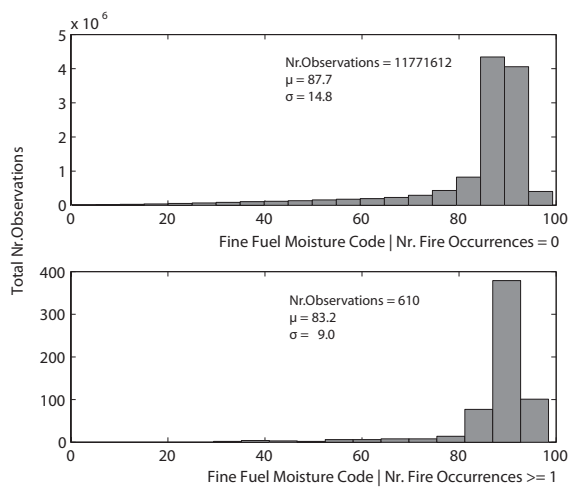
Figure 4.9: Histograms of FFMC (2006-2010) conditional on fire occurrence on Cyprus
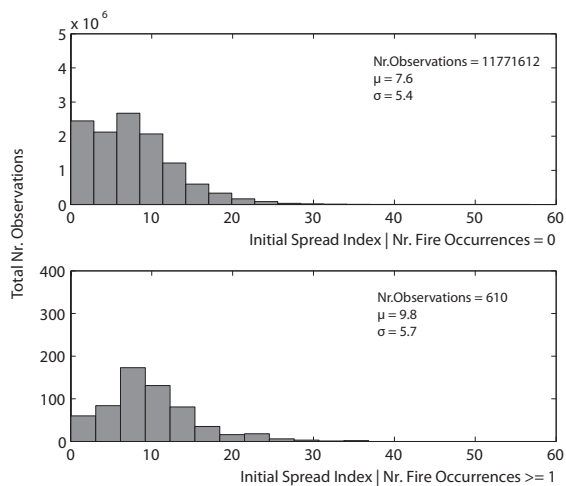
Figure 4.10: Histograms of ISI (2006-2010) conditional on fire occurrence on Cyprus
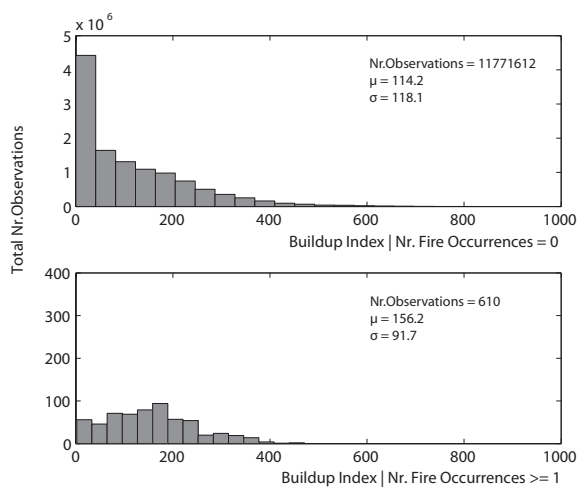
Figure 4.11: Histograms of BUI (2006-2010) conditional on fire occurrence on Cyprus
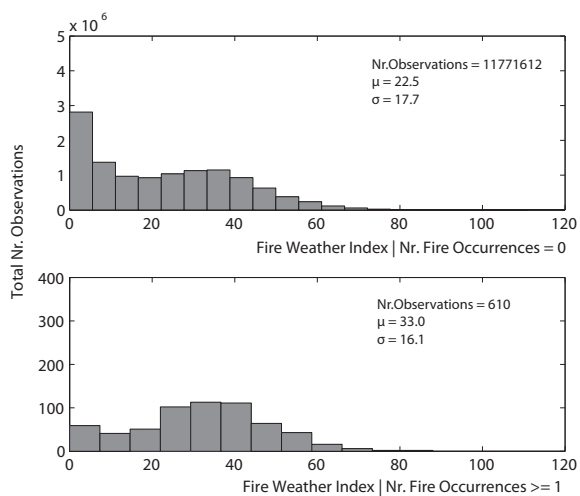
Figure 4.12: Histograms of FWI (2006-2010) conditional on fire occurrence on Cyprus
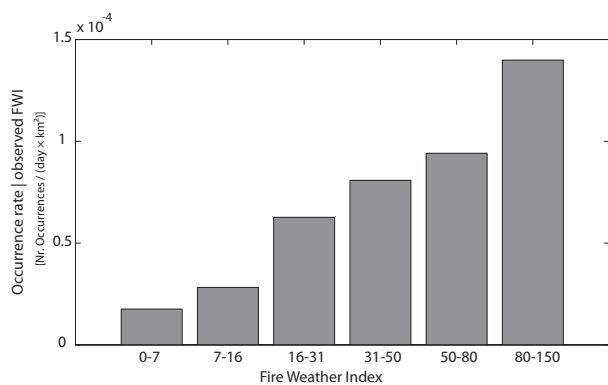
Figure 4.13: Observed mean occurrence rate [Nr. Fires/day x km²] conditional on FWI class for 2006-2010 on Cyprus
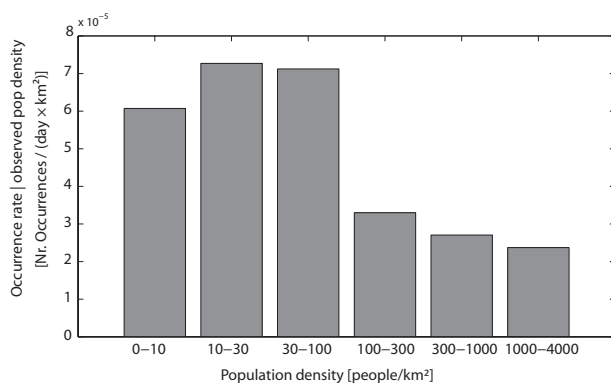
Figure 4.14: Observed mean occurrence rate [Nr. Fires/day x km²] conditional on population density [people/km²] for 2006-2010 on Cyprus
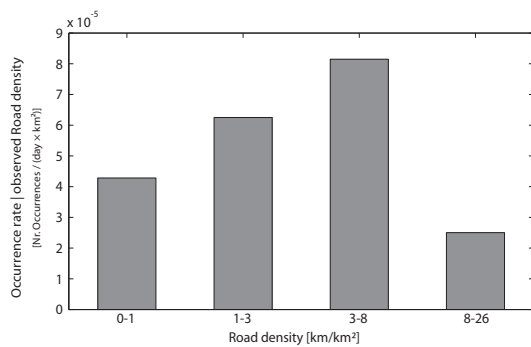
Figure 4.15: Observed mean occurrence rate [Nr. Fires/day x km²] conditional on road density [km/km²] for 2006-2010 on Cyprus
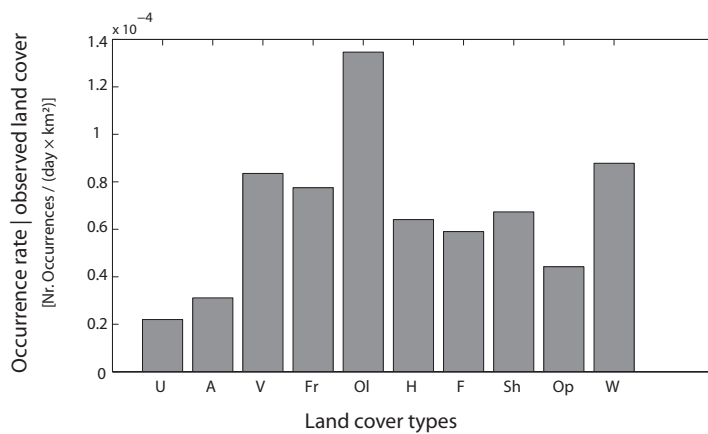
Figure 4.16: Observed mean occurrence rate [Nr. Fires /day x km²] conditional on land cover types for 2006-2010 on Cyprus

U: urban areas, A: arable land, V: vineyards, Fr: fruits and berry plantations, Ol: olive groves,
H: heterogeneous agricultural areas, F: forests, Sh: shrub and/or herbaceous vegetation associations,
Op: open spaces with little or no vegetation, W: wetlands and water bodies

(a)

(b)

(c)

Wind Speed (km/h)
- 10 - 15
- 15 - 20
- 20 - 25
- 25 - 30
- 30 - 35

Temperature (°C)
- 10 - 15
- 15 - 20
- 20 – 25
- 25 - 30

Relative Humidity (%)
- 40 - 50
- 50 - 60
- 60 - 70
- 70 - 80
- 80 - 90

0 10 Km

N
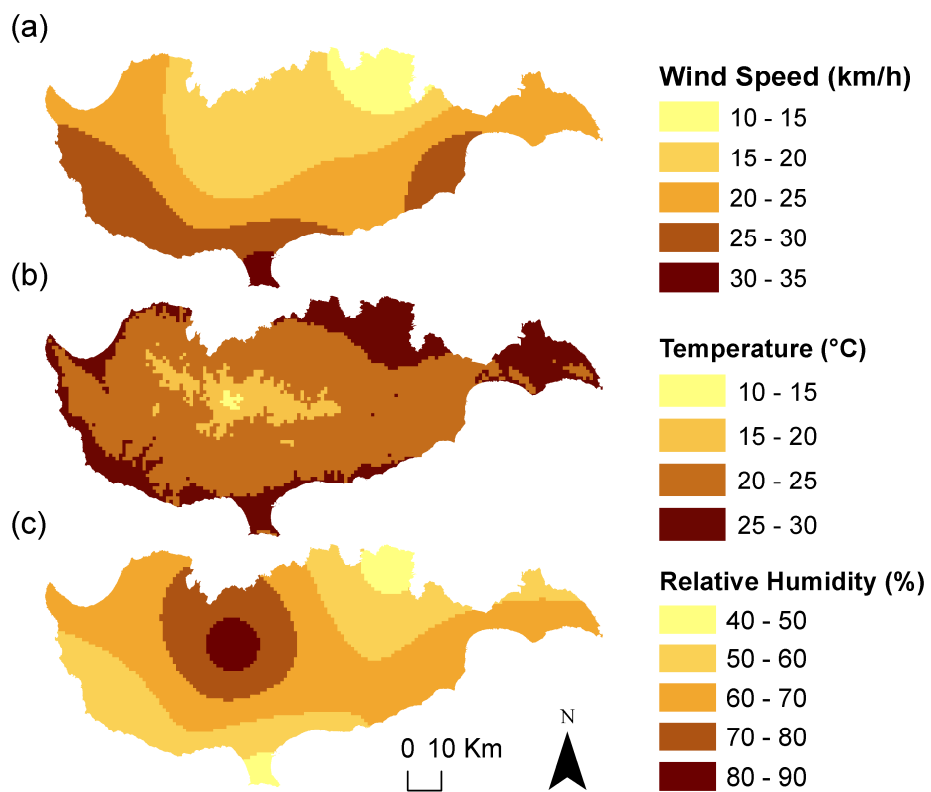
Figure 4.17: Interpolated weather parameters, (a) wind speed [km/h]; (b) temperature [° C]; (c) relative humidity [%] on the 8th October 2010 on Cyprus
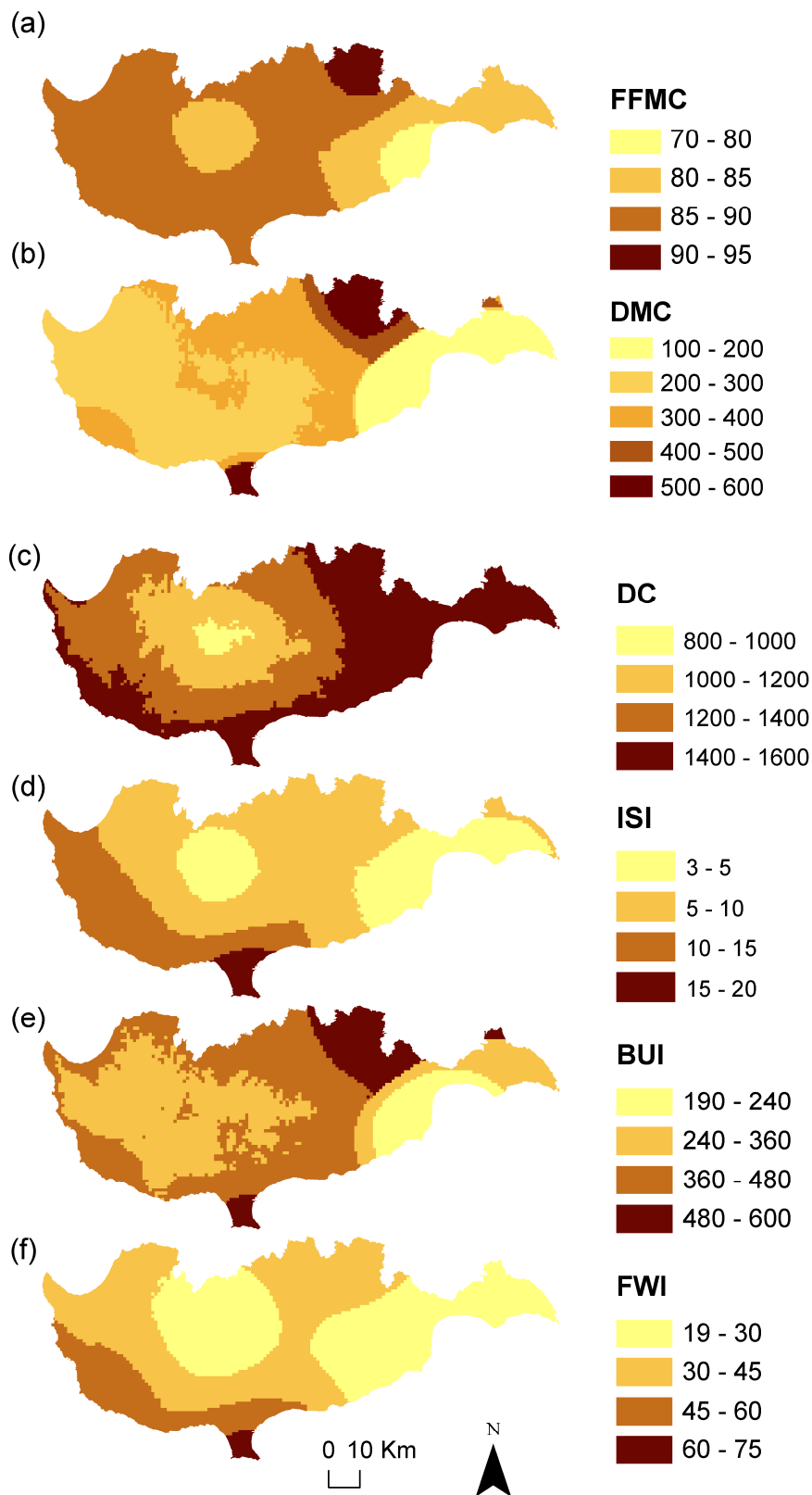
Figure 4.18: Components of the CFFWIS on the 8th October 2010 on Cyprus
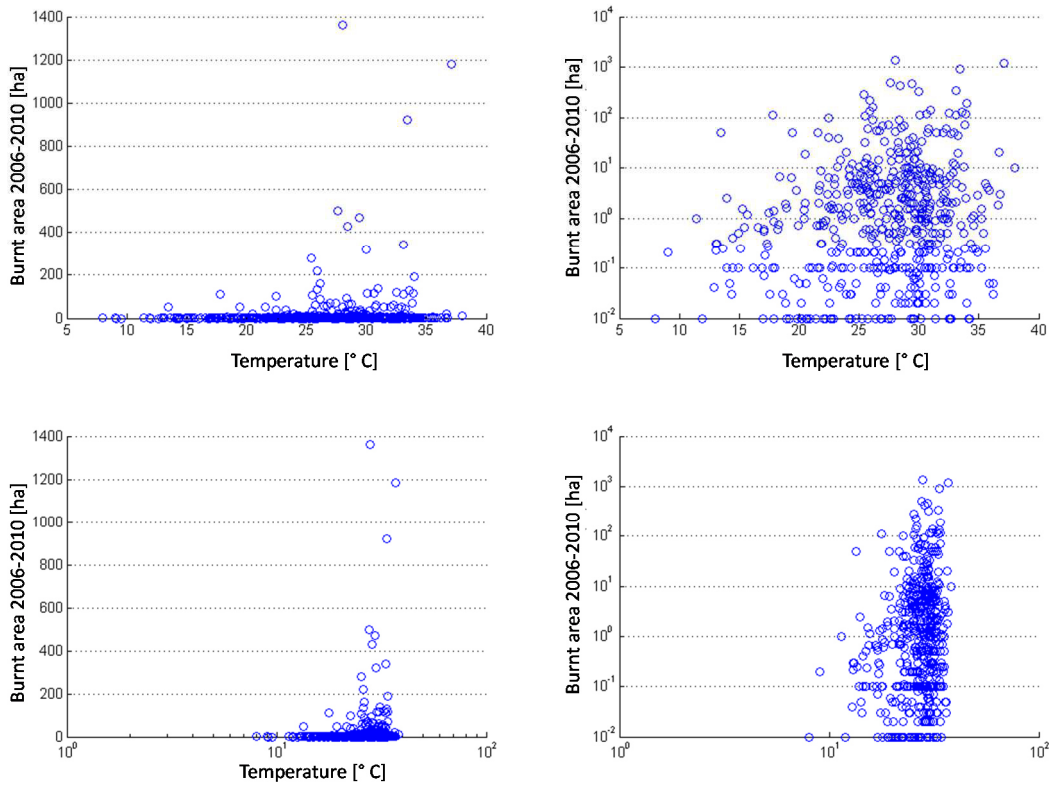
Figure 4.19: Burnt area of fire events (2006-2010) versus Temperature [° C] in linear and logarithmic scale
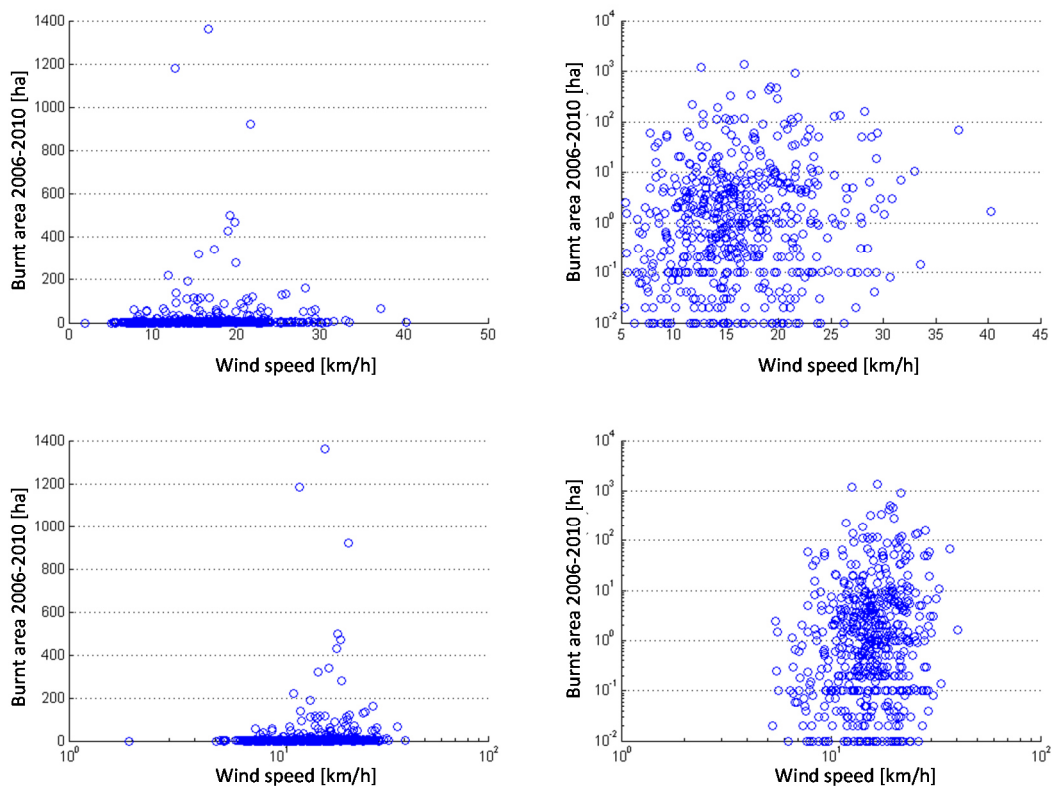
Figure 4.20: Burnt area of fire events (2006-2010) versus Wind speed [km/h] in linear and logarithmic scale

Table 4.3: Fire periods and registered damages on Cyprus (NatCatSERVICE, Munich Re)

Fire Period	Location	Damages description	House Losses
20 June 2007-16 July 2007	Kalavasos, Asgata	Forest fires, high temperatures >40°C. Several houses, buildings destroyed. Evacuated: 5 villages.	several buildings
June 2008	West of Larnaka, Sina Oros near Limassol	Forest-, brushfires. 5 houses, holiday homes destroyed. Farmland affected. Injured: 5 firefighters.	5 houses

4.3 South France

4.3.1 Description

South France is chosen for model application due to typical Mediterranean climate and land uses. The study area covers two regions, Languedoc-Roussillon and Provence-Alpes-Côte d'Azur.

Languedoc-Roussillon is divided into five administrative departments and comprises 1545 municipalities. Its area is 27 376 km² and it has 2 686 054 residents (year 2012). In the last decade the region experienced a fast population growth in the largest cities Montpellier, Nîmes and Perpignan. The area has two mountain regions, Pyrénées-Orientales in the south (summit Pic Carlit, 2921m) and Massif Central in the north (summit Mont Lozére, 1699m).

The climate is characterized by short mild winters (average temperature 8 °C) and long dry hot summers (average temperature 24 °C). Due to the varying topography of the area, it can be divided in four climate types. The mountainous areas (Pyrénées, Montaignes Noirs, Cévennes), the foothills of the mountainous areas with warmer temperatures but various microclimate and land use dominated by vineyards, pines and shrubs, the coastal plain characterized by vineyards and urban and peri-urban areas (cities Motpellier, Perpignan, Narbonne, Bézier) and the agricultural area in the western part beyond Carcassone. The Mistral and the Tramontana winds are strong cool dry winds that can reach wind speed over 100 km/hr. Mistral affects mostly the eastearn Gard department coming from the north, whereas Tramontana blows in from the sea into the coastal plains of Hérault, Aude and Pyrénées-Orientales.

Provence-Alpes-Côte d'Azur is divided into six departments and comprises 963 municipalities. It covers an area of 31 400 km² and has 4 900 000 residents. The topography of the region varies, with high-lying summits in the north (summit Bare des Ecrins, 4102m) facing the plane coast where major cities (Nice, Cannes, Marseille) are located. Land use is predominantly forest, shrubs and agricultural land.

The climate of the region shows high variability especially in the precipitation due to the varying topography. The south encounters wet winters and dry summers with almost no precipitation, which makes the coastal plain more susceptible to fires.

4.3.2   Input data

Table 4.4 summarizes the employed data, the resolution and their sources. Figure 4.21 shows the digital elevation model, the weather stations, the fire events (2000-2011) and the municipalities of both regions. Figure 4.22 shows the fire events (2000-2011) classified based on the resulting burnt area. Most of the fires resulted to burnt area < 1km², and two fire events burnt larger areas (27-67 km²). Figure 4.23 shows the population density [Nr. people/km²], the street density [km/km²] and the land cover types in Languedoc-Roussillon and Provence-Alpes-Côte d'Azur.

Table 4.4: Data types, resolution and sources for South France

Data	Resolution		Source	Additional information
	spatial	temporal		
Digital Elevation Model (DEM)	15m x 15m		ASTER GDEM (Ministry METI Japan & NASA)	
Land cover	250m x 250m		Corine Land cover 2006 (European Environmental Agency)	44 land cover types 1:100,000 (version13)
Admin. borders	municipality		ARTICQUE Solutions Group	
Population	municipality		Statistical Service of France (INSEE)	census 2009
Road network			Open Street Map	
Fire Events	DFCI coordinates	Date 2000-2011	Prométhée Forest Fire Database	
Temperature Wind speed Relative humidity Precipitation		Daily 2000-2011 24hr Daily 2000-2011	Deutscher Wetterdienst (DWD) MétéoFrance	35 Weather Stations

4.3.3   Preliminary data analysis

Figure 4.24 shows the observed mean occurrence rate of fires as a function of the population density. The mean occurrence rate increases with increasing population density. This is contrary to the result in Figure 4.14, where the occurrence rate increases in rural areas with increasing population density and for urban areas then decreases.

Figure 4.25 shows the observed mean occurrence rate of fires as a function of the street density. The occurrence rate increases for increasing street density in rural areas (street density < 15 km/km²) and a decrease can be observed for urban areas (street density > 15 km/km²). This result agrees with the result shown in Figure 4.15.

Figure 4.26 shows the observed mean occurrence rate of fires as a function of the land over types. Olive groves followed by urban areas (it can be assumed that this is mainly in the wildland urban interface buffer zone) show the highest mean occurrence rate. Vineyards, heterogeneous agricultural areas and forests follow. As in Figure 4.16, the areas covered by olives have the highest mean occurrence rate.
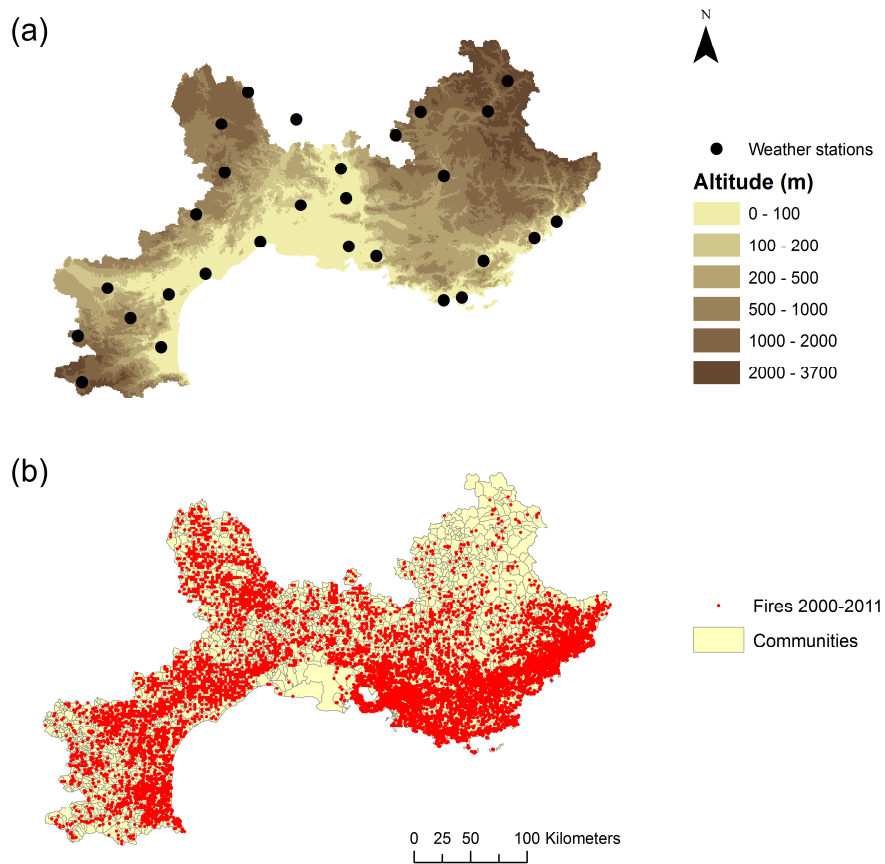
Figure 4.21: (a) DEM and weather stations and (b) fire events (2005-2011) and municipalities for study areas Languedoc-Roussillon and Provence-Alpes-Côte d'Azur

Figure 4.27 shows the interpolated values of the weather parameters on a specific day (25th July 2009). It can be seen that the temperature (Figure 4.17c) is also adapted to the elevation based on the normal lapse rate.

Figure 4.28 and Figure 4.29 show the calculated values of the CFFWIS components on the 25th July 2009. FFMC takes very high values, as expected due to dryness. It is also obvious the

influence that temperature (Figure 4.27c) has on this component. DMC is also influenced by wind speed (Figure 4.27a) and DC from temperature. In this map the relation between the components ISI and BUI and FWI can also be seen. FWI results from the combination of the ISI and the BUI.
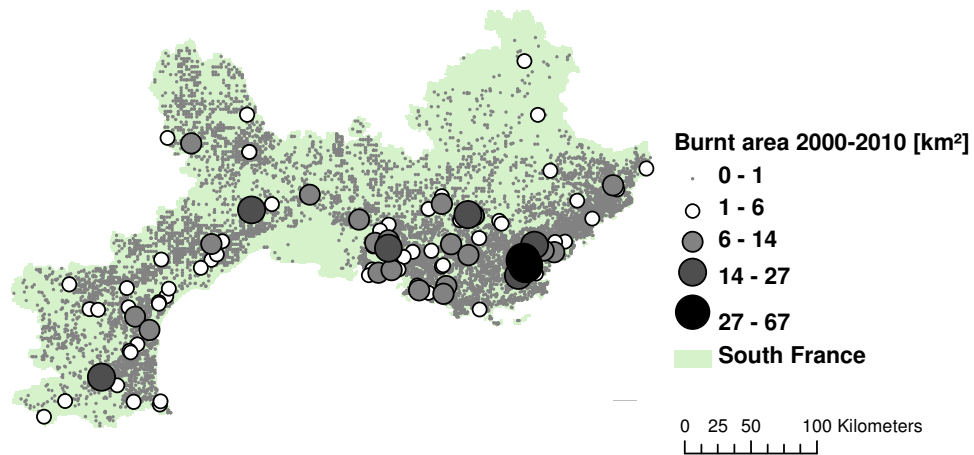
Figure 4.22: Fire events 2000-2010 in South France classified based on the resulting burnt area [km²]

Table 4.5 shows the losses for different fire periods, as they are registered in the NatCatSERVICE database of Munich Re.

(a)

Population density

(People/km^2)

- 0 - 50
- 50 - 250
- 250 - 500
- 500- 1000
- 1000 - 2000
- 2000 - 25000

(b)

Street density

km/km^2

- 0 - 2
- 2 - 5
- 5 – 12
- 12 - 50

(c)

Corine Land Cover

- Urban/artificial areas
- Arable land
- Permanent crops
- Pastures
- Heterogenous agriculture
- Forests
- Shrubs/herbaceous
- Open space, little/no vegetation
- Water bodies

0   25   50   100 Kilometers
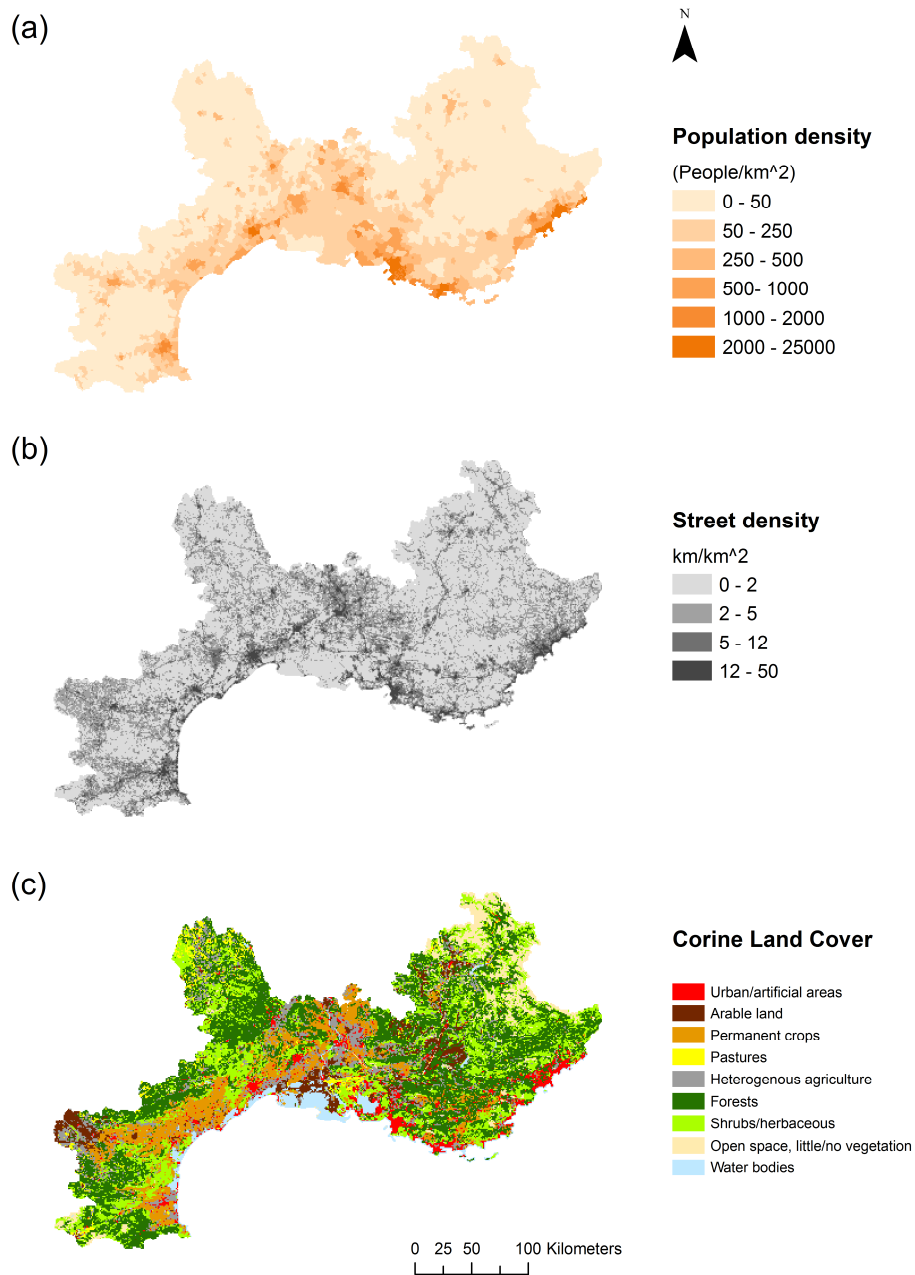
Figure 4.23: (a) Population density [Nr. People/km²], (b) Street density [km/km²] and (c) Land cover types in Languedoc-Roussillon and Provence-Alpes-Côte d'Azur
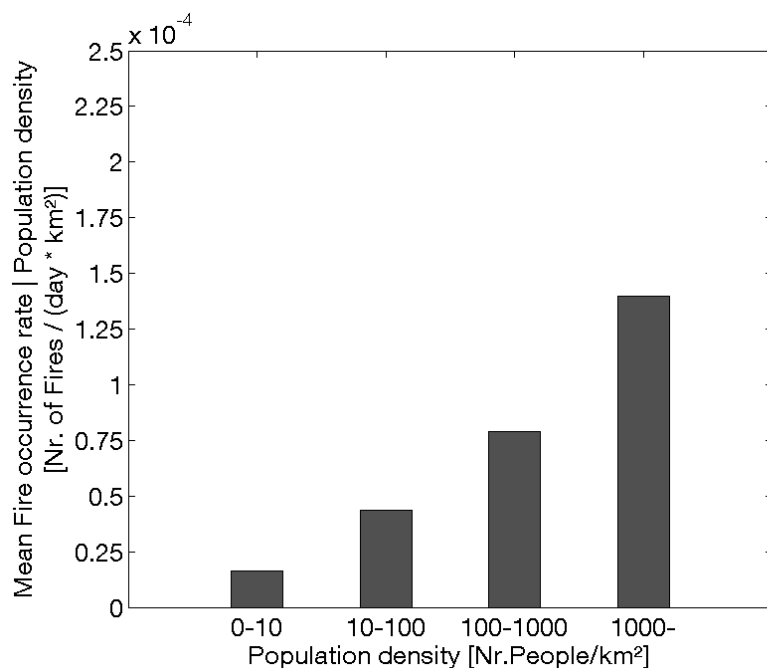
Figure 4.24: Observed mean occurrence rate [Nr. Fires/day x km²] conditional on population density [Nr. People/km²] for 2005-2011 in Languedoc-Roussillon and Provence-Alpes-Côte d'Azur
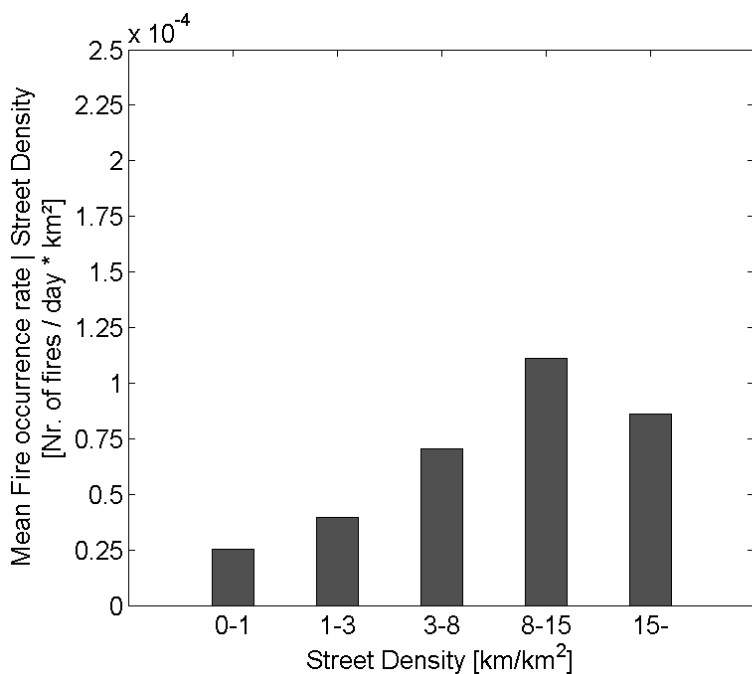
Figure 4.25: Observed mean occurrence rate [Nr. Fires/day x km²] conditional on street density [km/km²] for 2005-2010 in Languedoc-Roussillon and Provence-Alpes-Côte d'Azur
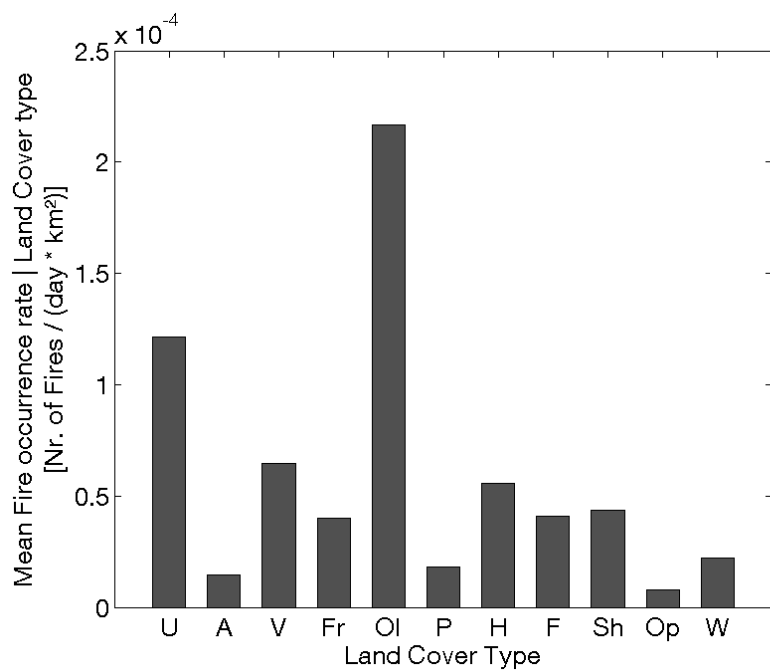
Figure 4.26: Observed mean occurrence rate [Nr. Fires/day x km²] conditional on land cover types for 2005-2010 in Languedoc-Roussillon and Provence-Alpes-Côte d'Azur

U: urban areas, A: arable land, V: vineyards, Fr: fruits and berry plantations, Ol: olive groves, P: pastures
H: heterogeneous agricultural areas, F: forests, Sh: shrub and/or herbaceous vegetation associations,
Op: open spaces with little or no vegetation, W: wetlands and water bodies
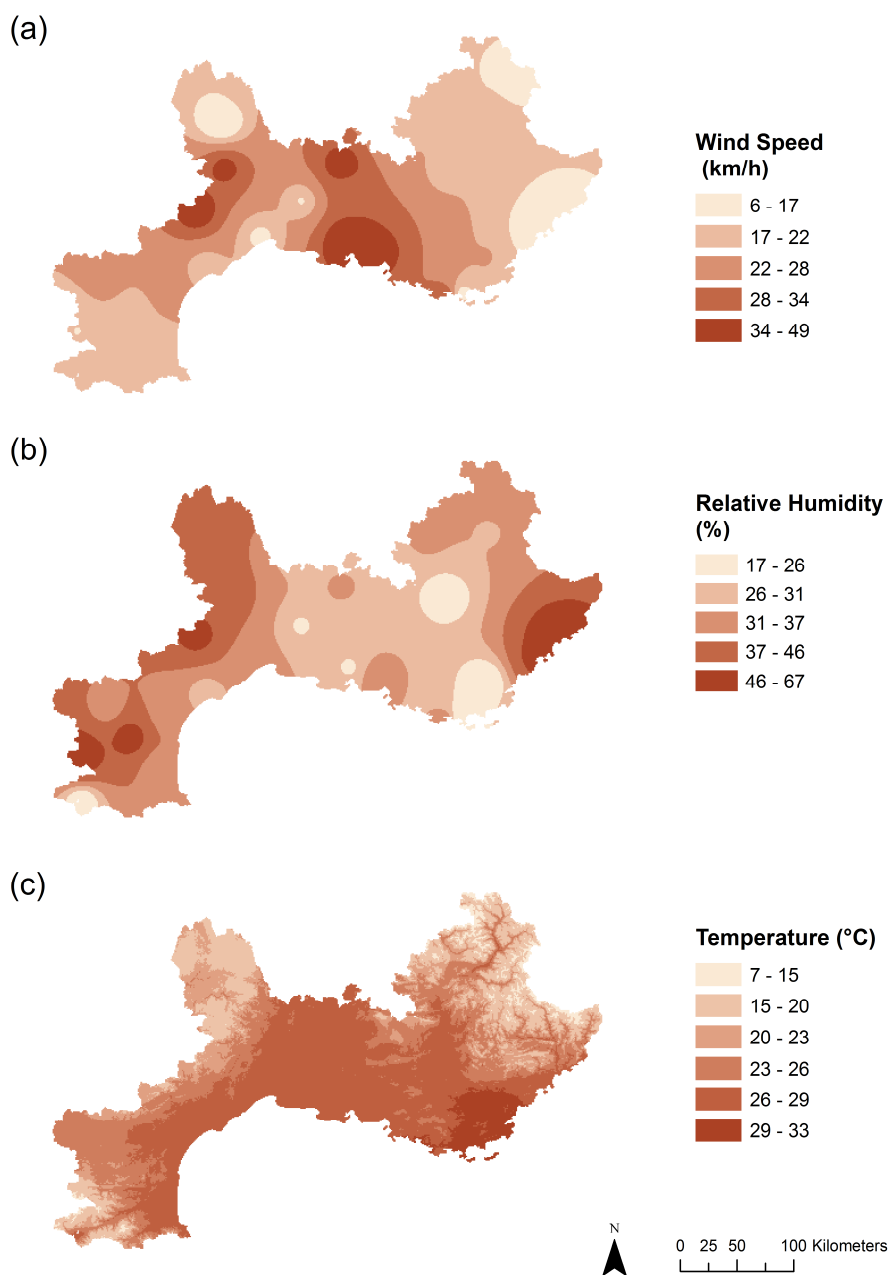
Figure 4.27: Interpolated weather parameters (a) wind speed [km/h]; (b) relative humidity [%]; (c) temperature [° C] on the 25th July 2009 in Languedoc-Roussillon and Provence-Alpes-Côte d'Azur

(a)

FFMC

	0 - 87
	87 - 90
	90 - 96

(b)

DMC

	10 - 70
	70 - 100
	100- 150
	150- 200
	200- 260

(c)

DC

	200 - 400
	400- 460
	460- 520
	520 - 580
	580 - 640

N

0 25 50   100 Kilometers
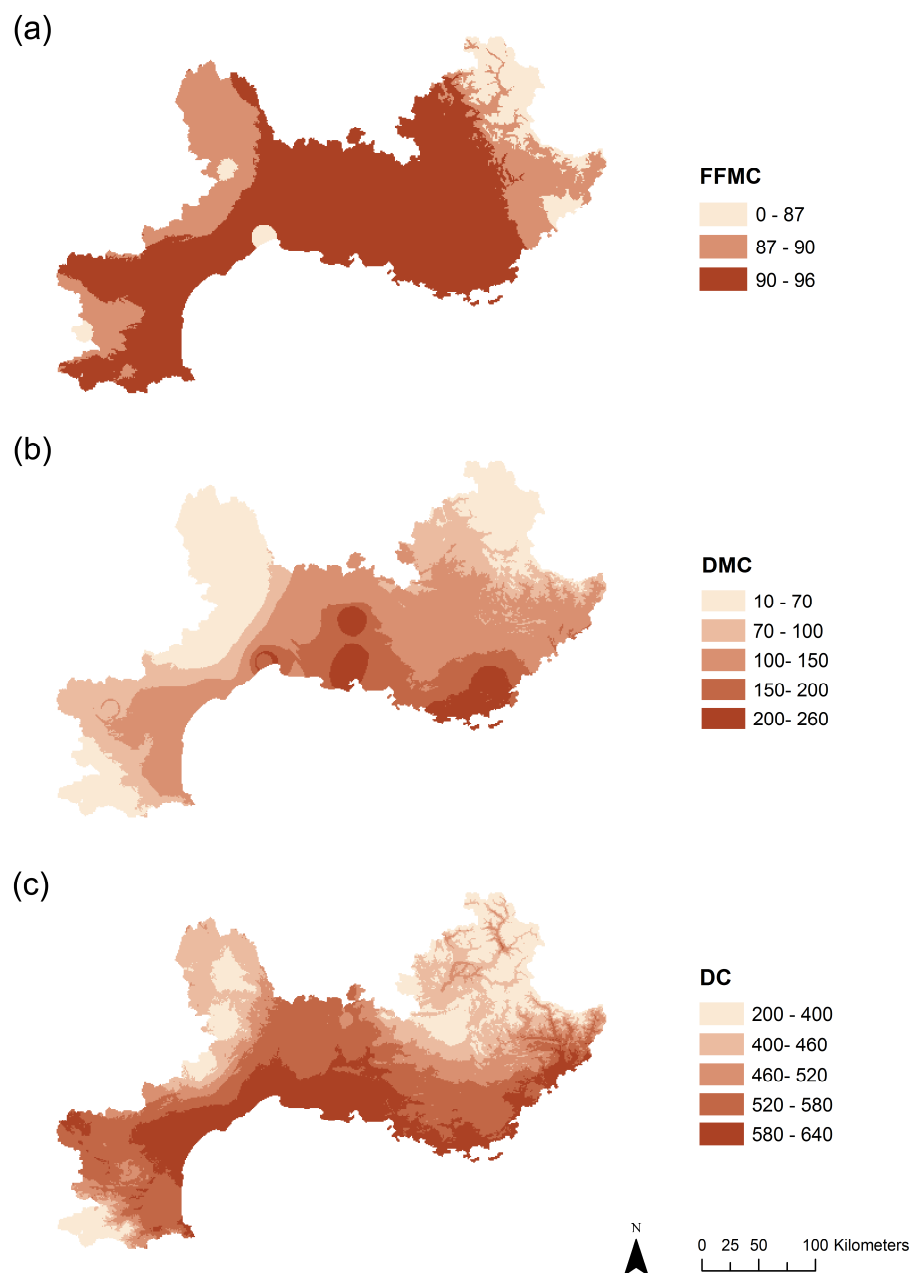
Figure 4.28: Calculated components of the CFFWIS (a) FFMC; (b) DMC; (c) DC on the 25th July 2009 in Languedoc-Roussillon and Provence-Alpes-Côte d'Azur

(a)

(b)

(c)
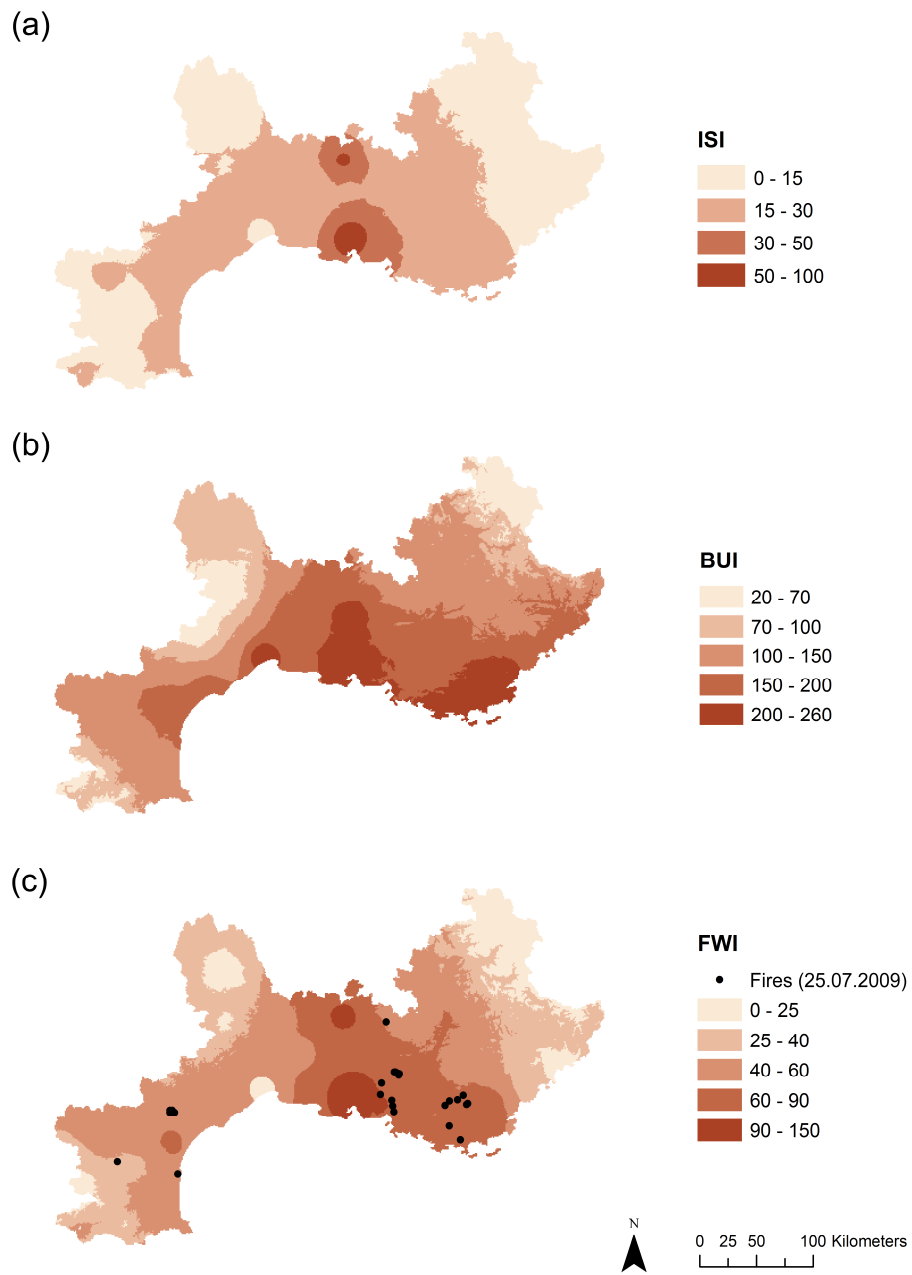
Figure 4.29: Calculated components of the CFFWIS (a) ISI; (b) BUI; (c) FWI and fire occurrences on the 25th July 2009 in Languedoc-Roussillon and Provence-Alpes-Côte d'Azur

Table 4.5: Selected fire periods and registered damages in South France (NatCatSERVICE, Munich Re)

Fire Period	Location	Damages description	House Losses
8.-9.10.2011	Languedoc-Roussillon, Herault	Brush fire Wind speeds up to 80 km/h Structures burnt	Structures burnt
21.-23.8.2011	Auvergne, Cantal; Languedoc Roussillon, Lozère; Poitou-Charentes, Charente	Several forest fires (esp. pine trees) >2.6 km² burnt Injured: 5 (fire fighters)	
22.-23.7.2009	Marseille, Cassis	Forest fires (manmade fire) 4 houses, farmhouse destroyed	4 houses
4.-24.7.2007	Provence, Alpes-Maritime, Mandelieu-la-Napoule, Theoule-sur-mer; Cote Azur, Var, Ramatuelle	Several forest fires >20 km² of land burnt 1 house destroyed Roads, highways closed Injured: 5 Evacuated: 3,000.	1 house
5.7.-8.8.2005	Corce; Haute-Provence, Manosque, Gréoux-les-Bains, Saint-Martin-les-Eaux, Saint Raphael, Aix-en-Provence	Drought conditions for several weeks Intense mistral wind >1,500 seats of fire 10 houses damaged >100 km² of brush, forest destroyed Power lines cut off 50,000 households without electricity Injured: 5 Evacuated: 650 Also affected: Spain, Portugal, Italy	10 houses

4.4 Summary

Chapter 4 introduces the reader in the study areas Rhodes, the Republic of Cyprus and South France. The data types, resolution and sources are described. This preliminary data analysis gives an overview on the factors influencing fire occurrences and burnt area. The mean occurrence rate of fires increases for higher values of population density and street density and decreases in urban areas. Olive groves are the areas with the highest mean fire occurrence rate. First maps of the interpolated values of the weather parameters are shown as well as maps with the calculated values of the CFFWIS components. The results of the components are compared with the observed fire occurrences. Among the components of the CFFWIS, ISI, BUI and FWI show a potential in predicting fire occurrences, in opposition to FFMC which remains high independently of the fire occurrence. Neither weather parameters, nor the components of the CFFWIS show linearity with the resulting burnt area. The potential of the CFFWIS componets to predict fire occurrence will be studied in depth in Chapter 5. Moreover, their ability to predict fire size (resulting burnt area) will be discussed in Chapter 6. Finally, registered losses for selected fire periods from the worldwide database NatCatSERVICE (Munich Re) are shown for both Cyprus and South France. The limited availability of damage data is also discussed.

5 Fire occurrence model

Accurate fire occurrence prediction is essential for an efficient planning of preventive and mitigating measures. Due to the random nature of fire occurrences and uncertainties in the influencing factors, such a prediction should ideally be probabilistic. In this chapter, probabilistic daily fire prediction models are developed for the Mediterranean at the meso-scale, based on Poisson regression, which uses readily available spatial and weather data. Influencing factors included in the models are weather conditions, land cover and human presence. The models are learned with data from Rhodes from the period 2000-2009 and Cyprus from the period 2006-2010. The probabilistic prediction is verified with a test data set and is illustrated with maps for selected days. Main part of what is presented here is published in Papakosta and Straub (2015).

5.1   Introduction

The prediction of the occurrence and extend of fire incidents is of great importance for the planning of precautionary, preventive and mitigating measures (danger communication, evacuation preparedness, dead fuel clearing activities, fire-fighting infrastructure, property insurance). Due to the random nature of fire occurrences and uncertainties in the influencing factors, such a prediction must necessarily be probabilistic. Various probabilistic models are proposed in the literature, including Poisson models (e.g. Cunningham and Martell 1973; Mandallaz and Ye 1997; Syphard *et al.* 2008), logistic regression (e.g. de Vasconcelos *et al.* 2001; Preisler *et al.* 2004; Kalabokidis *et al.* 2007; Syphard *et al.* 2008; Chuvieco *et al.* 2009; Arndt *et al.* 2013), multiple regression (e.g. Sebastián-López *et al.* 2008; Oliveira *et al.* 2012), neural networks (e.g. de Vasconcelos *et al.* 2001; Vasilakos *et al.* 2007; Vasilakos *et al.* 2009) and Bayesian networks (Dlamini 2009). Recently, machine learning algorithms have been found to be well suited for modeling and predicting fire occurrences, due to their larger flexibility compared with classical regression analysis. In particular, the Maxent (maximum entropy) algorithm (Parisien and Moritz 2009) and methods based on

decision tree learning, such as the random forest algorithm (Massada *et al.* 2012; Oliveira *et al.* 2012) have been applied. The appropriate model choice depends on the selected influencing factors and their spatial and temporal resolution, as well as the purpose of the model prediction.

Past probabilistic models of fire occurrence use weather factors, anthropogenic factors or combinations thereof as explanatory variables (Plucinski 2012). The effect of climatic factors is often represented by components of the Canadian Forest Fire Weather Index System (CFFWIS) (Martell *et al.* 1987; Martell *et al.* 1989; Wotton *et al.* 2003). In these studies, the temporal resolution is daily, the spatial resolution is regional. Various studies have looked into the combined effect of weather and anthropogenic factors (Cardille *et al.* 2001; Pew and Larsen 2001; Amatulli *et al.* 2006; Kalabokidis *et al.* 2007; Syphard *et al.* 2008; Vilar *et al.* 2010; Padilla and Vega-García 2011; Miranda *et al.* 2012; Oliveira *et al.* 2012; Martínez-Fernández *et al.* 2013). The temporal resolution of these studies is seasonal or yearly, and thus the weather factors include mean, minimum and maximum temperatures, as well as cumulative precipitation. Common explanatory variables representing anthropogenic influences used are population density, land use, distances to human-built infrastructures (e.g. Catry *et al.* 2009), but many additional variables were studied, e.g. distance to campground (Chou *et al.* 1993), holidays (Mandallaz and Ye 1997), ownership of housing (Cardille *et al.* 2001), proximity to urban areas and roads (Romero-Calcerrada *et al.* 2008), unemployment rate (Oliveira *et al.* 2012), rural exodus by means of population decrease (Martínez-Fernández *et al.* 2013), hiking trail density (Arndt *et al.* 2013). The spatial resolution in these studies varies from cellular (1 km² grid) (e.g. Pew and Larsen 2001) to regional.

In this chapter a daily probabilistic model for fire occurrences in Mediterranean climates is developed, which includes both natural and anthropogenic factors. Such a daily predictive model aims to provide better predictions, than models based only on weather conditions, due to human influence on fire occurrences in the Mediterranean. The model, which has fine temporal and spatial resolution, can eventually be helpful as a fire management tool. In the proposed model, the influence of weather conditions is represented by the Canadian Forest Fire Weather Index System (CFFWIS) (Van Wagner 1987) (Section 2.3), which – although it was originally developed for Canadian climates and vegetation – is commonly used for predicting fire occurrence in the Mediterranean Viegas *et al.* 1999; Camia and Amatulli 2009. This necessitates that the interpretation of the CFFWIS indicators to categorize fire danger level (e.g., low, moderate, high) is adjusted to the specifics of the Mediterranean climates (Moriondo *et al.* 2006; Giannakopoulos *et al.* 2011; Dimitrakopoulos *et al.* 2011).

In the model proposed and investigated in this chapter, the anthropogenic influence is represented through spatial variables such as land cover type and road density, which was found to be a relevant indicator of fire occurrence in e.g. (Amatulli *et al.* 2006; Yang *et al.* 2007; Syphard *et al.* 2008 and Oliveira *et al.* 2012). In contrast to previous studies, the proposed model combines a high spatial resolution (1km²) with a high temporal resolution (daily) for predicting fire occurrence. In addition, the model includes weather conditions (as expressed through the CFFWIS), topography and vegetation in combination with anthropogenic factors. The model is based on a Poisson regression (Section 3.3). Its results are daily maps of fire occurrence rates.

A first model with spatial resolution the municipality is introduced and applied to the island of Rhodes. The second model is applied to the Republic of Cyprus, where the model parameters are learnt from observed fire events (see Chapter 4). The data is separated into a learning set and a verifying set, which allows investigating the predictive power of the proposed model. It is found that the best prediction can be achieved by combining the natural and anthropogenic factors. The main factors describing anthropogenic influences are found to be land cover, population and road density.

5.2   Probabilistic model for predicting fire occurrence

Two BN models are here proposed. The first model is shown in Figure 5.1. The model is able to estimate wildfire occurrence rates based on temporal and spatial data. Here, the spatial reference of the model is the municipality level (administrative unit), to account for the available data (i.e. fire records that are available only for a municipality without geo-reference as in Rhodes study area). The temporal reference is one day. Therefore, the BN represents the factors influencing wildfire occurrence in a municipality (as specified by the corresponding node) during a particular day.

The nodes of the model represent variables influencing wildfire occurrence. Grey nodes represent the variables used for the calculation of the daily fuel moisture and are treated separately in the parameter estimation. Every node has a number of discrete mutually exclusive states, meaning that continuous random variables (such as *Area* or *Human population density*) are discretized.

The nodes *Municipality*, *Area* and *Human population density* can be determined from spatial and demographic data. In case of missing data, these nodes could be random. *Land cover* has labeled states that are related to fuel type (e.g. forest, natural grasslands, olive groves, artificial surface, etc.) and the probability of occurrence of each fuel type is taken as the proportion of the area covered within a municipality.

The node *FFMC* (Fine Fuel Moisture Code) represents the continuous variable fuel moisture of fine fuels (Section 2.3). The node is a child of the weather variables (*Temperature, Wind speed, Relative humidity* and *Precipitation*) and the fuel moisture of the previous day. The daily values of *FFMC* are calculated deterministically with the equations given in Appendix.

The node *Occurrence rate* represents the mean number of wildfire occurrences per day and km². In this model, the rate is a function only of *Land cover*, *Human population density* and *FFMC*, which includes all weather related variables. The occurrence rate is not observable and is estimated based on historical data with the EM algorithm (Section 3.1.1).

For given daily rate of occurrence λ and area α, the number of wildfires during a day can be modeled by a Poisson distribution, assuming independence among fire events for given occurrence rate (see Section 3.3). The CPT of the number of occurrences N is therefore obtained as,

$$\Pr(N = k \mid \lambda, \alpha) = \frac{(\lambda\alpha)^k}{k!}\exp(-\lambda\alpha), \qquad k = 0,1,2,\dots \tag{5.1}$$

wherein λ [day^{-1}km^{-2}] is the occurrence rate and α [km²] is the area.
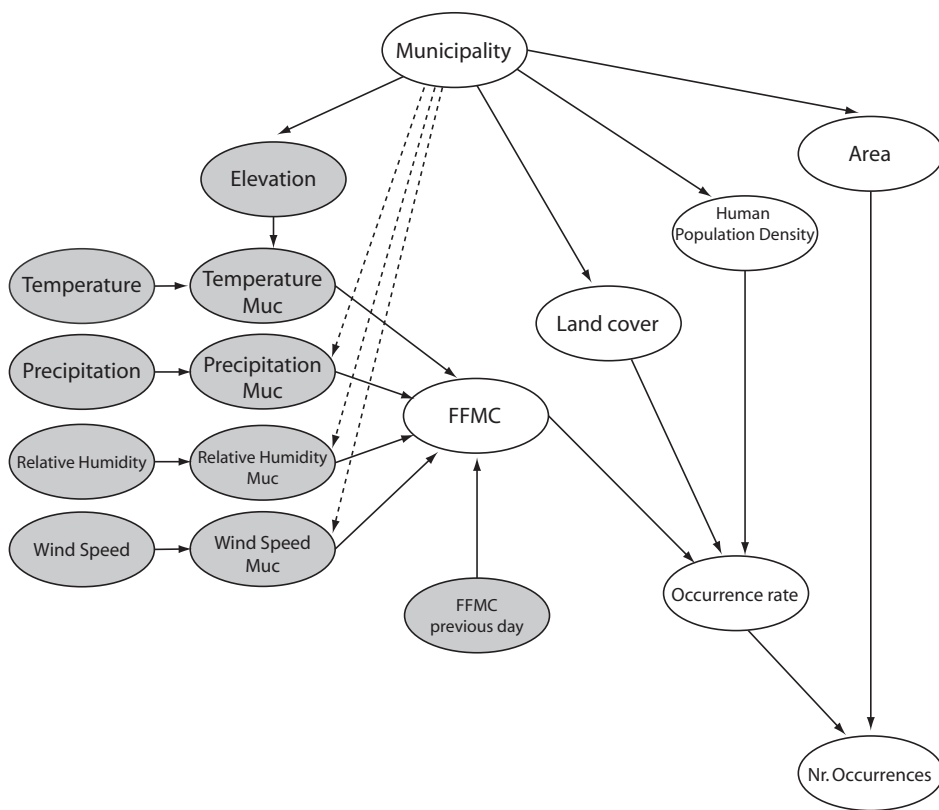
Figure 5.1: BN for fire occurrences using FFMC at the municipality level

Figure 5.2 summarizes the second proposed probabilistic model by means of a BN. The BN models daily fire occurrence in a cell of 1 km², which is the spatial unit. This will be the model further used in this thesis to predict fire risk with 1 km² spatial resolution. This includes every wildland fire that is registered by the local authorities, independent of the burnt area. Different colors indicate different classes of variables. The variables in blue represent the weather conditions; the variables in orange are the components of the CFWIS, which result in a FWI value; the variables in yellow represent the anthropogenic influence and the vegetation. Finally, the variables in white are the predicted *Fire occurrence rate* and the actual *Fire Occurrences*. The yellow variables change over space but are constant in time, whereas all other variables change both in time and space.

In classical regression analysis, the variables are separated into explanatory and response variables (sometimes also referred to as independent and dependent variables) (Section 3.3). In the BN framework, no such separation is made. Instead, the causal relations between variables are modeled, which is why in Figure 5.2 there are links in-between weather variables and in-between white variables. As an example, road density is statistically dependent on the land cover type and the human population density. In the application presented in this chapter, there is no difference between the BN model and the regression model. In fact, a regression approach is used to estimate the parameters of the BN as explained later. However, when using the model for prediction, not all explanatory variables may be known with certainty. The BN allows modeling them as random variables. As an example, the forecasted weather variables will be uncertain, which can be directly implemented in the BN.
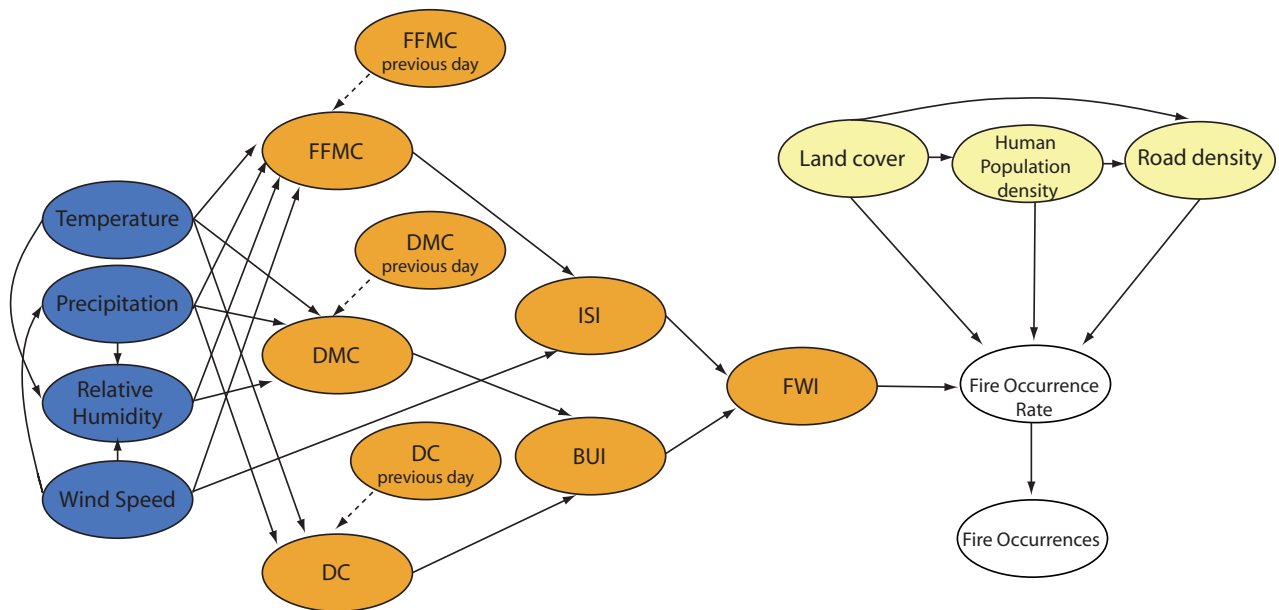
Figure 5.2: BN for fire occurrence using all the components of the CFFWIS in 1km² spatial resolution

Data is available for all weather variables as well as all yellow variables. All these variables are continuous, with the exception of land cover, which has labeled states that are related to fuel type (e.g. forest, natural grasslands, olive groves, artificial surface, etc.). The orange variables are defined by the CFWIS functions following Appendix I. For given values of the weather variables, they are defined deterministically.

The fire occurrence rate λ, which is defined as the mean number of fires per day and km², is estimated from the data. In the model, it is a function of land cover, human population density, road density and FWI. The variable fire occurrences $N \in 0,1,2,...$ is the number of fires in one cell on one day. As explained before for a given daily fire occurrence rate λ, the number of fires follows a Poisson distribution, assuming independence among fire events for given occurrence rate.

Observations of N are used to estimate λ based on Poisson regression (Section 3.3).

5.3   Parameter estimation

The parameters of the model in Figure 5.1 are estimated based on the EM algorithm. The model is applied to the study area of Rhodes (see also Chapter 4). The daily values at noon are extracted and used as an input for the FFMC calculations (Appendix I). In the case of missing values of relative humidity and wind speed at noon, values from the previous measurement at 09:00 are utilized. In the case of a missing temperature value, the recorded value of the previous day at noon is taken. Since there is only one official weather station on the island, the weather variables at other locations are inferred from the data obtained at this station. For temperature, the value in each municipality is estimated based on the normal lapse rate. After the data pre-processing and the FFMC calculation,

each of the municipality is described by spatial information, daily weather conditions and FFMC for the time period 2000-2009, and recorded fire events (2,555 events).

The model in Figure 5.2 is applied to Cyprus (see also Chapter 4). After the data pre-processing, weather interpolation and FWI calculation, each of the 6,447 grid cells is described by spatial information, noon daily weather conditions and FWI, and recorded fire events for the period 2006-2010 (11,768,570 records). Only the records of the period 2006-2009 (9,419,067 records) are used for parameter estimation.

Poisson regression with MLE is employed following Chapter 3. Various candidate models for the fire occurrence rate λ were learnt with the data. All models differ only in the selection of parameters employed. From these models, five were selected and are presented here.

5.4   Results

5.4.1   Rhodes

The main result of the parameter estimation for the model of Figure 5.1 is the PMF of the occurrence rate conditional on the FFMC, the land cover and the human population density. To show the influence of each of these three factors individually, we evaluate the BN by fixing only the corresponding factor. Because the factors are not d-separated in the BN (they are connected through the common node municipality), they are statistically dependent. Therefore, this approach slightly overestimates the influence of the individual factors. However, by also fixing the remaining factors, this effect was investigated and found to be small. The advantage of fixing only one factor at a time is that the results are then averaged over the remaining factors and are thus more representative, since they are effectively based on a larger number of underlying data.

Figure 5.3 shows the mean occurrence rate for different ranges of human population density. The occurrence rate increases with increasing values of human population density.
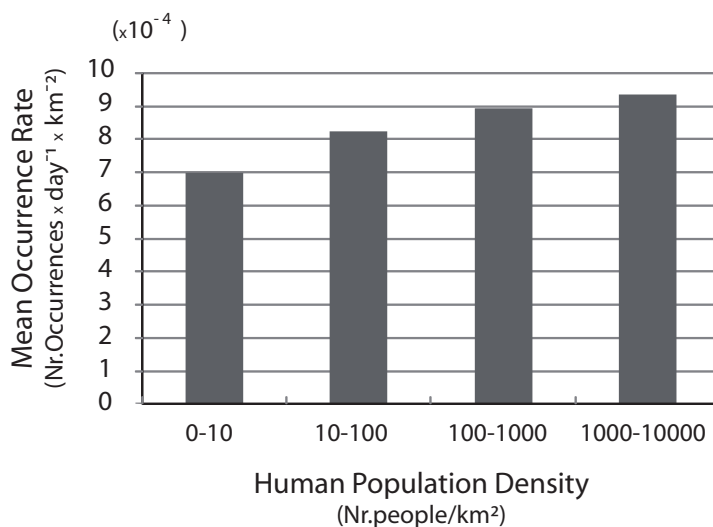
Figure 5.3: Mean fire occurrence rate and human population density for Rhodes

A slight influence of the land cover on the mean occurrence rate is observable (Figure 5.4). The agricultural areas (arable land, permanent crops of vineyards and olive groves, heterogeneous agricultural areas) have higher mean occurrence rates than the natural/semi natural areas (forests, scrub/herbaceous vegetation and natural grasslands, open spaces with little or no vegetation). In heterogeneous agricultural areas, where complex cultivation patterns and settlements are mixed, the occurrence rate is the highest among all land covers.
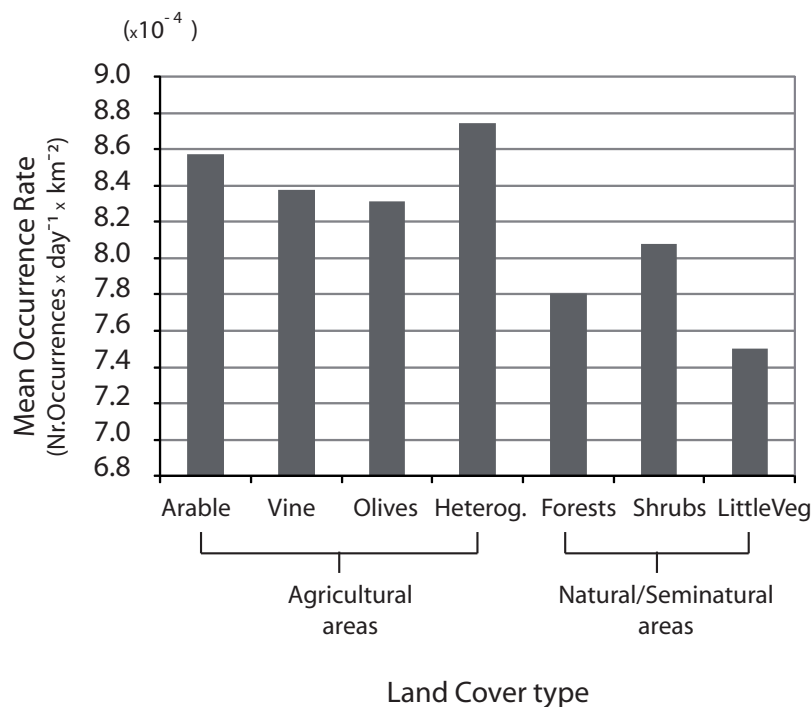
Figure 5.4: Mean fire occurrence rate and land cover types for Rhodes

FFMC is found to have only slight influence on the occurrence rate, which is estimated as $8.35 \cdot 10^{-4}$ [Nr.Occurrences x day^{-1} x km^{-2}] for FFMC values in the range of $0-40$ and $8.59 \cdot 10^{-4}$ [Nr.Occurrences x day^{-1} x km^{-2}] for FFMC values in the range of $95-100$. This is also supported by the figures presented in Chapter 4 (Figure 4.2 and Figure 4.3), where FFMC values are generally high, and the only large changes occur during and after rainfall events and the corresponding means and standard deviations of FFMC conditional on fire occurrences exhibit similar trends.

5.4.2 Regression analysis

Alternative candidate models are shown in Table 5.1. Tested variables were the CFFWIS components BUI, ISI and FWI. The null model (M_Null) includes only the intercept as an explanatory variable. Models M_BUI, M_ISI and M_FWI include as sole variables BUI, ISI and FWI respectively. M_BUI_ISI includes both BUI and ISI.

The models were trained with data from Cyprus for 2006-2009. The results of the Poisson regression are shown in Table 5.1. The table includes the estimated parameters, the AIC score and the maximum log-likelihood with respect to the learning set (log-likelihood 2006-2009). M_Null has as expected the lowest maximum likelihood score, among the tested models. The model

including both BUI and ISI (M_BUI_ISI) performed better than M_BUI and M_ISI, and all three models proved to perform worse than M_FWI.

Table 5.1: Alternative models with explanatory variables and estimated parameters (Cyprus 2006-2009)

Explanatory variables	*Parameters*	Alternative candidate models				
		M_Null	M_BUI	M_ISI	M_BUI_ISI	M_FWI
Intercept	β_0	-9.88	-10.21	-10.43	-10.50	-10.61
BUI	β_1		0.0027		0.0016	
ISI	β_2			0.0637	0.0483	
FWI	β_3					0.0278
log-likelihood (2006-2009)		-5266.8	-5236.2	-5228.2	-5219.9	-5198.4
AIC (2006-2009)		10536.0	10476.0	10460.0	10446.0	10400.8

Table 5.2 shows the selected models M1 to M5. The models are arranged according to increasing number of explanatory variables, starting from M1 that includes FWI as the sole variable (M_FWI), to M5 with 12 variables, including FWI, road and population density and land cover types.

As an example, the predicted rate of fires according to model M5 is,

$$\lambda = \exp(-10.90 + 0.0329 \cdot \text{FWI} + 0.3217 \cdot \text{Road density} - 0.0234 \cdot (\text{Road density})^2 - 0.0010 \cdot \text{Pop density} - 0.9681 \cdot \text{Arable} + 0.3235 \cdot \text{Permanent} - 0.0760 \cdot \text{Heterogeneous} + 0.1057 \cdot \text{Forest} + 0.0486 \cdot \text{Shrubs} - 0.1882 \cdot \text{OpenSpaces} - 1.1863 \cdot \text{Urban/Wet/Pastures}) \tag{5.2}$$

In models M2, M3 and M5, road density as well as (road density)² are included as explanatory variables, to represent the non-linear effect of road density on the fire occurrence rate observed from Figure 4.15 in Chapter 4. It is important to stress that road and population density are highly positively correlated, and are also dependent on land cover type. The influence of human presence is expressed by all these variables.

Based on the learning data set, model M5 performs best, as it exhibits the lowest AIC, followed by M3 and M4. The estimated parameters of the explanatory variables FWI, road density and population density in all models M1-M5 are consistent. In models M4 and M5, the estimated parameters of the land cover types take slightly different values. They are higher in M4 due to the fact that in M5 the additional terms in the link function describing road and population density on average take a value slightly above zero.

Table 5.2: Selected models with explanatory variables and estimated parameters (Cyprus 2006-2009)

Explanatory variables	*Parameters*	Selected Models				
		M1	M2	M3	M4	M5
Intercept	β_0	-10.61	-10.95	-10.92	-10.90	-10.90
FWI	β_1	0.0278	0.0282	0.0302	0.0327	0.0329
Road density [km/km²]	β_2		0.3236	0.3198		0.3217
(Road density)² [km/km²]	β_3		-0.0324	-0.0276		-0.0234
Population dens. [people/km²]	β_4			-0.0018		-0.0010
Arable	β_5				-0.6501	-0.9681
Permanent*	β_6				0.8383	0.3235
Heterogeneous	β_7				0.4098	-0.0760
Forest	β_8				0.3497	0.1057
Shrub/Herbaceous	β_9				0.3279	0.0486
Open spaces	β_{10}				-0.1310	-0.1882
Urban-Wet-Past**	β_{11}				-0.9556	-1.1863
log-likelihood (2006-2009)		-5198.4	-5166.1	-5151.2	-5147.3	-5111.9
AIC (2006-2009)		10400.8	10340.2	10312.4	10312.6	10247.8

* Permanent crops include olives, vineyards and fruits

** Urban-Wet-Past variable includes Urban areas, Wetlands and Pastures

It is also worthwhile noting that the variables describing road and population density in Model M5 are not independent of the land use type. Pearson's correlation coefficient ρ between population density and urban & wetlands land cover type is 0.48 and between road density and urban & wetlands is 0.59. Therefore, the variables population and road density in model M5 partly express the fact that fires are less likely in urban areas. In M4, where these variables are not present, this effect is fully described by β_{11} alone.

Eq. (3.18) from Chapter 3 is used to compare the sensitivity of the studied models to changes in the explanatory variables. Table 5.3 shows the relative change of λ, as predicted by M5, when changing one explanatory variable and keeping all others fixed. For FWI, population density and road density, the change of the variable is equal to one standard deviation σ, whereas the land cover types change from 0 to 1.

Table 5.3: Relative change of occurrence rate $\frac{\Delta\lambda}{\lambda}$ with changing explanatory variables of model M5 for Cyprus. For continuous variables FWI, population density and road density, the change of the variable is equal to one standard deviation σ

Explanatory variables	Δx	$\left(\frac{\Delta\lambda}{\lambda}\right)_i$, Eq. 3.7
FWI	σ=17.7	0.791
Population density	σ=316	-0.271
Road density	σ=3.23	0.614 *
(Road density)²		
Arable	1	-0.620
Permanent	1	0.382
Heterogeneous	1	-0.073
Forest	1	0.111
Shrub/Herbaceous	1	0.050
Open spaces	1	-0.172
Urban-Wet-Past	1	-0.695

$* \left(\frac{\Delta\lambda}{\lambda}\right)_i = \exp[\Delta x(\beta_2 + 2\,\beta_3\mu_{RD} + \beta_3\Delta x)]$, with $\mu_{RD} = 2.09$ being the mean value of road density.

5.4.3   Prediction

Daily observations of Cyprus in 2010 are used to verify the predictive ability of the proposed models. Table 5.4 shows the log-likelihood as estimated from each model with parameters learned from the 2006-2009 dataset for the entire data of 2010. Model M5 predicts the highest log likelihood for the 2010 data set.

Table 5.4: Predicted log-likelihood values for the entire 2010 data set of Cyprus

2010	M_Null	M1	M2	M3	M4	M5
Log-likelihood	-1404.9	-1388.6	-1383.2	-1388.7	-1380.6	-1377.1

Four days in 2010 with the highest number of fires are selected to investigate and demonstrate the prediction of the fire occurrence rate with the model (whose parameters were learnt by data for 2006-2009).

Figure 5.5 shows the expected number of fires as predicted by the models on October 8, 2010. This is the day with the highest number of fires in 2010 (5 fires). For the weather conditions and the components of the CFFWIS of that day see Figure 4.17 and Figure 4.18. The maps of Figure 5.5 illustrate the increasing model complexity in going from M1 to M5. Model M1 takes into account only the influence of FWI, whereas M2 includes also road density. For this reason, the prediction with M2 shows a bigger spatial variability than the one with M1. M3 includes additionally population density, and due to the high positive correlation between road and population density, the resulting map shows little difference to the map of M2. The map created with model M4 shows the influence of both FWI and land cover types, whereas the map produced with Model M5 is the result of the combination of models M4 and M3, including FWI, road and population density and land cover types.

In Figure 5.6 - Figure 5.8, the equivalent maps are shown for different days. Three fires occurred on these days. The resulting maps exhibit similar characteristics with those in Figure 5.5. Urban centers are clearly visible in the maps as the areas with permanent low expected fires predicted by all models.

Table 5.5 summarizes the predicted fire occurrence rates for each grid cell with fire occurrence on the investigated days. The model with the highest predicted rate is highlighted for each cell. Models M4 and M5 generally predict higher occurrence rates than model M1, which includes only the influence of FWI.

To assess the predictive power of the model, it is not sufficient to only focus on the prediction of fire occurrences. The prediction in all cells must be compared to account for the predicted probability when no fire occurred. It is reminded, that M5 had the best predictive power for the whole data set of 2010 as demonstrated in Table 5.4. The probability of the observed fire and no-fire events, as predicted by the models, in the entire area in 2010 can be compared. This probability is equal to the likelihood of the final models computed with the 2010 data.

Based on the predicted occurrence rate in each cell and day of 2010 in the study area, Table 5.6 shows the estimates of the log-likelihood of the whole study area with and without the fire cells. For example, on October 8 the log-likelihood of model M1 in the 5 cells with fires is -48.52. Therefore, the probability of these events according to M1 was $\exp(-48.52) = 8.5 \cdot 10^{-22}$. Likewise, the probability of not having any fires in the remaining cells is predicted as $\exp(-0.464) = 0.63$.
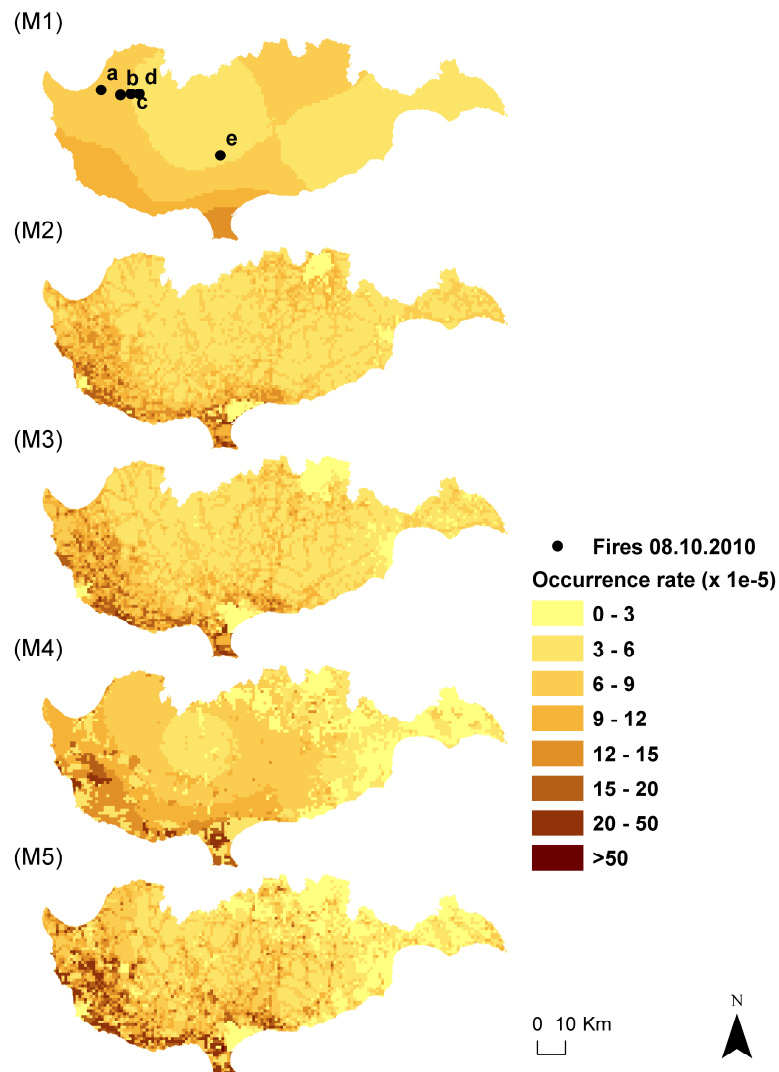
Figure 5.5: Expected fires predicted by different regression models on 8th October 2010 (day with maximum number of fires in 2010). Black dots represent the registered fires on this day (a – e). The predictions are estimated by the models M1, M2, M3, M4, M5
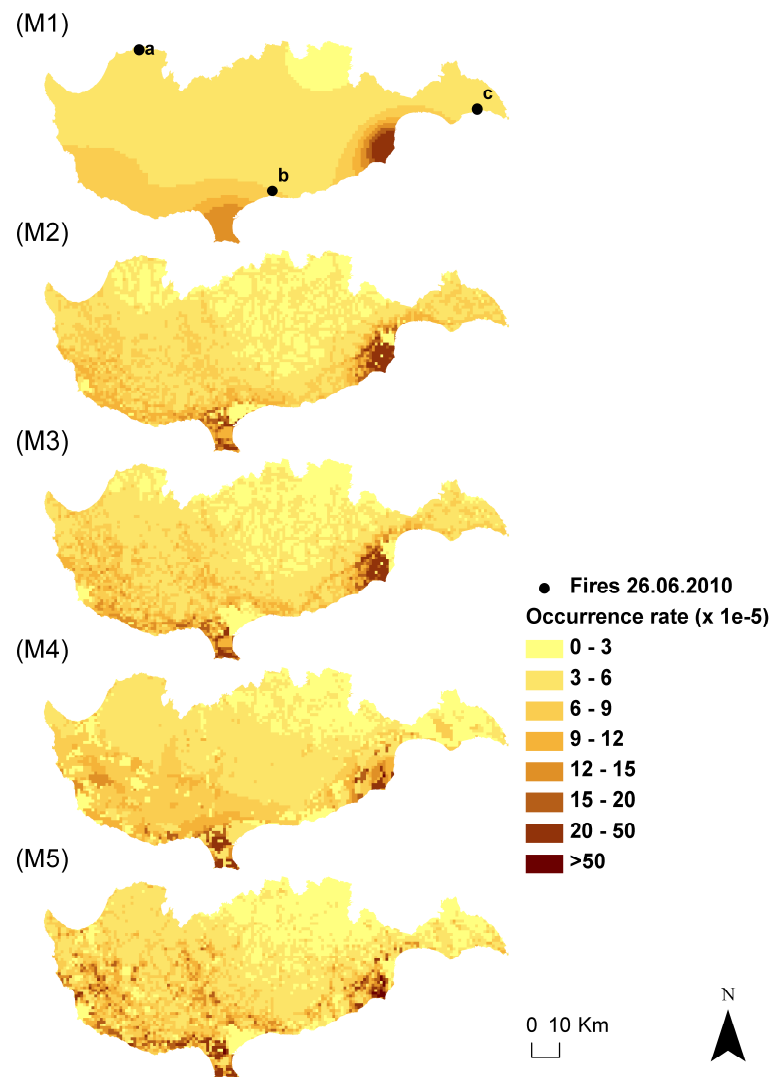
Figure 5.6: Expected fires predicted by different regression models on 26th June 2010 (day with second maximum number of fires and largest resulted burnt area (3.4 km² = 340 ha) in 2010). Black dots represent the registered fires on this day (a – c). The predictions are estimated by the models M1, M2, M3, M4, M5
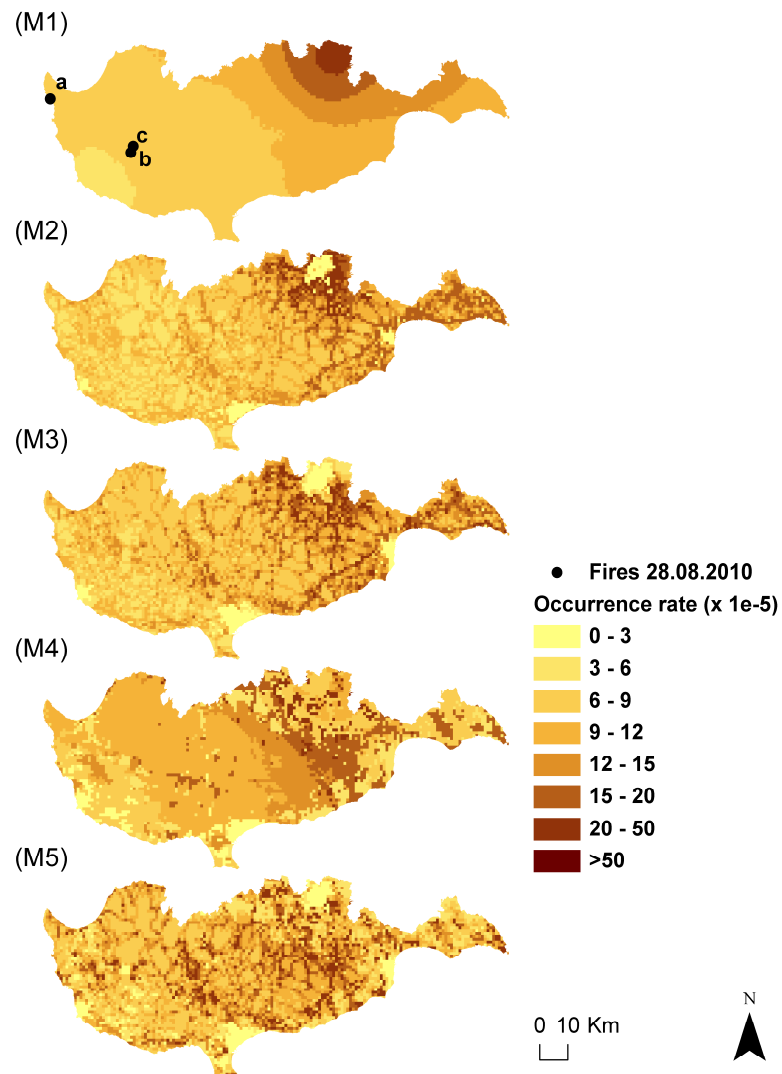
Figure 5.7: Expected fires predicted by different regression models on 28th August 2010 (day with second maximum number of fires (3 Fires) in 2010). Black dots represent the registered fires on this day (a – c). The predictions are estimated by the models M1, M2, M3, M4, M5
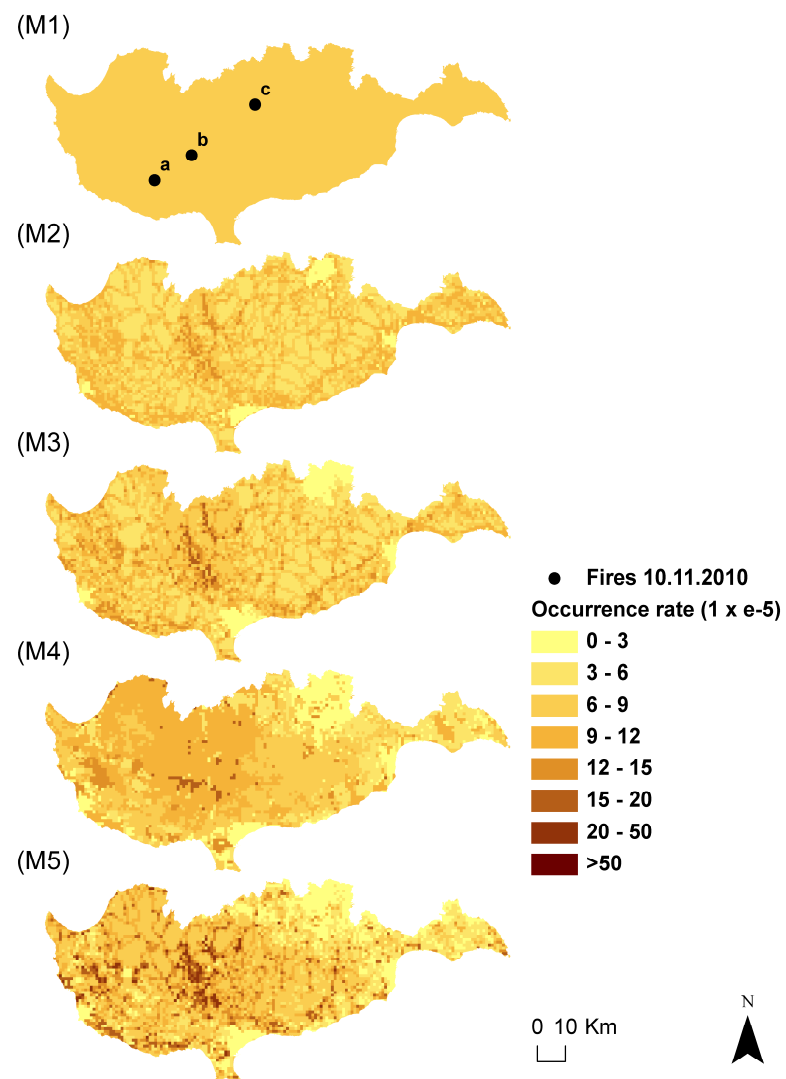
Figure 5.8: Expected Fires predicted by different regression models on 10th November 2010 (day with second maximum number of fires (3 Fires) in 2010). Black dots represent the registered fires on this day (a – c). The predictions are estimated by the models M1, M2, M3, M4, M5

Table 5.5: Predicted fire occurrence rate at the locations of fires shown in Figure 5.5 - Figure 5.8. The highest prediction rate in each case is highlighted in grey

		fire occurrence rate (x 10^{-5} d^{-1} km^{-2})				
	Models	M1	M2	M3	M4	M5
Day in 2010	Fire locations					
8 October	a	7.2	7.1	7.8	9.1	9.4
	b	6.4	4.6	5.1	8.1	6.4
	c	6.0	4.3	4.8	7.5	5.9
	d	5.7	6.3	7.0	7.0	8.8
	e	5.4	4.0	4.4	6.6	5.3
26 June	a	3.9	5.3	5.8	4.7	5.9
	b	6.2	8.4	8.6	7.6	10.9
	c	5.1	8.0	8.0	6.0	10.7
28 August	a	7.4	6.3	6.9	9.4	8.4
	b	6.7	8.6	9.5	9.1	10.3
	c	6.6	8.6	9.7	3.1	4.3
10 November	a	6.9	5.0	5.6	8.9	7.0
	b	7.8	6.0	6.5	16.6	10.5
	c	7.3	7.8	8.4	9.5	10.9

Table 5.6: Predicted log-likelihood values for cells with fires on the selected days in 2010 for models M_Null and M1 – M5. Values shown in parenthesis are the log-likelihood values for the cells without fire

Day in 2010	# fires	M_Null	M1	M2	M3	M4	M5
8 October	5	-49.4 (-0.3299)	-48.52 (-0.464)	-49.39 (-0.432)	-48.93 (-0.429)	-47.42 (-0.471)	-47.85 (-0.485)
26 June	3	-29.64 (-0.3299)	-29.72 (-0.406)	-28.66 (-0.380)	-28.55 (-0.377)	-29.17 (-0.349)	-28.00 (-0.378)
28 August	3	-29.64 (-0.3299)	-28.75 (-0.651)	-28.39 (-0.635)	-28.08 (-0.658)	-29.96 (-0.723)	-28.62 (-0.714)
10 November	3	-29.64 (-0.3299)	-28.56 (-0.461)	-29.08 (-0.464)	-28.82 (-0.484)	-27.29 (-0.509)	-27.85 (-0.508)
Log-likelihood for entire data of 2010		-1404.9	-1388.6	-1383.2	-1388.7	-1380.6	-1377.1

Table 5.5 shows that the best model is not always the one that predicts the highest occurrence rate for locations with observed fires, due to an over-prediction of the occurrence rate for locations without fires. The best model in each case is the one that best discriminates the locations with fire occurrences from those without. This is described by the sum of the likelihood values for all cells and all days. When considering the verifying data set 2010, the model M5 has the highest log-likelihood value, indicating the best prediction performance. Based on the learning data set, models M5 and M4 were found to perform best (Table 5.5). It may be therefore concluded that overall model M5 provides the best prediction.

The receiver operating characteristic (ROC) curves provide an additional indicator of the prediction performance of the models (Section 3.3.2.2). Figure 5.9 shows the corresponding ROC curves for the dataset of 2010 and each Model M1-M5. Model M5 has the largest AUC (Figure 5.9), i.e. it performs best among the other models, whereas model M1 has the lowest AUC.

The effect of the influencing variables on the probability of fire occurrence from the BN model of Figure 5.2 is shown in Table 5.7. The most influencing states are the higher values of FWI, the urban areas (population density 300-4000 People/km²) and the open spaces. The less influencing states are low road density (0-5 km/km²), shrubs and heterogeneous cultivation.

For the study area of South France, Figure 5.10 shows the predicted fire occurrence rate on the 25th July 2009, from models M1 and M5 (see also Figure 4.27 – Figure 4.29). With black dots the corresponding registered fire events (27 fires) on that day, which was the max daily amount of fires for 2009. The map results from the application of Eq. 5.2 on South France. The proposed models (M1 – M5) were not applied on South France, due to the size of the area and the time series. Nevertheless, in the next chapters (Chapter 7 and Chapter 8), applications of the BN models of fire effects and fire risk on South France are included.
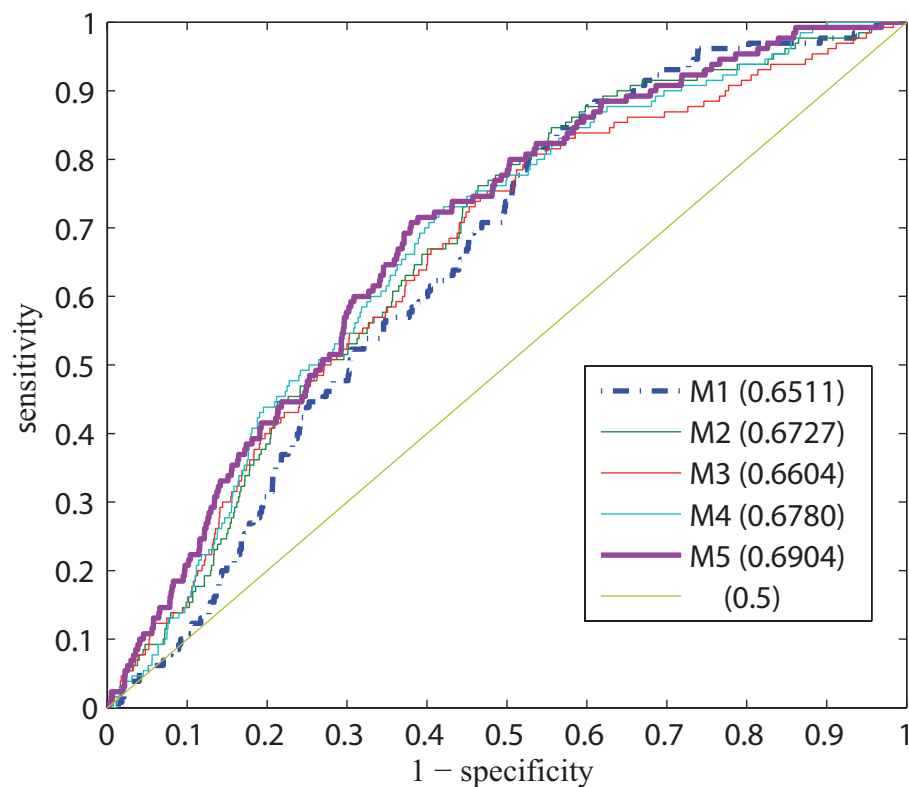
Figure 5.9: ROC curves and AUC values (in brackets) for models M1-M5

Table 5.7: Effect of influencing variables on fire occurrence probability

Variable	States	Pr(Fire) (x 10^{-5}) Prior: $9.45 \cdot 10^{-5}$	Change in Probability [%]
FWI	0-10	4.50	- 52
	10-30	7.22	- 24
	30-60	16.00	+ 70
	60-120	28.20	+199
Land cover types	1 : Urban/Wetland/Pastures	2.17	- 77
	2: Arable land	2.72	- 71
	3: Permanent crops	13.30	+ 40
	4: Heterogeneous agriculture	8.31	- 12
	5: Forests	18.00	+ 91
	6: Shrubs/Herb. vegetation	9.34	- 1
	7: Open spaces	22.10	+133
Population density	0-20	7.81	- 17
	20-300	7.78	- 18
	300-4,000	32.10	+240
Road density	0-0.5	9.36	- 1
	0.5-2	7.35	- 22
	2-26	11.60	+ 23

(a)

Occurrence rate (x 1e-5)

- 0 - 4
- 4 - 8
- 8 - 16
- 16 - 32
- 32 - 64
- 64 – 128
- 128 - 256
- 256 - 512
- 512 - 1024
- Fires 25.07.2009

(b)

N

0 25 50   100 Km
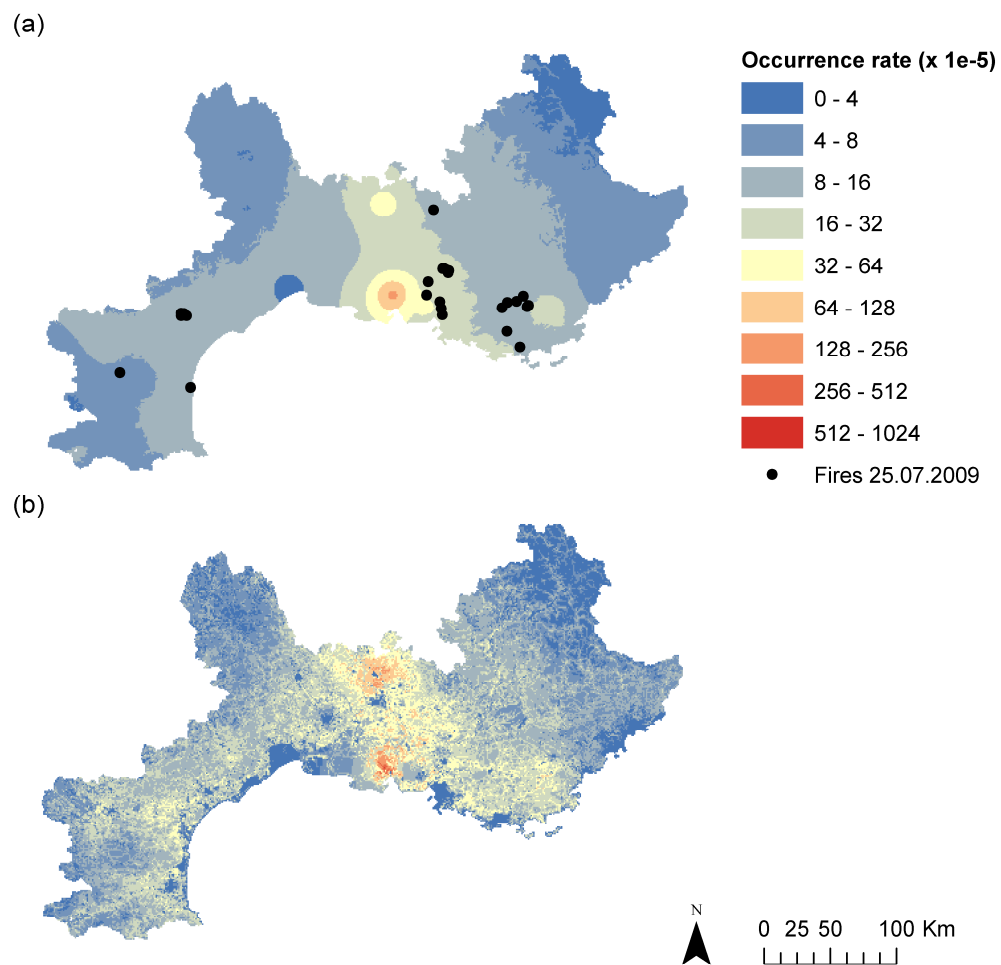
Figure 5.10: Expected fires predicted by different regression models on 25th July 2009 (day with maximum number of fires (27 fires). Black dots represent the registered fires on this day. The predictions are estimated by the models M1 (a) and M5 (b)

5.5   Summary

The investigations in Chapter 5 are a step towards an improved prediction of fire occurrence in the Mediterranean for fire management purposes. The probabilistic modeling approach selected provides a quantitative metric of the ability of different explanatory variables to predict daily fire occurrence. Of particular interest is the ability of the FWI, which was developed for Canada, to predict fire danger in the Mediterranean. In previous empirical studies, the components of the CFFWIS (FFMC - expressing fine fuel moisture, ISI - representing relative fire spread expected immediately after ignition and BUI - expressing moisture content of heavier fuels) were found to be relevant indicators for predicting people-caused fire occurrence in Canada (Martell et al. 1987; Martell et al. 1989; Wotton et al. 2003). As shown in this chapter, the FWI is a good indicator for fire danger also in the Eastern Mediterranean. However, it is also demonstrated that the prediction ability of FWI alone is limited. The component FFMC shows low prediction ability, due to the high values in fire season. A model that additionally includes land cover types, population density and road density is found to provide significantly improved predictions. However, care should be taken not to introduce redundant variables (e.g. both population and road density are higher in urban areas). This dependency must be considered when transferring the model to other regions. Due to the randomness of fire occurrence, there is a limitation to any prediction. Therefore, while the developed models are able to identify days and locations with higher fire risks, they are not - and will not - be able to deterministically predict fire occurrences in advance. Nevertheless, the predictions can support the planning of preventive and mitigating measures. Importantly, they also improve the understanding of influential factors and provide better predictions than models currently used, that take under account only FWI (e.g. European Forest Fire Information System-EFFIS).

6 Fire size model

Fires occur every year in fire prone areas and the vegetation is partly adjusted to this phenomenon. Most of the times the conditions do not favour radical fire spread and fires can be successfully contained. When weather conditions, topography and fuel accumulation favour fire spread, this leads to uncontrollable fires resulting to severe damages. Modelling of fire behaviour is an essential task for realistic fire risk management tools, in order to account for the specifics of extreme fire danger conditions. In this chapter a model representing influencing factors of severe fire events is presented and an application to the study area Cyprus is shown. Sensitivity analysis shows the influence of the factors on the resulting burnt area. Maps of the predicted burnt area conditional on specific days with high burnt areas of the dataset Cyprus 2010 are presented. Main part of what is presented here is based on Zwirglmaier *et al.* (2013).

6.1 Introduction

After a fire occurs, it depends on various factors, whether it will spread rapidly resulting to an uncontrollable fire with several hot spots. The main factors influencing fire spread are the topography of the area (slope and aspect), the weather conditions and the fuels (Rothermel 1983).

Many studies have investigated and have found critical the influence of the following factors on fire behavior; fuel type, structure and density (e.g. Rothermel 1972;Albini 1979;Dimitrakopoulos 2002;Stephens and Moghaddas 2005), wind and slope (e.g. Rothermel 1972;Rothermel 1983;Cruz *et al.* 2004) and fuel moisture (e.g. Van Wagner 1977;Albini 1979).

In literature, there are both physics-based and operational models predicting fire behavior (Scott 2006). Physics-based models are based on combustion chemistry, fluid dynamics and heat transfer (e.g. Butler *et al.* 2004;Cruz *et al.* 2006a;Cruz *et al.* 2006b). They demand intensive calculations and costly operations, for this they are not widely applied in fire management problems (Scott 2006;Mitsopoulos and Dimitrakopoulos 2007). Operational models are mathematical models based

on observations of unplanned and experimental fires (e.g. Stocks *et al.* 2004). They have great speed of calculations and can be easily used and therefore can be applied at large temporal and spatial scales on fire management problems. Although physics-based models can be applied widely, operational models can be applied to conditions similar to the ones on which they have been built. Also semi-empirical model exist, that are a combination of heat transfer analysis, laboratory experiments, computer simulations and heat observations (e.g. Van Wagner 1977) (Dimitrakopoulos *et al.* 2007). Some of the outputs of the above models are flame length, flame height, frontal fire intensity, rate of spread, type of fire etc.

The fire behavior models can also be classified based on the type of fire they predict (Johnston *et al.* 2005) into surface fire behavior models (e.g. Rothermel 1972) and crown fire behavior models (e.g. Van Wagner 1993).

Both deterministic and probabilistic approaches for predicting fire behavior and fire size can be found in the literature. Deterministic approaches are semi-physical or semi-empirical models that combine physical equations of heat generation and transfer with characteristics of the fuels and are calibrated with empirical data (Schaaf *et al.* 2007). Probabilistic approaches are more recent and use e.g. logistic regression techniques to predict crown fires (e.g. Cruz *et al.* 2003;Cruz *et al.* 2004) or large fire occurrence (e.g. Preisler *et al.* 2004;Bradstock *et al.* 2009;Finney *et al.* 2011) and cellular automaton approaches (e.g. Hargrove *et al.* 2000;Johnstone *et al.* 2011). Probabilistic approaches have the limitation that they lack physical reasoning (Schaaf *et al.* 2007).

For decision making, there are fire management applications, which include one or more models or systems and give as output characteristics of the fire (e.g. fire growth simulation, fire spotting) and thus support fire management (Cruz and Alexander 2010). In fire simulators fire starts from a source, spreads outward growing in size, assuming an elliptical shape with the major axis in the direction most favorable to spread (Rothermel 1972). Such applications widely used are the Canadian Forest Fire Behavior Prediction System (Forestry Canada 1992), NEXUS (Scott 1999), FARSITE (Finney 2004), FlamMap (Finney 2006), BehavePlus (Andrews 2009), PROMETHEUS (Tymstra *et al.* 2010) and PHOENIX RapidFire (Chong *et al.* 2012). The empirical models of Rothermel (1991) and Van Wagner (1993) are incorporated in these applications.

The Canadian Forest Fire Behavior Prediction System (Forestry Canada 1992) is a subsystem of the Canadian Forest Fire Danger Rating System. Its operational models for spread rate and fuel consumption were derived from empirical studies. As inputs are used fuel types, the components FFMC, ISI and BUI of the CFFWIS, wind speed and direction, topography (percent slope and upslope direction), foliar moisture content and the type and duration of the prediction. The system gives primary and secondary outputs. Primary outputs are rate of spread, fuel consumption, head fire intensity and fire description. Among the secondary outputs are fire area and perimeter and head, flank and back fire spread distances.

FARSITE is a fire area simulator, that produces vector fire perimeters (polygons) at specific time intervals (Finney 2004). It incorporates several models of surface and crown fire, point-source fire accelerator, spotting and fuel moisture. The vertices of the produced polygons give information on the spread rate and the fire intensity. These are interpolated to produce raster maps of fire behavior, thus a 2d simulation of fire behavior. The input variables are topography (elevation, slope, aspect), fuel model, canopy cover, crown characteristics, temperature, humidity, precipitation, wind speed and direction.

BehavePlus Fire Modeling System (Andrews 2009) is the successor to BEHAVE (Andrews 1986) and is broadly used for wildland fire prediction. The system models fire behavior and effects. It incorporates different mathematical models for fire behavior, fire effects and fire environment based on specific fuel and moisture conditions. It gives as output among others rate of spread, flame

length, spotting distance, scorch height, tree mortality and fuel moisture. Several input variables are required, such as fuel models, fuel load characteristics, fuel surface area-to-volume ratios, fuel heat content, P-G (palmetto-gallberry) fuel characteristics, canopy characteristics, fuel moisture characteristics, wind speed characteristics, temperature and terrain variables.

In this chapter a fire behavior model that predicts burnt area in the meso-scale is introduced. This model is based on Zwirglmaier *et al.* (2013), where the structure of different BN models is learnt with data and their predictive ability is compared. In contrast to the above described prediction systems, this model aims to give expected burnt area of fires in 1 km² spatial resolution and does not consider the elliptical form of the fire. The model combined with the previously described fire occurrence model (Chapter 5) serves as a fire hazard model. The proposed model uses weather conditions, fuel types, fuel moisture and topography as input variables. The model is applied to the study area of Cyprus (2006-2009).Year 2010 is used as a verification dataset to make predictions. The resulting predictions are shown in maps and diagrams.

6.2   Probabilistic model for predicting fire size

The fire size model presented in Figure 6.1 is adapted from Zwirglmaier (2012) and Zwirglmaier et al. (2013). The variables are chosen from a wider range of potential variables to represent the processes influencing the resulting burnt area of a fire. The variables were selected as a result of BN model structure with automatic structure learning algorithms. The process followed to achieve the structure of the proposed model and the CPTs of the variables is described later on in Section 6.3.

As already mentioned above the main factors influencing fire behavior, and as a result fire size are the type and accumulation of fuels, the fuel moisture, the weather conditions and the topography. Type and accumulation of the fuels are here described by land cover types. The fuel moisture is expressed by the components of the CFFWIS. Weather conditions are expressed by the variables temperature, relative humidity, wind speed, wind direction and precipitation, which influence also fuel moisture. Different time steps are included, which are based on the availability of data (21 days, 14 days, 7 days, 3 days, 1 day, actual). Wind and Topography are described by the directly observable variables wind speed, wind direction, slope and aspect. The relative direction of the wind to the slope is included as the difference between aspect and wind direction. In the fire size model, the target/predicted node is *Burnt area*. Although other variables can express more accurately fire behavior (e.g. fire intensity, rate of spread, spotting activity), here due to the availability of data fire size will be described by the resulting burnt area.

In the proposed model, *Burnt area* is influenced by *Fire occurrence*, *Land cover* types, *Topography*, *Recent weather conditions*, and *Fire behavior indices*. The latter three are hidden variables, meaning that there are no available observations for them and their CPTs are learned via the EM algorithm (see also Section 3.1.1). They are included to reduce the number of parents of the node *Burnt area*. *Topography* combines the influence of the variables *Wind Speed* [km/h], *Slope* [°] and *Aspect Minus Wind Direction* [same, opposite, perpendicular]. *Recent weather conditions* summarizes the effect of Relative humidity (*RH*) [%], *Mean RH over the last 3 days* [%], *Mean RH over the last 21 days* [%], *Accumulated precipitation over the last 21 days* [mm], *Mean temperature of the last day* [°C] and *Mean temperature over the last 7 days* [°C]. *Initial fire behavior* influences the three indices of the CFFWIS, namely Fine Fuel Moisture Code (*FFMC*), Initial Spread Index (*ISI*) and Build-up index (*BUI*).

The BN for fire occurrence (Chapter 5) is included in the BN for fire behavior. The fire occurrence model triggers the fire size model. The variable *Fires* is a parent node of the variable *Burnt area, so*. The variable *Land cover*, which is used for predicting the *Fire occurrence rate*, is also influencing the *Burnt area* directly. However, the node *LC grouped* is introduced to group the land cover types grouped in fewer classes. This reduces the number of free parameters of the variable *Burnt area* and facilitates parameter learning with hidden variables (EM algorithm).
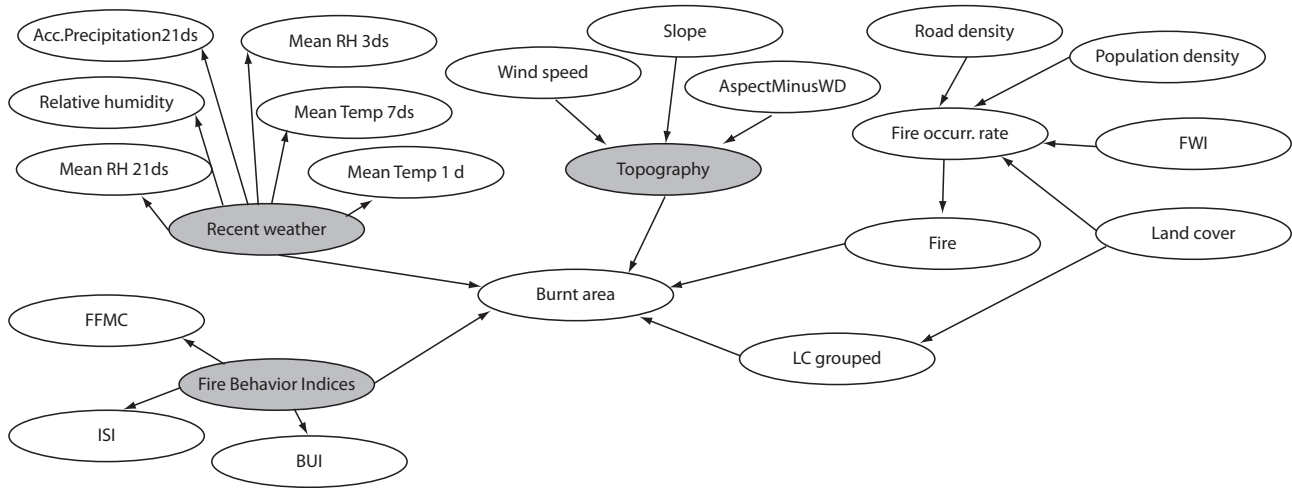
Figure 6.1: Bayesian network for the prediction of Burnt area. Hidden variables are shown in grey. Indices of the CFFWIS - FWI: Fire Weather Index, FFMC: Fine Fuel Moisture Code, ISI: Initial Spread Index, BUI: Built-Up Index.

6.3 Model structure, nodes discretization and parameter estimation

In order to achieve the structure of the BN for burnt area prediction, the first step is to select the overall relevant variables to account for the influencing factors on fire size. Among the variables, which are indirectly influencing burnt area, it is not clear which of the variables are relevant, non-informative or redundant. Moreover, it is also not clear how the variables influence each other, so a graph representing causal relationships cannot be easily obtained. Since knowledge is unavailable, observations can be used to learn automatically the structure of the model. In the case of a large amount of variables, structure learning has limitations.

The structure of a BN can be learned by either a score-based approach, where among several generated candidate graphs the one with the highest score (Bayesian Information Criterion, Akaike Information Criterion) (Section 3.3.2.1) is selected, or a constraint-based approach, where a graph is constructed based on the independence properties derived from the data (Zwirglmaier *et al.* 2013).

The proposed model is based on structure learning by constraint-based approach. Two algorithms have been used to generate model structure and identify relevant variables. The PC algorithm and the NPC algorithm (Necessary Path Condition). Both algorithms generate in the first step an undirected graph and in the second step the links between the variables are oriented. They perform independence tests on a dataset, thus for each pair of variables a set of nodes is found for which these variables are conditionally on this set of nodes independent according to the data. If all

the derived independence properties are actual properties of the underlying distribution and not due to random noise, then the PC algorithm will give the correct undirected graph. The NPC to overcome the problem of random noise checks the independencies for consistency. Based on generated conditions for each of the links in the graph, the NPC results to the shortest possible necessary path. To orient the links, the converging connections (Section 3.1) are first oriented and then the remaining links are oriented in a way that no further converging connections and no directed cyclic paths are created.

The structure learning process is limited, when large amount of variables is involved. Here, smaller graph structures are learned and based on the resulting links, the relevant variables are identified. Weather conditions are taken in different time steps and their relevance to burnt area is investigated E.g. among the variables *Accumulated precipitation* of the last 21 days, 14 days, 7 days, 3 days, 1 day and actual, the variable of the last 21 days was identified to be of greater importance and was included in the final model. The same time steps were checked for temperature and relative humidity and the relevant ones were chosen. The final model is then constructed based on relevant variables and phenomenological reasoning.

The relevant variables are grouped and the dependencies between these groups are modeled with the hidden variables *Topography*, *Recent Weather*, *Fire Behavior Indices* (Figure 6.1). The hidden variables are not observable and their parameters are learnt with the EM algorithm (Section 3.1.1). In this way, the joint influence of a set of variables can be modeled, reducing the number of links to the target variable (Straub and Der Kiureghian 2010), and less parameters are needed to specify the model. The variable *Topography* expresses the combination of the influence of the variables *Wind speed*, *Slope* and *AspectMinusWindDirection.* In order to model dependencies between the variables *FFMC*, *BUI* and *ISI*, which were found relevant, the variable *Fire Behavior Indices* is introduced as a common parent. The variable *Recent weather* is introduced as a common parent of the relevant weather parameters.

The variable *Land cover* of the fire occurrence model has 7 states. To reduce the number of parameters needed to specify the CPT of the target variable *Burnt area*, the variable *LC grouped* is introduced, which groups the initial *Land cover* types into 3 classes (Table 6.1). The three states of the *LC grouped* are defined based on data from Cyprus 2006-2009 related to the mean fire size in each *Land cover* class (Table 6.2). The first class includes urban/wetland/pasture, heterogeneous agriculture and shrubs, which had the highest mean fire size. The second class includes arable land, forests and permanent crops, whose mean fire size follows. Open spaces are assigned to the third class.

Table 6.1: LC grouped with respect to Land cover types

LC grouped	Land cover
1	1: Urban, wetland, pasture 4: Heterogeneous agriculture 6: Shrubs/Herbaceous
2	2: Arable land 3: Permanent crops 5: Forests
3	7: Open spaces

Table 6.2: Burnt area, number of fires and mean fire size for different land cover types on Cyprus (2006-2009)

Land cover class	Burnt area [km²]	No. Fires	Mean fire size [km²]	% burnt area
1.Urban/wetland/pasture	12.39	33	0.38	13.89
2.Arable land	5.62	53	0.11	6.24
3.Permanent crops	1.77	34	0.05	1.99
4.Heterogeneous agric.	33.24	123	0.27	37.28
5.Forests	5.84	101	0.06	6.55
6.Shrubs/Herbaceous	30.25	131	0.23	33.92
7.Open spaces	0.06	5	0.01	0.07
Sum	89.17	480		100

In order to perform inference in the BN model, the continuous random variables which should be included in the BN are discretized with the class-attribute interdependence maximization measure (CAIM) (Kurgan and Cios 2004). This method maximizes the interdependency between an indicator variable and the target variable (here the *Burnt area*) but does not account for the possible interdependencies between indicator and target variables when considered together. Therefore, since the variables *Wind speed*, *Slope* and *AspectMinusWindDirection* influence *Burnt area* jointly, they are discretized using equal frequency discretization.

The variable Burnt area is discretized with exponential binning based on Zwirglmaier *et al.* (2013) and Scherb (2014). The four intervals are chosen with exponential alike character. Table 6.3 summarizes the exponential binning of the Cyprus data (2006-2009) based on the resulting burnt area and the occurring fires. Most of the fires of the dataset resulted to a small burnt area ($0 - 0.01$ km²) and only 18 fires ended to bunrt area > 1 km². The resulting states of all variables are shown in Table 6.4. The parameters of the model are then learnt with data from the study area Cyprus (2006-2009) (Section 4.2).

Table 6.3: Exponential binning of the variable burnt area for Cyprus 2006-2009 (Scherb 2014)

	Burnt area 2006-2009 [km²]			
	[0-0.01]	[0.01-0.1]	[0.1-1]	[1-inf]
Area [km²]	0.6281	5.8348	17.4915	65.213
Fire count	274	138	50	18
Mean area [km²]	0.0023	0.0423	0.3489	3.623

Table 6.4: Variables, number of states and state description of the fire size model

Variable	No. states	State description
Burnt area [km²]	4	0-0.01 0.01-0.1 0.1-1 1-inf
FFMC	3	0-86.2 86.2-88.6 88.6-99
BUI	3	0-84.1 84.1-281.8 281.8-inf
ISI	3	0-3.9 3.9-26.6 26.6-inf
Fire behavior indices	2	moderate low
Land cover type (LC) grouped	3	1: 1,4,6 2: 2,3,5 3: 7
Sum precipitation 21 days [mm]	3	0-15.2 15.2-33.2 33.2-inf
Relative humidity [%]	4	0-26.3 26.3-68.4 68.4-73.2 73.2-100
Mean rel. humidity 3days [%]	4	0-50.5 50.5-61.8 61.8-67.1 67.1-100
Mean rel. humidity 21days [%]	3	0-38.1 38.1-51.5 51.5-100
Mean Temperature 1day [°C]	4	-inf-21.8 21.8-31.1 31.1-32 32-inf
Mean Temperature 7 days [°C]	3	-inf-21.8 21.8-30.4 30.4-inf
Recent weather	4	dry moderate dry moderate humid humid
Wind speed [km/h]	4	0-11.6 11.6-15.1

		15.1-19.2
		19.2-inf
Slope [°]	4	0-4
		4-8
		8-15
		15-90
AspectMinusWindDirection	3	same
		perpendicular
		opposite
Topography	3	middle
		gradual
		steep

6.4   Results

The dataset 2010 is used to demonstrate the predictive ability of the model. Figure 6.2 shows the pathway of the daily sum of the predicted burnt area over the 6447 cells of the study area. As expected the prediction increases during the late spring until autumn. Note that this is the sum of the predictions over the study area and that the daily predictions vary a lot between the study area cells. Figure 6.3 shows the predicted burnt area per land cover type. The highest values are predicted for shrubs/herbaceous vegetation (type 6, burnt area= 18.27 km²), heterogeneous cultivations (type 4, burnt area=14.62 km²) and forests (type 5, burnt area=7.93 km²).
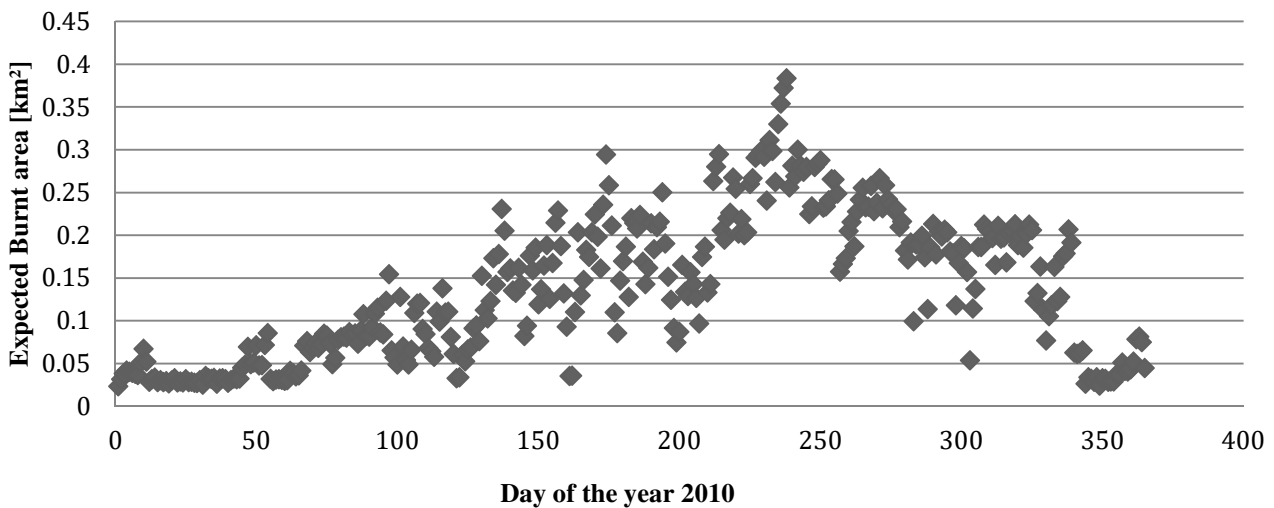
Figure 6.2: Daily expected sum of burnt area [km²] for the dataset Cyprus 2010
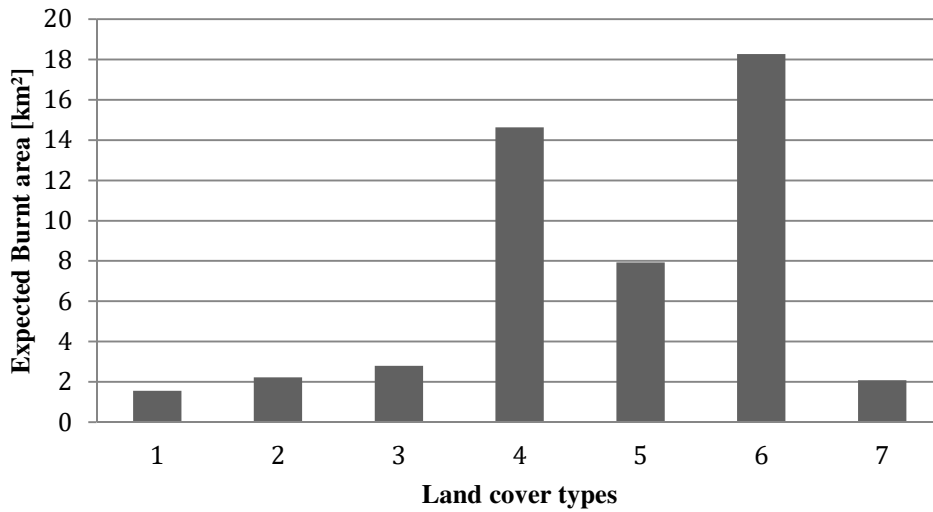
Figure 6.3: Expected burnt area [km²] per land cover type for the dataset Cyprus 2010

Table 6.5 shows a confusion matrix and the accuracy values of the model. The confusion matrix presents for each combination of predicted interval and observed interval the number of corresponding cases. These predictions are conditioned on a fire occurrence. The model predicts better the fires of the first interval (0-0.01 km²) and performs worse for higher burnt areas (1-inf km²). The overall correctly predicted burnt area for the year 2010, B, can be calculated, by taking the mean value of the actual burnt area in the intervals and multiply it with the diagonal values of the confusion matrix, thus with the number of correctly predicted burnt areas. For the last interval $[1 - inf]$, the mean value of the recorded burnt area is 3.6229 km². The overall predicted burnt area is then,

$$
\begin{aligned}
B &= 52 \cdot 0.0023 \text{ km}^2 + 14 \cdot 0.0423 \text{ km}^2 + 2 \cdot 0.3498 \text{ km}^2 + 0 \cdot 3.6229 \text{ km}^2 \\
&= 1.41 \text{ km}^2
\end{aligned}
\tag{6.1}
$$

The actual value of the burnt area for 2010 is 17.5 km² resulting from 131 fires. Four bigger fires in the interval $[1 - inf]$ resulted in 10.47 km² and 13 fires in the interval $[0.1 - 1]$ resulted in 5.47 km². The rest of the fires from the first two intervals ($[0 - 0.01]$ and $[0.01 - 0.1]$) resulted in 1.54 km². This shows that the proposed model is rather weak in predicting fires of higher resulting burnt area. Nevertheless, the model performs well for fires with small resulting burnt areas. This is due to the fact that in the learning dataset of the model (Cyprus 2006-2009) most of the fires registered resulted in a burnt area of the first interval $[0 - 0.01]$. As a result the model performs better for this interval.

Table 6.5: Confusion matrix and accuracy values of the fire size model for the validation dataset Cyprus 2010

Actual burnt area [km²]	Predicted burnt area for 2010 [km²]					Accuracy		
	[0-0.01]	[0.01-0.1]	[0.1-1]	[1-inf]	sum		%	Fraction
[0-0.01]	52	16	3	0	71		0.73	52/71
[0.01-0.1]	22	14	6	0	42		0.33	14/42
[0.1-1]	7	4	2	0	13		0.15	2/13
[1-inf]	2	2	0	0	4		0	0/4
					130	Overall	0.52	68/130

Table 6.6 shows a sensitivity analysis of the model. Evidence is given in each state of the variables and the information is propagated in the network. The prior probability of the variable Burnt area being > 0.1 km² is updated to the posterior. The most influencing state of the land cover type is open spaces. This is due to shortage of available data for this land cover type (i.e. only 5 fires occurred in open spaces in 2006-2009 resulting to 0.06 km², see also Table 6.2). Steep topography increases the probability of having burnt area > 0.1 km² by 69%. Humid recent weather lowers the same probability by 34% and dry recent weather increases the probability by 46%.

Table 6.6: Influence of variables on burnt area

Variable	States	Pr(BurntArea>0.1) Prior=$1.70 \cdot 10^{-5}$	Change in Probability [%]
LCgrouped	1: 1,4,6	$1.65 \cdot 10^{-5}$	-3
	2: 2,3,5	$1.56 \cdot 10^{-5}$	-8
	3: 7	$6.54 \cdot 10^{-5}$	+284
Topography	1:middle	$1.97 \cdot 10^{-5}$	+16
	2:gradual	$8.59 \cdot 10^{-6}$	-50
	3:steep	$2.88 \cdot 10^{-5}$	+69
Recent weather	1: dry	$2.49 \cdot 10^{-5}$	+46
	2: moderate dry	$1.82 \cdot 10^{-5}$	+7
	3: moderate humid	$1.28 \cdot 10^{-5}$	-25
	4: humid	$1.12 \cdot 10^{-5}$	-34
Fire behavior indices	1: moderate	$1.78 \cdot 10^{-5}$	+4
	2: low	$1.35 \cdot 10^{-5}$	-21

To demonstrate the coupling of the BN with the GIS, four days of the year 2010 are selected, the days with the maximum resulting burnt area. The day with the largest burnt area is the 6th June (4.3 km²). Large fires occurred also on the 22nd August (1.15 km²) and 14th November (2.22 km²). On the 1st January 2010 the model predicts very low burnt area in the whole study area. On the 6th June 2010 the values raise mainly on the eastern side of the study area, whereas on the 22nd August 2010 the highest values of burnt area on individual cells are predicted. The predicted values are lower on the 14th November 2010. Table 6.7 summarizes the accumulated predicted burnt area [km²] over the study area. The highest value is predicted for the 22nd August 2010. Since these are the extreme days of the year 2010, it is expected that the model underestimates the burnt area.

When choosing the days with the highest fire occurrences in 2010 (see also Figure 5.5 – Figure 5.8) the resulting prediction is shown in Figure 6.5. For these days the model predicts values closer to the actual resulting burnt area (Table 6.8).

Table 6.7: Accumulated predicted expected burnt area, mean and standard deviation [km²] for days of 2010 with maximum registered burnt area, together with the actual burnt area. The results are conditional on fire occurrence

Date	Accumulated predicted expected Burnt area [km²]	Mean [km²]	Standard deviation	Actual Burnt area [km²]
01.01.2010	0.02	$4 \cdot 10^{-6}$	$3 \cdot 10^{-6}$	0
06.06.2010	0.23	$36 \cdot 10^{-6}$	$31 \cdot 10^{-6}$	4.3
22.08.2010	0.26	$41 \cdot 10^{-6}$	$57 \cdot 10^{-6}$	1.15
14.11.2010	0.21	$32 \cdot 10^{-6}$	$28 \cdot 10^{-6}$	2.22

Table 6.8: Accumulated predicted expected burnt area, mean and standard deviation [km²] for days of 2010 with maximum fire occurrences, together with the actual burnt area. The results are conditional on fire occurrence

Date	Accumulated predicted expected Burnt area [km²]	Mean [km²]	Standard deviation	Actual Burnt area [km²]
26.06.2010	0.11	$17 \cdot 10^{-6}$	$29 \cdot 10^{-6}$	3.4
28.08.2010	0.28	$44 \cdot 10^{-6}$	$54 \cdot 10^{-6}$	0.0034
08.10.2010	0.17	$27 \cdot 10^{-6}$	$31 \cdot 10^{-6}$	0.0005
10.11.2010	0.20	$30 \cdot 10^{-6}$	$26 \cdot 10^{-6}$	0.0654
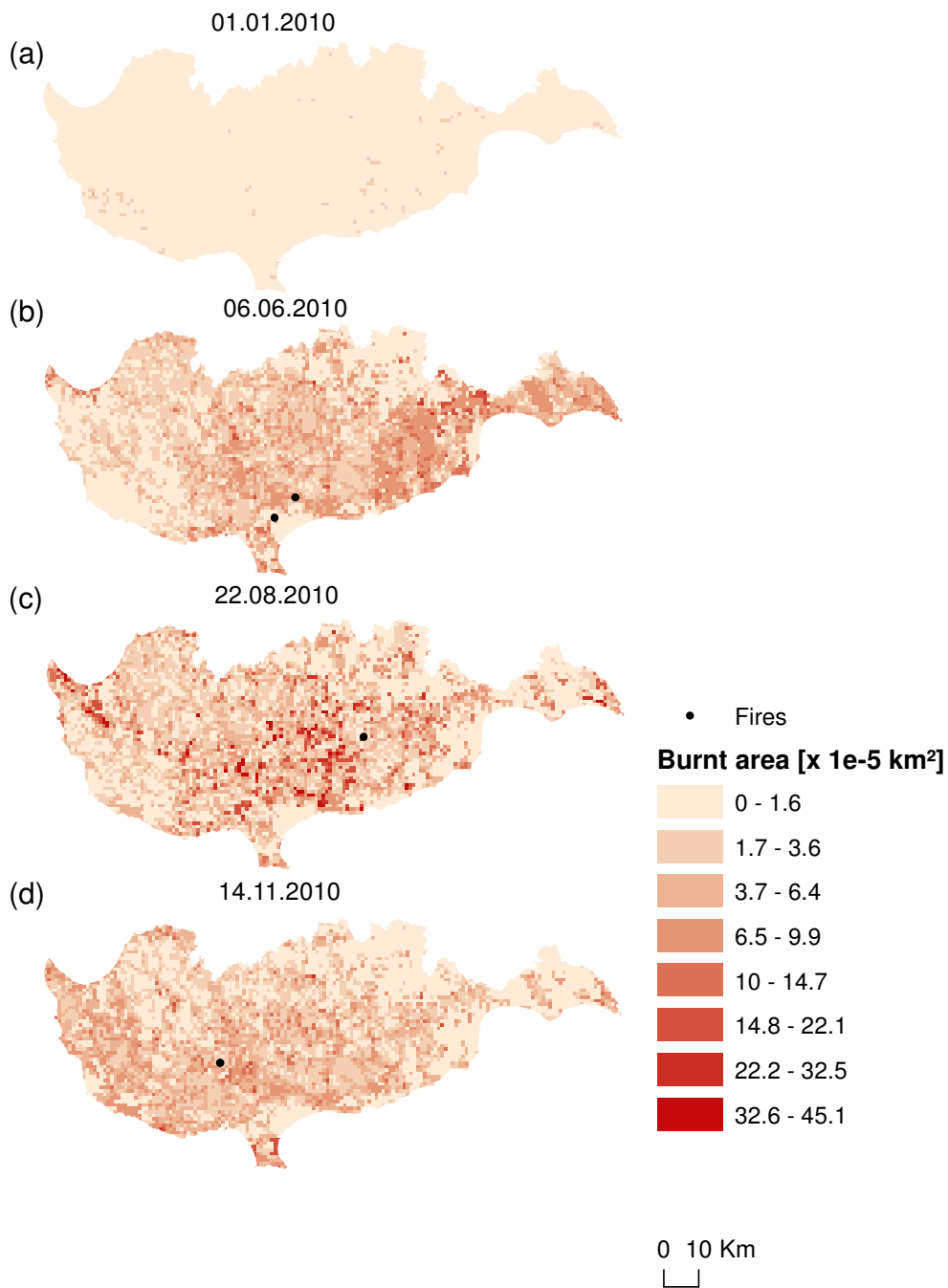
Figure 6.4: Predicted burnt area [km²] on days of 2010 with max recorded burnt area (in brackets the real burnt area):
(a) 1st January (no fire events), (b) 6th June (4.3 km²), (c) 22nd August (1.15 km²), (d) 14th November (2.22 km²)
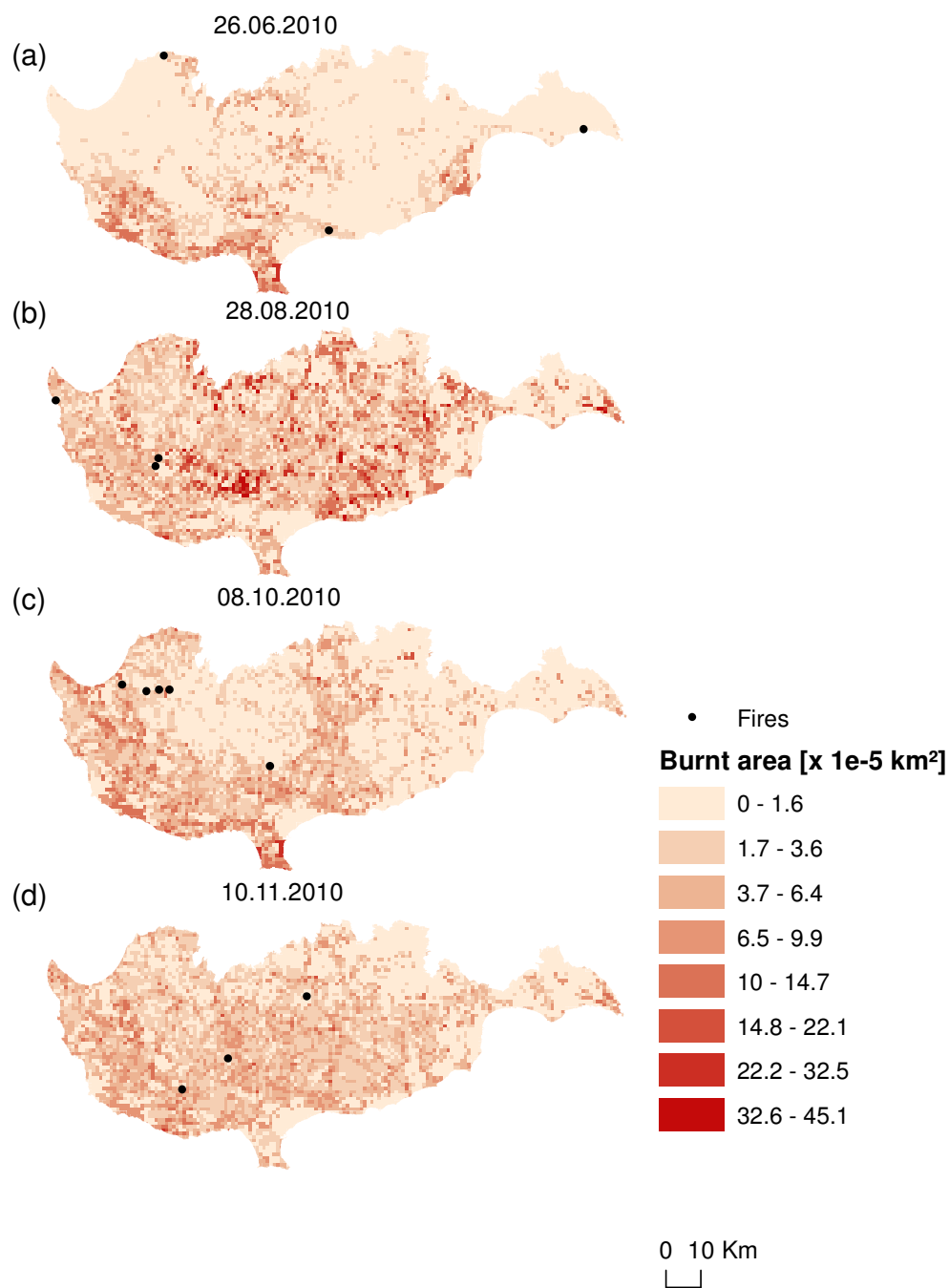
Figure 6.5: Predicted burnt area [km²] on different days of 2010 with max recorded fire occurrences (in brackets the real burnt area): (a) 26th June (3.4 km²), (b) 28th August (0.0034 km²), (c) 8th October (0.0005 km²), (d) 10th November (0.0654 km²)

6.5   Summary

Chapter 6 introduces a fire size model at the meso-scale that predicts resulting burnt area [km²] is introduced. The model takes into account land cover types, initial fire behavior conditions (as expressed by ISI and BUI of the CFFWIS), topography (wind speed, slope and aspect minus wind direction) and recent weather conditions (e.g. accumulated precipitation over the last 21 days). Contrary to fire behavior models, which use fuel models to estimate fuel flammability and fire spread potential, the proposed model utilizes land cover types and therefore offers fire size predictions. Hidden variables – thus non-observable variables - are implemented in the modeling to reduce the dimensions of the CPT of the child variable burnt area and therefore to facilitate the learning process. The parameters of the model are learnt with data from Cyprus for 2006-2009 with the EM algorithm. As validation dataset is chosen the dataset Cyprus 2010. The daily accumulated burnt area over the whole study area for 2010 is calculated. The model predicts higher burnt areas during the season spring to autumn, as a result of dryer weather conditions. The model predicts better smaller fires (0-0.01 km² burnt area), due to the fact that these fires are highly represented in the learning dataset Cyprus 2006-2009. Eight representative days of 2010 (one in the winter period with no fires occurring, three with the maximum resulting burnt areas of the year and four with the highest number of fire occurrences) are chosen to visualize the prediction ability of the model.

7 Fire effects model

Wildfire effects estimation regarding direct losses on structures is sparsely investigated in the literature, and often focuses on certain case studies, which do not result in generalized wildfire effects predictive models.

In this chapter, two fire effects models are introduced that quantify the potential damages to houses and to vegetated areas in the meso-scale. The parameters of the models are learnt with data from Cyprus and Greece. The models predict the expected damage cost [€] under specific hazard characteristics, either for known fire events or for hypothesised conditions of the whole study area. Data from Cyprus and South France are used to demonstrate the predictive ability of the models. The proposed models will be incorporated with the fire occurrence and fire behaviour model to quantify fire risk to houses and vegetated areas in Chapter 8.

7.1   Introduction

Various investigations in the literature concern the influence of the fires on the vegetation. However, research devoted to assessing the effects of wildfires on construction damages is relatively limited and the interest on quantitative models has been quite recent. Some studies examined the correlation of house losses to weather-related fire danger classification indices (e.g. Blanchi *et al.* 2010;Harris *et al.* 2012), to their arrangement and location (e.g.Syphard *et al.* 2012) and to fuel variables and their distance from houses (e.g. Gibbons *et al.* 2012). Other studies assessed the vulnerability of houses in conjunction with ecosystem characteristics (e.g. biodiversity, conservation status) (e.g. Chuvieco *et al.* 2013). The literature in this field also includes a significant number of case studies documenting house damages due to wildfires (e.g. Lynch 2004;Xanthopoulos 2008). However, these case studies do not result in generalized predictive

models that allow performing cost assessments at other sites with similar conditions. Reports on community wildfire protection plans use rating systems to assess wildfire occurrence danger and effects (Ohlson *et al.* 2003;OFD 2004;ECONorthwest 2007). Rating systems are also often used to evaluate the susceptibility of items at risk and the degree of loss on the basis of expert knowledge (Tutsch *et al.* 2010;Penman *et al.* 2013). Moreover, empirical research on the subject is hindered by incomplete, sporadic and aggregated documentation of effects of past events (Gibbons *et al.* 2012). The above highlight the need for better tools for the prediction of expected effects due to fires to support fire management decisions.

As already described in Section 2.1 (Eq. 2.2), the expected consequences for given hazard characteristics (risk) can be expressed as,

$$R(h) = \mathrm{E}_D[C \mid H = h] = \int_D \mathrm{f}(d|h)\, C(d,h) dd \qquad (7.1)$$

wherein $\mathrm{E}_{H,D}$ denotes the expected value with respect to D. $\mathrm{f}(d|h)$ describes the vulnerability as the probability of damage D conditional on the hazard H, i.e. it, and $C(d,h)$ is the cost as a function of damage and hazard.

Here, the expected cost from house losses or from vegetated area losses conditional on fire hazard characteristics $\mathrm{E}_D = [C|H]$ is estimated. In order to quantify consequences, vulnerability and exposure indicators are identified, which are related to the degree of loss and the items at risk. A wildfire effects assessment system at the meso-scale is developed, i.e. at a 1km^2 spatial resolution. Exemplarily, the system focuses on damages to houses and to vegetated areas, expressed in monetary values. It is based on a BN model, which includes variables expressing hazard characteristics, houses and vegetated areas at risk and their susceptibility. As a case study, the proposed BNs are applied to Cyprus. The parameters of the models are learnt with both data and expert knowledge. Past wildfire disaster events from the period 2006-2010 are chosen to demonstrate the predictive ability of the house damage model. The BNs are coupled with a Geographic Information System (GIS) and maps of expected effects with evidence given to hazard characteristics are provided to illustrate the results. The predictions are compared with the damages registered in the NatCatSERVICE database of the reinsurance company Munich Re.

7.2   Factors influencing house damage

Losses due to wildfires are influenced by both natural and anthropogenic factors. The main factors influencing fire losses are the presence and intensity of the fire, the flammability of the exposed objects and the suppression effectiveness. Interrelations of the influencing factors are present, e.g. fire characteristics and flammability of items influence the result of fire suppression. For houses, the main factors influencing losses are fire characteristics (flame length, fire intensity, spread rate, burning ember density), house design and construction materials, the surroundings of the house (defensible space, distance from forest, fuel accumulation) and fire suppression effectiveness (Blanchi *et al.* 2010;Gibbons *et al.* 2012).

Houses usually either survive a fire or get totally destroyed (Cohen 2000;Blong 2003). Combustion requires all three fire triangle elements (fuel, heat, oxygen) (Figure 2.3), and a house will only ignite if all elements are present. Fire impact may include convective heating or direct contact of the flames, radiant heat flux from nearby flames and airborne firebrands (Cohen

2000;Koo *et al.* 2010;Mell *et al.* 2010). Radiant heat from an intense fire can cause house ignitions within a 40m distance from the flame (Cohen 2000;Cohen 2004). A reduction of cover (from 90% to 5%) of trees and shrubs within 40m of houses could potentially reduce house loss by an average of 43% (Gibbons *et al.* 2012). Embers lifted from a fire (sometimes lifted by fire whirls occurring in large-scale forest fires) can be transported by strong winds to long distances up to 3 km (Albini 1979;Koo *et al.* 2010) and can result in ignitions at landing positions.

The characteristics of a building structure and its immediate surroundings influence the probability of ignition and therefore survival (Cohen 2000). Structure flammability depends on exterior construction materials (e.g. roof type and roof material influence the ignition by firebrands (Koo *et al.* 2010;Gibbons *et al.* 2012)) and construction design (e.g. number, size and characteristics of openings). Fire resistant roof materials include metal, clay tile and asphalt shingles (FSBC 2003). Homes should not be considered simply as potential victims of wildland fire, but also as potential fuels facilitating the continuation of the fire in their location (Cohen 2000). Therefore, building density is also included in studies of house losses due to wildfires (Gibbons *et al.* 2012). Poor fire crew access may explain why housing clusters with fewer roads are more vulnerable. However, it has been documented in numerous cases that houses with low ignitability can survive high intensity fires, whereas houses with high ignitability may be destroyed during lower intensity fires (Cohen 2000).

7.3   Probabilistic model for predicting house losses

A BN model is introduced here for assessing effects to houses caused by wildfires (Figure 7.1). Houses are here defined as independent living units in a building. The model estimates the house damage cost, thus the monetary restoration cost from the direct damage of the fire on the houses, to be paid by the owners, or as premiums by insurance or state.The model is developed for the Mediterranean island of Cyprus and can be applied to areas with similar characteristics. The BN includes variables that correspond to hazard, exposure, vulnerability and costs. Connecting arcs show the causal relationships among the variables. The BN serves to model the probabilistic relation between damage D and cost C for given hazard H, allowing the computation of the risk $R(h)$ for given hazard following Eq. 7.1.

Figure 7.1: Bayesian Network for effects to houses caused by wildfires

Wildfire hazard *H* is characterized by the variables *Burnt area*, the *Fire type* and the Fire Weather Index (*FWI*) of the Canadian Forest Fire Weather Index System (Lawson and Armitage 2008). *Fire type* distinguishes among a surface fire with flame length <3.5m, a surface fire with flame length >3.5m and a crown fire. As a rule more intense wildfires, i.e. those with longer flame lengths, are more difficult to extinguish and thus result in larger burnt areas (Rothermel and Deeming 1980). *Burnt area* is here expressing wildfire severity and the variables describing the fire hazard are included in the fire occurrence and fire size models (see also Chapter 5 and Chapter 6). In the proposed model, the arc connecting *Burnt area* and *Fire type* is contrary to this causal relationship. Such a contra-causal connection is possible in BN if it is ensured that no other independence properties are violated (Straub and Der Kiureghian 2010). It is used here to allow extension of the proposed BN to a larger BN that includes a fire size prediction expressed by the resulting burnt area as given in Chapter 6. The probability distribution of the *Fire type* conditional on *Burnt area* is determined based on data.

Exposure nodes in the BN describe the exposure of the system (items at risk). *Urban/Rural* discriminates urban from rural areas, which influences the *House density* [house/km²] and the *House stock. House stock* accounts for the house type portfolio in the meso-scale. It describes the combination of house types in 1km², which include single houses, semi-detached/row houses, and apartments. The *House stock* classification influences the costs of rebuilding, which is here taken as the construction value of the houses in monetary terms. The above variables were chosen to represent the exposure of the houses based on their arrangement and surrounding conditions. At the applied meso-scale level, the portfolio of the variable *House stock* is the combination of types in percentage in 1 km² and is defined specifically for the test-bed area. The definition of *House stock* can vary, when modelling in different scale and test-bed area. This variable is here adapted to the

test-bed area. *House stock* has two states: 40s_25r_35a, (40% of the houses are single houses, 25 % row houses and 35% apartments) and 70s_20r_10a (70% single houses, 20% row houses, 10% apartments). In the application on South France, the variable House stock is considered random.

The nodes influencing the vulnerability variable *Fire containment in 24 hrs* are based on Plucinski *et al.* (2012), where a logistic regression analysis is performed to determine the effect of multiple variables on fire containment (Table 7.1). The probability of Fire Containment in 24 hrs can be derived from,

$$\Pr(Fire\ Containment) = b_0 + b_1 F(G)FDI + b_2 ground\ time + b_3 air\ time \qquad (7.2)$$

In the BN*, Fire containment in 24 hrs* depends on *Vegetation type* (forest/shrub/grass), fire weather conditions (*FWI*), *Time for ground attack* and the air /no *air suppression* actions. *Distance to next fire station* [km] describes the shortest distance to the next fire station and influences the variable *Time for ground attack* [min]. The later is the travelling time that a vehicle needs to cover this distance. The response time of a fire crew is defined as 5 min. The mean vehicle velocity is assumed to be 70km/hr. In the BN applied here, *FWI* influences only the result of the suppression effectiveness and not the fire itself (*Burnt area*, *Fire type*) as it should and can be found in Chapter 5. The reason for this is that in this chapter given hazard characteristics are assumed and the hazard itself is not modelled. Since the model of Plucinski *et al.* (2012) contains the equivalent fire danger indicator FFDI (Forest Fire Danger Index)/GFDI (Grass Fire Danger Index) used in Australia (McArthur 1967), an adaptation of *FFDI* to *FWI* values is based on Dowdy *et al.* (2010). The *FWI* is chosen to represent fire weather conditions because of its ability to represent the influence of weather conditions on fire danger in the Mediterranean (Papakosta and Straub 2015). *FWI* is calculated from daily weather conditions (input 12:00 temperature, relative humidity, wind speed and 24hr precipitation). *Land cover types* refer to the Corine 2006 land cover type nomenclature and influences the variable *Vegetation type*. *Vegetation type* can be grass, forest, shrub and non burnable. *Air suppression* can be either present or absent (yes/no). The above variables are chosen to express the suppression result and how it influences the house damages. *Construction type* categorizes the houses based on the construction materials and roof type. It is also a combination of constructions in the 1 km² cell, and includes construction materials such as stone/mud, single/insulated brick and roof types such as flat concrete or inclined roof with tiles. The definition of *Construction type* can vary, when modelling at different scales and for different areas.

The vulnerability node *House damages* represents the degree of damage to the house portfolio in the cell. The node *House damages* is influenced by *Fire type*, *Fire containment in 24 hrs*, *Construction type* and *House stock*. As mentioned before it is assumed that a house is either totally damaged or stay intact after a fire. The CPT of *House damages* is obtained through a normalized summation of the individual damage from each influencing variable, as explained in more details in the test bed application. The definition of this variable can vary based on the modelling scale and the available data set.

The node *House damage cost* (HDC) in Figure 7.1 expresses the house damage cost in the 1 km² cell as a product of the *House damage*, the *Construction value*, the *House density* and the *Burnt area*. HDC is expressed in monetary terms [€].

The BN is coupled with a GIS as explained in Section 3.2. Spatial feature groups, such as points, lines and polygons are processed, stored and managed in the GIS database (see also Chapter 4). The geospatial features are associated with variables in the BN. In each cell (1 km²), a copy of

the BN represents the wildfire effect. Spatial dependence is represented through the dependence of the observed indicator variables, but not through the BN itself.

The parameters of the exposure indicators are learned with the attribute data of the geospatial features. Thus, the CPTs of the variables *Land cover*, *Urban/Rural*, *House density*, *Construction type* and *Distance to next fire station* are learned with data from the geodatabase (Figure 4.7). The hazard characteristics are fixed, thus the state of the variables *Burnt area*, *Fire type* and *FWI* is defined. This evidence is propagated through the network and the posterior marginal distributions of each variable are computed.

Table 7.1: Fire Containment in 24hrs: regression parameters (Plucinski 2012;Plucinski *et al.* 2012)

		b_0	b_1	b_2	b_3
Vegetation Type	Suppression	intercept	F/G FDI	ground time	air time
grass	ground	2.41124	-0.02454	-0.51708	
forest	ground	1.168703	-0.024632	-0.20104	
shrub	ground	1.664122	-0.019558	-0.282204	
grass	ground & air	4.80436	-0.042789	-0.66977	-0.3253
forest	ground & air	3.83561	-0.05031	-0.29845	-0.34783
shrub	ground & air	3.75257	-0.03704	-0.3184	-0.08101

7.4   Probabilistic model for predicting vegetated area losses

Figure 7.2 introduces the BN for the effects to vegetated areas induced by wildfires. The model estimates the vegetation damage cost, thus the monetary restoration cost from the direct damage of the fire on the vegetation, to be paid by the owners or the state. In this model the definition of the Hazard is identical with the previous model on house damage. The exposure indicators are different to represent the vegetated areas. The variable *Land Cover type* is the parent of the variable *Corine vegetation*. The latest summarizes all the land cover types with vegetation (e.g. permanent crops, forests, natural grasslands) of the Corine nomenclature. *Restoration cost* and *Restoration time* are defined conditional on *Corine vegetation*. *Restoration cost* here is the amount of money paid either as premium from the EU Rural Development Programs (forest, transitional woodland) or as given from JRC (Oehler *et al.* 2012). *Restoration time* [yrs] is the average time needed for the vegetated area to achieve its former condition.
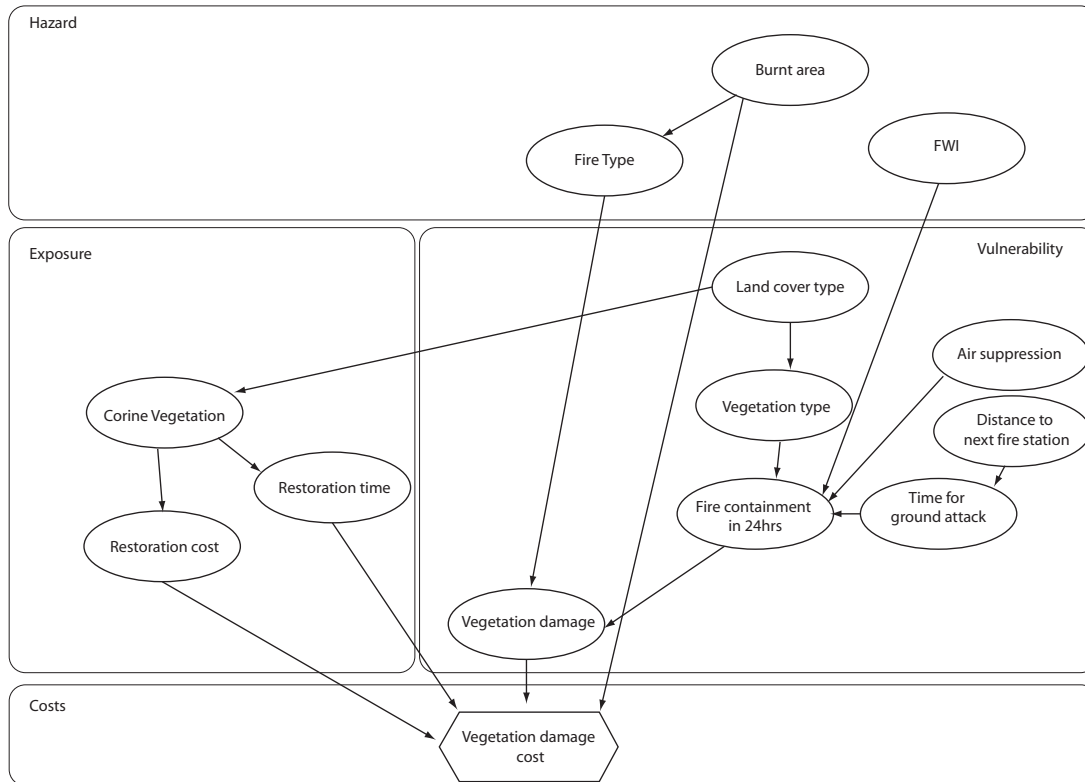
Figure 7.2: Bayesian Network for effects to vegetation by wildfires

The vulnerability node *Vegetation damage* represents the degree of damage, i.e. the vulnerability of the vegetation in the cell. The vulnerability is influenced by *Fire type* and *Fire containment in 24 hrs*. It is expressed as percentage of vegetation totally damaged in 1 km². The CPT of *Vegetation damage* is assumed conditional on the variable *Fire type*. This variable is introduced to represent vulnerability of the vegetation in the meso-scale. Here damage accounts for total damage. The definition of this variable can vary based on the modelling scale and the available data set.

The node *Vegetation damage cost* (VDC) in Figure 7.2 expresses the vegetation damage cost in monetary terms [€] in the 1 km² cell as a product of the *Vegetation damage*, the *Burnt area*, the *Restoration cost* and the *Restoration time* as,

$$
\begin{aligned}
Vegetation\ &Damage\ Cost \\
&= Vegetation\ damage \cdot Burnt\ area \cdot Restoration\ cost \\
&\cdot (1+r)^{Restoration\ time}
\end{aligned}
\tag{7.3}
$$

wherein r is the discount rate 3%. The model predicts the vegetation damage cost [€] in a 1 km² spatial resolution. The final product of the model is the utility node "*Vegetation damage cost*".

7.5   Variable definition and parameter estimation

The parameters of the model are learnt with data from the test-bed area Cyprus (2006-2009) (see also Section 4.2). Fires occur with an annual mean occurrence rate of $5.5 \cdot 10^{-5} \frac{Fires}{day \cdot km^2}$ (Section 4.2.3). The average burnt area in the 2006-2010 period was 21 km²/year (Cyprus Forest Service).

Table 7.2 summarizes the modeling of the BNs variables for the test-bed area. The definitions of the discrete states of the variables are provided as well as the sources for the conditional probabilities defining the variables. It is reminded that the spatial resolution of the model is 1 km², which is of relevance for the definition of the variables.

The variable *Fire type* and its CPT on *Burnt area* need to be defined based on data. Such data are not available for Cyprus so a data set is used that includes the Fire type, the resulting Burnt area and the House damages of 196 fire events that took place in the Wildland Urban Interface (WUI) in Greece in the 1993-2003 period (Hellenic Agricultural Organization Demeter). Wildfire conditions in Greece are generally considered similar to those in Cyprus as the two countries have Mediterranean climate and similar forest vegetation. Figure 7.3 shows a boxplot of the fire type versus the resulting burnt area for Greece. The data set is used to learn the CPT of the variable Fire type.
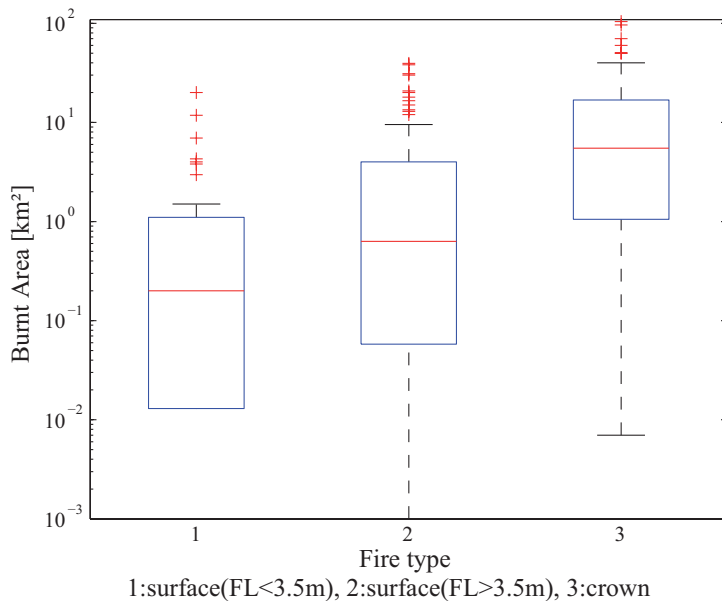
Figure 7.3: Boxplot of Burnt area [km²] versus Fire type
1: surface fire (flame length<3.5m), 2: surface fire (flame length>3.5m), 3: crown fire

Table 7.2: Description of BN variables and data sources for the definition of the conditional probability tables

Variable	# states	States	Source of probability distribution and additional information
Fire type	3	1 2 3	1: surface fire with flame length < 3.5m 2: surface fire with flame length >3.5m 3: crown fire Classification based on fire events in WUI Greece 1993-2003
Burnt area [km²]	7	$0 - 10^{-12}$ 10^{-12}-0.01 0.01 - 0.1 0.1 - 1 1 - 3 3 - 10 10 - 30	Historical fire events (2006-2010) Data source: Department of Forest, Ministry of Agriculture Cyprus
Distance to next fire station [km]	3	0 - 5 5 - 10 10 - 30	Edited from fire station locations Data source: Cyprus Fire Service
Time for ground attack [min]	4	5 - 10 10 - 15 15 - 20 20 - 25	Ground troop response time assumed to be 5 min. Conditional on distance to next fire station. Vehicle travel velocity assumed 70 km/h
FWI	4	0 - 10 10 - 30 30 - 60 60 - 120	FWI calculated from interpolated weather data from 5 weather stations Source: Deutscher Wetterdienst (DWD), Cyprus Meteorological Service (Papakosta and Straub 2015)
Land cover	7	1 2 3 4 5 6 7	1: Urban/Wetland/Pastures 2: Arable land 3: Permanent crops 4: Heterogeneous agriculture 5: Forests 6: Shrubs/Herbaceous vegetation 7: Open spaces Edited from Corine Land Cover map (version 13) Data source: European Environmental Agency
Vegetation type	4	Grass Forest Shrub No burn	Conditional on Land cover types Edited from Corine Land Cover map (version 13) Data source: European Environmental Agency
Air suppression	2	no yes	no: 50% yes: 50% Probabilities assumed
Fire Containment in 24 hrs		yes no	Conditional on Vegetation type, FWI, Air suppression, Time for ground attack Probabilities calculated based on regression models from Plucinski *et al.* 2012
Urban/Rural	2	Urban Rural	Classified based on population density values Urban >120 residents/km² Rural <120 residents/km²
House Stock	2	40s_25r_35a 70s_20r_10a	s: single houses r: row houses a: apartments (% percentage) Probabilities from data from Service 2010

Construction Type	2	5t_15s_80i 10t_25s_65i	t: traditional house, stone/mud wall s: single brick wall/flat roof house i: insulated brick/inclined roof (% percentage) Edited from Service 2012 Florides *et al.* 2001 p. 228 Nemry and Uihlein 2008, p.A147 Probabilities from data (Service 2010)
House density [Nr. Houses/ km²]	6	0 - 3 3 - 10 10 - 30 30 - 100 100 - 300 300 - 1,000 1,000 - 3,000	Based on Nr. dwellings (houses) statistics and municipality borders Data source: Statistical Service Cyprus
Construction value [x 10³ €]	4	0 - 10 10 - 50 50 - 100 100 - 500	Customized to House stock based on mean value and range for each building type, data from: Service 2010, p. 160 (Table 14: Building permits authorized by type of project 2010)
House damages	2	no damage minor major	minor: <20% major: >20% Conditional on fire type based on fire events in WUI Greece 1993-2003 Conditional on fire containment assumed 60% minor, 40% major Conditional on construction type based on scores from: OFD 2004, p.11-12 ECONorthwest 2007, Appendix C, page C-8 Conditional on house stock (defensible space) based on scores: OFD 2004, p.11-12
Corine Vegetation	15	211 212 221 222 223 241 242 243 311 312 321 323 324 No Vegetation	211: Non-irrigated Arable 212: Permanent Irrigated Land 221: Vineyards 222: Fruit Trees 223: Olives 241: Annual Crops Permanent 242: Complex Cultivation Patterns 243: Land Occupied Agriculture 311: Broad Leaved Forest 312: Coniferous Forest 321: Natural Grasslands 323: Sclerophyllous Vegetation 324: Transitional Woodland-Shrub Data source: Corine Land Cover map (version 13) European Environmental Agency
Restoration cost [x 10² €]	4	0 - 300 300 – 1,000 1,000 - 3,000 3,000 – 10,000	Conditional on Corine Vegetation, based on the afforestation premiums paid through the EU Rural Development Programs (Oehler *et al.* 2012) see also Table 7.3
Restoration time [yrs]	3	1 5 15	Conditional on Corine Vegetation, based on expert knowledge as given in (Oehler *et al.* 2012) see also Table 7.3

Vegetation damage	3	no damage minor major	minor: <20% major: >20% Conditional on fire type assumed Fire type 1: 90% minor, 10% major Fire type 2: 60% minor, 40% major Fire type 3: 20% minor, 80% major

The CPT of *House damages* results as a normalized summation of the individual contributions to the damage from each of the influencing variables. The influence of *Fire type* on *House damages* is quantified using the Greek dataset. The failure of *Fire containment in 24hrs* is assumed to lead to minor *House damages* with 60% probability and major *House damages* with 40% probability. The *Construction type* of houses in Cyprus includes mainly three types of structures. Traditional houses, mostly built in the period prior to 1945 with stone or mud walls and roofs with wood parts (Nemry and Uihlein 2008), are considered the most vulnerable. The vulnerability of houses built with single brick walls and flat reinforced concrete roofs in the period $1946 - 1970$ (Nemry and Uihlein 2008) is considered to be low, and newer houses with insulated brick walls and inclined roofs with ceramic tiles are the most fire resistant. The vulnerability of *House stock* classes (single houses, row houses, apartments) based on the possible flammability of their surroundings is considered to be high for single houses, medium for row houses and low for apartments (Long and Randall 2004; OFD 2004).

Table 7.3 summarizes the restoration cost and the restoration time as given in Oehler *et al.* (2012). The highest restoration costs have the forested areas, followed by transitional woodland shrubs and permanent agriculture areas.

Table 7.3: Average restoration cost [€/ha] and average restoration period [yrs] for different Corine land cover types in Europe (Oehler *et al.* 2012)

CORINE class	average restoration cost in Europe [€/ha]	average restoration period [yrs]
211: Nonirrigated Arable	868	1
212: Permanent Irrigated Land	868	1
221: Vineyards	3271	5
222: FruitTrees	3111	5
223: Olives	3351	15
241: Annual Crops Permanent	668	1
242: Complex Cultivation Patterns	758	1
243: Land Occupied Agriculture	509	1
311: Broad Leaved Forest	9339	15
312: Coniferous Forest	6618	15
321: Natural Grasslands	254	1
323: Sclerophyllous Vegetation	254	1
324: Transitional Woodland-Shrub	5364	5

7.6 Results

7.6.1 House Damage Cost

Figure 7.4 illustrates the BN estimate of the *House Damage Cost* (HDC) conditional on a fire with the mildest hazard conditions, i.e. with *Burnt area* < 0.01 km² and *Fire type* 1 (surface fire with flame length < 3.5m). *FWI* is not fixed, thus the variable *FWI* is considered random. For each node in the BN, the posterior marginal distribution of the variable is shown together with the expected house damage cost, given the corresponding state. In this example, even variables that are known for each cell are considered as random, such as *Land use*. The results are therefore representative for a randomly selected cell in the test-bed area. The expected HDC for a randomly selected cell of the test-bed area is 331 € for the assumed hazard conditions. For different *Land Cover types*, the expected HDC varies from 0 (for urban areas and wetlands) to 588 € (for forested areas).

In Figure 7.4 cells with higher *House density* are expected to have higher HDC. The same applies to cells with higher construction values. Areas with forests (*Land cover type*: 5) as the dominant land use are expected to have the highest house damage cost, followed by shrubs (*Land cover type*: 6) and permanent crops (*Land cover type*: 3). Furthermore, the higher the *FWI*, expressing the fire danger due to weather conditions, the higher the expected HDC.

Figure 7.5, Table 7.4 and Figure 7.6 show the computed expected HDC in an average cell, where one of the variables is varied.

Figure 7.5 shows the HDC as a function of the *Burnt area*. As expected, the cost increases with increasing *Burnt area*. *Burnt area* > 1 [km²] exceeds the area of the cell, and in these cases the cost in an average cell is overestimated. The neighboring cells are then assumed to have similar characteristics as the cell where fire occurs.

Table 7.4 shows expected HDC conditional on *Fire type*. As expected the HDC for crown fires is highest.
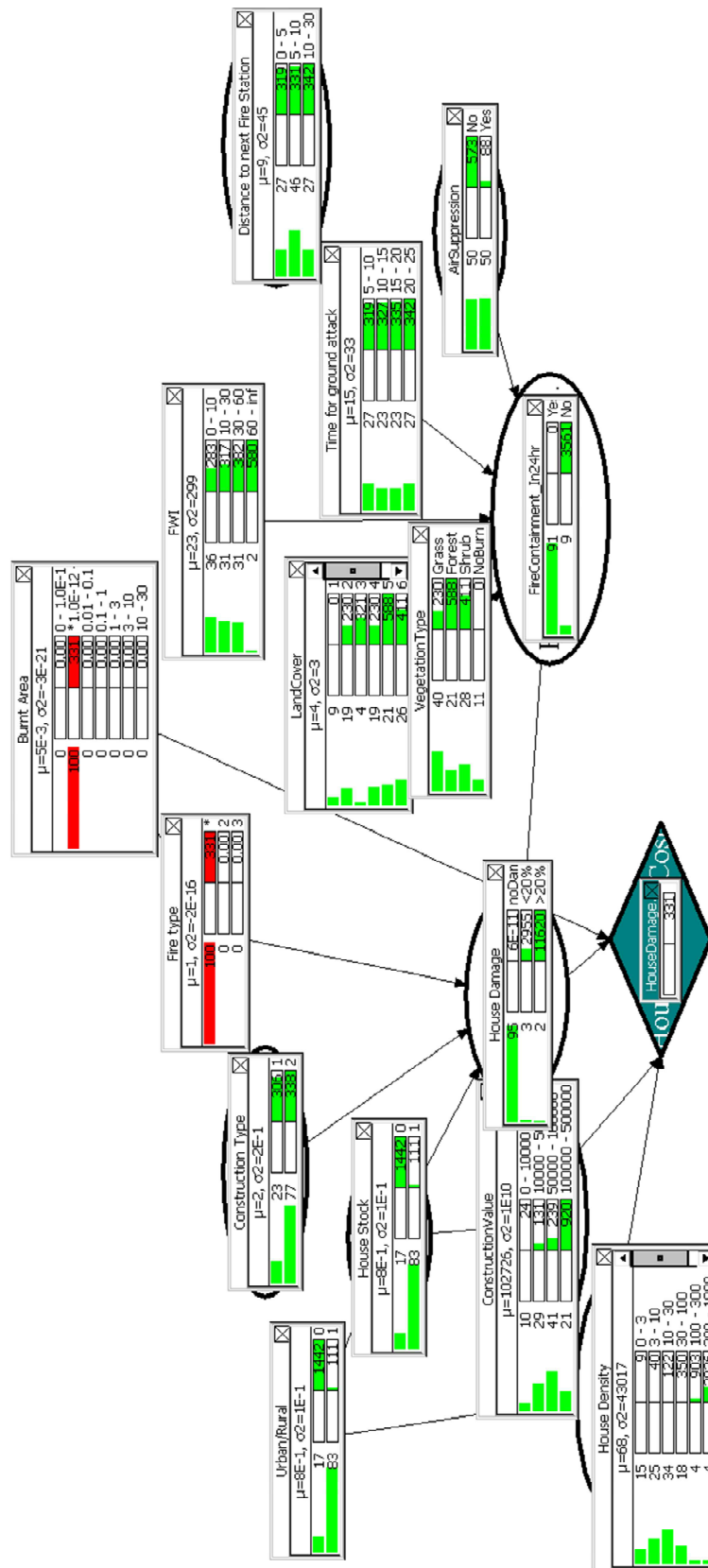
Figure 7.4: Expected house damage cost [€] for average cell, estimated for burnt area < 0.01 [km²] and fire type 1 (screenshot from HUGIN)
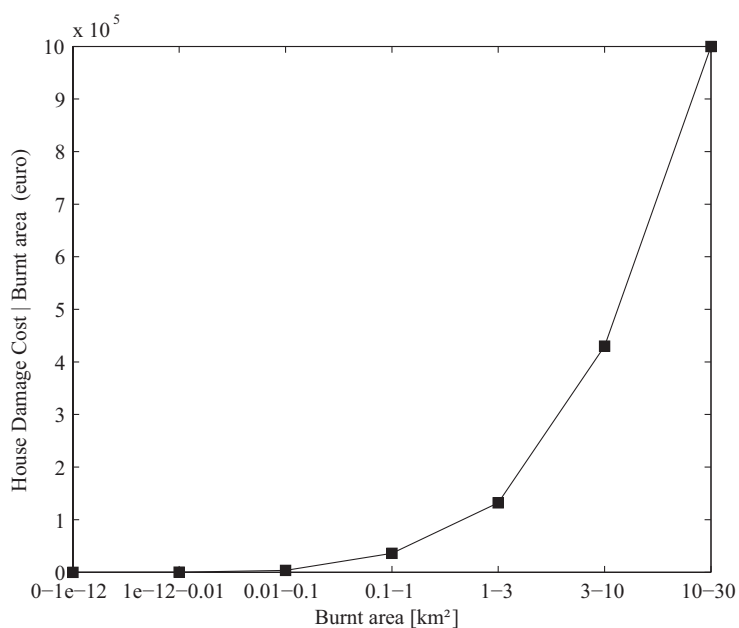
Figure 7.5: Expected house damage cost [€] conditional on burnt area [km²]

Table 7.4: Expected house damage cost [€] conditional on Fire type. Fire types 1 and 2 correspond to surface fires with different flame lengths (1: flame length < 3.5m, 2: flame length > 3.5 m) and fire type 3 corresponds to crown fires.

Fire type	1	2	3
House damage cost [€]	$189 \cdot 10^3$	$237 \cdot 10^3$	$565 \cdot 10^3$

Figure 7.6 shows expected HDC conditional on *House density*. Cells with higher *House density* (urban areas) are expected to register higher HDC when affected by wildfires. In this model, the influence of *House density* on the characteristics of the fire itself is neglected. This dependence is included when combining the BN with the hazard model (Chapter 8).
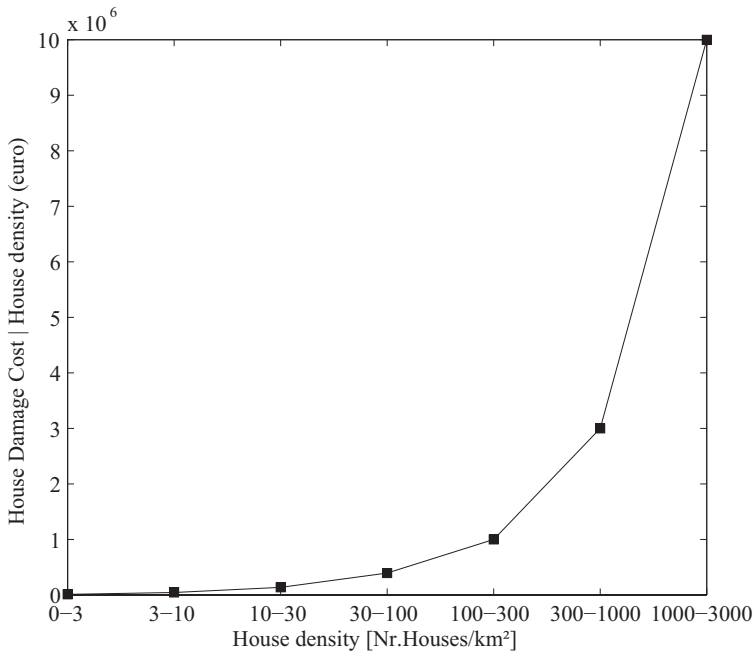
Figure 7.6: Expected house damage cost [€] conditional on house density [Nr.Houses/km²]

Table 7.5 shows the influence of the variables on the resulting HDC. The highest influence on HDC have the variables (in decreasing order) *House density*, *Fire containment in 24 hrs*, *Urban/rural*, *Burnt area*, *Construction value*, *Land cover*, *Air suppression* and *Fire type*. The influence of the variable *Vegetation type* on the HDC is identical to the influence of the *Land cover type*. The influence of the variable *House stock* on the HDC is identical to the influence with the variable *Urban/rural*. This is due to the deterministic connection that these variables have with their parents. The prior expected HDC for an average cell of the study area is $372 \cdot 10^3$ €. As an example, when there is evidence that the resulting *Burnt area* is in the interval $10 - 30$ km², the expected HDC for an average cell becomes $1e6$, thus increases by 168.74 %.

Table 7.5: Effect of influencing variables on house damage cost

Variable	Possible States of the Variable	House damage cost without setting an initial variable value [€] Prior: 372107	Change in % relative to the average
Burnt area	0	0	-100.00
	≤0.01	327	-99.91
	0.01 - 0.1	3,606	-99.03
	0.1 - 1	36,178	-90.28
	1 - 3	132,109	-64.50
	3 - 10	430,013	+15.56
	10 - 30	1,000,000	+168.74
Fire type	1	189,346	-49.12
	2	236,698	-36.39
	3	564,797	+51.78
Construction type	5t_15s_80i	300,138	-19.34
	10t_25s_65i	380,281	+2.20
Urban/Rural	urban	2,000,000	+437.48
	rural	124,350	-66.58
House stock	40s_25r_35a	2,000,000	+437.48
	70s_20r_10a	124,350	-66.58
Construction value	0 - 10,000	27,012	-92.74
	10,000 - 50,000	147,407	-60.39
	50,000 - 100,000	269,023	-27.70
	100,000 - 500,000	1,000,000	+168.74
House density	0 - 3	10,283	-97.24
	3 - 10	44,560	-88.03
	10 - 30	137,108	-63.15
	30 - 100	394,046	+5.90
	100 - 300	1,000,000	+168.74
	300 - 1000	3,000,000	+706.22
	1,000 - 3,000	10,000,000	+2,587.40
House damage	no damage	0	-100
	minor	3,000,000	+706.22
	major	10,000,000	+2,587.40
FWI	0 - 10	317,951	-14.55
	10 - 30	356,196	-4.28
	30 - 60	430,156	+15.60
	60 - 120	652,301	+75.30
Distance to next fire station	0-5	359,457	-3.40
	5-10	372,086	-0.01
	10-30	385,139	+3.50
Time for ground attack	5 - 10	359,457	-3.40
	10 - 15	367,806	-1.15
	15 - 20	376,365	+1.16
	20 - 25	385,139	+3.50
Air suppression	no	644,701	+73.26
	yes	99,513	-73.26
Fire Containment in 24 hrs	yes	0	-100
	no	4,000,000	+974.96
Land cover	1	0	-100
	2	259,325	-30.31

	3	361,066	-2.97
	4	259,325	-30.31
	5	661,341	+77.72
	6	462,807	+24.38
	7	0	-100
Vegetation type	Grass	259,325	-30.31
	Forest	661,341	+77.72
	Shrub	462,807	+24.38
	No vegetation	0	-100

Two examples of past fire periods are selected to demonstrate the BN-GIS coupling and illustrate the estimated HDC for each of the observed fire events (Figure 7.7 and Figure 7.8). Based on the hazard characteristics (*Burnt area* and *FWI*) and the exposure and vulnerability indicators, the model estimates the expected HDC for each cell (1 km²) in which a fire occurred. The results vary from 0 to $570 \cdot 10^3$ €. Table 7.6 compares the estimated expected HDC with the losses registered in the NatCatSERVICE database (Munich Re). The aggregated expected house damage cost from all fire events for the period is also given. The NatCatSERVICE database gives information on the number of houses damaged, and not on the resulting house damage cost, which hinders a direct validation of the BN results. It is also noted that the BN model provides expected values, which do not necessarily have to coincide with the actual observed losses for a single event. Nevertheless, the comparison of Table 7.6 shows that the BN model gives results that are in agreement with actual recorded losses.
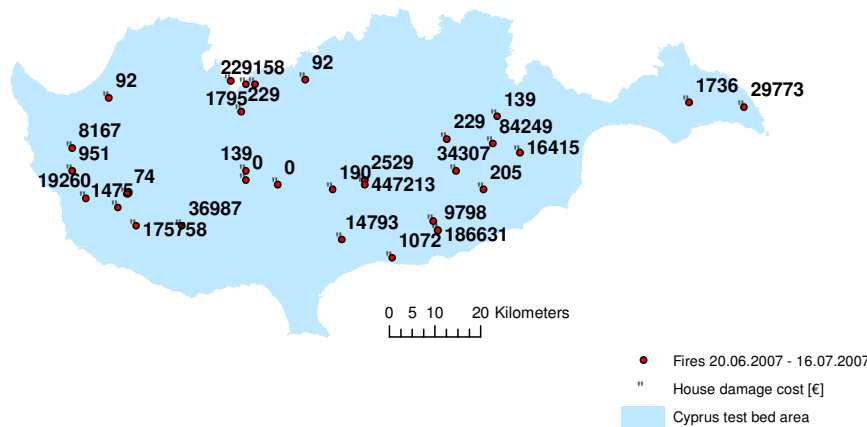
Figure 7.7: Expected house damage cost [€] for fires in the period 20. June 2007-16. July 2007 on Cyprus
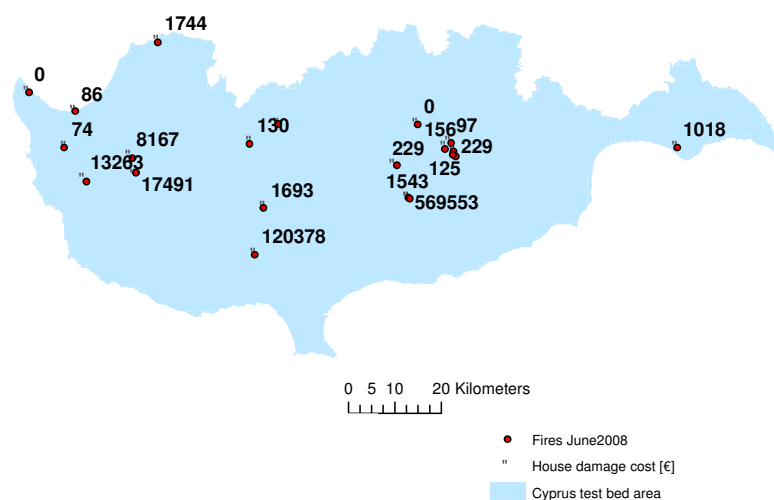
Figure 7.8: Expected house damage cost [€] for fires in June 2008 on Cyprus

Table 7.6: Aggregated Expected HDC compared to registered losses for two past fire periods

Fire Period	Aggregated Burnt Area [km²]	Aggregated estimated expected HD cost [€]	Losses as recorded in NatCatSERVICE	Estimated Losses [€] *
20 June 2007- 16 July 2007	34	$1110 \cdot 10^3$	several buildings	
June 2008	19.54	$760 \cdot 10^3$	5 houses	$725 \cdot 10^3$

* Estimated Losses= NatCatSERVICE x Mean House construction value ($145 \cdot 10^3$ €)

The proposed model is also applied on the test-bed area of South France for one fire period. Fire season 05.07.2005 – 08.08.2005 is chosen to demonstrate the predictive ability of the model (see also Table 4.5). Evidence is given on the variables Burnt area, Land cover types and FWI. All the other exposure and vulnerability variables are assumed random. The model estimates the expected HDC for each cell in which a fire occurred. The results vary from 0 to $5821 \cdot 10^3$ (Figure 7.9). The NatCatSERVICE database gives information on the number of houses damaged. The comparison between the predicted HDC and the actual recorded losses is shown in Table 7.7. The estimated losses are again multiplied with the mean house construction value on Cyprus, to agree with the distribution of the construction value used in the model, which is derived from data of Cyprus. The estimated losses are at the magnitude of $165 \cdot 10^5$€. According to the data from NatCatSERVICE, during this fire period, only 10 houses were damaged, which leads to a cost of $145 \cdot 10^4$ €. The model predicts much higher losses. Other sources reported (08.08.2005) fires due to high temperatures and worst drought in six decades and the evacuation of some 3200 residents and tourists at Pradet in the Var (http://globaldisasterwatch.blogspot.de/p/2005-disasters-from-july-december.html)(retrieved 13.03.15). No other data was available for estimation control.
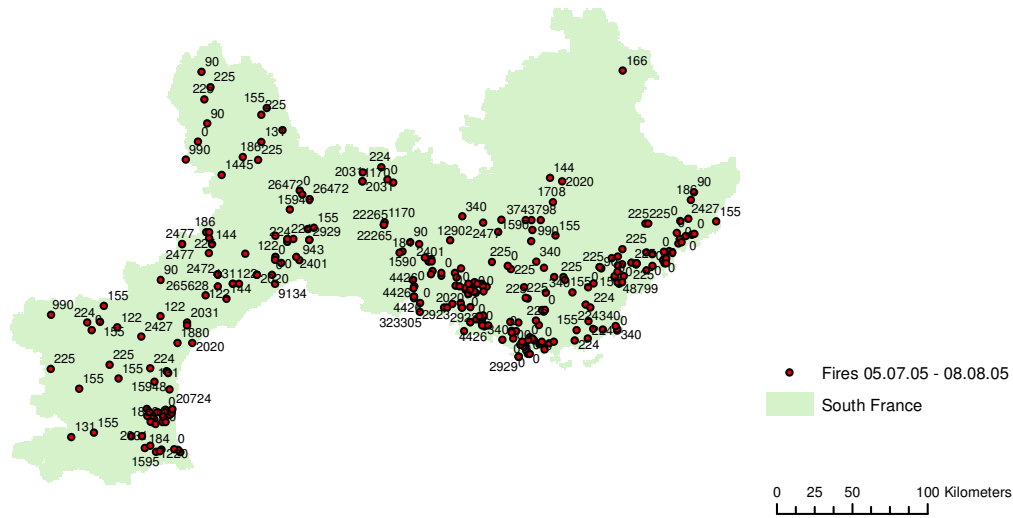
Figure 7.9: Expected house damage cost [€] for fires in the period 5. July 2005-8. August 2005 on South France

Table 7.7: Aggregated Expected HDC compared to registered losses for one fire period (South France)

Fire Period	Aggregated Burnt Area [km²]	Aggregated estimated expected HD cost [€]	Losses as recorded in NatCatSERVICE	Estimated Losses [€] *
5 July 2005- 8 August 2005	65.42	$164 \cdot 10^5$	10 houses	$145 \cdot 10^4$

* Estimated Losses= NatCatSERVICE x Mean House construction value ($145 \cdot 10^3$ €)

Figure 7.10 and Figure 7.11 show the estimated HDC for the entire test-bed area of Cyprus conditional on a specific fire occurring throughout the island. The maps result from the BN-GIS coupling. Figure 7.10 shows the expected HDC conditional on *Burnt area* < 0.01 km², *Fire type* = 1, once with random *FWI* values and once with fixed *FWI* = 60. For *FWI*= 60, which denotes dryer vegetation conditions, the expected HDC rises in the whole area, except for the urban areas. Urban areas have the lowest HDC, due to the lack of flammable vegetation and higher probability of fire containment. The peri-urban areas (WUI) represent the coexistence of residential areas and natural vegetation and have the highest expected HDC values.

Figure 7.11 shows expected HDC conditional on *Burnt area* = 10 − 30 km² and *Fire type* = 3, once with random *FWI* values and once with fixed *FWI* = 60. The highest values are again estimated in the peri-urban areas, followed by forested areas. The forested areas have higher expected HDC, since these are the areas affected by crown fires (*Fire type* = 3). The effect of neighboring forested areas is neglected in this model. The WUI cells are still the most threatened for house damage.

Figure 7.12 and Figure 7.13 show the estimated HDC for the test-bed area South France conditional on a specific fire occurring throughout the area. The expected HDC is conditional on the same hazard conditions as in Figure 7.10 and Figure 7.11. Again for *FWI*=60, which denotes dryer vegetation conditions, the expected HDC rises in the whole area, except for the urban areas. Urban

areas have the lowest HDC and the peri-urban areas (Wildland-Urban Interface, WUI) have the highest expected HDC values. Figure 7.13 shows expected HDC conditional on *Burnt area* $= 0 - 30 \ km^2$ and *Fire type* $= 3$, once with random *FWI* values and once with fixed *FWI* $= 60$. The highest values are again estimated in the peri-urban areas, followed by forested areas (see also Figure 4.26).
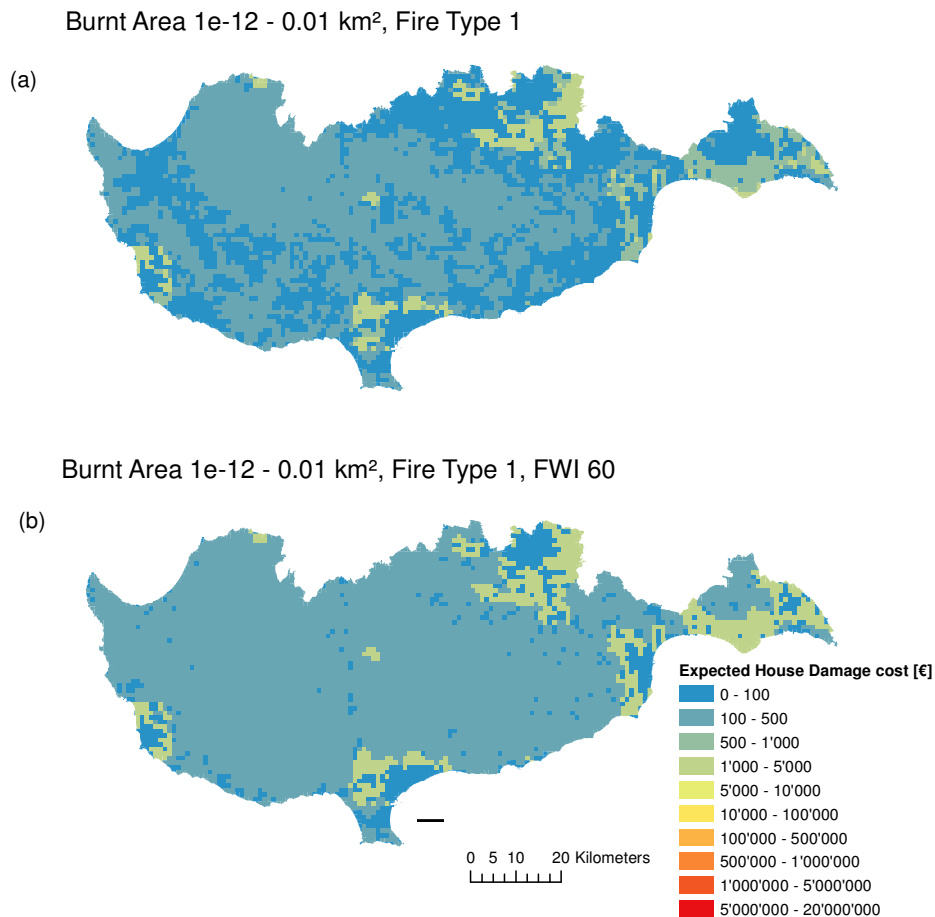
Figure 7.10: Expected house damage cost [€] conditional on burnt area = 10^{-12} - 0.01 km², fire type = 1, random FWI (a) and FWI=60 (b) on Cyprus

The results agree with other studies, which claim that the WUI is expected to have higher damages (e.g. Mozumder *et al.* 2009; Gibbons *et al.* 2012; Syphard *et al.* 2012). Moreover, the influence of higher fire danger conditions (FWI= 60) on the expected house losses agrees with previous studies, showing that the majority of losses occur on days with intensive fire weather conditions (e.g. Blanchi *et al.* 2010).

Burnt Area 10-30 km², Fire Type 3

(a)

Burnt Area 10-30 km², Fire Type 3, FWI 60

(b)

Expected House Damage cost [€]

0 - 100
100 - 500
500 - 1'000
1'000 - 5'000
5'000 - 10'000
10'000 - 100'000
100'000 - 500'000
500'000 - 1'000'000
1'000'000 - 5'000'000
5'000'000 - 20'000'000

0 5 10   20 Kilometers
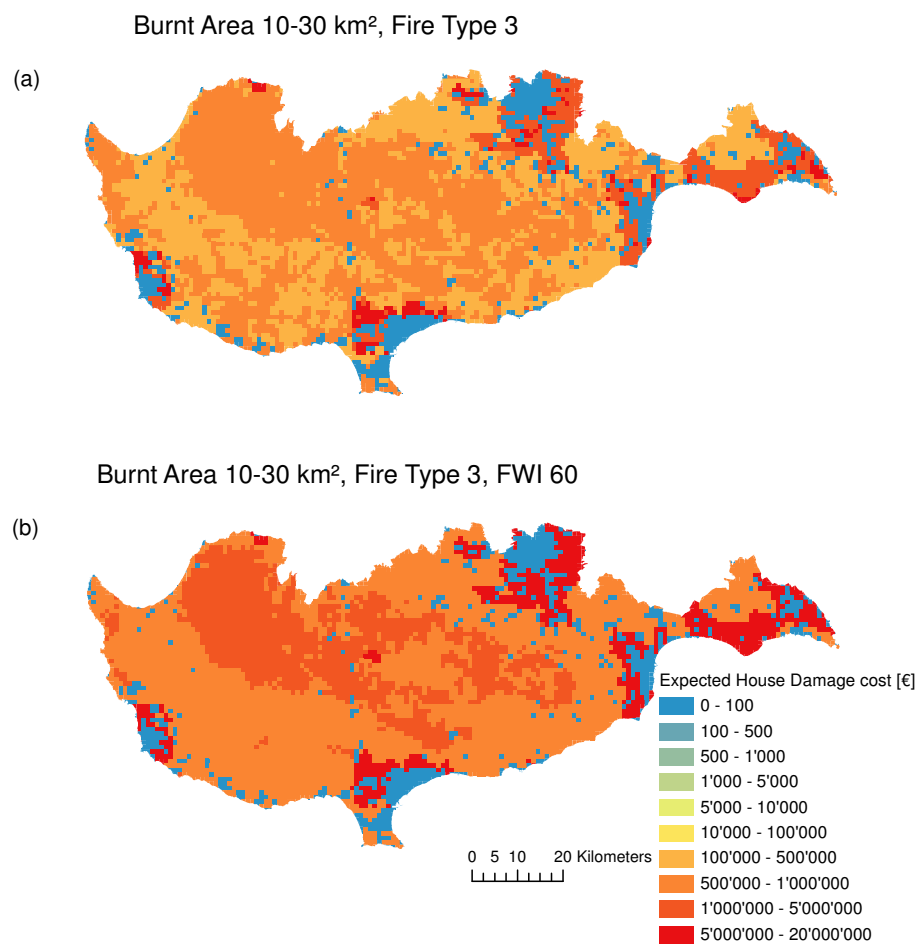
Figure 7.11: Expected house damage cost [€] conditional on burnt area = 10 - 30 km², fire type = 3, random FWI (a) and FWI=60 (b) on Cyprus

(a)

Burnt area 1e-12 - 0.001 km², Fire type 1

(b)

Burnt area 1e-12 - 0.001 km², Fire type 1, FWI 60

Expected house damage cost [€]

- 0 - 100
- 100 - 500
- 500 - 1'000
- 1'000 - 5'000
- 5'000 - 10'000
- 10'000 - 100'000
- 100'000 - 500'000
- 500'000 - 1'000'000
- 1'000'000 - 5'000'000
- 5'000'000 - 20'000'000

0   25   50   100 Km
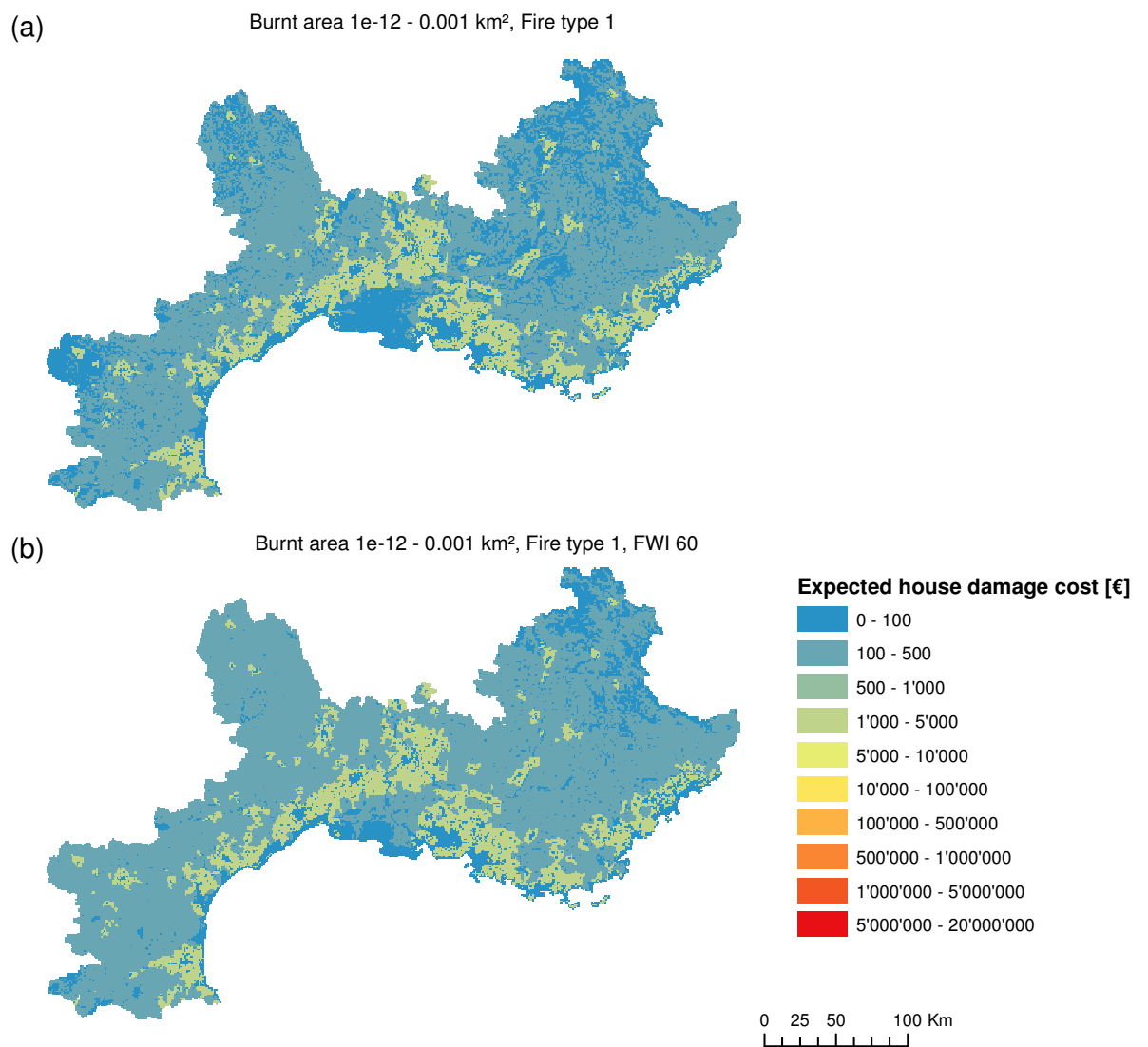
Figure 7.12: Expected house damage cost [€] conditional on burnt area = 10^{-12} - 0.01 km², fire type = 1, random FWI (a) and FWI=60 (b) on South France

(a)   Burnt area 10 - 30 km², Fire type 3

(b)   Burnt area 10 - 30 km², Fire type 3, FWI 60

Expected house damage cost [€]

- 0 - 100
- 100 - 500
- 500 - 1'000
- 1'000 - 5'000
- 5'000 - 10'000
- 10'000 - 100'000
- 100'000 - 500'000
- 500'000 - 1'000'000
- 1'000'000 - 5'000'000
- 5'000'000 - 20'000'000

0   25   50   100 Km
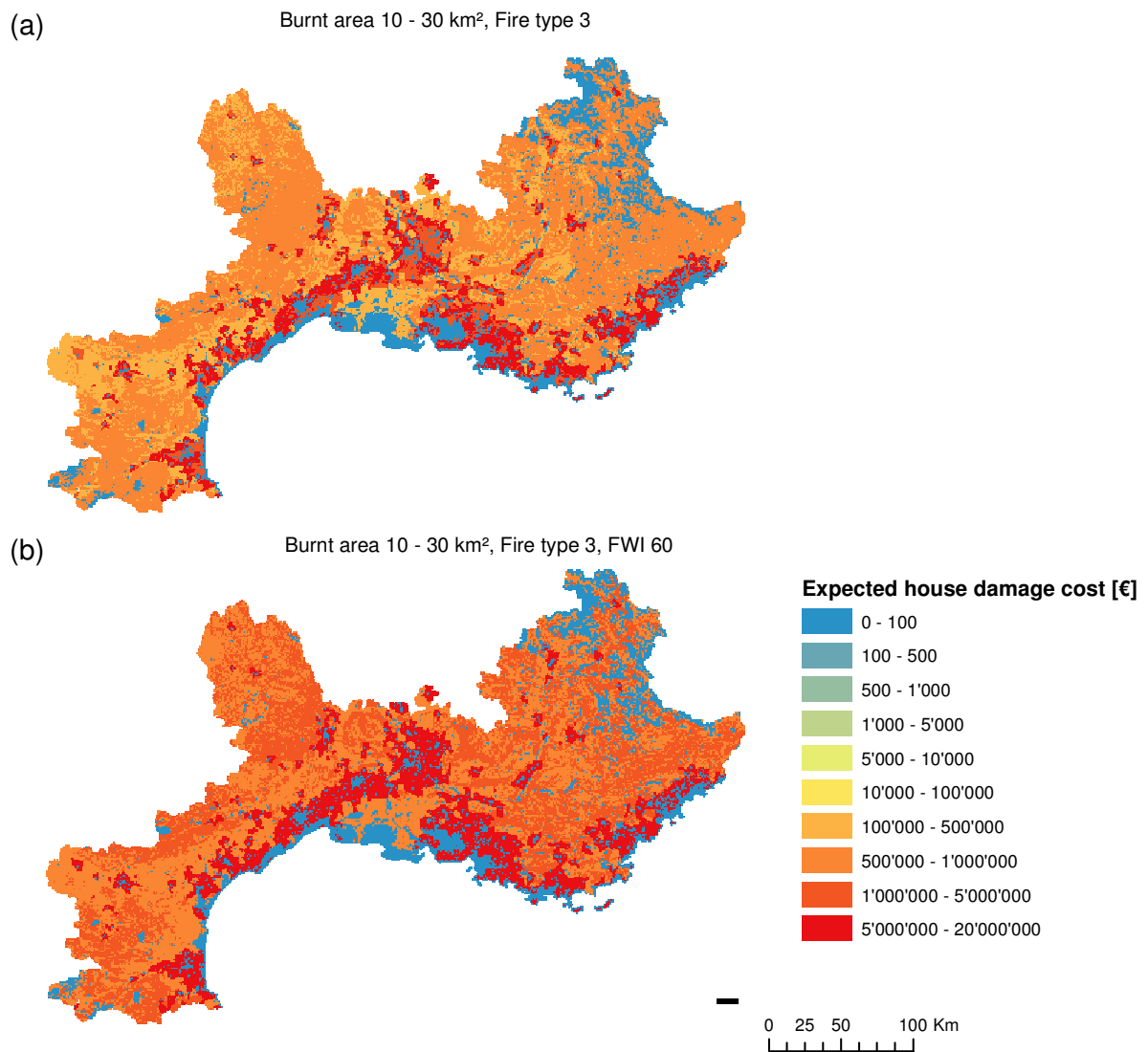
Figure 7.13: Expected house damage cost [€] conditional on burnt area = 10 - 30 km², fire type = 3, random FWI (a) and FWI=60 (b) on South France

7.6.2 Vegetation Damage Cost

Figure 7.14 illustrates the BN estimate of the *Vegetation Damage Cost* (VDC) conditional on a fire with the lowest hazard conditions, i.e. with *Burnt area* < 0.01 km² and *Fire type* 1 (surface fire with flame length < 3.5 m). *FWI* is not fixed. In each node, the posterior marginal distribution of the variable is shown together with the expected vegetation damage cost, given the corresponding state. Again in this example, even variables that are known for a given location are considered as random, such as land use. The results are therefore representative for a randomly selected cell in the test-bed area. The expected VDC for a randomly selected cell of the test-bed area is 241 €. For different Land Cover types, the expected HDC varies from 0 (for urban areas and wetlands) to 803 € (for forested areas).
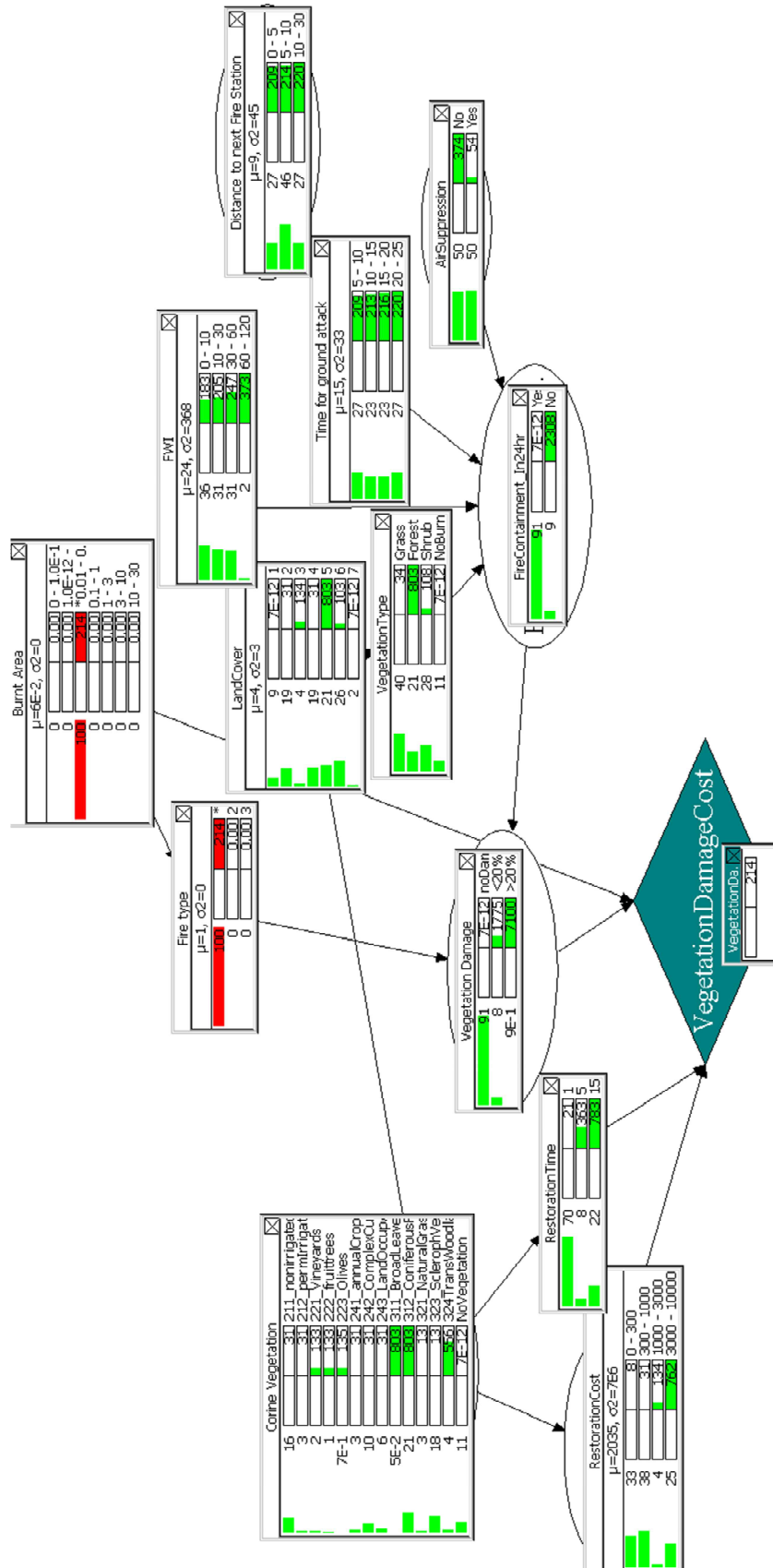
Figure 7.14: Expected vegetation damage cost [€] for average cell, estimated for burnt area 0.01 - 0.1 [km²] and fire type 1 (screenshot from HUGIN)

Areas with forests (*Land cover type*: 5) as the dominant land cover type are expected to have the highest VDC, followed by transitional woodland shrubs (*Land cover type*: 6) and permanent crops (*Land cover type*: 3, Corine land cover: vineyards, fruit trees, olives). Furthermore, the higher the *FWI*, expressing the fire danger due to weather conditions, the higher the expected VDC.

Figure 7.15, Figure 7.16 and Table 7.8 show the computed expected VDC in an average cell, where one of the variables is varied. Figure 7.15 shows the VDC as a function of the *Burnt area*. *Burnt area* > 1 [km²] exceeds the area of the cell, and in these cases the cost in an average cell is overestimated. The neighboring cells are then assumed to have similar characteristics with the cell where fire occurs.

Table 7.8 shows expected VDC conditional on fire type. As expected the HDC for crown fires is highest.
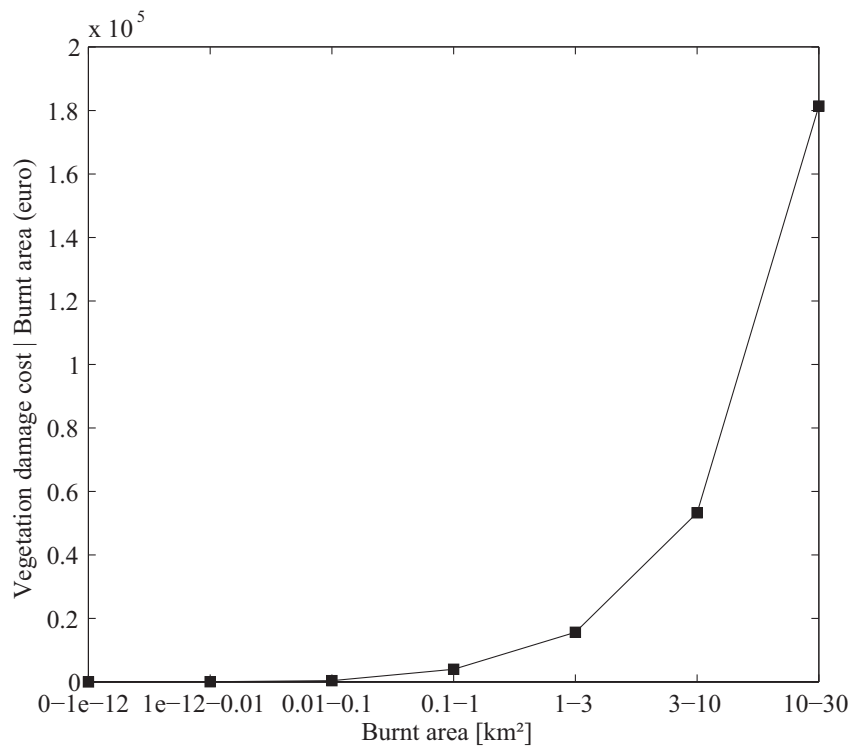
Figure 7.15: Expected vegetation damage cost [€] conditional on burnt area [km²]

Table 7.8: Expected vegetation damage cost [€] conditional on Fire type

Fire type	1	2	3
Vegetation damage cost [€]	$11 \cdot 10^3$	$24 \cdot 10^3$	$86 \cdot 10^3$

Figure 7.16 shows expected VDC conditional on *Corine vegetation* type. Cells with forests (311 and 312) are expected to register the highest VDC when affected by wildfires, followed by transitional woodland shrubs (324) and permanent crops (221, 222, 223).
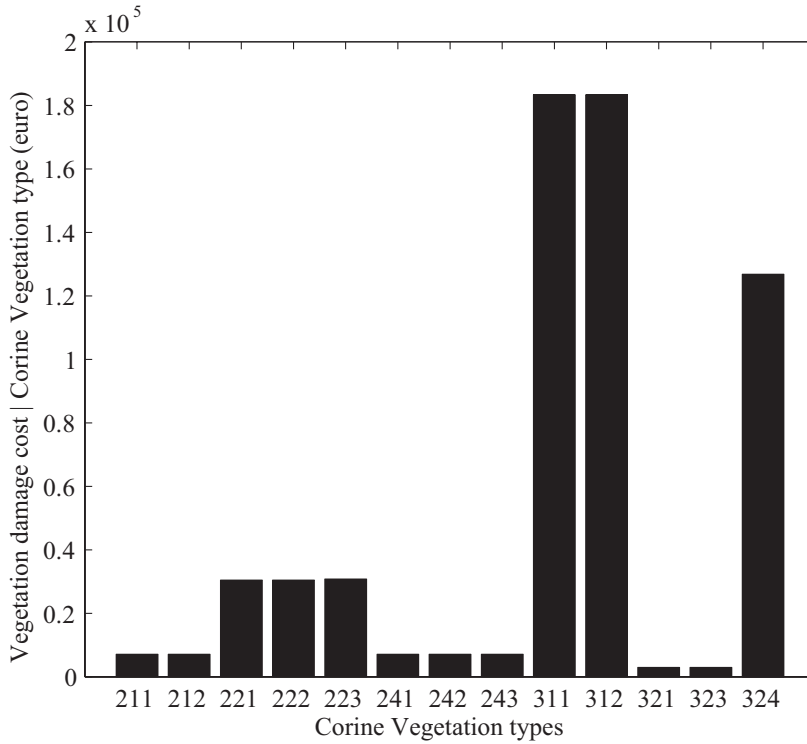
Figure 7.16: Expected vegetation damage cost [€] conditional on Corine Vegetation type (see also Table 7.3)

Table 7.9 shows the influence of the variables on the resulting VDC. The highest influence on VDC have the variables (in decreasing order) *Fire containment in 24 hrs*, *Corine vegetation* types, *Burnt area*, *Restoration time*, *Restoration cost* and *Air suppression*. The influence of the variable *Vegetation type* on VDC is identical to the influence of the variable land cover type. This is due to the deterministic connection between them. The prior expected VDC for an average cell of the study area is $49 \cdot 10^3$ €. As an example, when there is evidence that the resulting *Burnt area* is in the interval $10 - 30$ km², the expected VDC for an average cell becomes $181 \cdot 10^3$ €, thus increases by 271 %.

Table 7.9: Effect of influencing variables on vegetation damage cost

Variable	Possible States of the Variable	Vegetation damage cost without setting an initial variable value [€] Prior: 48917	Change in % relative to the average
Burnt area [km²]	0	0	-100
	≤0.01	31	-99.94
	0.01 - 0.1	371	-99.24
	0.1 - 1	3,937	-91.95
	1 - 3	15,582	-68.15
	3 - 10	53,254	+8.87
	10 - 30	181,363	+270.76

Fire type	1	11,156	-77.19
	2	24,104	-50.72
	3	85,781	+75.36
Corine Vegetation	211	7,078	-85.53
	212	7,078	-85.53
	221	30,439	-37.77
	222	30,439	-37.77
	223	30,800	-37.04
	241	7,078	-85.53
	242	7,078	-85.53
	243	7,078	-85.53
	311	183,345	+274.81
	312	183,345	+274.81
	321	2,915	-94.04
	323	2,915	-94.04
	324	126,802	+159.22
	No Vegetation	0	-100
Restoration cost [x 10² €]	0 - 300	1,913	-96.09
	300 - 1000	7,078	-85.53
	1000 - 3000	30,495	-37.66
	3000 - 10000	173,938	+255.58
Restoration time [yrs]	1	4,688	-91.42
	5	82,879	+69.43
	15	178,809	+265.54
Vegetation damage	no damage	0	-100
	minor	138,537	+183.21
	major	875,505	+1,689.8
FWI	0 - 10	41,856	-14.43
	10 - 30	46,857	-4.21
	30 - 60	56,487	+15.47
	60 - 120	85,224	+74.22
Distance to next fire station	0 - 5	47,763	-2.36
	5 - 10	48,919	0
	10 - 30	50,098	+2.41
Time for ground attack	5 - 10	47,763	-2.36
	10 - 15	48,529	-0.79
	15 - 20	49,308	+0.80
	20 - 25	50,098	+2.41
Air suppression	no	85,403	+74.59
	yes	12,430	-74.59
Fire Containment in 24 hrs	yes	0	-100
	no	526,670	+976.66
Land cover	1	0	-100
	2	7,078	-85.53
	3	30,495	-37.66
	4	7,078	-85.53
	5	183,345	+274.81
	6	23,445	-52.07
	7	0	-100
Vegetation type	Grass	7,859	-83.93

	Forest	183,345	+274.81
	Shrub	24,632	-49.65
	No vegetation	0	-100

Figure 7.17 and Figure 7.18 show the estimated VDC for the test-bed area of Cyprus conditional on a specific fire occurring throughout the island. Figure 7.17 shows the expected VDC conditional on *Burnt area* < 0.01 km², *Fire type* = 1, once with random *FWI* values and once with fixed *FWI* = 60. For *FWI* = 60, which denotes dryer vegetation conditions, the expected VDC rises in the forested areas (see also Figure 4.5).

Figure 7.18 shows expected VDC conditional on *Burnt area* = $10 - 30 \ km^2$ and *Fire type* = 3, once with random *FWI* values and once with fixed *FWI* = 60. The urban areas are expected to have 0 € of VDC. The highest values are estimated in the forested areas.

Figure 7.19 and Figure 7.20 show the estimated VDC for the test-bed area South France conditional on a specific fire occurring throughout the area. The expected VDC is conditional on the same hazard characteristics as in Figure 7.17 and Figure 7.18 respectively. For *FWI* = 60 the expected VDC rises in the forested areas (see also Figure 4.23c). The urban areas are expected to have 0 € of VDC. The highest values are estimated in the forested areas.
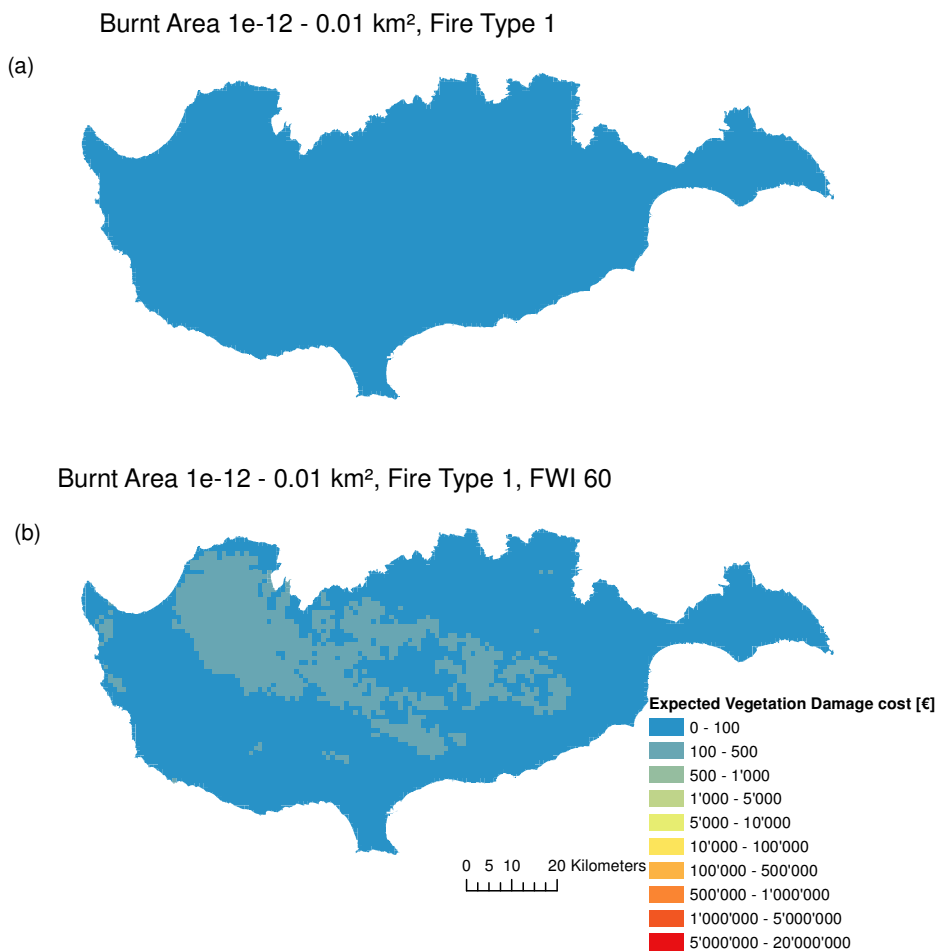
Figure 7.17: Expected vegetation damage cost [€] conditional on burnt area = 10^{-12} - 0.01 km², fire type = 1, random FWI (a) and FWI=60 (b) on Cyprus

Burnt Area 10-30 km², Fire Type 3

(a)

Burnt Area 10-30 km², Fire Type 3, FWI 60

(b)

Expected Vegetation Damage cost [€]
- 0 - 100
- 100 - 500
- 500 - 1'000
- 1'000 - 5'000
- 5'000 - 10'000
- 10'000 - 100'000
- 100'000 - 500'000
- 500'000 - 1'000'000
- 1'000'000 - 5'000'000
- 5'000'000 - 20'000'000

0 5 10   20 Kilometers
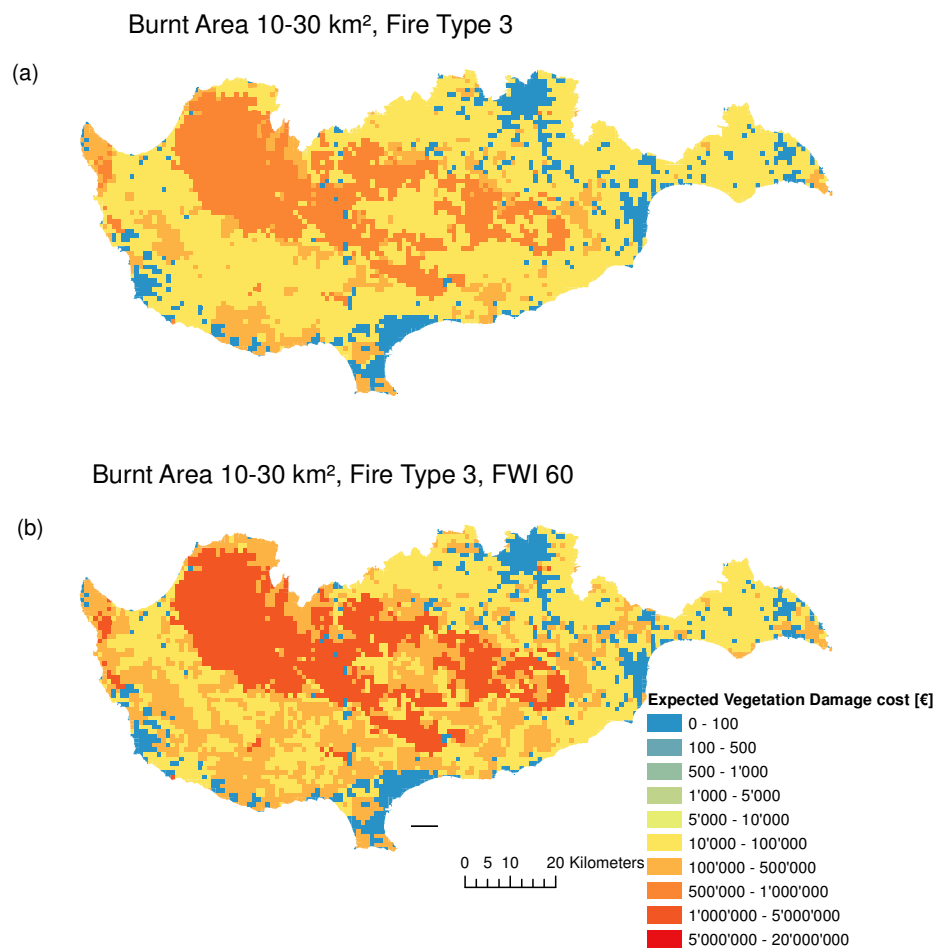
Figure 7.18: Expected vegetation damage cost [€] conditional on burnt area = 10 - 30 km², fire type = 3, random FWI (a) and FWI=60 (b) on Cyprus

(a)

Burnt area 1e-12 - 0.01 km², Fire type 1

(b)

Burnt area 1e-12 - 0.01 km², Fire type 1, FWI 60

Expected vegetation damage cost [€]

- 0 - 100
- 100 - 500
- 500 - 1'000
- 1'000 - 5'000
- 5'000 - 10'000
- 10'000 - 100'000
- 100'000 - 500'000
- 500'000 - 1'000'000
- 1'000'000 - 5'000'000
- 5'000'000 - 20'000'000

0   25   50   100 Km
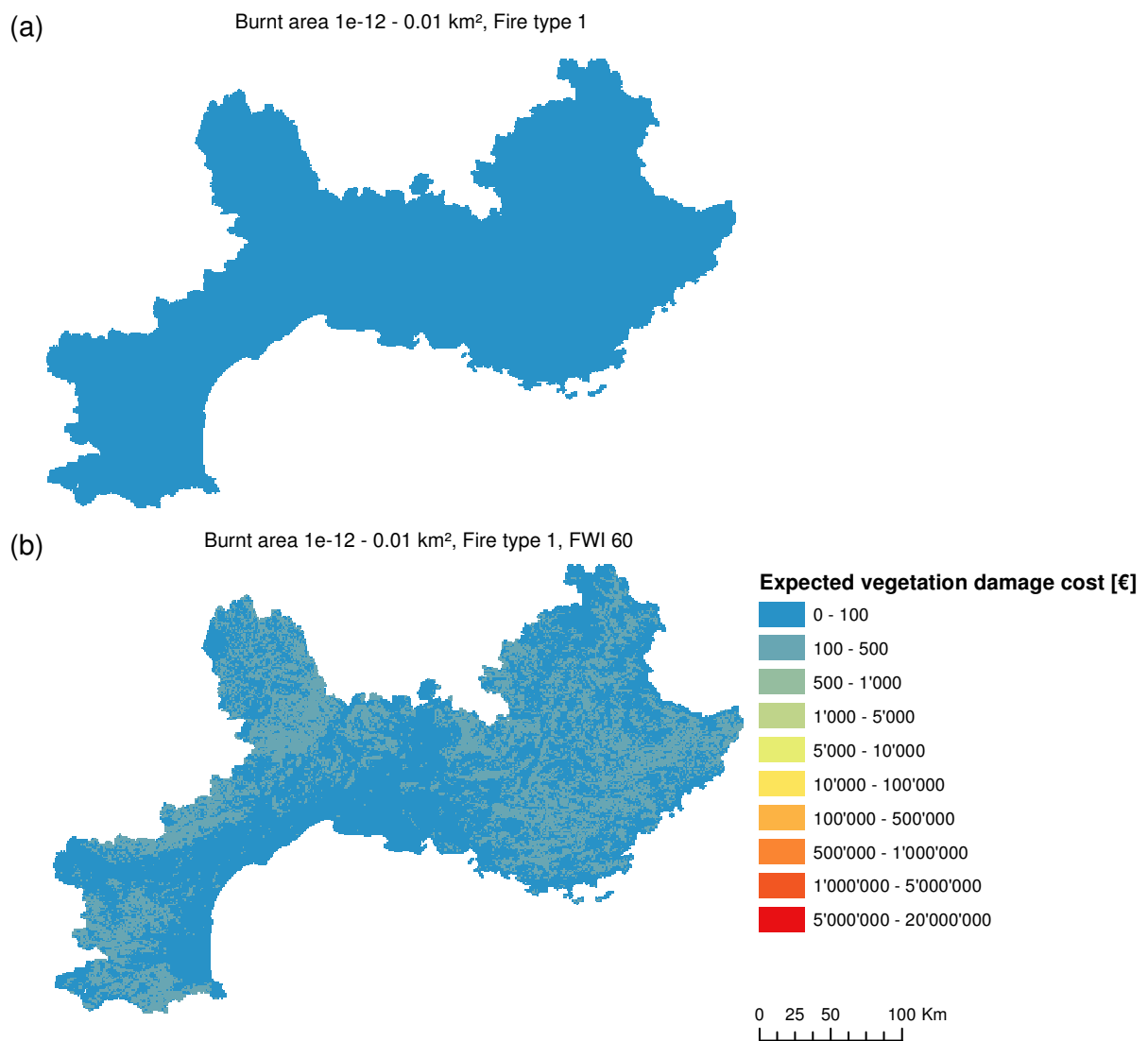
Figure 7.19: Expected vegetation damage cost [€] conditional on burnt area = 10^{-12} - 0.01 km², fire type = 1, random FWI (a) and FWI=60 (b) on South France

(a)

Burnt area 10 - 30 km², Fire type 1

(b)

Burnt area 10 - 30 km², Fire type 1, FWI 60

Expected vegetation damage cost [€]
- 0 - 100
- 100 - 500
- 500 - 1'000
- 1'000 - 5'000
- 5'000 - 10'000
- 10'000 - 100'000
- 100'000 - 500'000
- 500'000 - 1'000'000
- 1'000'000 - 5'000'000
- 5'000'000 - 20'000'000

0   25   50   100 Km
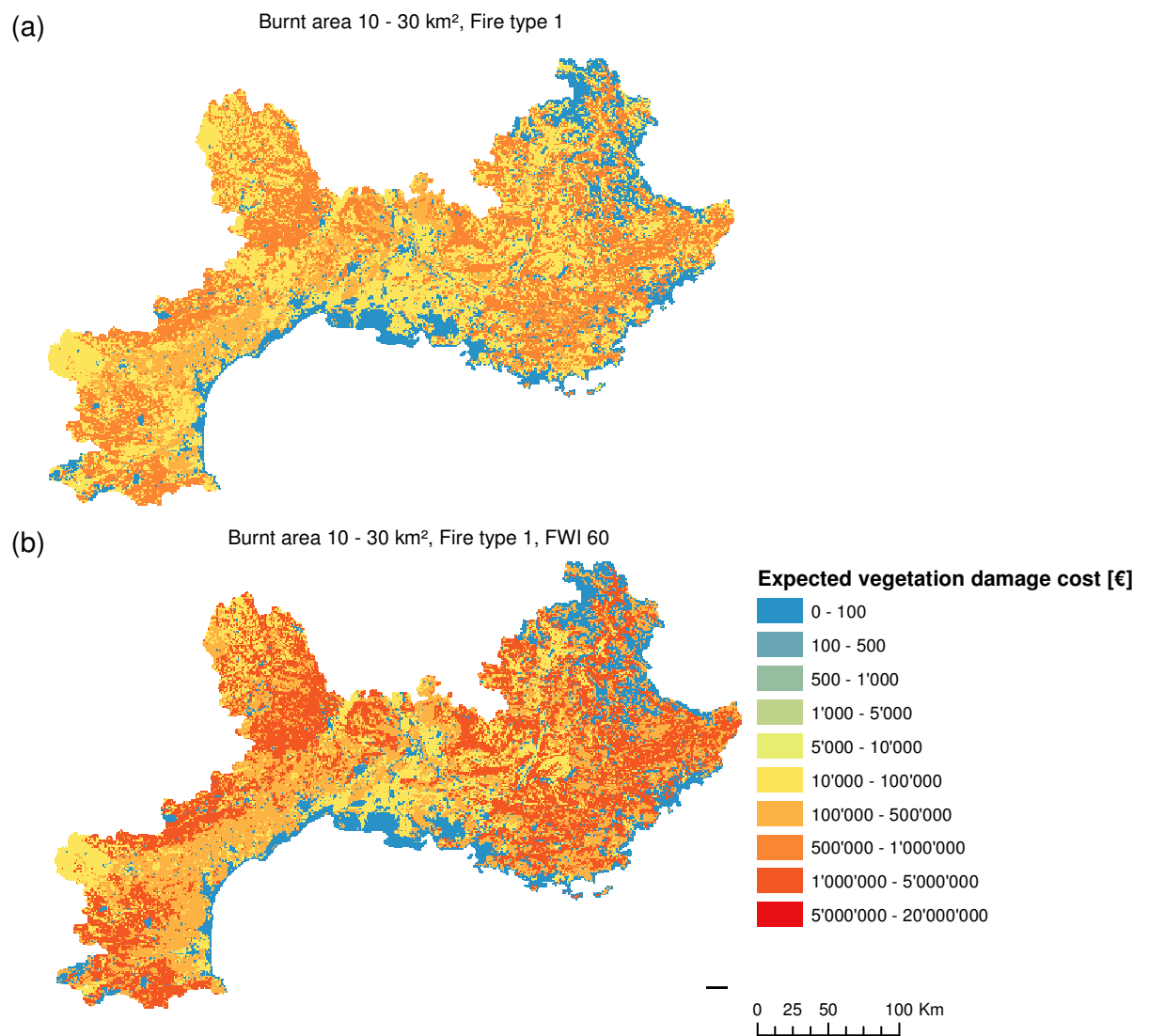
Figure 7.20: Expected vegetation damage cost [€] conditional on burnt area = 10 - 30 km², fire type = 3, random FWI (a) and FWI=60 (b) on South France

7.7   Summary

Predictive models for wildfire effects that provide monetary estimates of effects to houses and vegetation are an important component of risk assessment. Such a model can be used to support preparedness measures (e.g. fire crew allocation, fuel reduction). In Chapter 7 two models are introduced that estimate expected damage cost to houses and vegetation for given fire characteristics. The effect estimation is here facilitated by BNs, which allow modeling the damage cost of wildfires in the meso-scale with respect to different hazard characteristics and include vulnerability and exposure indicators. The model is applied to the Mediterranean island of Cyprus and to South France. First expected house damage cost maps are presented. The results show that larger house damage cost can be expected for higher burnt areas and house densities, and more hazardous fires. WUI are expected to experience the highest damages, a result which agrees with previous studies (e.g. Mozumder *et al.* 2009;Gibbons *et al.* 2012;Syphard *et al.* 2012). The highest vegetation damage cost are expected for forested areas, followed by shrubs and permanent crops. The estimated damage for specific fire periods on Cyprus and in South France is examined. The model gives realistic estimations of the damages. However, the available data on recorded damages for the verification of results are sparse. More and exact data on the fire damages would support model validation.

8 Fire risk model

In this chapter the fire risk predictive model is presented, which integrates the probabilistic models of fire hazard (presented in Chapter 5 and Chapter 6) and fire effects (presented in Chapter 7) in one model. Due to the randomness inherent in the wildfire process and because the modeling is subject to uncertainty in all three stages (occurrence, behavior/size, damages), fire risk prediction is ideally carried out in a probabilistic format. In the previous chapters (Chapter 5 – Chapter 7) it is shown how fire occurrences are influenced by weather conditions, human presence and vegetation types. Fire size is influenced mainly by local weather conditions (e.g. wind speed), topography and fuels. Fire damages depend to a large extent on fire severity and the vulnerability of assets.

8.1   Risk model for house damage and vegetation damage

Figure 8.1 introduces the fire risk model. The model integrates the three previously presented models (Chapter 5 – Chapter 7). It consists of:

(1) The fire occurrence model (yellow color), which includes as predictive variables weather conditions (expressed by the Fire Weather Index - *FWI* of the Canadian Forest Fire Weather Index System - CFFWIS), *land cover* types, *population* and *road density*, and predicts the probability of a fire occurring in each spatial-temporal unit, i.e. daily and per 1km². The node *Fire N* can be in two states, either no fire occurrence or fire occurrence. The probability of fire occurrence summarizes the probability of Fire N > 0 as derived by the Poisson distribution (Section 5.2). The CPT of *Fire occurrence rate* λ is based data from the calculation of λ for each cell of Cyprus study area based on Model 5 (Section 5.4.2).

(2) The fire size model (orange color), triggered by the occurrence model (*Fire N*), and is influenced by the actual and past weather conditions (*Recent weather*), the *Fire Behavior indices* of the CFFWIS (*FFMC*, *ISI*, *BUI*) and *Topography* (*Wind speed*, *Slope*, *AspectMinusWindDirection*).

(3) The effects model (green color), which predicts the expected losses related to houses and vegetated areas conditional on fire hazard. The fire hazard is characterized by the resulting *Burnt area* [km²] and *Fire type*. Vulnerability (resistance capacity) and exposure (values at risk) indicators are used to quantify the damage. The latest depends also on the fire suppression efficiency (see also Chapter 7). Variables representing vulnerability are *Construction type, Air suppression, Distance to next fire station, Time for ground attack, Fire containment in 24hrs, House damage, Vegetation damage*. Variables representing exposure are *Urban/Rural, House density, House stock, Construction value, Corine vegetation, Restoration cost, Restoration time*.

The final results of the combined model are the risk to houses (expected house damage cost [€]) and the risk to vegetation (expected vegetation damage cost [€]). As already shown in Eq. 2.1 (Section 2.1) the risk can be formulated as,

$$R = \mathrm{E}_{H,D}[C] = \int_H p(H) \int_D p(D|H)C(D,H)dD \; dH \tag{8.1}$$

wherein H is the hazard, D the resulting damages and C the consequences (i.e. effects). In the presented model, hazard H is expressed by *Burnt area* (*detailed*) and *Fire type*. The damages D, i.e. the vulnerability, is expressed by the variables House damage and Vegetation damage, the variable *Fire Containment in 24 hrs* and its parent nodes. The effects nodes *House damage cost* and *Vegetation damage cost* are a function of the hazard variable *Burnt area detailed*, the vulnerability variables *House damage* and *Vegetation damage* respectively and the exposure variables.

The node *Burnt area* is identical to the node *Burnt area* of the Fire size model (Chapter 6) and the node *BurntAreaDetailed* is identical to the node *Burnt area* of the fire effects model (Chapter 7). The latest has more intervals in the range of $1 - 30$ km². The reason for this choice in the modelling, is made to restrict the number of states and thus the CPT of the variable *Burnt area* in the size model (Chapter 6) and as a result to allow parameter learning with the limited fire data set of Cyprus 2006-2009. The node *Burnt area detailed* is a child of the node *Burnt area* with more intervals in the range of $1 - 30$ km², in order to give more precise estimations of the expected cost for large fires. The CPT of the node *Burnt area detailed* is learnt with the same fire data set of Cyprus 2006-2009.
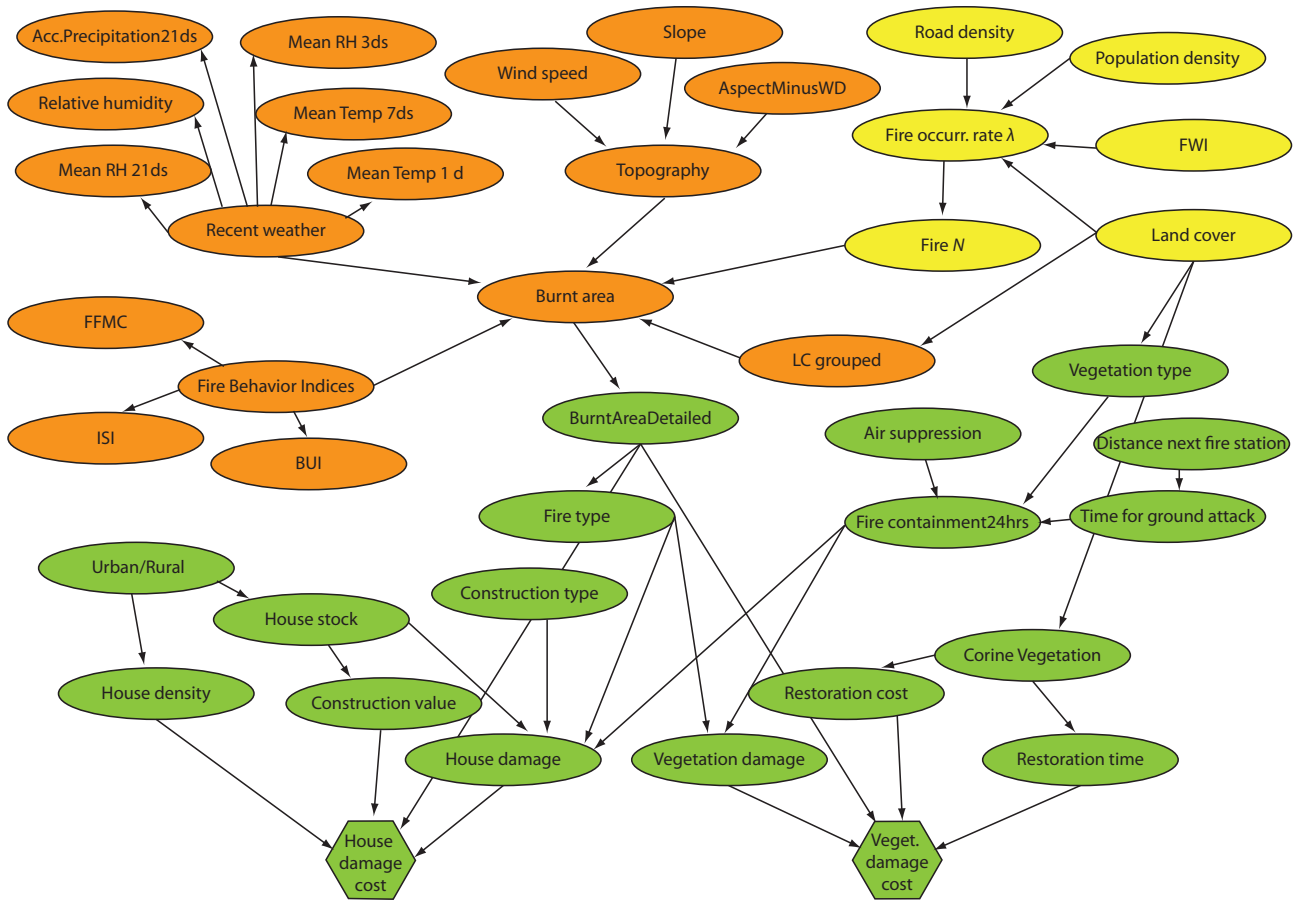
Figure 8.1: Fire risk model. The model includes the three models presented in Chapter 5 – Chapter 7. The fire occurrence model (yellow), the fire size model (orange) and the fire effects model (green).

8.2 BN computations

As already explained in Chapter 5 – Chapter 7, the parameters of the model are learnt with data from the study area Cyprus (2006-2009). The model is then applied on Cyprus 2010 and South France 2003 and 2010. The variables, their states and data sources are identical with those shown in Table 6.3 and Table 7.2. A description of the variables, which are not included in those tables is given in Table 8.1.

Table 8.1: Description of BN variables and data sources for the definition of the conditional probability tables of the fire risk model

Variable	#states	States	Source of probability distribution and additional information
Population density [People/km²]	3	0 - 20 20 - 300 300 - inf	Source: Statistical Service Cyprus (census 2011)
Road density [km/km²]	3	0 - 0.5 0.5 - 2 2 - inf	Source: Open Street Map
Fire occurrence rate λ $\left[\dfrac{Fires}{day \cdot km^2}\right]$	19	$0 - 10^{-9}$ $10^{-9} - 10^{-8}$ $10^{-8} - 10^{-7}$ $10^{-7} - 10^{-6}$ $10^{-6} - 5 \cdot 10^{-6}$ $5 \cdot 10^{-6} - 10^{-5}$ $10^{-5} - 2 \cdot 10^{-5}$ … $8 \cdot 10^{-5} - 9 \cdot 10^{-5}$ $9 \cdot 10^{-5} - 0.0001$ $0.0001 - 0.0005$ $0.0005 - 0.001$ $0.001 - 0.01$ $0.01 - 0.1$	Based on Equation 5.2 (Fire occurrence Model 5 in Chapter 5)
Fire N	2	1 0	Based on Equation 5.1 with $\alpha = 1\ km^2$
Burnt area [km²]	5	$0 - 10^{-12}$ $10^{-12} - 0.01$ $0.01 - 0.1$ $0.1 - 1$ $1 - inf$	Historical fire events (2006-2010) Data source: Department of Forest, Ministry of Agriculture Cyprus
Burnt area detailed [km²]	7	$0 - 10^{-12}$ $10^{-12} - 0.01$ $0.01 - 0.1$ $0.1 - 1$ $1 - 3$ $3 - 10$ $10 - inf$	Historical fire events (2006-2010) Data source: Department of Forest, Ministry of Agriculture Cyprus
Fire type	4	0 1 2 3	0: no fire 1: surface fire with flame length < 3.5m 2: surface fire with flame length >3.5m 3: crown fire Classification based on fire events in WUI Greece 1993-2003

Figure 8.2 and Figure 8.3 both show screenshots of the risk model for different conditions. The figures are here given to demonstrate the prediction made by the model with and without given evidence. In Figure 8.2 no evidence is given for the cell showing the risk to houses and vegetation for an average cell in an average day. In Figure 8.3 evidence is given on the weather (FWI and Accumulated precipitation 21 days) and cell characteristics (Land cover, Slope).

Figure 8.2: Expected house damage cost [€] and vegetation damage cost [€] for average cell, without evidence given (screenshot from HUGIN)
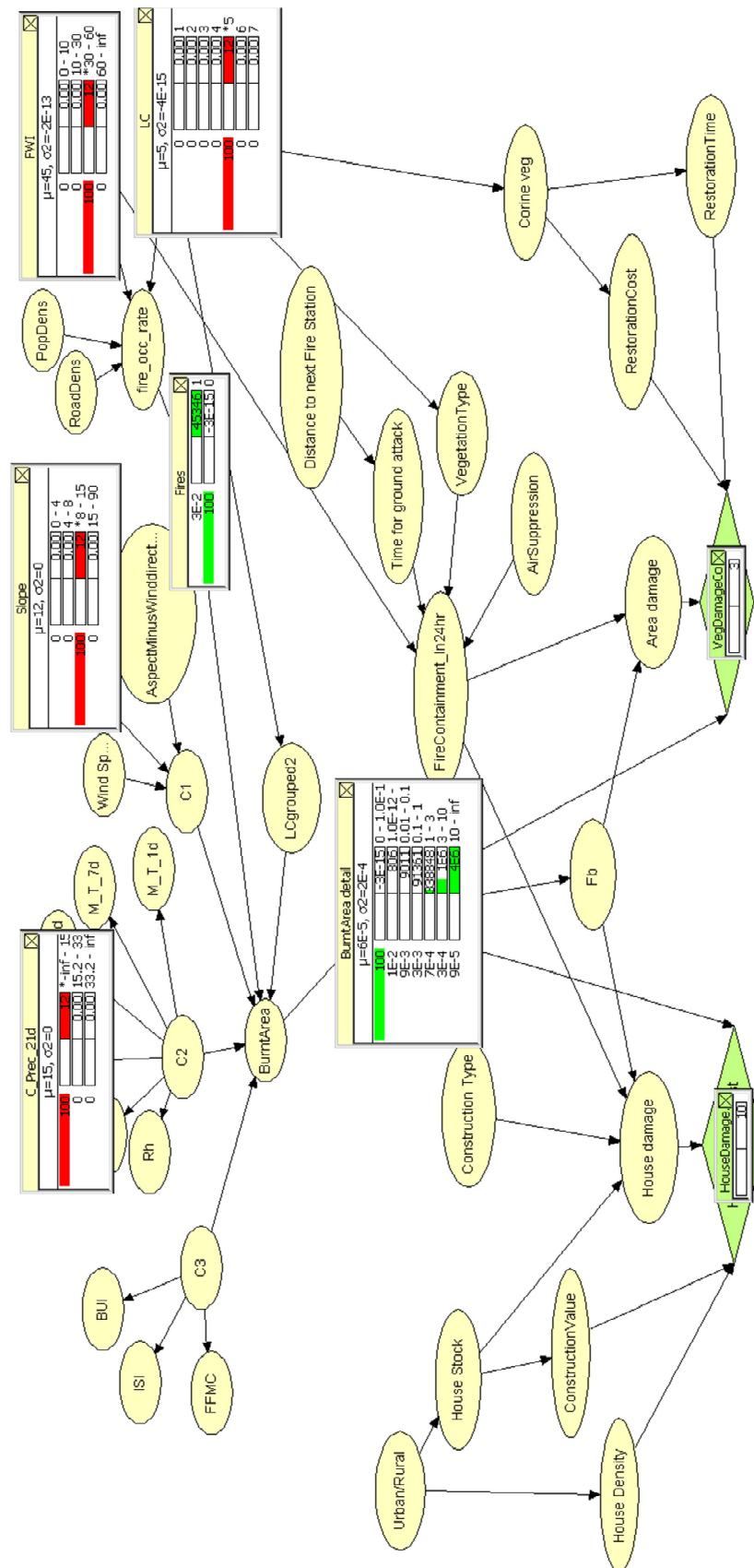
Figure 8.3: Expected house damage cost [€] and vegetation damage cost [€] with evidence given on weather (FWI, Accumulated precipitation 21 days) and cell characteristics (Land cover, Slope) (screenshot from HUGIN)

8.3 Results

8.3.1 Sensitivity analysis

In order to show the influence of the variables on the risk to houses and vegetation, the variance of risk for each variable is calculated (Table 8.2). The prior risk to houses for an average cell of the study area is 3 €. The intermediate results for each state of the variables are shown in Table AIII-1 (Appendix III). Table 8.2 gives the variables in decreasing order of their influence on the risk to houses. The highest influence on risk to houses have the variables *Burnt Area, Vegetation damage, House damage*, *Fire type*, *Fires, House density Fire occurrence rate*, *Fire containment in 24 hrs, Urban/Rural*. The variable *Vegetation type* has identical influence with the variable *Land cover type*. The variable *House stock* has identical influence with the variable *Urban/rural*. This is due to the deterministic connection that these variables have with their parent variables in the BN. Table AIII-1 (Appendix III) also includes the relative increase of the risk to houses, when evidence is given in each state of the variables. As an example, when there is evidence that the resulting *Burnt area* is in the interval $10 - \inf$ km², the risk to houses for an average cell becomes $2 \cdot 10^6$, thus increases by $+6.66 \cdot 10^7$ %.

The prior expected vegetation damage cost for an average cell of the study area is 0.4 €. Table 8.3 summarizes the influence of the variables on risk to vegetation. The detailed intermediate results can be found in Table AIII-2 (Appendix III). The highest influence on risk to vegetation have the variables (in decreasing order) *Burnt area*, *Vegetation damage*, *House damage*, *Fire type*, *Fires, Fire occurrence rate*, *Fire containment in 24hrs*, *Urban/Rural*. As an example, when there is evidence that the land cover type is forest (type 5), the expected vegetation damage cost for an average cell becomes 2 €, thus increases by $+400$ %.

Table 8.2: Variable influence on house risk [€]

Variable V	Variance $\mathrm{Var}_V[\mathrm{Risk}] = \sum (\mathrm{Risk}(V) - \mathrm{Risk})^2 \cdot p(v)$
Burnt area	2,605,708.59
Vegetation damage	802,008.91
House damage	356,008.91
Fire type	162,031.91
Fires	83,208.91
House density	3,964.62
Fire occur. rate	664.00
Fire Containment in 24hrs	78.75
Urban/Rural	20.32
House stock	20.32
Construction value	7.60
FWI	4.99
Land cover	4.61
Restoration cost	3.77
Pop. density	3.45
Restoration time	2.68
Recent Weather	0.73
Road density	0.64
Topography	0.21
Fire behavior indices	0.17
Construction type	0

Table 8.3: Variable influence on vegetation risk [€]

Variable V	Variance $\text{Var}_V[\text{Risk}] = \sum(\text{Risk}(V) - \text{Risk})^2 \cdot p(v)$
Burnt area	38,036.86
Vegetation damage	25,314.16
House damage	8,183.04
Fire type	4,326.18
Fires	1,606.16
Fire occur. rate	42.40
Fire Containment in 24hrs	1.32
Restoration time	0.69
Land cover	0.61
Pop. density	0.20
Restoration cost	0.19
FWI	0.09
Recent Weather	0.01
Road density	0
Topography	0
Fire behavior indices	0
Construction type	0
Urban/Rural	0
House stock	0
Construction value	0
House density	0

8.3.2   Cyprus

The fire risk model is applied on Cyprus 2010. Figure 8.4 - Figure 8.6 show timelines for Cyprus 2010 of the predicted daily fire risk to houses (Figure 8.4), vegetation (Figure 8.5) and both (Figure 8.6). As expected, the risk to houses increases gradually between April (day 91) and August (day 240), and decreases gradually from September (day 241) to December (day 370) (Figure 8.4). The highest value is predicted on the 25.August (32,995 €). The same trend can be observed for the predicted fire risk to vegetation (Figure 8.5). The maximum value predicted is on the 26. August (5,396 €). For the overall risk the highest value is 36,740 € (Figure 8.6). In all three figures, fire risk increases from April to August. This is due to the weather conditions in spring-summer that lead to dryer vegetation (low precipitation, high temperature, high wind speed) (see also Figure 4.2 and Figure 4.8). As shown in Figure 8.1 in the proposed model weather variables and CFFWIS components influence *Fire occurrence rate*, *Burnt area* and *Fire containment in 24hrs*, and so during the spring-summer period they favor fire occurrence and fire spread (burnt area) and hinder fire containment, leading as a result to higher risk on those days.
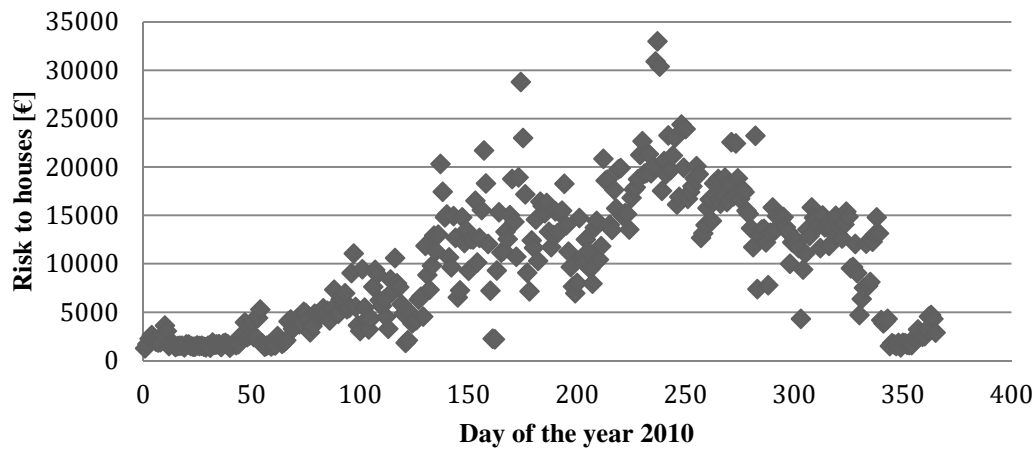
Figure 8.4: Daily predicted fire risk to houses [€] for Cyprus 2010

Figure 8.5: Daily predicted fire risk to vegetation [€] for Cyprus 2010
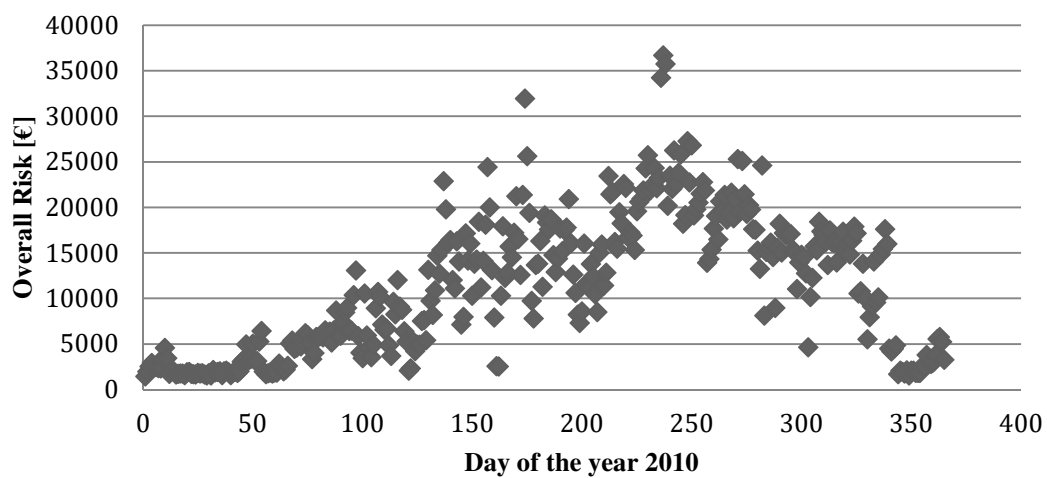
Figure 8.6: Daily predicted fire risk to houses and vegetation [€] for Cyprus 2010

Four days in 2010 are chosen to demonstrate the predictions of the risk model in maps; a day in winter (01.01.2010), in which low risk values are expected, and 3 days with the highest recorded burnt area in 2010. As expected, FWI takes low values in winter days and higher values in summer days (Figure 8.**7**). The highest risk to houses over the whole area is predicted on 06.06.10 (21,735 €) (Figure 8.8) and the highest risk to vegetation over the whole area is predicted on 22.08.10 (2,768 €) (Figure 8.9). In areas with higher FWI, risk to houses and vegetation is higher. Moreover, the WUI areas are the ones, where the highest risk to houses is predicted (Figure 8.8), which is in agreement with previous studies (Beringer 2000;Cohen 2000;Haight *et al.* 2004;Mozumder *et al.* 2009;Mell *et al.* 2010) (see also Chapter 7). On the other hand, regarding the risk to vegetation (Figure 8.9), forested areas on Cyprus have the highest risk to vegetation due to fuel availability and high restoration cost and time (Table 7.3).
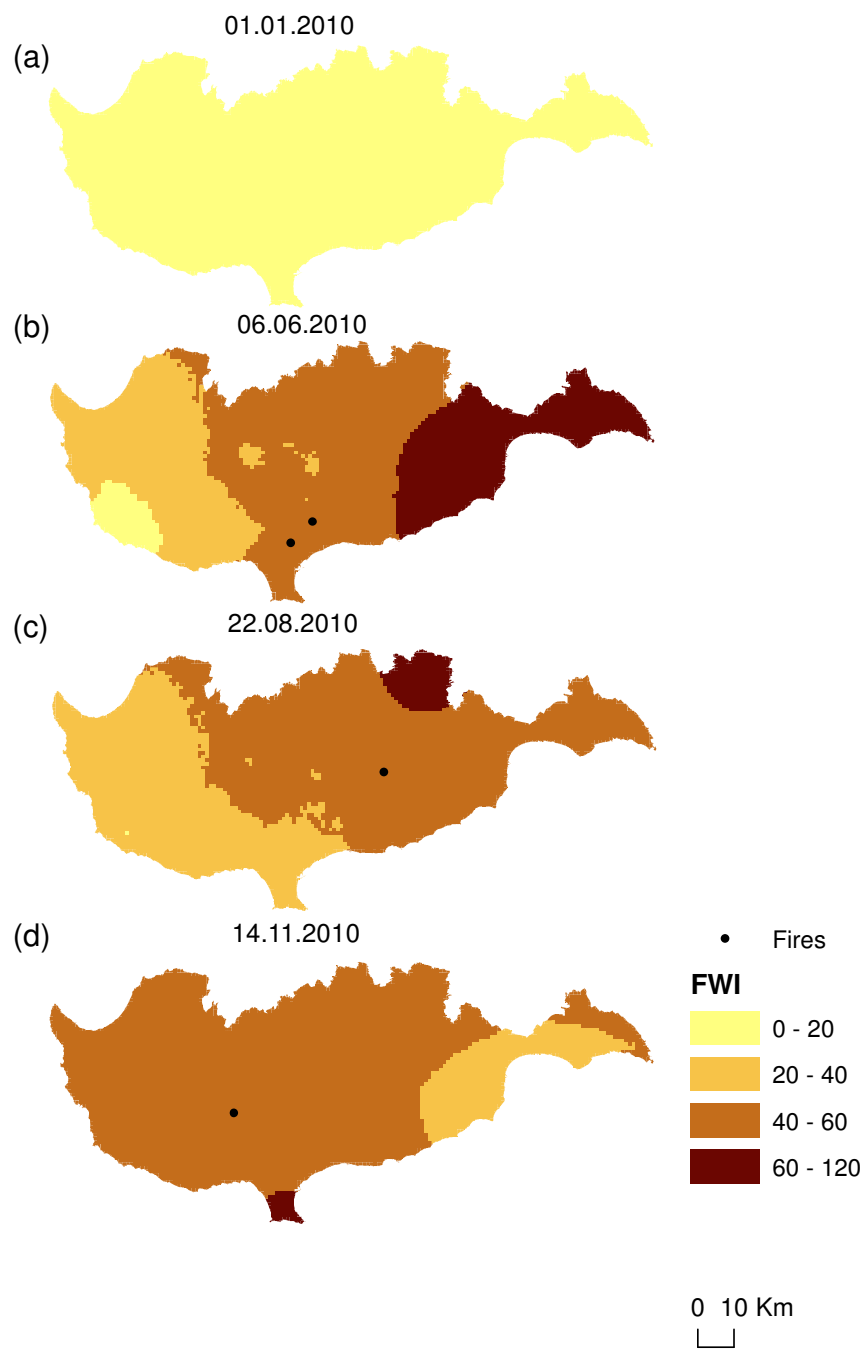
Figure 8.7: FWI and fire events on different days of 2010 (in brackets the total burnt area):
(a) 11th January (no fire events), (b) 6th June (4.3 km²), (c) 22 August (1.15 km²), (d) 14th November (2.22 km²)

Figure 8.8: Predicted fire risk to houses [€] on different days of 2010 (in brackets the accumulated risk over the entire area): (a) 1st January (1,268 €), (b) 6th June (21,735 €), (c) 22 August (19,379 €), (d) 14th November (13,880 €)

Figure 8.9: Predicted fire risk to vegetation [€] on different days of 2010 (in brackets the accumulated risk over the entire area): (a) 1st January (198 €), (b) 6th June (2,718 €), (c) 22 August (2,768 €), (d) 14th November (2,353 €)

8.3.3   South France

The proposed fire risk model is also applied to South France for 2003 and 2010. In 2003 a very destructive fire season with 1937 occurring fires and 306.68 km² burnt resulted in several structures damaged and thousands of people evacuated from their houses (http://news.bbc.co.uk/2/hi/europe/3105339.stm). Year 2010 with 802 fires occurred and 54.92 km² burnt area is the last available year of the data set and the same year as for Cyprus.

Figure 8.10 and Figure 8.11 show the daily predicted risk to houses and vegetation respectively for years 2003 and 2010 over the whole area. In 2003 the predicted risk to houses and to vegetation is higher than during 2010. However, the highest daily risk is predicted for 2010. The same trend can be seen as expected for the overall risk for these years (Figure 8.12). Daily risk increases during the fire period April (day 120) to August (day 240) and decreases later on. The trend is similar to the results shown for Cyprus 2010 (Figure 8.6). The peak of the predicted fire risk occurs in 2003 in July (day 210), earlier than in 2010 (August, day 240). Particularly destructive fires occurred indeed earlier in 2003 (29.07.2003, Source: http://news.bbc.co.uk/2/hi/europe/3105339.stm) than in 2010 (31.08.2010, Source: http://www.english.rfi.fr/france/20100901-fires-ravage-southern-france). This supports the reliability of the prediction of the fire risk model.

To demonstrate the prediction of risk in maps, four days have been chosen for 2003 (Figure 8.10 - Figure 8.12). These are the days in which the highest burnt areas of the year were recorded.

As previously for Cyprus, the risk is higher in the peri-urban areas and in areas with permanent crops (rural areas with available fuels and structures) (see also land cover types in Figure 4.31(c)). Figure 8.15 shows the predicted fire risk to vegetation [€] for the same days. It should be noticed, that a lower classification of the risk is here chosen, in order to differentiate between lower risk values. Here, forested and agricultural areas have higher vegetation risk values.

Predictions of risk for respective days in 2010 for South France are included in Appendix III (Figure AIII-1 – Figure AIII-3). The maps show similar distribution of the risk as in the days of 2003.
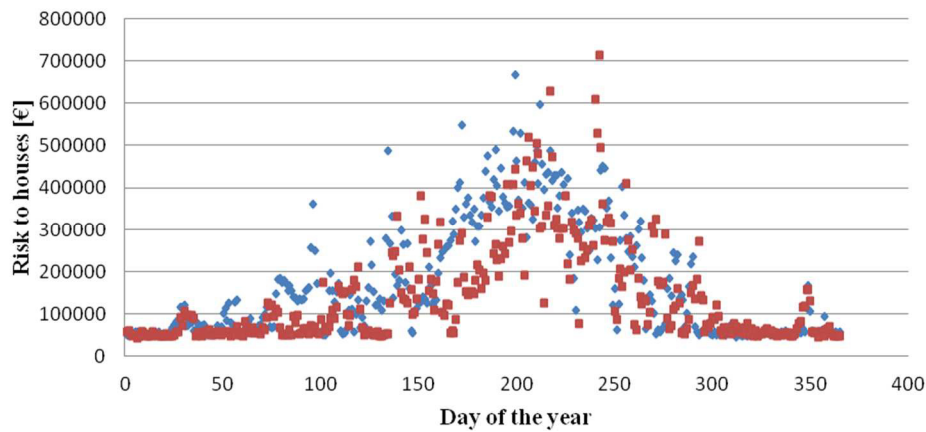
Figure 8.10: Daily predicted fire risk to houses [€] for South France 2003 and 2010
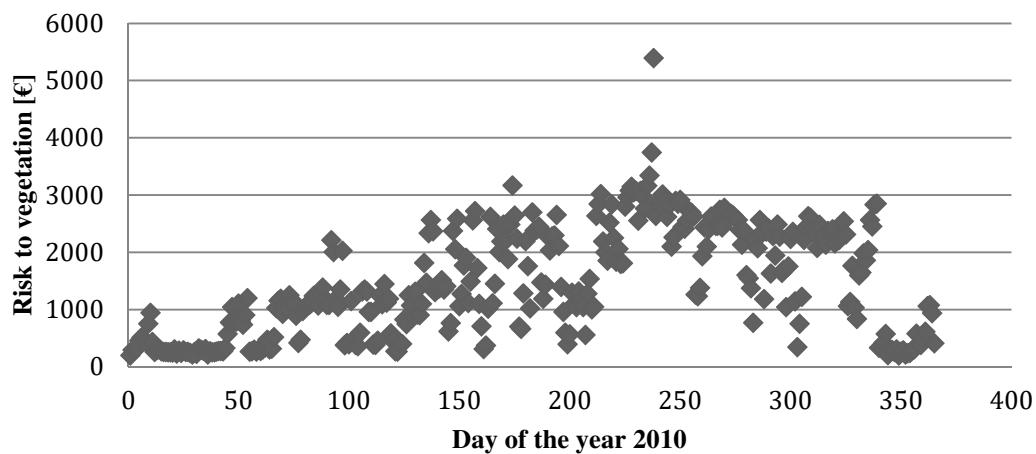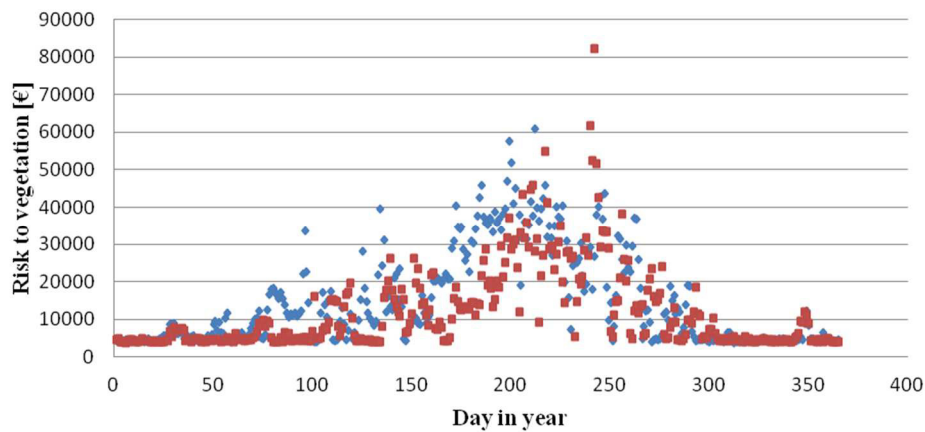

Figure 8.11: Daily predicted fire risk to vegetation [€] for South France 2003 and 2010
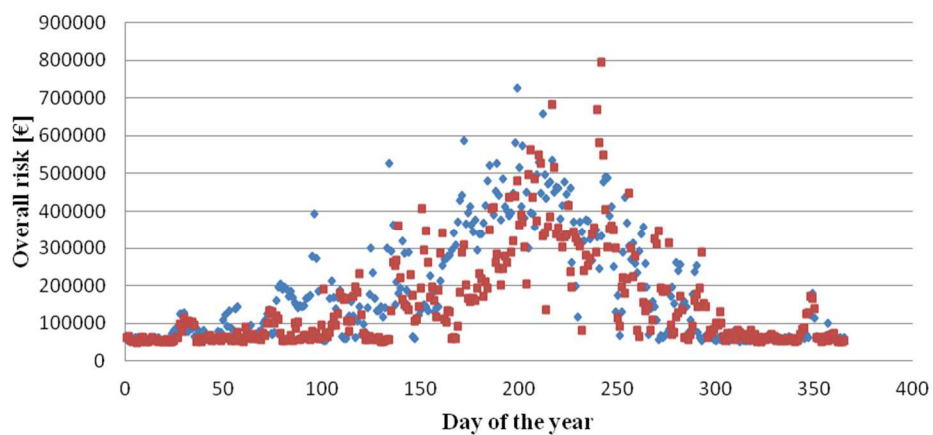
Figure 8.12: Daily predicted fire risk to houses and vegetation [€] for South France 2003 and 2010

(a)   01.01.2003

(b)   17.07.2003

(c)   28.07.2003

•   Fires

FWI

0 - 20

20 - 40

40 - 60

60 - 200

(d)   31.08.2003

N

0   50   100   200 Kilometers
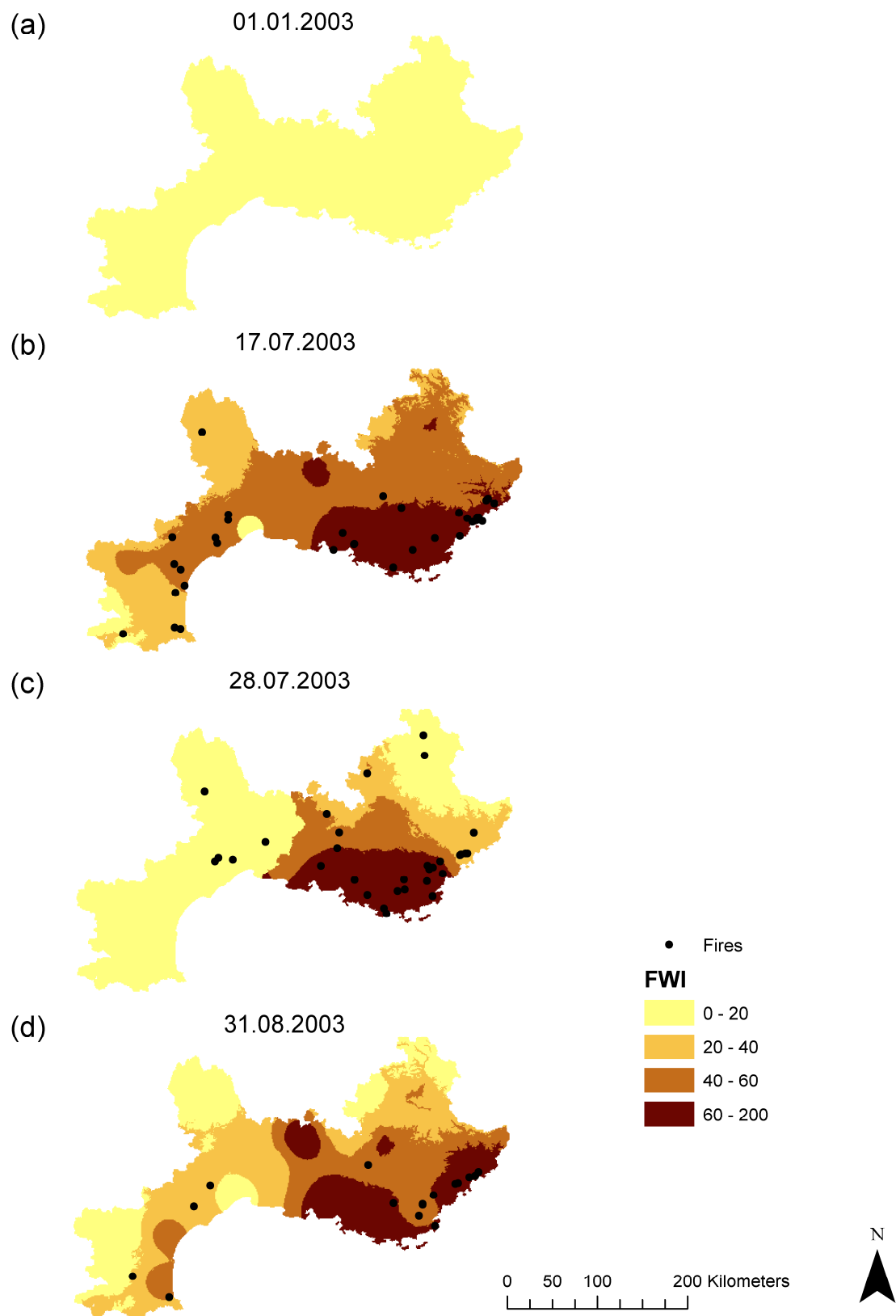
Figure 8.13: FWI and fire events on different days of 2003 in South France (in brackets the burnt area):
(a) 1st January (no fire events), (b) 17th July (67.44 km²), (c) 28th July (56.46 km²), (d) 31st August (27.26 km²)
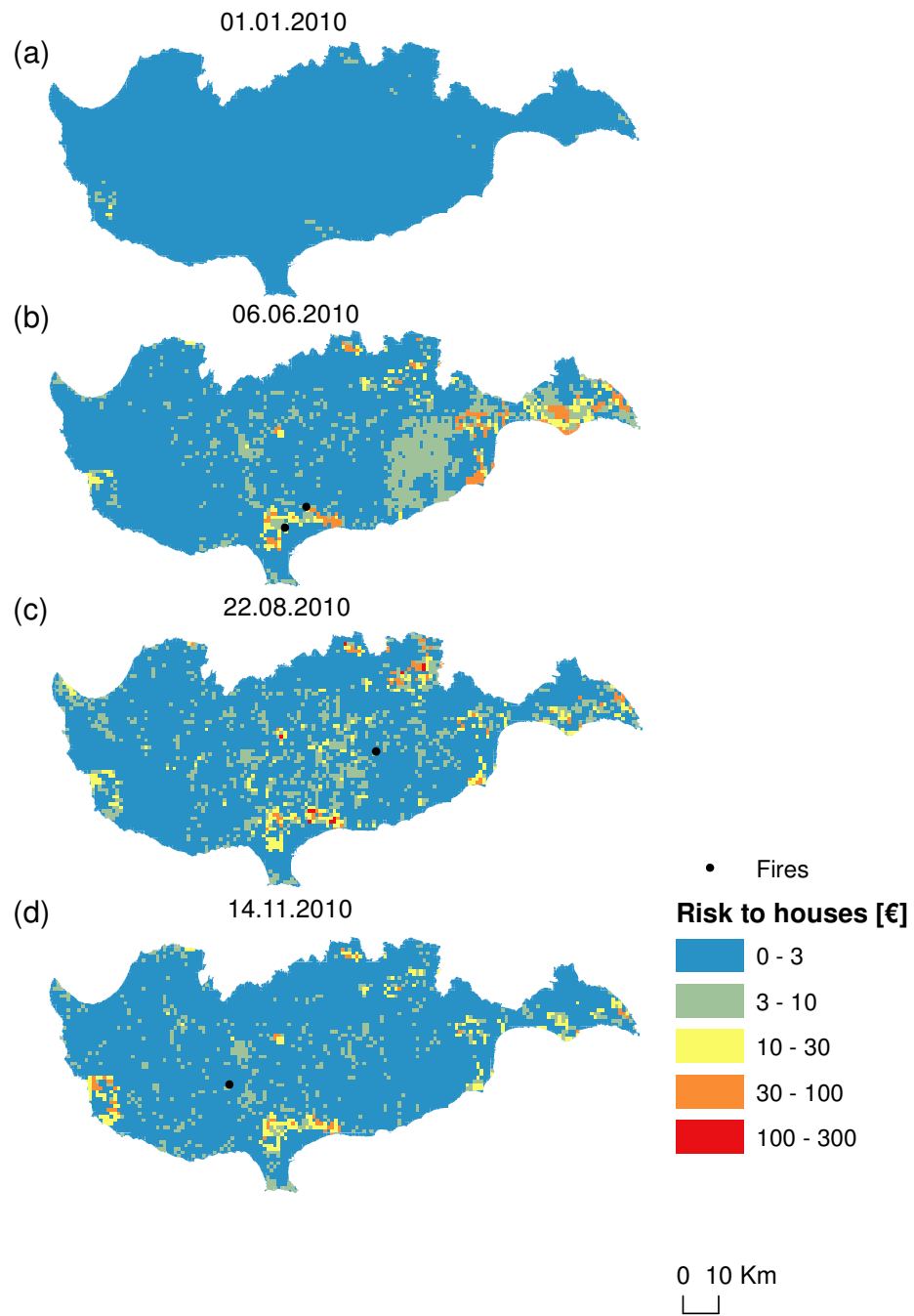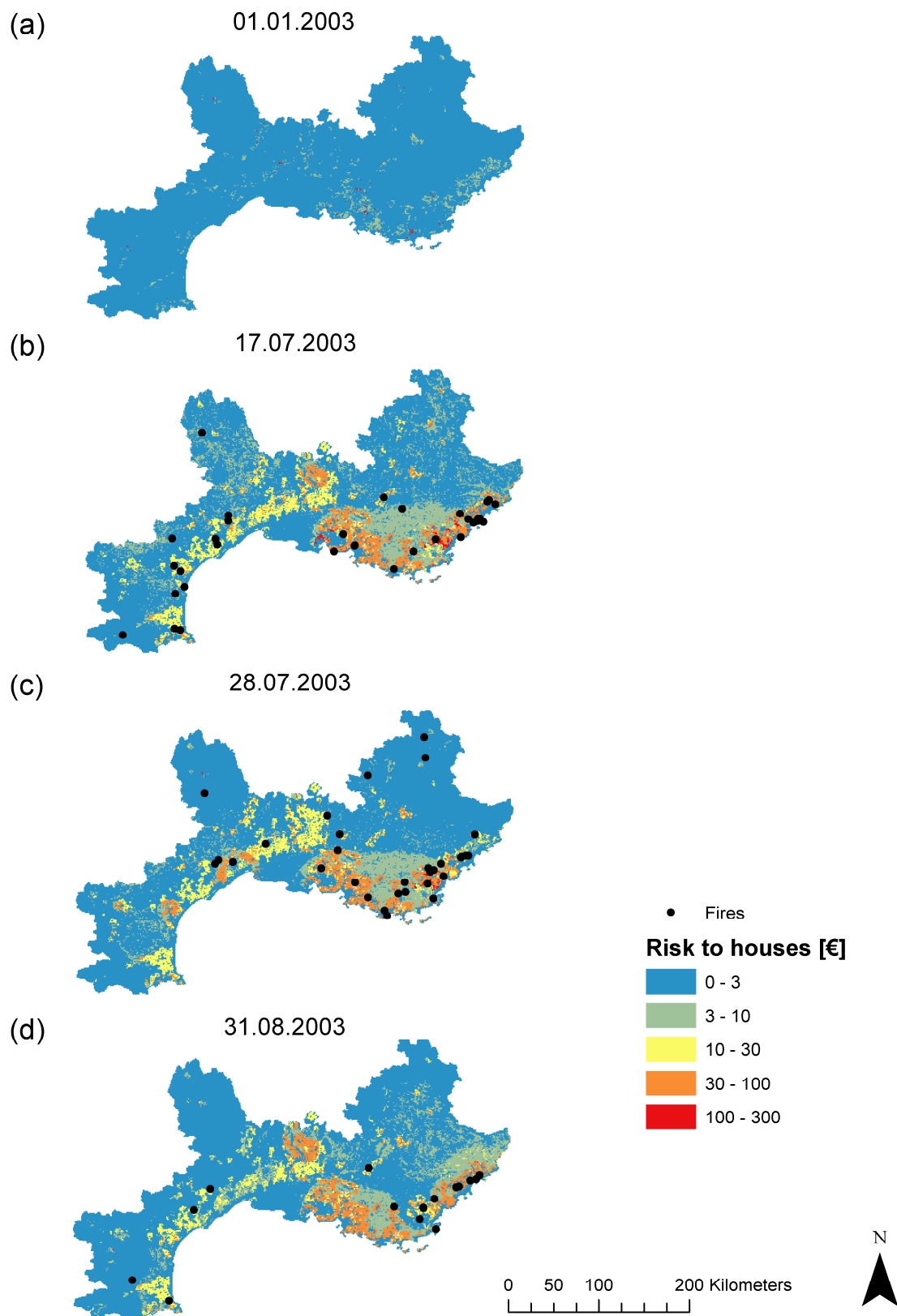
Figure 8.14: Predicted fire risk to houses [€] on different days of 2003 in South France (in brackets the accumulated risk over the whole area): (a) 1st January (51,240 €), (b) 17th July (534,075 €), (c) 28th July (460,916 €), (d) 31st August (440,192 €)
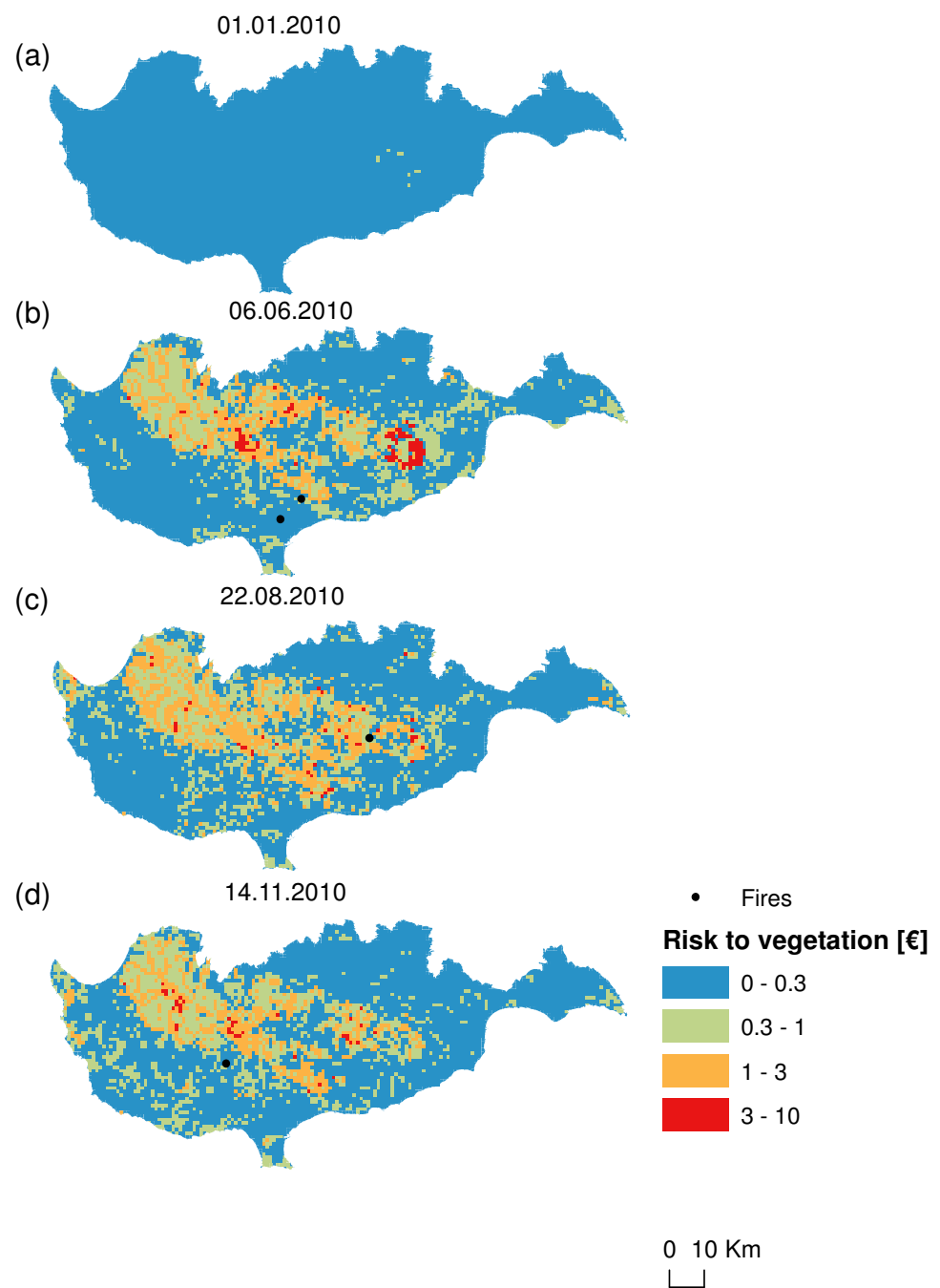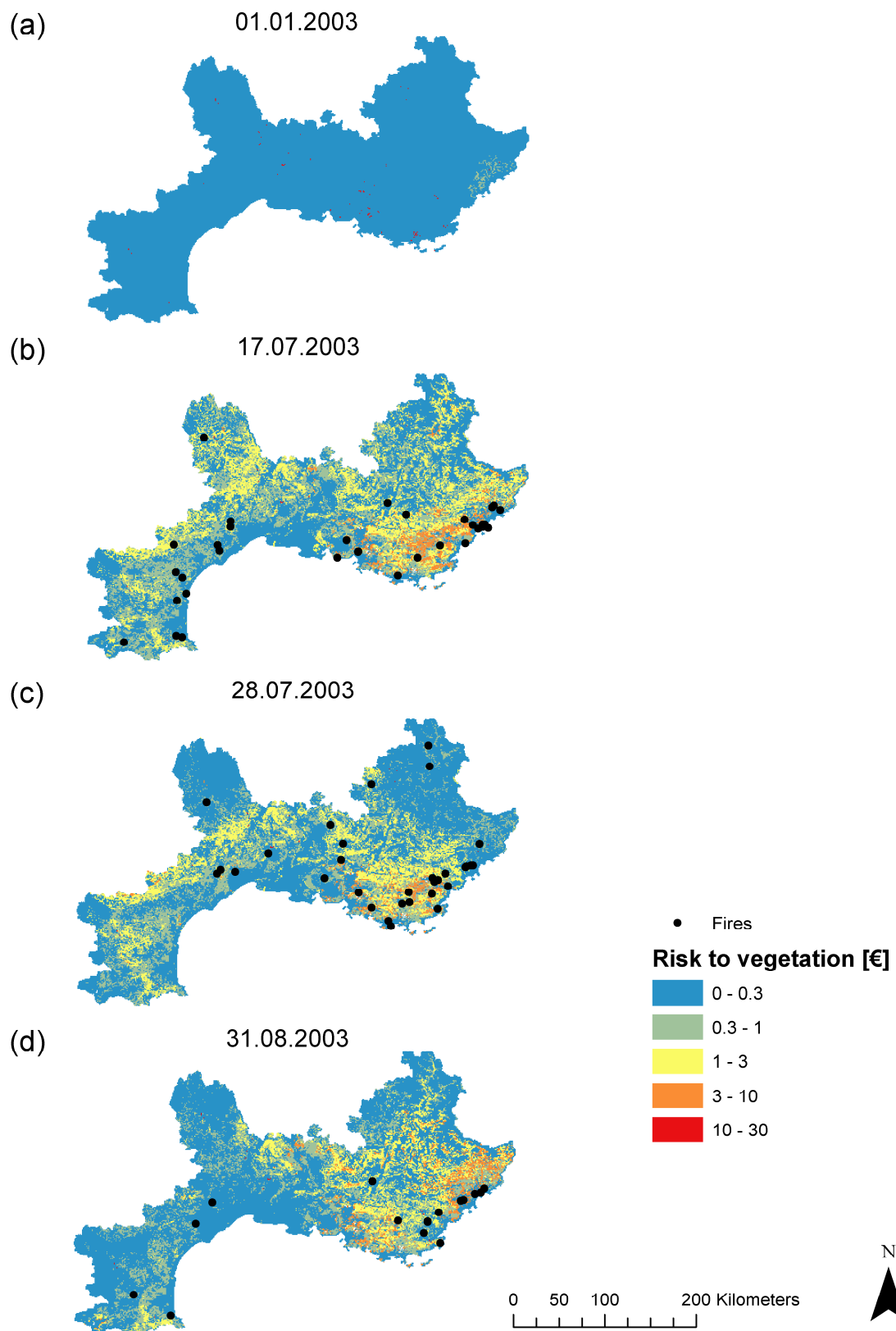
Figure 8.15: Predicted fire risk to vegetation [€] on different days of 2003 in South France (in brackets the accumulated risk over the whole area): (a) 1st January (4,231 €), (b) 17th July (46,864 €), (c) 28th July (35,248 €), (d) 31st August (37,838 €)

8.4   Summary

Chapter 8 gives an insight into the final fire risk model. The proposed BN model results from the combination of the three previously presented models. The fire occurrence model (Chapter 5), the fire size model (Chapter 6) and the fire effects model (Chapter 7). The CPTs of the model are learned with data from Cyprus 2006-2009. The model is applied on data from Cyprus 2010 and from South France 2003 and 2010. The time series for these years show that the risk to houses and vegetation increases from April to August and decreases from September to December. Certain days with historic fires resulting to large burnt areas are chosen to map the predicted risk to houses and vegetation on the study areas. The peri-urban areas (WUI), thus the areas with coexisting structures and vegetation have the highest predicted risk to houses. The forested and agricultural areas have the highest fire risk to vegetation. For South France the pick of the predictions agrees with the destructive fires that occurred in these years, with several damaged houses, thousands of peoples evacuated from their houses and hundreds of km² of vegetated areas burnt.

9 Conclusion

9.1 Summary

Fires are common during summer periods in the Mediterranean. Mild wet winters and extended dry hot summers form fire prone environments; strong katabatic foehn winds intensify occurring fires, making fire suppression a demanding, dangerous and time/resource consuming task. Although weather favours fire spread, it is mainly humans responsible for fire ignitions in the Mediterranean. Most fires are started by people, either on purpose (e.g. arson) or by accident (e.g. campfire, agricultural activities). Record temperatures in the past (e.g. Greece 2007, Russia 2010) dried the accumulated fuels and facilitated the rapid spread of occurred fire events with enormous effects on humans and the environment. Such extreme conditions are expected to be more often in the future according to future climate change scenarios. Effective wildfire risk prediction in high temporal and spatial resolution can therefore prove an important tool to support fire management. Both preventive and mitigating measures can benefit from it. From risk accounting of endangered areas in the insurance industry, to decision making in suppression crew allocation, fire risk quantification can be a valuable tool for the private and the public sector.

Fire risk can be estimated as a function of hazard occurrence probability and consequences. The hazard is characterized by the occurrence and severity. Consequences can be direct/indirect, or tangible/intangible. Consequences are a function of vulnerability and exposure of the affected items (e.g. human lives, properties, infrastructure and vegetation). Vulnerability describes the degree of expected damage as a function of hazard intensity. Exposure refers to the items at risk, such as house density. Risk is thus expressed by hazard, vulnerability and exposure (Figure 2.1). Indicators, thus measurable variables are used to quantify vulnerability and exposure. Due to the randomness inherent in the wildfire process and because the modeling is subject to uncertainty in all three stages (occurrence, behavior, damages), fire risk prediction is ideally carried out in a probabilistic format.

Available data and expert knowledge should be incorporated for parameter learning. Moreover, the applications need to deal with (partly incomplete) data from various sources.

This thesis aims to provide a methodology for fire risk modeling and introduce a daily fire risk prediction model in the meso-scale for Mediterranean areas. The model results in daily fire risk estimations demonstrated in maps.

The modeling is carried out with Bayesian Networks (BN), due to their capability to model complex processes with random variables and the associated uncertainties. Three BNs are introduced to account for the three stages of the wildfire process (occurrence, behavior, consequences) as shown in Chapter 5, Chapter 6 and Chapter 7 respectively. The fire occurrence model is based on the results of a Poisson regression (Chapter 5). The models include variables expressing weather conditions, fuel moisture, topography, land cover, construction characteristics, human presence, and infrastructure and suppression efficiency. The composition of the three models results to the wildfire risk model, which predicts daily wildfire risk to houses and vegetated areas in 1km² spatial resolution (Chapter 8). The BN is coupled with a Geographic Information System (GIS), to enable estimation of the model parameters (Conditional Probability Tables (CPT) of the variables) and risk mapping (Section 3.2). The models are applied on three study areas of the Mediterranean (Rhodes, Cyprus, South France).

9.2   Discussion

The selected probabilistic modeling approach in Chapter 5 provides a quantitative metric of the ability of different explanatory variables to predict daily fire occurrence. The weather influence on fire occurrence is expressed by the fire danger indicator "Fire Weather Index" (FWI) developed originally for Canada. FWI proved to have better fire occurrence predictive ability than the intermediated components of the CFFWIS. The observed FWI values in the Mediterranean case study areas are mostly in a limited range only (see also Figure 4.12), which limits the ability of the FWI alone to discriminate days and locations with high fire danger from those with low fire danger. This indicates that there might be potential in adjusting the definition of the FWI to local conditions in agreement with Dimitrakopoulos *et al.* (2011). It may also be investigated if selected weather parameters should be included as explanatory variables in addition to the FWI. Moreover, in agreement with previous studies, it is found that including anthropogenic factors as explanatory variables can significantly improve the prediction of fire occurrence. The comparison of different models showed that a model with land cover types, population and road density (all readily available data) has a significantly better predictive ability than one based on *FWI* alone, which is in operation in present by the EU as the European Forest Fire Information System (EFFIS) (Figure 2.10). Since such data is readily available, it is straightforward to include it in forecasting systems. However, including additional variables in the modeling should be done with caution to avoid redundant variables and the interdependencies should be taken into account. Already the three included explanatory variables (land cover type, population and road density) are partly redundant and inter-dependent, e.g. both population and road density are higher in urban areas. Moreover, due to the randomness of fire occurrence, there is a limitation to any prediction. While the developed models are able to identify days and locations with higher fire risks, they are not - and will not - be able to deterministically predict fire occurrences in advance. Nevertheless, the predictions can support the planning of fire preventive and mitigating measures, such as fuel reduction and fire

crew allocation. Importantly, they also improve the understanding of influential factors on fire occurrence.

The fire size model of Chapter 6 predicts resulting burnt area [km²] in the meso-scale and does not consider the elliptical form of the fire. Furthermore, this model does not result to characteristics of a fire usually predicted by fire behavior systems, such as fire intensity, flame length or spread rate. This is due to lack of data of these variables for the study areas concerned. In case of data availability, an extension of the presented model including also the relevant variables is possible and should be considered. The model takes into account land cover types, initial fire behavior conditions (as expressed by components of the Canadian Forest Fire Weather Index System (CFFWIS)), topography (wind speed, slope, aspect minus wind direction) and recent weather conditions (e.g. accumulated precipitation over the last 21 days) (Figure 6.1). The proposed model is based on structure learning by constraint-based approach and phenomenological reasoning and includes hidden (i.e. non-observable) variables. The model predicts higher burnt areas from spring to autumn, as a result of dryer weather conditions. The model is able to predict accurately small fires (0-0.01 km²), due to the fact that these fires are highly represented in the learning dataset Cyprus 2006-2009. Additional data on fires resulting to large burnt area could be used to update the CPT of the variable *Burnt area* and therefore improve the predicting ability of the model for bigger fires.

In the fire effects model of Chapter 7 hazard characteristics are expressed by *Burnt area* [km²], *Fire type* and *FWI*. The model accounts for fire suppression effectiveness. House damage cost is based on the construction value of houses. Vegetation damage cost is based on the premiums paid for vegetation restoration by the EU. The meso-scale modeling requires that the indicators are representative for a 1 km² spatial unit. This makes the modeling more demanding, as it is necessary to identify representative states not of individual houses, but rather of portfolios of houses, e.g. house stock, construction type. This introduces uncertainties in house damage estimation at the meso-scale. The results show that higher house damage cost can be expected for bigger burnt areas and house densities, and more hazardous fires. The WUI is expected to experience the highest house damages. The highest vegetation damages are expected for forested areas, followed by shrubs and permanent crops. This is due to the higher mean occurrence rate in these areas (Figure 4.16 and Figure 4.26) and the higher cost and time of restoration (Table 7.3).

The overall fire risk model, which results from the combination of the three previously presented models, is described in Chapter 8. Yearly, the predicted risk to houses and vegetation increases from April to August and decreases from September to December. The peri-urban areas (WUI), thus the areas with coexisting structures and vegetation, show the highest predicted risk to houses. The forested and agricultural areas have the highest fire risk to vegetation. This agrees with previous studies, which stress the high fire risk in WUI areas (e.g.Beringer 2000;Cohen 2000;Haight *et al.* 2004;Mozumder *et al.* 2009;Mell *et al.* 2010). In the proposed model, this is due to the higher mean occurrence rate in these areas (Figure 4.16 and Figure 4.26) and the higher cost and time of restoration (Table 7.3). Yearly, the risk rises from spring to the end of summer and decreases gradually during autumn. For South France the year 2003 is expected to have higher fire risk than 2010. This prediction agrees with the destructive fires that occurred in South France in 2003, with several damaged houses, thousands of peoples evacuated from their houses and hundreds of km² of vegetated areas burnt. The proposed fire risk model is flexible and can be easily extended to include other variables or get updated with additional information on the existing variables. This allows the modeling of other types of fire induced losses (e.g. human safety) or of the fire hazard in higher complexity. Finally, it is demonstrated that the presented model can be

used in its current state in areas with similar characteristics to the ones used for model calibration, to predict daily fire risk to houses and vegetation in the meso-scale.

9.3   Main contributions of the thesis

The proposed fire occurrence model contributed to the first research objective of this thesis (Chapter 1.1), thus to develop a probabilistic fire occurrence model that includes as influencing variables both weather conditions and human involvement to account for ignitions related to humans, and improve the currently used fire danger models. After data analysis for the identification of variables influencing the fire hazard phenomenon, Poisson regression with forward selection of explanatory variables was realized to predict fire occurrence probability with incorporation in the model of both environmental (FWI) and anthropogenic (e.g. population density) influencing factors. BNs were employed for the modeling of fire occurrence and fire size with random variables representing the main driving factors of the fire phenomenon. The fire occurrence and fire size model predict the fire hazard per day (temporal resolution) and km² (spatial resolution). The fire size model is a result of automatic structure learning with convenient algorithms and phenomenological reasoning, which predicts the resulting burnt area [km²] in the meso-scale; the model incorporates both observable and non-observable variables. Direct and tangible fire effects on houses and vegetation are quantified in monetary terms [€] with vulnerability and exposure indicators. The latest are included in the BNs as random variables. Sensitivity analysis of the models identified the influence of the variables on the expected fire damage cost and the fire risk. To support parameter learning, predictions and result visualization the BNs area coupled with a GIS. Parameter learning is done with readily available data of three study areas of the Mediterranean region and incorporation of expert knowledge. Results include predictions of fire occurrence rate $\left[\frac{Nr.Fires}{km^2 \cdot day}\right]$, burnt area [km²] and expected damage cost [€] on houses and vegetation for verification data sets and daily maps with 1 km² spatial resolution for Cyprus and South France. Overall, the present thesis presents a novel fire risk predicting model, which is flexible and can be easily extended to include other variables or get updated with additional information on the existing variables. In this way other types of fire induced losses or the fire hazard in more complexity can be modelled. The presented model can be used in its current state in areas with similar characteristics to predict daily fire risk to houses and vegetation in the meso-scale.

9.4   Outlook

This thesis presented a novel probabilistic fire risk model to be used for areas with climatic and anthropogenic conditions similar to those of the Mediterranean countries. Even so, there are limitations that have been identified during the realization of this thesis as discussed above and aspects that should be addressed in future works.

In the fire occurrence model, further explanatory variables describing anthropogenic factors (e.g. power line networks, campsites) may be included in the analysis. However, care should be taken not to introduce redundant variables. Already the three included explanatory variables (land cover type, population and road density) are partly redundant and inter-dependent. E.g., both

population and road density are higher in urban areas. This dependency must be considered when transferring the model to other regions. The predictive ability of other fuel moisture indicators can be additionally studied and if relevant, they can be included in the model. Fuel types, could be an additional variable in the model; in this case the dependency to land cover types should be represented.

In the fire size model, the data set of fires from Cyprus (2006-2009) included mainly small burnt areas ($< 0.01 \, k\text{m}^2$). As a result the model predicts smaller fires with higher accuracy than bigger fire events. The predictive ability of the model can be improved, when additional data sets of fires with bigger resulting burnt areas are employed for model updating. Fuel moisture indicators other than of the CFFWIS should be studied and when relevant included in the model. The proposed model predicts burnt area and neglects other important fire characteristics; fire intensity, spread rate and flame length are essential predicted variables for model application regarding fire crew allocation. To achieve the prediction of fire characteristics and the probability of transition of a fire from surface to crown, fuel models should be incorporated. As a result the model will be a fire behavior model, rather than a fire size model.

In the fire effects model, additional influencing variables can be added to increase model accuracy. These include (i) the adjacent vegetation influencing house damages, (ii) evacuation status and permanent/non-permanent house use to account for the suppression attempts of the resident, (iii) the existence of fire protection plans in the community level to account for the residents preparedness of protecting their houses from fire and (iv) the existence of house insurance against fire, which also influences the residents behaviour in case of fire. The BN model is flexible, and these (and other) variables can be included by adding them as nodes, together with the appropriate links. Their inclusion does however require that quantitative models of their influence on the house damage, or on other variables of the BN, are available. In this thesis limited data on real damages are used for model validation. Additional available data on actual house and vegetation damages and fire characteristics can be valuable for the parameter learning and the model validation. The above can increase model accuracy and lead to better estimations.

In the fire risk model, additional data sets of other study areas should be used to update the probability distributions of the random variables and thus raise the predictive ability of the model. The loose coupling of BN-GIS chosen proved to be of limited flexibility and high calculation time, especially for larger study areas (e.g. South France). A more flexible and user friendly database for this data set will improve data management, querying and analysis. It will also enable model updating and increase model performance. A more complex coupling of the BN-GIS requiring little user intervention and offering a more user-friendly application for non GIS experts in fire management should be considered. Actions could include a flexible interface (e.g. a dialog box), for defining the input data to the BN (e.g. daily weather prediction), the execution of the evidence propagation in the BN software with a plug-in module in the GIS environment with call-back functions, the output of the beliefs of the BN and the direct visualization in the GIS (e.g. Yassemi *et al.* 2008;Jolma *et al.* 2011).

Future work towards better predictive models can include the above proposed methods and/or incorporate in the BNs external models already in operation. Predicting, adapting, extending, replacing, predicting, adapting…The work towards reliable tools to model fire phenomena and expected losses is continuous; nevertheless, understanding and improvements are nowadays fast, among others due to data availability and powerful visualization and modelling tools. The present work aimed to contribute towards better fire risk predictive models to support fire prevention and mitigation measures for the protection of human life and property in the Mediterranean and aspires the presented models to be adapted, further investigated, extended and eventually replaced in the perpetual work in progress of science.

Appendix I

Equations of the
Canadian Forest Fire Weather Index System

The following equations and notations are taken from Van Wagner and Pickett (1985)

Weather

T	-	noon temperature , °C
H	-	noon relative humidity, %
W	-	noon wind speed, km/h
r_0	-	rainfall in open, measured once daily at noon, mm
r_f	-	effective rainfall, FFMC
r_e	-	effective rainfall, DMC
r_d	-	effective rainfall, DC

Fine Fuel Moisture Code (FFMC)

m_0	-	fine fuel moisture content from previous day
m_r	-	fine fuel moisture content after rain
m	-	fine fuel moisture content after drying
E_d	-	fine fuel EMC for drying
E_w	-	fine fuel EMC for weting
k_0	-	intermediate step in calculation of k_d
k_d	-	log drying rate, FFMC, $log_{10}m/day$
k_l	-	intermediate step in calculation of k_w
k_w	-	log wetting rate, $log_{10}m/day$
F_0	-	previous day's FFMC
F	-	FFMC

Duff Moisture Code (DMC)

M_0	-	duff moisture content from previous day
M_r	-	duff moisture content after rain
M	-	duff moisture content after drying
K	-	log drying rate in DMC, $log_{10}m/day$
L_e	-	effective day length in DMC, hours
b	-	slope variable in DMC rain effect
P_0	-	previous day's DMC
P_r	-	DMC after rain
P	-	DMC

Drought Code (DC)

Q - moisture equivalent of DC, units of 0.254 mm
Q_0 - moisture equivalent of previous day's DC
Q_r - moisture equivalent after rain
V - potential evapotranspiration, units of 0.254 mm water/day
L_f - day length adjustment in DC
D_0 - previous day's DC
D_r - DC after rain
D - DC

Fire Behavior Indexes (ISI, BUI, FWI)

$f(W)$ - wind function
$f(F)$ - fine fuel moisture function
$f(D)$ - duff moisture function
R - Initial Spread Index (ISI)
U - Buildup Index (BUI)
B - FWI (intermediate form)
S - FWI (final form)

Severity Rating

DSR - Daily Severity Rating

Fine Fuel Moisture Code (FFMC)

$$m_0 = 147.2\,(101 - F_0)/(59.5 + F_0) \tag{1}$$

$$r_f = r_0 - 0.5, \quad r_0 > 0.5 \tag{2}$$

$$m_r = m_0 + 42.5 r_f \left(e^{-\frac{100}{251 - m_0}} \right) \left(1 - e^{-\frac{6.93}{r_f}} \right), \qquad m_0 \leq 150 \tag{3a}$$

$$m_r = m_0 + 42.5 r_f \left(e^{-\frac{100}{251 - m_0}} \right) \left(1 - e^{-\frac{6.93}{r_f}} \right) + 0.0015(m_0 - 150)^2 r_f^{0.5}, \qquad m_0 > 150 \tag{3b}$$

$$E_d = 0.942 H^{0.679} + 11 e^{(H-100)/10} + 0.18(21.1 - T)(1 - e^{-0.115H}) \tag{4}$$

$$E_w = 0.618 H^{0.753} + 11 e^{(H-100)/10} + 0.18(21.1 - T)(1 - e^{-0.115H}) \tag{5}$$

$$k_0 = 0.424 \left[1 - \left(\frac{H}{100} \right)^{1.7} \right] + 0.0694 W^{0.5} [1 - \left(\frac{H}{100} \right)^{8}] \tag{6a}$$

$$k_d = k_0 \cdot 0.581 e^{0.0365T} \tag{6b}$$

$$k_l = 0.424 \left[1 - \left(\frac{100 - H}{100} \right)^{1.7} \right] + 0.0694 W^{0.5} [1 - \left(\frac{100 - H}{100} \right)^{8}] \tag{7a}$$

$$k_w = k_1 \cdot 0.581 e^{0.0365T} \tag{7b}$$

$$m = E_d + (m_0 - E_d) \cdot 10^{-k_d} \tag{8}$$

$$m = E_w - (E_w - m_0) \cdot 10^{-k_w} \tag{9}$$

$$F = 59.5(250 - m)/(147.2 + m) \tag{10}$$

$$r_e = 0.92r_0 - 1.27, \quad r_0 > 1.5 \tag{11}$$

1. Previous day's F becomes F_0 .

2. Calculate m_0 by Equation (1).

3. a. If $r_0 > 0.5$, calculate r_f by Equation 2.
   b. Calculate m_r from r_f and m_0
      i. If $m_0 \le 150$, use Equation 3a.
      ii. If $m_0 > 150$, use Equation 3b.
   c. m_r becomes the new m_0.

4. Calculate E_d by Equation 4.

5. a. If $m_0 > E_d$ calculate k_d by Equations 6a and 6b.
   b. Calculate m by Equation 8.

6. If $m_0 < E_d$ calculate E_w by Equation 5.

7. a. If $m_0 < E_w$ calculate k_w by Equations 7a and 7b.
   b. Calculate m by Equation 9.

8. If $E_d \geq m_0 \geq E_w$ let $m = m_0$.
9. Calculate F from m by Equation 10. This is today's FFMC.

Restrictions:
1) When $r_0 \geq 0.5mm$, the rainfall routine (Equations 3a and 3b) must be omitted.
2) When $m_r > 250$, let $m_r = 250$.

Duff Moisture Code (DMC)

$$M_0 = 10 + e^{(5.6348 - \frac{P_0}{43.43})} \tag{12}$$

$$b = 100/(0.5 + 0.3P_0), \quad P_0 \leq 33 \tag{13a}$$

$$b = 14 - 13lnP_0, \quad 33 < P_0 \leq 65 \tag{13b}$$

$$b = 6.2lnP_0 - 17.2, \quad P_0 > 65 \tag{13c}$$

$$M_r = M_0 + 1000r_e/(48.77 + br_e) \tag{14}$$

$$P_r = 244.72 - 43.43\ln(M_r - 20) \tag{15}$$

$$K = 1.894(T + 1.1)(100 - H)L_e 10^{-6} \tag{16}$$

$$P = P_0(or\ P_r) + 100K \tag{17}$$

1. Previous day's P becomes P_0.

2. a. If $r_0 > 1.5$, calculate r_e by Equation 11.
    b. Calculate M_0 from P_0 by Equation 12.
    c. Calculate b by Equation 13a, 13b or 13c.
    d. Calculate M_r by Equation 14.
    e. Convert M_r to P_r by Equation 15. P_r becomes new P_0.

3. Take L_e (effective day length) from Table below.

Month	J	F	M	A	M	J	J	A	S	O	N	D
L_e	6.5	7.5	9.0	12.8	13.9	13.9	12.4	10.9	9.4	8.0	7.0	6.0

4. Calculate K by Equation 16.

5. Calculate P from P_0 by Equation 17. This is today's DMC

Restrictions:
1) If $r_0 < 1.5$, the rainfall routine (Equations 11 to 15) must be omitted.
2) Negative values of P_r resulting from Equation 15 must be raised to zero.
3) If $T < -1.1$ use $T = -1.1$.

Drought Code (DC)

$$r_d = 0.83r_0 - 1.27, \quad r > 2.8 \tag{18}$$

$$Q_0 = 800e^{\frac{-D_0}{400}} \tag{19}$$

$$Q_r = Q_0 + 3.937r_d \tag{20}$$

$$D_r = 400\ln(\frac{800}{Q_r}) \tag{21}$$

$$V = 0.36(T + 2.8) + L_f \tag{22}$$

$$D = D_0(or\ D_r) + 0.5V \tag{23}$$

1. Previous day's D becomes D_0.

2. a. If $r_0 > 2.8$, calculate r_d by Equation 18.
   b. Calculate Q_0 from D_0 by Equation 19.
   c. Calculate Q_r by Equation 20.
   d. Convert Q_r to D_r by Equation 21. D_r becomes new D_0.

3. Take L_f (Daylength factor) from Table below.

Month	J	F	M	A	M	J	J	A	S	O	N	D
L_f	-1.6	-1.6	-1.6	0.9	3.8	5.8	6.4	5.0	2.4	0.4	-1.6	-1.6

4. Calculate V by Equation 22.
5. Calculate D from D_0 (or D_r) by Equation 23. This is today's DC.

Restrictions:
1) If $r_0 < 2.8$ the rainfall routine (Equations 18 to 21) must be omitted.
2) If $D_r < 0$, take $D_r = 0$.
3) If $T < -2.8$ use in Equation 22 $T = -2.8$.
4) If $V < 0$ by Equation 22, let $V = 0$.

Initial Spread Index (ISI)

$$f(W) = e^{0.05039W} \tag{24}$$

$$f(F) = 91.9e^{-0.1386m}[1 + \frac{m^{5.31}}{4.93 \cdot 10^7}] \tag{25}$$

$$R = 0.208f(W)f(F) \tag{26}$$

Buildup Index

$$U = \frac{0.8PD}{P + 0.4D}, \quad P \leq 0.4D \tag{27a}$$

$$U = P - \left[1 - \frac{0.8D}{P + 0.4D}\right][0.92 + (0.0114P)^{1.7}], \quad P > 0.4D \tag{27b}$$

Fire Weather Index

$$f(D) = 0.626U^{0.809} + 2, \quad U \leq 80 \tag{28a}$$

$$f(D) = \frac{1000}{25 + 108.64e^{-0.023U}}, \quad U > 80 \tag{28b}$$

$$B = 0.1Rf(D) \tag{29}$$

$$lnS = 2.72(0.434lnB)^{0.647}, \quad B > 1 \tag{30a}$$

$$S = B, \qquad\qquad\qquad B \leq 1 \tag{30b}$$

1. Calculate $f(W)$ and $f(F)$ by Equations 24 and 25.

2. Calculate R by Equation 26. This is today's ISI.

3. Calculate U by Equation 27a or Equation 27b.

4. Calculate $f(D)$ by Equation 28a or Equation 28b.

5. Calculate B by Equation 29.

6. Calculate S by Equation 30a or Equation 30b.

Appendix II

Figure AII-1: Burnt area of fire events (2006-2010) versus Relative humidity [%] in linear and logarithmic scale

Figure AII-2: Burnt area of fire events (2006-2010) versus Precipitation [mm] in linear and logarithmic scale

Figure AII-3: Burnt area of fire events (2006-2010) versus FFMC in linear and logarithmic scale

Figure AII-4: Burnt area of fire events (2006-2010) versus DMC in linear and logarithmic scale
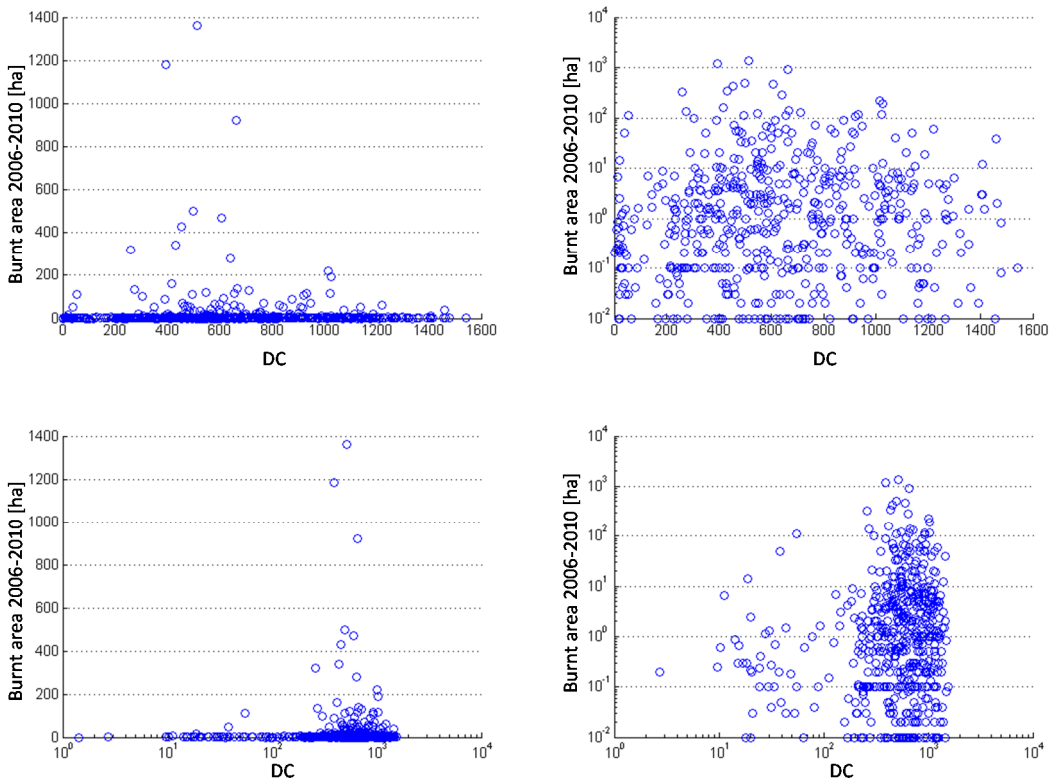
Figure AII-5: Burnt area of fire events (2006-2010) versus DC in linear and logarithmic scale
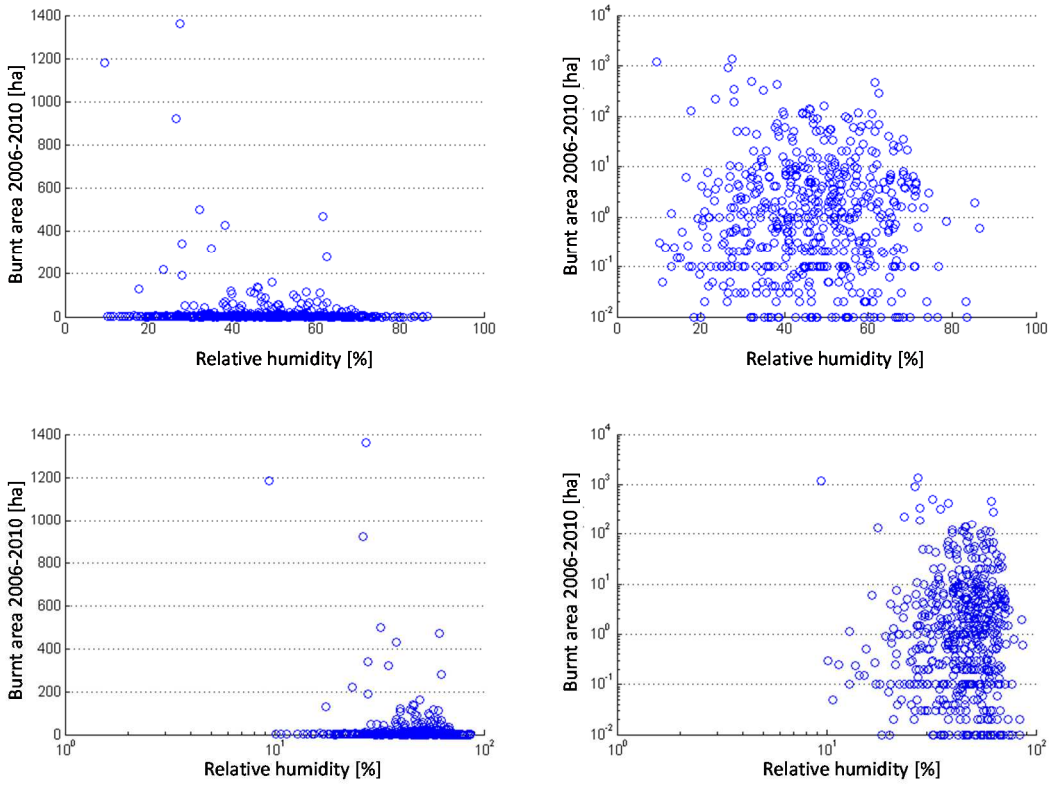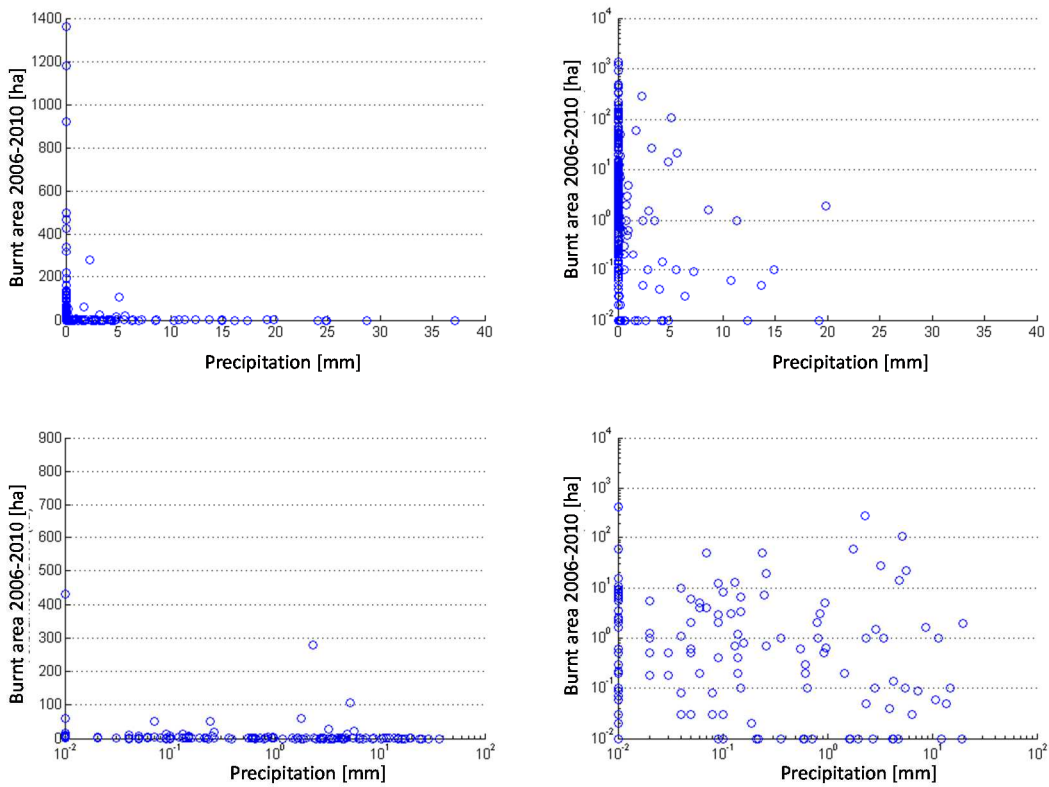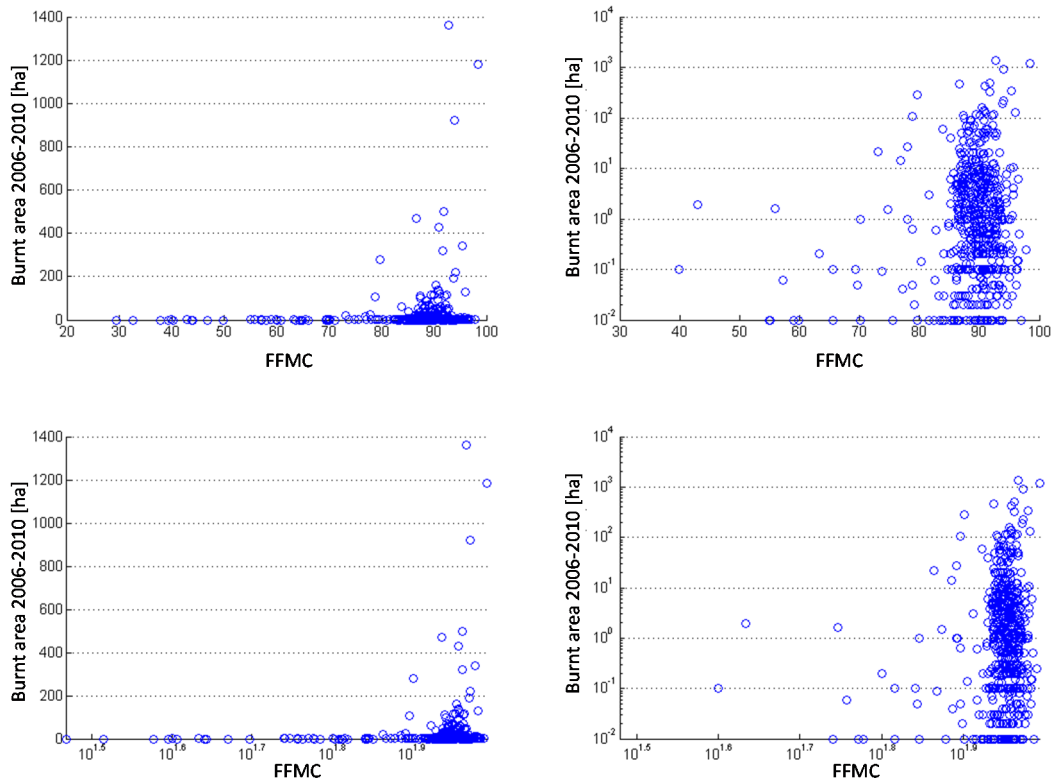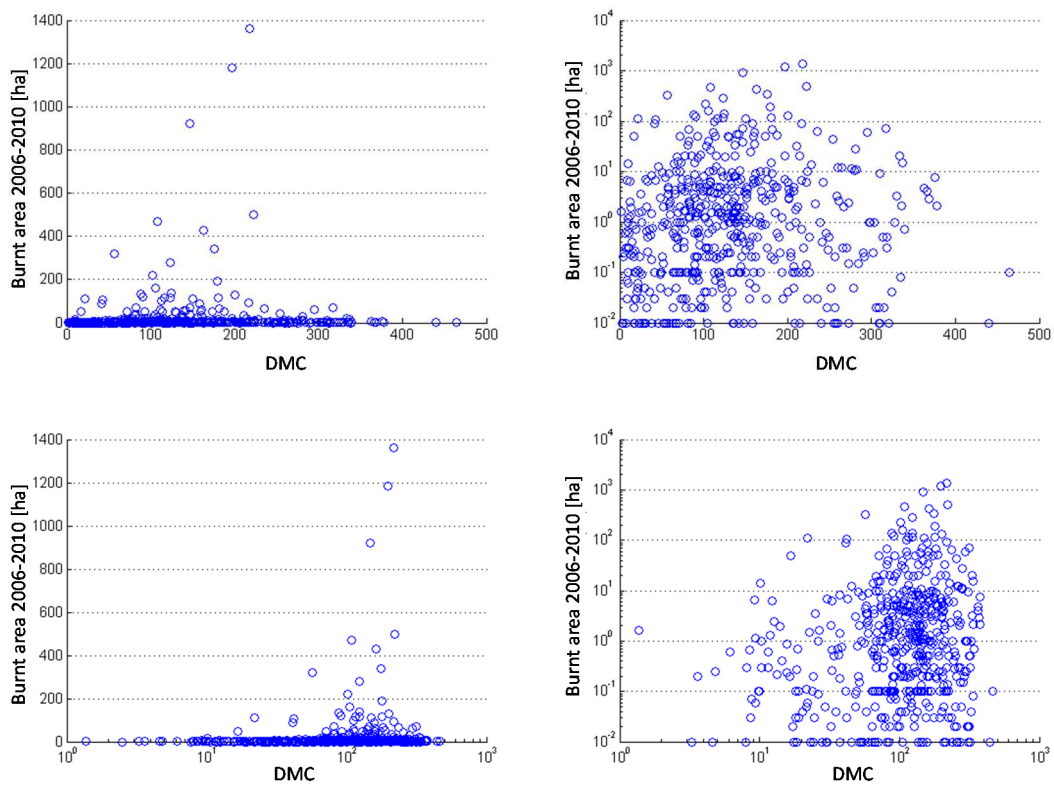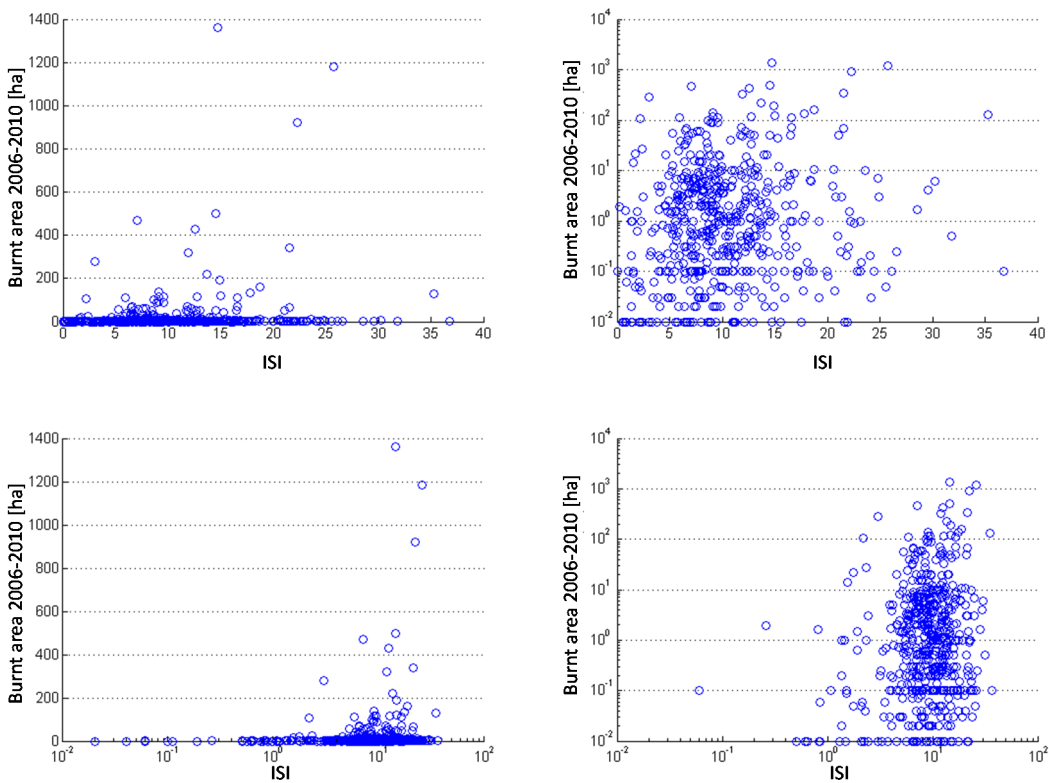

Figure AII-6: Burnt area of fire events (2006-2010) versus ISI in linear and logarithmic scale
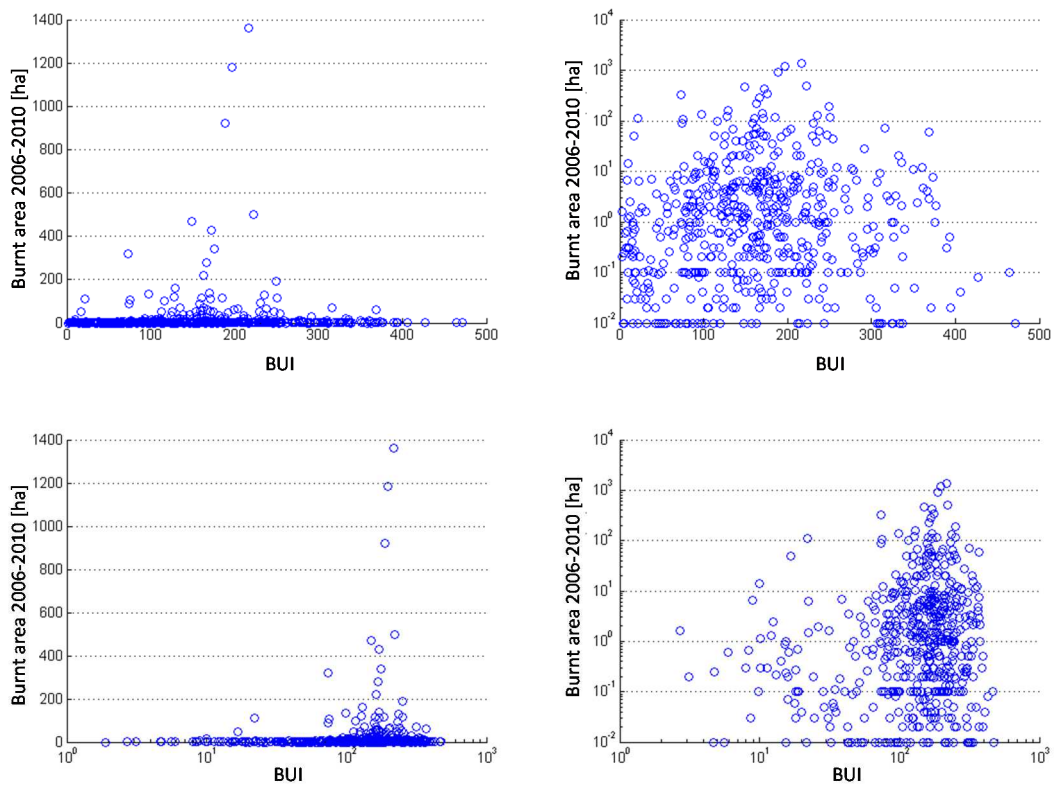
Figure AII-7: Burnt area of fire events (2006-2010) versus BUI in linear and logarithmic scale
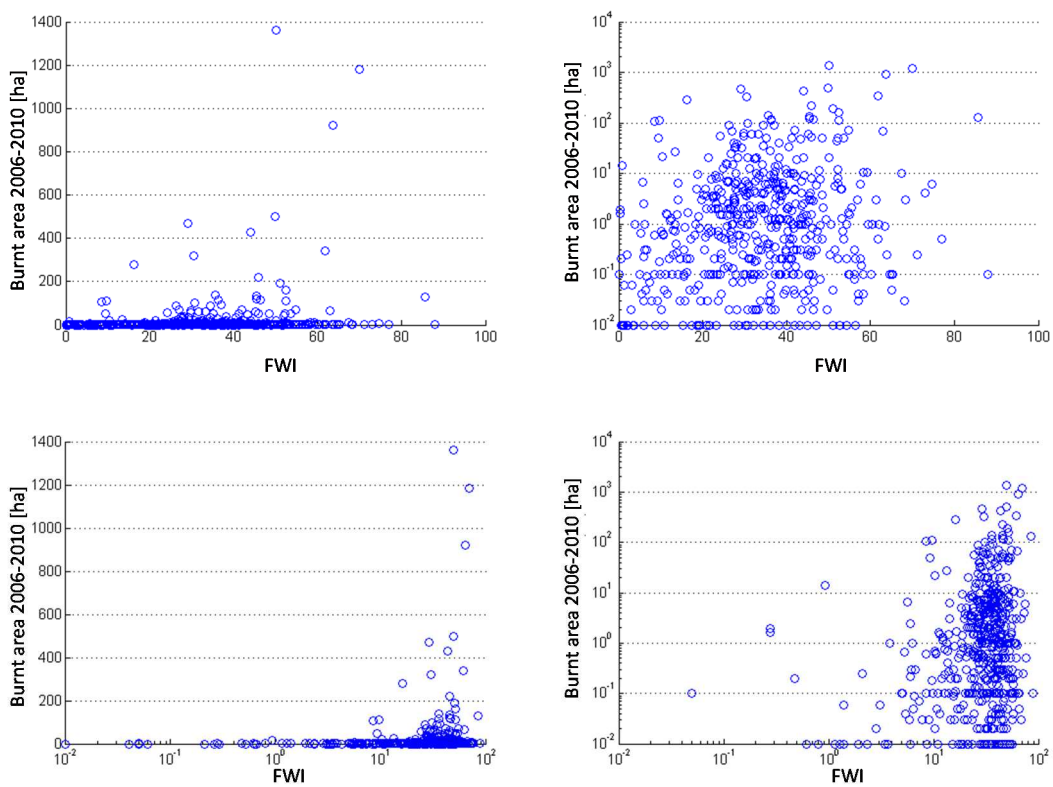
Figure AII-8: Burnt area of fire events (2006-2010) versus FWI in linear and logarithmic scale

Appendix III

Table AIII-1: Effect of influencing variables on house risk [€]

Variable V	Possible States of the Variable	Risk to houses without setting an initial variable value [€] Risk(V) Prior risk: Risk = 3	Probability of Variable being in the state $p(v)$	Change in % relative to the average $\dfrac{\text{Risk}(V) - \text{Risk}}{\text{Risk}} \cdot 100$	R $= (\text{Risk}(V)$ $- \text{Risk})^2 \cdot p(v)$	Variance $\sum R$
FWI	0-10	1	0.36	-66.66	1.44	4.99
	10-30	2	0.31	-33.33	0.31	
	30-60	5	0.31	+66.66	1.24	
	60-inf	13	0.02	+333.33	2	
Land cover	1	0	0.09	-100	0.81	4.61
	2	$4 \cdot 10^{-1}$	0.19	-86.66	1.28	
	3	3	0.04	0	0	
	4	2	0.19	-33.33	0.19	
	5	6	0.21	+100	1.89	
	6	4	0.26	+33.33	0.26	
	7	0	0.02	-100	0.18	
Pop. density [People/km²]	0-20	2	0.47	-33.33	0.47	3.45
	20-300	2	0.46	-33.33	0.46	
	300-inf	9	0.07	+200	2.52	
Road density [km/km²]	0-0.5	3	0.36	0	0	0.64
	0.5-2	2	0.32	-33.33	0.32	
	2-inf	4	0.32	+33.33	0.32	
Fire occur. rate λ $\left[\dfrac{Fires}{day \cdot km^2}\right]$	$0\text{-}10^{-9}$	10^{-5}	$3 \cdot 10^{-4}$	-99.99	0	664.00
	$10^{-9}\text{-}10^{-8}$	10^{-4}	$4 \cdot 10^{-4}$	-99.99	0	
	$10^{-8}\text{-}10^{-7}$	$8 \cdot 10^{-4}$	$6 \cdot 10^{-4}$	-99.97	0.01	
	$10^{-7}\text{-}10^{-6}$	$4 \cdot 10^{-3}$	10^{-3}	-99.86	0.01	
	$10^{-6}\text{-}5 \cdot 10^{-6}$	$3 \cdot 10^{-2}$	$9 \cdot 10^{-3}$	-99	0.08	
	$5 \cdot 10^{-6}\text{-}10^{-5}$	$6 \cdot 10^{-2}$	0.07	-98	0.61	
	$10^{-5}\text{-}2 \cdot 10^{-5}$	$2 \cdot 10^{-1}$	0.14	-93.33	1.10	
	$2 \cdot 10^{-5}\text{-}3 \cdot 10^{-5}$	$5 \cdot 10^{-1}$	0.16	-83.33	1	
	$3 \cdot 10^{-5}\text{-}4 \cdot 10^{-5}$	$8 \cdot 10^{-1}$	0.13	-73.33	0.63	
	$4 \cdot 10^{-5}\text{-}5 \cdot 10^{-5}$	1	0.1	-66.66	0.4	
	$5 \cdot 10^{-5}\text{-}6 \cdot 10^{-5}$	2	0.08	-33.33	0.08	
	$6 \cdot 10^{-5}\text{-}7 \cdot 10^{-5}$	2	0.06	-33.33	0.06	
	$7 \cdot 10^{-5}\text{-}8 \cdot 10^{-5}$	2	0.05	-33.33	0.05	
	$8 \cdot 10^{-5}\text{-}9 \cdot 10^{-5}$	3	0.04	0	0	
	$9 \cdot 10^{-5}\text{-}0.0001$	3	0.03	0	0	
	0.0001-0.0005	11	0.14	+266.66	8.96	
	0.0005-0.001	31	$9 \cdot 10^{-4}$	+933.33	0.71	
	0.001-0.01	155	$3 \cdot 10^{-4}$	+5,066.7	6.93	
	0.01-0.1	1,467	$3 \cdot 10^{-4}$	$+4.88 \cdot 10^{-4}$	642.99	
Fires	yes	30,420	$9 \cdot 10^{-5}$	$+1.01 \cdot 10^{-6}$	83,400	83,208.91
	no	0	0.99	-100	8.91	
Topography	middle	3	0.38	0	0	0.21
	gradual	3	0.41	0	0	
	steep	4	0.21	+33.33	0.21	
Recent Weather	dry	4	0.27	+33.33	0.27	0.73
	moderate dry	3	0.27	0	0	
	moderate humid	2	0.26	-33.33	0.26	
	humid	2	0.20	-33.33	0.20	
Fire behavior indices	moderate	3	0.83	0	0	0.17
	low	4	0.17	+33.33	0.17	
Burnt area detailed	0	0	0.99	-100	8.91	2,605,708.6
	≤0.01	461	$5 \cdot 10^{-5}$	$+1.53 \cdot 10^{-4}$	10.49	

[km²]	0.01-0.1	4,796	$3 \cdot 10^{-5}$	+1.60000	689.19	
	0.1-1	47,400	10^{-5}	+158,000,000	220,000	
	1-3	152,401	$4 \cdot 10^{-6}$	+506,000,000	930,000	
	3-10	496,062	$2 \cdot 10^{-6}$	+1,653,000,000	4,900,000	
	10-inf	2,000,000	$5 \cdot 10^{-7}$	+666,000,000	2,000,000	
Fire type	0	0	0.99	-100	8.91	162,031.91
	1	16,163	$2 \cdot 10^{-5}$	+53,900,000	5,223	
	2	18,884	$5 \cdot 10^{-5}$	+62,900,000	1,780,000	
	3	83,328	$2 \cdot 10^{-5}$	+277,000,000	13,900,000	
Construction type	5t_15s_80i	3	0.23	0	0	0
	10t_25s_65i	3	0.77	0	0	
Urban/Rural	urban	13	0.17	+333.33	17	20.32
	rural	1	0.83	-66.66	3.32	
House stock	40s_25r_35a	13	0.17	+333.33	17	20.32
	70s_20r_10a	1	0.83	-66.66	3.32	
Construction value [€]	0-10,000	$2 \cdot 10^{-1}$	0.10	-93.33	0.78	7.60
	10,000-50,000	1	0.29	-66.66	1.16	
	50,000-100,000	2	0.41	-33.33	0.41	
	100,000-500,000	8	0.21	+166.66	5.25	
House density [Houses/km²]	0-3	$8 \cdot 10^{-2}$	0.15	-97.33	1.28	3,964.62
	3-10	$3 \cdot 10^{-1}$	0.25	-90	1.82	
	10-30	1	0.34	-66.66	1.36	
	30-100	3	0.18	0	0	
	100-300	8	0.04	+166.66	1	
	300-1,000	26	0.04	+766.66	21.16	
	1,000-3,000	78	$7 \cdot 10^{-1}$	+2500	3938	
House damage	no damage	0	0.99	-100	8.91	356,008.91
	minor	205,439	$4 \cdot 10^{-6}$	+685,000,000	16,900,000	
	major	788,617	$3 \cdot 10^{-6}$	+2,630,000,000	18,700,000	
Fire Containment in 24 hrs	yes	0	0.91	-100	8.19	78.75
	no	31	0.09	+933.33	70.56	
Vegetation damage	no damage	0	0.99	-100	8.91	802,008.91
	minor	173,440	$7 \cdot 10^{-6}$	+578,000,000	21,100,000	
	major	343,797	$5 \cdot 10^{-6}$	+1,140,000,000	59,100,000	
Restoration cost [€]	0-30,000	3	0.33	0	0	3.77
	30,000-100,000	1	0.38	-66.66	1.52	
	100,000-300,000	3	0.04	0	0	
	300,000-1,000,000	6	0.25	+100	2.25	

Table AIII-2: Effect of influencing variables on vegetation risk

Variable V	Possible States of the Variable	Risk to Vegetation without setting an initial variable value [€] $\text{Risk}(V)$ Prior risk: $\text{Risk} = 4e-1$	Probability of Variable being in the state $p(v)$	Change in % relative to the average $\dfrac{\text{Risk}(V) - \text{Risk}}{\text{Risk}} \cdot 100$	$R = (\text{Risk}(V) - \text{Risk})^2 \cdot p(v)$	Variance $\sum R$
FWI	0-10	$2\cdot10^{-1}$	0.36	-50	0.01	0.09
	10-30	$3\cdot10^{-1}$	0.31	-25	0	
	30-60	$7\cdot10^{-1}$	0.31	+75	0.03	
	60-inf	2	0.02	+400	0.05	
Land cover	1	0	0.09	-100	0.01	0.61
	2	10^{-2}	0.19	-97.50	0.03	
	3	$2\cdot10^{-1}$	0.04	-50	0	
	4	$5\cdot10^{-2}$	0.19	-87.50	0.02	
	5	2	0.21	+400	0.54	
	6	$2\cdot10^{-1}$	0.26	-50	0.01	
	7	0	0.02	-100	0	
Pop. density [People/km²]	0-20	$3\cdot10^{-1}$	0.47	-25	0.01	0.20
	20-300	$3\cdot10^{-1}$	0.46	-25	0.01	
	300-inf	2	0.07	+400	0.18	
Road density [km/km²]	0-0.5	$5\cdot10^{-1}$	0.36	+25	0	0
	0.5-2	$3\cdot10^{-1}$	0.32	-25	0	
	2-inf	$4\cdot10^{-1}$	0.32	0	0	
Fire occur. rate λ $\left[\dfrac{Fires}{day\cdot km^2}\right]$	$0-10^{-9}$	$3\cdot10^{-6}$	$3\cdot10^{-4}$	-99.99	0	42.40
	$10^{-9}-10^{-8}$	$3\cdot10^{-5}$	$4\cdot10^{-4}$	-99.99	0	
	$10^{-8}-10^{-7}$	$2\cdot10^{-4}$	$6\cdot10^{-4}$	-99.95	0	
	$10^{-7}-10^{-6}$	10^{-3}	10^{-3}	-99.75	0	
	$10^{-6}-5\cdot10^{-6}$	$2\cdot10^{-3}$	$9\cdot10^{-3}$	-99.50	0	
	$5\cdot10^{-6}-10^{-5}$	$2\cdot10^{-3}$	0.07	-99.50	0.01	
	$10^{-5}-2\cdot10^{-5}$	$9\cdot10^{-3}$	0.14	-97.75	0.02	
	$2\cdot10^{-5}-3\cdot10^{-5}$	$5\cdot10^{-2}$	0.16	-87.50	0.02	
	$3\cdot10^{-5}-4\cdot10^{-5}$	$8\cdot10^{-2}$	0.13	-80	0.01	
	$4\cdot10^{-5}-5\cdot10^{-5}$	10^{-1}	0.1	-75	0.01	
	$5\cdot10^{-5}-6\cdot10^{-5}$	$2\cdot10^{-1}$	0.08	-50	0	
	$6\cdot10^{-5}-7\cdot10^{-5}$	$2\cdot10^{-1}$	0.06	-50	0	
	$7\cdot10^{-5}-8\cdot10^{-5}$	$2\cdot10^{-1}$	0.05	-50	0	
	$8\cdot10^{-5}-9\cdot10^{-5}$	$3\cdot10^{-1}$	0.04	-25	0	
	$9\cdot10^{-5}-0.0001$	$3\cdot10^{-1}$	0.03	-25	0	
	0.0001-0.0005	1	0.14	+150	0.05	
	0.0005-0.001	5	$9\cdot10^{-4}$	+1150	0.02	
	0.001-0.01	38	$3\cdot10^{-4}$	+9,400	0.42	
	0.01-0.1	374	$3\cdot10^{-4}$	+9,340,000	41.87	
Fires	yes	4225	$9\cdot10^{-5}$	+105,600,000	1,606	1,606.16
	no	0	0.99	-100	0.16	
Topography	middle	$3\cdot10^{-1}$	0.38	-25	0	0
	gradual	$4\cdot10^{-1}$	0.41	0	0	
	steep	$5\cdot10^{-1}$	0.21	+25	0	
Recent Weather	dry	$6\cdot10^{-1}$	0.27	+50	0.01	0.01
	moderate dry	$3\cdot10^{-1}$	0.27	-25	0	
	moderate humid	$3\cdot10^{-1}$	0.26	-25	0	

	humid	$5 \cdot 10^{-1}$	0.20	+25	0	
Fire behavior indices	moderate	$4 \cdot 10^{-1}$	0.83	0	0	0
	low	$5 \cdot 10^{-1}$	0.17	+25	0	
Burnt area detailed [km²]	0	0	0.99	-100	0.16	38,036.86
	≤0.01	63	$5 \cdot 10^{-5}$	+1,560,000	0.20	
	0.01-0.1	634	$3 \cdot 10^{-5}$	+15,800,000	12.04	
	0.1-1	6368	10-5	+159,000,000	405.46	
	1-3	19885	$4 \cdot 10^{-6}$	+497,000,000	1,582	
	3-10	67960	$2 \cdot 10^{-6}$	+1,700,000,000	9,237	
	10-inf	231448	$5 \cdot 10^{-7}$	+5,790,000,000	2,680,000	
Fire type	0	0	0.99	-100	0.16	4,326.18
	1	1109	$2 \cdot 10^{-5}$	+27,700,000	24.58	
	2	2225	$5 \cdot 10^{-5}$	+55,600,000	247.44	
	3	14238	$2 \cdot 10^{-5}$	+356,000,000	4,054	
Construction type	5t_15s_80i	$4 \cdot 10^{-1}$	0.23	0	0	0
	10t_25s_65i	$4 \cdot 10^{-1}$	0.77	0	0	
Urban/Rural	urban	$4 \cdot 10^{-1}$	0.17	0	0	0
	rural	$4 \cdot 10^{-1}$	0.83	0	0	
House stock	40s_25r_35a	$4 \cdot 10^{-1}$	0.17	0	0	0
	70s_20r_10a	$4 \cdot 10^{-1}$	0.83	0	0	
Construction value [€]	0-10,000	$4 \cdot 10^{-1}$	0.10	0	0	0
	10,000-50,000	$4 \cdot 10^{-1}$	0.29	0	0	
	50,000-100,000	$4 \cdot 10^{-1}$	0.41	0	0	
	100,000-500,000	$4 \cdot 10^{-1}$	0.21	0	0	
House density [Houses/km²]	0-3	$4 \cdot 10^{-1}$	0.15	0	0	0
	3-10	$4 \cdot 10^{-1}$	0.25	0	0	
	10-30	$4 \cdot 10^{-1}$	0.34	0	0	
	30-100	$4 \cdot 10^{-1}$	0.18	0	0	
	100-300	$4 \cdot 10^{-1}$	0.04	0	0	
	300-1,000	$4 \cdot 10^{-1}$	0.04	0	0	
	1,000-3,000	$4 \cdot 10^{-1}$	$7 \cdot 10^{-1}$	0	0	
House damage	no damage	$2 \cdot 10^{-1}$	0.99	-50	0.04	8,183.04
	minor	34,598	$4 \cdot 10^{-6}$	+865,000,000	4,788	
	major	33,638	$3 \cdot 10^{-6}$	+841,000,000	3,395	
Fire Containment in 24 hrs	yes	0	0.91	-100	0.15	1.32
	no	4	0.09	+900	1.17	
Vegetation damage	no damage	0	0.99	-100	0.16	25,314.16
	minor	9,115	$7 \cdot 10^{-6}$	+228,000,000	582	
	major	70,331	$5 \cdot 10^{-6}$	+1,760,000,000	247,320,000	
Restoration cost [€]	0-30,000	$2 \cdot 10^{-2}$	0.33	-95	0.05	0.19
	30,000-100,000	$3 \cdot 10^{-2}$	0.38	-92.50	0.05	
	100,000-300,000	$2 \cdot 10^{-1}$	0.04	-50	0	
	300,000-1,000,000	1	0.25	+150	0.09	
Restoration time [yrs]	1	$2 \cdot 10^{-2}$	0.70	-95	0.10	0.69
	5	$6 \cdot 10^{-1}$	0.08	+50	0.03	
	15	2	0.22	+400	0.56	
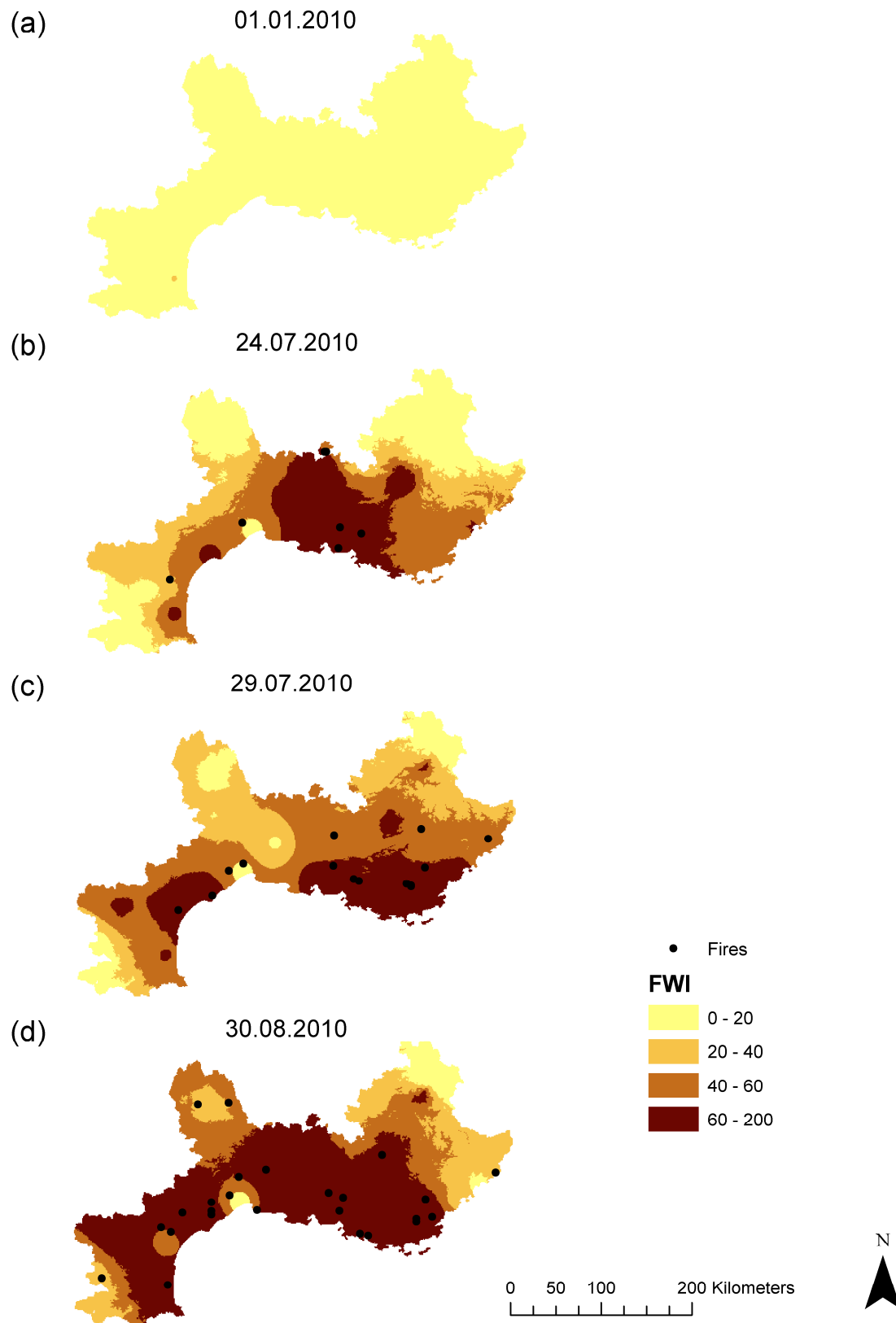
Figure AIII-1: FWI and fire events on different days of 2010 in South France (in brackets the burnt area):
(a) 1st January (no fire events), (b) 24th July (9.15 km²), (c) 29th July (2.25 km²), (d) 30th August (29.51 km²)

Figure AIII-2: Predicted fire risk to houses [€] on different days of 2010 in South France (in brackets the accumulated risk over the whole area): (a) 1st January (56,377 €), (b) 24th July (462,885 €), (c) 29th July (50,4% €), (d) 30th August (712,487 €)
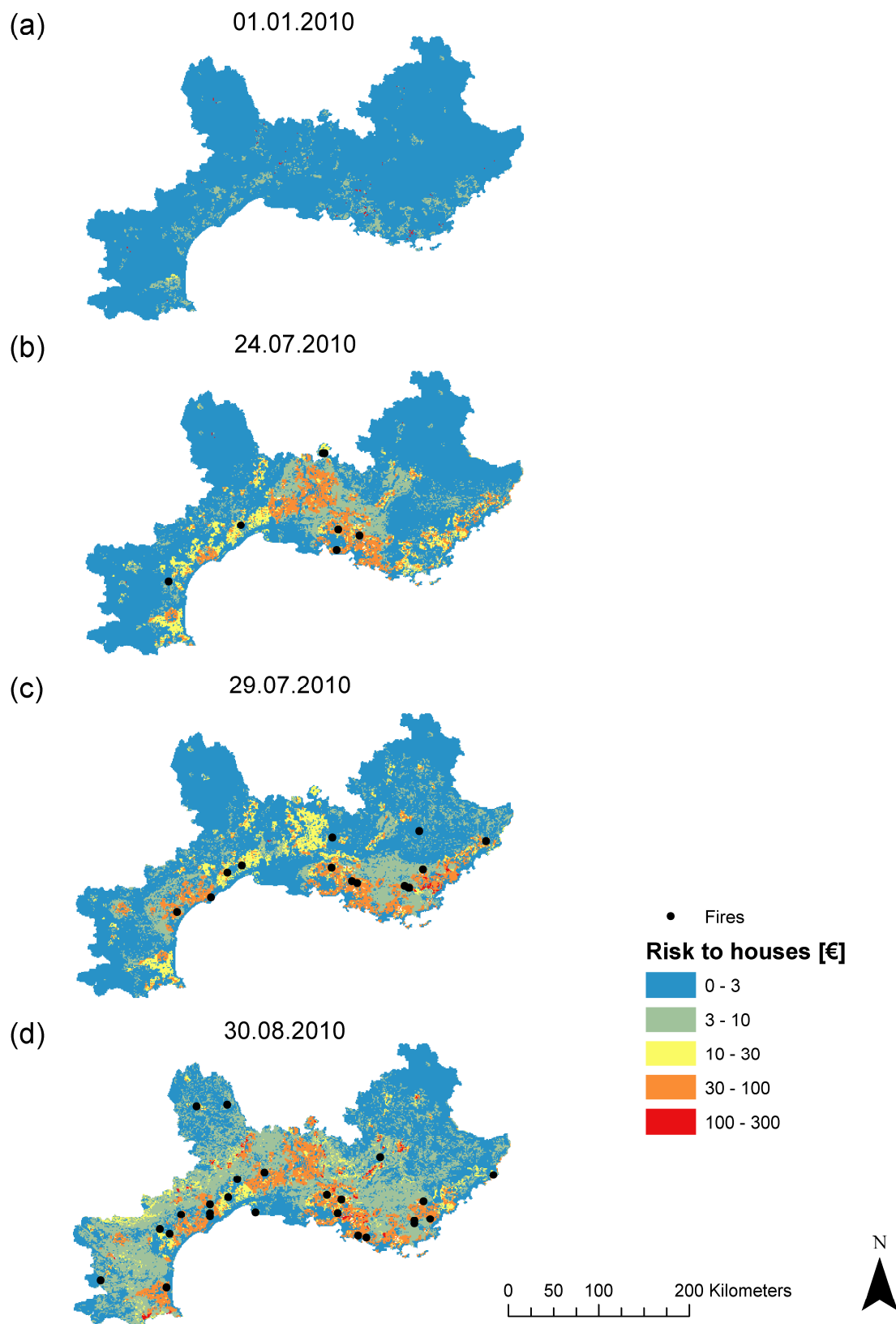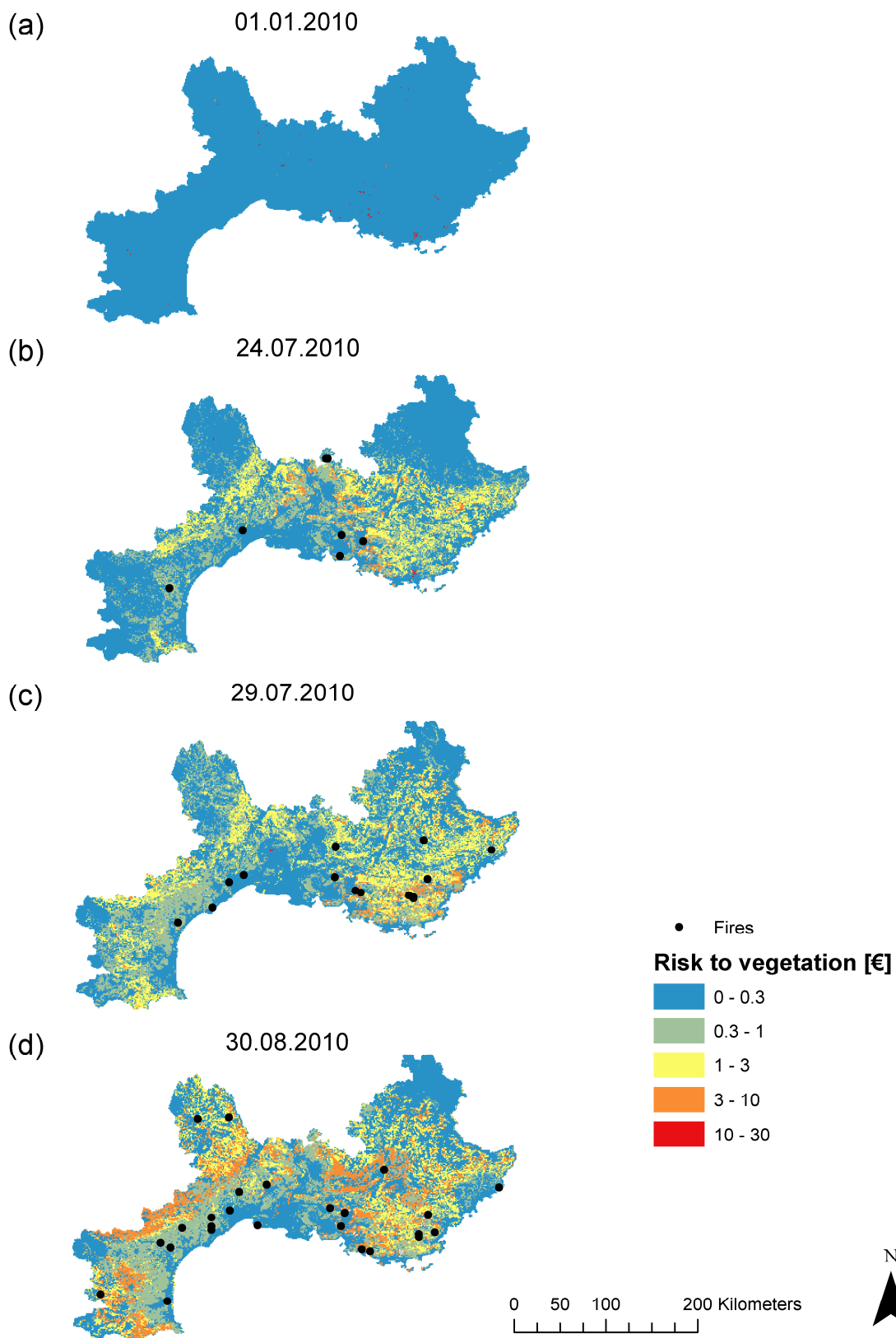
Figure AIII-3: Predicted fire risk to vegetation [€] on different days of 2010 in South France (in brackets the accumulated risk over the whole area): (a) 1st January (4,539 €), (b) 24th July (32,926 €), (c) 29th July (44,596 €), (d) 30th August (82,124 €)

Appendix IV

The following publications of the author are directly related to and were published during the present PhD research work:

Papakosta P and Straub D (2011). Effect of Weather Conditions, Geography and Human Involvement on Wildfire Ignition: A Bayesian Network Model Applications of Statistics and Probability in Civil Engineering, ICASP11. K. Faber, Nishijima. Zurich, CRC.

Papakosta P, Klein F, König S, Peters S and Straub D (2012) Linking spatio-temporal data to the Fire Weather Index to estimate the probability of wildfire in the Mediterranean. EGU General Assembly Conference Abstracts. Vienna. **14**.

Papakosta P, Öster J, Scherb A and Straub D (2013). Fire occurrence prediction in the Mediterranean: Application to Southern France. EGU General Assembly Conference Abstracts.Vienna. **15**.

Papakosta P and Straub D (2013). A Bayesian network approach to assessing wildfire consequences Proceedings of the 11th International Conference on Structural Safety & Reliability. G. Deodatis, B. R. Ellingwood and D. M. Frangopol. New York, USA, CRC Press.

Papakosta P, Scherb A, Zwirglmaier K and Straub D (2014) Estimating daily fire risk in the mesoscale by means of a Bayesian network model and a coupled GIS. In 'Advances in forest fire research'. I. d. U. d. Coimbra. Coimbra, Portugal**:** 725-735.

Papakosta P and Straub D (2015) "Probabilistic prediction of daily fire occurrence in the Mediterranean with readily available spatio-temporal data." *iForest (in review).*

Papakosta P, Xanthopoulos G and Straub D (2015) "Probabilistic prediction of wildfire vulnerability and damages to houses in the meso-scale with Bayesian network." *International Journal of Wildland Fire (in review).*

Terminology

The following definitions of wildfire related terms found in this thesis are taken from USDA (2016) and NWCG (2014):

Air attack	The deployment of fixed-wing or rotary aircraft on a wildland fire, to drop retardant or extinguishing agents, shuttle and deploy crews and supplies, or perform aerial reconnaissance of the overall fire situation.
Arson	At common law, the malicious and willful burning of another's dwelling, outhouse or parcel; by most modern statutes, the intentional and wrongful burning of someone else's, or one's own, property. Frequently requires proof of malicious or wrongful intent
Aspect	Cardinal direction toward which a slope faces
Average annual precipitation	The expected amount of annual rainfall
Behave	A system of interactive computer programs for modeling fuel and fire behavior
Buildup Index	A relative measure of the cumulative effect of daily drying factors and precipitation on fuels with a ten-day timelag
Burn severity	A qualitative assessment of the heat pulse directed toward the ground during a fire. Burn severity relates to soil heating, large fuel and duff consumption, consumption of the litter and organic layer beneath trees and isolated shrubs, and mortality of buried plant parts
Campfire	A fire that was started for cooking or warming that spreads sufficiently from its source to require action by a fire control agency

Canopy	The stratum containing the crowns of the tallest vegetation present (living or dead)
Climate	The prevalent or characteristic meteorological conditions of any place or region, and their extremes
Combustion	The rapid oxidation of fuel in which heat and usually flame are produced. Combustion can be divided into four phases: pre-ignition, flaming, smoldering, and glowing
Conduction	Heat transfer through a material from a region of higher temperature to a region of lower temperature
Containment	The status of a wildfire suppression action signifying that a control line has been completed around the fire, and any associated spot fires, which can reasonably be expected to stop the fire's spread
Cover type	The designation of a vegetation complex described by dominant species, age, and form
Crown fire	The movement of fire through the crowns of trees or shrubs more or less independently of the surface fire
Dead fuels	Fuels with no living tissue in which moisture content is governed almost entirely by atmospheric moisture (relative humidity and precipitation), dry-bulb temperature, and solar radiation
Defensible space	An area either natural or manmade where material capable of causing a fire to spread has been treated, cleared, reduced, or changed to act as a barrier between an advancing wildland fire and the loss to life, property, or resources. In practice, "defensible space" is defined as an area a minimum of 30 feet (9.14 meters) around a structure that is cleared of flammable brush or vegetation
Detection	The act or system of discovering and locating fires
Digital Elevation Model	A set of points which defines the terrain as numbers for computer applications. This data may be used to draw contours, make orthophotos, slope maps, and drive fire models
Drought index	A number representing the net effect of evaporation, transpiration and precipitation in producing cumulative moisture depletion in deep duff or upper soil layers
Dry bulb temperature	The temperature of the air measured in the shade 4-8 feet (1.22-2.44 meters) above the ground
Duff	The layer of decomposing organic materials lying below the litter layer of freshly fallen twigs, needles, and leaves and immediately above the mineral soil

Evacuation	An organized, phased, and supervised withdrawal, dispersal, or removal of civilians from dangerous or potentially dangerous areas, and their reception and care in safe areas
Exposure	Property that may be endangered by a fire burning in another structure or by a wildfire (item at risk)
Fine fuels	Fast-drying fuels, generally with a comparatively high surface area-to-volume ratio, which are less than 1/4-inch in diameter and have a timelag of one hour or less. These fuels readily ignite and are rapidly consumed by fire when dry
Fire	Rapid oxidation, usually with the evolution of heat and light; heat, fuel, oxygen and interaction of the three
Fire behavior	The manner in which a fire reacts to the influences of fuel, weather and topography
Fire behavior prediction system	A system that uses mathematical equations to predict certain aspects of fire behavior in wildland fuels when provided with data on fuel and environmental conditions
Fire cause	Source of fire's ignition. For statistical purposes fires are grouped into broad cause classes. The nine general causes (used in the U.S.) are lightning, campfire, smoking, debris burning, incendiary, machine use (equipment), railroad, children, and miscellaneous
Fire crew	An organized group of firefighters under the leadership of a crew leader or other designated official
Fire effects	The physical, biological, and ecological impacts of fire on the environment
Fire front	The part of a fire within which continuous flaming combustion is taking place. Unless otherwise specified the fire front is assumed to be the leading edge of the fire perimeter. In ground fires, the fire front may be mainly smoldering combustion
Fire intensity	A general term relating to the heat energy released by a fire
Fire perimeter	The entire outer edge or boundary of a fire
Fire season	1) Period(s) of the year during which wildland fires are likely to occur, spread, and affect resource values sufficient to warrant organized fire management activities. 2) A legally enacted time during which burning activities are regulated by state or local authority

Fire triangle	Instructional aid in which the sides of a triangle are used to represent the three factors (oxygen, heat, fuel) necessary for combustion and flame production; removal of any of the three factors causes flame production to cease
Fire weather	Weather conditions that influence fire ignition, behavior and suppression
Flame height	The average maximum vertical extension of flames at the leading edge of the fire front. Occasional flashes that rise above the general level of flames are not considered. This distance is less than the flame length if flames are tilted due to wind or slope
Flame length	The distance between the flame tip and the midpoint of the flame depth at the base of the flame (generally the ground surface); an indicator of fire intensity
Fuel	Combustible material. Includes, vegetation, such as grass, leaves, ground litter, plants, shrubs and trees, that feed a fire
Fuel bed	An array of fuels usually constructed with specific loading, depth and particle size to meet experimental requirements; also, commonly used to describe the fuel composition in natural settings
Fuel model	Simulated fuel complex (or combination of vegetation types) for which all fuel descriptors required for the solution of a mathematical rate of spread model have been specified
Fuel moisture	The quantity of moisture in fuel expressed as a percentage of the weight when thoroughly dried at 212 degrees Fahrenheit (104.44 degrees Celsius)
Fuel reduction	Manipulation, including combustion, or removal of fuels to reduce the likelihood of ignition and/or to lessen potential damage and resistance to control
Fuel type	An identifiable association of fuel elements of a distinctive plant species, form, size, arrangement, or other characteristics that will cause a predictable rate of fire spread or difficulty of control under specified weather conditions
Ground fuel	All combustible materials below the surface litter, including duff, tree or shrub roots, punchy wood, peat, and sawdust that normally support a glowing combustion without flame
(Fire) Hazard	The physical phenomenon of a fire occurring and spreading
Hazard reduction	Any treatment of a hazard that reduces the threat of ignition and fire intensity or rate of spread
Head of fire	The side of the fire having the fastest rate of spread
Initial attack	The actions taken by the first resources to arrive at a wildfire to protect lives and property, and prevent further extension of the fire

Keech Byram Drought Index	Commonly-used drought index adapted for fire management applications, with a numerical range from 0 (no moisture deficiency) to 800 (maximum drought)
Litter	Top layer of the forest, scrubland, or grassland floor, directly above the fermentation layer, composed of loose debris of dead sticks, branches, twigs, and recently fallen leaves or needles, little altered in structure by decomposition
Live fuels	Living plants, such as trees, grasses, and shrubs, in which the seasonal moisture content cycle is controlled largely by internal physiological mechanisms, rather than by external weather influences
National Fire Danger Rating Systems	A uniform fire danger rating system that focuses on the environmental factors that control the moisture content of fuels
Preparedness	Condition or degree of being ready to cope with a potential fire situation
Prescribed fire	Any fire ignited by management actions under certain, predetermined conditions to meet specific objectives related to hazardous fuels or habitat improvement
Prevention	Activities directed at reducing the incidence of fires, including public education, law enforcement, personal contact, and reduction of fuel hazards
Rate of spread	The relative activity of a fire in extending its horizontal dimensions. It is expressed as a rate of increase of the total perimeter of the fire, as rate of forward spread of the fire front, or as rate of increase in area, depending on the intended use of the information.
Relative humidity	The ratio of the amount of moisture in the air, to the maximum amount of moisture that air would contain if it were saturated. The ratio of actual pressure to the saturated vapor pressure
Ressources	1) Personnel, equipment, services and supplies available, or potentially available, for assignment to incidents. 2) The natural resources of an area, such as timber, crass, watershed values, recreation values, and wildlife habitat
Risk	The combination of the probability of an event and its negative consequences (UNISDR Terminology); the expected consequences (effects) of an event
Smoldering fire	A fire burning without flame and barely spreading
Spot fire	A fire ignited outside the perimeter of the main fire by flying sparks or embers

Spotting	Behavior of a fire producing sparks or embers that are carried by the wind and start new fires beyond the zone of direct ignition by the main fire
Supression	All the work of extinguishing or containing a fire, beginning with its discovery
Timelag	Time needed under specified conditions for a fuel particle to lose about 63 percent of the difference between its initial moisture content and its equilibrium moisture content. If conditions remain unchanged, a fuel will reach 95 percent of its equilibrium moisture content after four timelag periods
Uncontrolled fire	Any fire which threatens to destroy life, property, or natural resources
Vulnerability	The degree of expected damage as a function of hazard intensity
Wildland fire	Any non-structure fire, other than prescribed fire, that occurs in the wildland (aka wildfire)
Wildland Urban Interface	The line, area or zone where structures and other human development meet or intermingle with undeveloped wildland or vegetative fuels

Abbreviations

The following abbreviations are found in this thesis:

AIC	-	Akaike Information Criterion
API	-	Application Programming Interface
AUC	-	Area Under Curve
BN	-	Bayesian Network
BUI	-	Buildup Index
CAIM	-	Class-Attribute Interdependence Maximization (measure)
CFFDRS	-	Canadian Forest Fire Danger Rating System
CFFWIS	-	Canadian Forest Fire Weather Index System
CPT	-	Conditional Probability Table
DC	-	Drought Code
DMC	-	Duff Moisture Code
EFFIS	-	European Forest Fire Information System
FFDI	-	Forest Fire Danger Index
FFMC	-	Fine Fuel Moisture Code
GFDI	-	Grass Fire Danger Index
HDC	-	House Damage Cost
EM	-	Expectation – Maximization (algorithm)
FWI	-	Fire Weather Index
GIS	-	Geographic Information System
ID	-	Identification
IDW	-	Inverse Distance Weighting
ISI	-	Initial Spread Index
MLE	-	Maximum Likelihood Estimation
MTC	-	Mediterranean Type Climate
NPC	-	Necessary Path Condition (algorithm)
PMF	-	Probability Mass Function
ROC	-	Receiver Operating Characteristic (curve)
VDC	-	Vegetation Damage Cost
WUI	-	Wildland-Urban Interface

Bibliography

Akaike H (1974). "A new look at the statistical model identification." *IEEE Transactions on Automatic Control* **19**(6): 716–723.

Albini FA (1979). Spot fire distance from burning trees: A predictive model. Ogden, Utah, USA, Intermountain Forest and Range Experiment Station, Forest Service, US Department of Agriculture. **INT-56**.

Amatulli G, Rodrigues MJ, Trombetti M and Lovreglio R (2006). "Assessing long term fire risk at local scale by means of decision tree technique." *Journal of Geophysical Research: Biogeosciences (2005–2012)* **111**(G4).

Andrews PL (1986). BEHAVE: fire behavior prediction and fuel modeling system-Burn subsystem. General Technical Report, Intermountain Research Station Ogden**:** 134.

Andrews PL (2009). BehavePlus fire modeling system, version: 5.0 Variables. General Technical Report, Rocky Mountain Research Station**:** 124.

Arndt N, Vacik H, Koch V, Arpaci A and Gossow H (2013). "Modeling human-caused forest fire ignition for assessing forest fire danger in Austria." *iForest-Biogeosciences & Forestry* **6**(6).

Aspinall WP, Woo G, Voight B and Baxter PJ (2003). "Evidence-based volcanology: application to eruption crises." *Journal of Volcanology and Geothermal Research* **128**(1): 273-285.

Bayraktarli YY, Ulfkjaer J, Yazgan U and Faber MH (2005). On the application of Bayesian Probabilistic Networks for earthquake risk management. Augusti et al. (eds) (Hg.) 2005 – Safety and Reliability of Engineering (Proc. ICOSSAR 05, Rome), Millpress.

Bensi MT (2010). A Bayesian Network methodology for infrastructure seismic risk assessment and decision support Dissertation, University of Berkeley, California.

Beringer J (2000). "Community fire safety at the urban/rural interface: the bushfire risk." *Fire Safety Journal* **35**(1): 1-23.

Blanchi R, Lucas C, Leonard J and Finkele K (2010). "Meteorological conditions and wildfire-related houseloss in Australia." *International Journal of Wildland Fire* **19**(7): 914-926.

Blaser L, Ohrnberger M, Riggelsen C and Scherbaum F (2009). Bayesian Belief Network for tsunami warning decision support. ECSQARU 2009. C. Sossai and G. Chemello. Berlin Heidelberg, Springer. **LNAI 5590:** 757–786.

Blong R (2003). "A new damage index." *Natural Hazards* **30**(1): 1-23.

Bradstock RA, Cohn JS, Gill AM, Bedward M and Lucas C (2009). "Prediction of the probability of large fires in the Sydney region of south-eastern Australia using fire weather." *International Journal of Wildland Fire*(18): 932–943.

BritishColumbiaForestService (not given). The home owners Firesmart Manual - Protect your home from wildfire. http://www.embc.gov.bc.ca/ofc/interface/pdf/homeowner-firesmart.pdf.

Butler BW, Finney MA, Andrews PL and Albini FA (2004). "A radiation-driven model of crown fire spread." *Canadian Journal of Forest Research* **34**: 1588-1599.

Byram GM (1959). Combustion of forest fuels. Forest fire: control and use. K. P. Davis. New York, McGraw-Hill**:** 61–89.

Camia A and Amatulli G (2009). Weather Factors and Fire Danger in the Mediterranean. Earth Observation of Wildland Fires in Mediterranean Ecosystems. E. Chuvieco, Springer**:** 71–82.

Cardille JA, Ventura SJ and Turner MG (2001). "Environmental and social factors influencing wildfires in the Upper Midwest, United States." *Ecological Applications* **11**(1): 111–127.

Carmel Y, Paz S, Jahashan F and Shoshany M (2009). "Assessing fire risk using Monte Carlo simulations of fire spread." *Forest Ecology and Management* **257**(1): 370-377.

Catry FX, Rego FC, Bação FL and Moreira F (2010). "Modeling and mapping wildfire ignition risk in Portugal." *International Journal of Wildland Fire* **18**(8): 921-931.

Chou YH, Minnich RA and Chase RA (1993). "Mapping Probability of Fire Occurence in San Jacinto Mountains, California, USA." *Environmental Management* **Vol. 17**(1): 129–140.

Chong D, Tolhurst K and Duff T (2012). PHOENIX Rapidfire 4.0's Convection and Ember Dispersal Model. Bushfire CRC.

Chuvieco E, Ed. (2009). Earth Observation of Wildland Fires in Mediterranean Ecosystems, Springer.

Chuvieco E, Aguado I, Yebra M, Nieto H, Salas J, Martín MP, Vilar L, Martínez J, Martín S and Ibarra P (2010). "Development of a framework for fire risk assessment using remote sensing and geographic information system technologies." *Ecological Modelling* **221**(1): 46-58.

Chuvieco E, González I, Verdú F, Aguado I and Yebra M (2009). "Prediction of fire occurrence from live fuel moisture content measurements in a Mediterranean ecosystem." *International Journal of Wildland Fire* **18**(4): 430-441.

Chuvieco E, Martínez S, Román MV, Hantson S and Pettinari ML (2013). "Integration of ecological and socio-economic factors to assess global vulnerability to wildfire." *Global Ecology and Biogeography* **23**(2): 245-258.

Cohen JD (2000). "Preventing disaster: Home ignitability in the wildland-urban interface." *Journal of Forestry* **98**(3): 15–21.

Cohen JD (2004). "Relating flame radiation to home ignition using modeling and experimental crown fires." *Canadian Journal of Forest Research* **34**(8): 1616-1626.

Cortner HJ, Gardner PD and Taylor JG (1990). "Fire hazards at the urban-wildland interface: What the public expects." *Environmental Management* **14**(1): 57-62.

Cruz MG and Alexander ME (2010). "Assessing crown fire potential in coniferous forests of western North America: a critique of current approaches and recent simulation studies." *International Journal of Wildland Fire* **19**(4): 377-398.

Cruz MG, Alexander ME and Wakimoto RH (2003). "Assessing the probability of crown fire initiation based on fire danger indices." *The Forestry Chronicle* **79**(5): 976-983.

Cruz MG, Alexander ME and Wakimoto RH (2004). "Modeling the likelihood of crown fire occurrence in conifer forest stands." *Forest Science* **50**(5): 640-658.

Cruz MG, Butler BW and Alexander ME (2006a). "Predicting the ignition of crown fuels above a spreading surface fire. Part II: model behavior and evaluation." *International Journal of Wildland Fire* **15**: 61-72.

Cruz MG, Butler BW, Alexander ME, Forthofer JM and Wakimoto RH (2006b). "Predicting the ignition of crown fuels above a spreading surface fire. Part I: model idealization." *International Journal of Wildland Fire* **15**: 47-60.

Cunningham AA and Martell DL (1973). "A stochastic model for the occurrence of man-caused forest fires." *Canadian Journal of Forest Research* **3**: 282–287.

de Vasconcelos MJP, Silva S, Tome M, Alvim M and Pereira JC (2001). "Spatial prediction of fire ignition probabilities: comparing logistic regression and neural networks." *Photogrammetric Engineering and Remote Sensing* **67**(1): 73-81.

Dimitrakopoulos AP (2002). "Mediterranean fuel models and potential fire behaviour in Greece." *International Journal of Wildland Fire* **11**(2): 127-130.

Dimitrakopoulos AP, Bemmerzouk AM and Mitsopoulos ID (2011). "Evaluation of the Canadian fire weather index system in an eastern Mediterranean environment." *Meteorological Applications* **18**: 83–93.

Dimitrakopoulos AP, Mitsopoulos ID and Raptis DI (2007). "Nomographs for predicting crown fire initiation in Aleppo pine (Pinus halepensis Mill.) forests." *European Journal of Forest Research* **126**(4): 555-561.

Dlamini WM (2009). "A Bayesian belief network analysis of factors influencing wildfire occurence in Swaziland." *Environmental Modelling & Software* **25**(2): 199–208.

Dowdy AJ, Mills GA, Finkele K and de Groot W (2010). "Index sensitivity analysis applied to the Canadian forest fire weather index and the McArthur forest fire danger index." *Meteorological Applications* **17**(3): 298-312.

ECONorthwest (2007). Linn County Community Wildfire Protection Plan. https://scholarsbank.uoregon.edu/xmlui/bitstream/handle/1794/5795/Linn_County_Wildfire_Plan.pdf?sequence=1.

Ederle S (2013). Vorhersage der Flächengröße von Großflächenbränden im Mittelmeerraum mittels linearer Regression. B.Sc., Technische Universität München.

FAO (2001). Global Forest Fire Assessment 1990-2000. Assessment Programme, Food and Agricultural Organization of the United Nations, Forestry department

Finney MA (2004). FARSITE: Fire area simulator-Model development and evaluation, United States Department of Cultivation**:** 52.

Finney MA (2006). An overview of FlamMap fire modeling capabilities. Fuels management—how to measure success: conference proceedings, USDA Forest Service, Rocky Mountain Research Station, Fort Collins, CO.

Finney MA, McHugh CW, Grenfell IC, Riley KL and Short KC (2011). "A simulation of probabilistic wildfire risk components for the continental United States." *Stochastic Environmental Research and Risk Assessment* **25**(7): 973-1000.

Flannigan MD, Amiro BD, Logan KA, Stocks BJ and Wotton BM (2005). "Forest fires and climate change in the 21st Century." *Mitigation and Adaptation Strategies for Global Change* **11**: 847–859.

Florides GA, Tassou SA, Kalogirou SA and Wrobel LC (2001). "Evolution of domestic dwellings in Cyprus and energy analysis." *Renewable energy*(23).

Forestry Canada FDG (1992). Development and Structure of the Canadian Forest Fire Behavior Prediction System. Information Report ST-X-3. F. Canada. Ottawa, Canada**:** 63.

ForestServiceBritishColumbia (2003). The home owners Firesmart Manual - Protect your home from wildfire. http://www.embc.gov.bc.ca/ofc/interface/pdf/homeowner-firesmart.pdf.

Giannakopoulos C, Karali A, Roussos A, Hatzaki M, Xanthopoulos G and Kaoukis K (2011). Evaluating present and future fire risk in Greece, JRC Scientific and Technical Reports.

Gibbons P, Van Bommel L, Gill AM, Cary GJ, Driscoll DA, Bradstock RA, Knight E, Moritz MA, Stephens SL and Lindenmayer DB (2012). "Land management practices associated with house loss in wildfires." *PloS one* **7**(1): e29212.

Grêt-Regamey A and Straub D (2006). "Spatially explicit avalanche risk assessment linking Bayesian networks to a GIS." *Natural hazards and Earth System Sciences* **6**: 911–926.

Haight RG, Cleland DT, Hammer RB, Radeloff VC and Rupp TS (2004). "Assessing fire risk in the wildland-urban interface." *Journal of Forestry* **102**(7): 41-48.

Hargrove WW, Gardner RH, Turner MG, Romme WH and Despain DG (2000). "Simulating fire patterns in heterogeneous landscapes." *Ecological modelling* **135**(2): 243-263.

Harris S, Anderson W, Kilinc M and Fogarty L (2012). "The relationship between fire behaviour measures and community loss: an exploratory analysis for developing a bushfire severity scale." *Natural hazards* **63**(2): 391-415.

He HS, Shang BZ, Crow TR, Gustafson EJ and Shifley SR (2004). "Simulating forest fuel and fire risk dynamics across landscapes—LANDIS fuel module design." *Ecological Modelling* **180**(1): 135-151.

Hernandez-Leal PA, Arbelo M and Gonzalez-Calvo A (2006). "Fire risk assessment using satellite data." *Advances in Space research* **37**(4): 741-746.

Jaiswal RK, Mukherjee S, Raju KD and Saxena R (2002). "Forest fire risk zone mapping from satellite imagery and GIS." *International Journal of Applied Earth Observation and Geoinformation* **4**(1): 1-10.

Jensen FV and Nielsen TD (2007). Bayesian Networks and Decision Graphs. NY, USA, Springer.

Johnson S, Low-Choy S and Mengersen K (2012). "Integrating Bayesian networks and geographic information systems: Good practice examples." *Integrated environmental assessment and management* **8**(3): 473-479.

Johnston P, Milne G and Klemitz D (2005). Overview of bushfire spread simulation systems. Bushfire CRC. Nedlands WA, Australia, The University of Western Australia.

Johnstone JF, Rupp TS, Olson M and Verbyla D (2011). "Modeling impacts of fire severity on successional trajectories and future fire behavior in Alaskan boreal forests." *Landscape Ecology* **26**(4): 487-500.

Jolma A, Lehikoinen A and Helle I (2011). Coupling Bayesian networks and geospatial software for environmental risk assessment. MODSIM2011, 19th International Congress on Modelling and Simulation, Modelling and Simulation Society of Australia and New Zealand.

JRC (2006). Forest Fires in Europe 2006. Joint Research Center (JRC) Scientific and Technical Reports. Italy, European Commission, JRC-IES, Land Management and Natural Hazards Unit (Ispra).

JRC (2011). Forest Fires in Europe 2010. Joint Research Center (JRC) Scientific and Technical Reports. Italy, European Commission, JRC-IES, Land Management and Natural Hazards Unit (Ispra).

Kalabokidis KD, Koutsias N, Konstantinidis P and Vasilakos C (2007). "Multivariate analysis of landscape wildfire dynamics in a Mediterranean ecosystem of Greece." *Area* **39**(3): 392-402.

Keeley JE (2009). "Fire intensity, fire severity and burn severity: a brief review and suggested usage." *International Journal of Wildland Fire* **18**(1): 116-126.

Keeley JE, Bond WJ, Bradstock RA, Pausas JG and Rundel PW (2012). Fire in Mediterranean ecosystems: Ecology, evolution and management. Cambridge, Cambridge Univ. Press.

Kjaerulff UB and Madsen AL (2013). Bayesian Networks and Influence Diagrams: A Guide to Construction and Analysis. New York, Springer.

Koo E, Pagni PJ, Weise DR and Woycheese JP (2010). "Firebrands and spotting ignition in large-scale fires." *International Journal of Wildland Fire* **19**(7): 818–843.

Kuehn NM, Riggelsen C and Scherbaum F (2011). "Modeling the joint probability of earthquake, site, and ground-motion parameters using Bayesian Networks." *Bulletin of the Seismological Society of America* **101**(1): 235–249.

Kurgan LA and Cios KJ (2004). "CAIM discretization algorithm." *Knowledge and Data Engineering, IEEE Transactions on* **16**(2): 145-153.

Lawson BD and Armitage OB (2008). Weather Guide for the Canadian Forest Fire Danger Rating System. Edmonton, Alberta, Canada, Natural Resources Canada, Canadian Forest Service, Northern Forestry Centre.

Leemans R and Cramer WP (1991). The IIASA database for mean monthly values of temperature, precipitation and cloudiness on a global terrestrial grid. RR-91-18. Vienna, Austria, International Institute for Applied Systems Analysis.

Leone V, Lovreglio R, Martín MP, Martínez J and Vilar L (2009). Human factors of fire occurrence in the Mediterranean. Earth Observation of Wildland Fires in the Mediterranean Ecosystems. E. Chuvieco, Springer**:** 149–170.

Long A and Randall C (2004). Wildfire Risk Assessment Guide for Homeowners: in the Southern United States, School of Forest Resources and Conservation, University of Florida (IFAS).

Lynch DL (2004). "What do forest fires really cost?" *Journal of Forestry* **102**(6): 42–49.

Mandallaz D and Ye R (1997). "Prediction of forest fires with Poisson models." *Canadian Journal of Forest Research* **27**: 1685–1694.

Marcot BG (2012). "Metrics for evaluating performance and uncertainty of Bayesian network models." *Ecological Modelling* **230**: 50-62.

Martell DL, Bevilacqua E and Stocks BJ (1989). "Modelling seasonal variation in daily people-caused forest fire occurrence." *Canadian Journal of Forest Research* **19**(12): 1555–1563.

Martell DL, Otukol S and Stocks BJ (1987). "A logistic model for predicting daily people-caused forest fire occurrence in Ontario." *Canadian Journal of Forest Research* **17**(5): 394–401.

Martínez-Fernández J, Chuvieco E and Koutsias N (2013). "Modelling long-term fire occurrence factors in Spain by accounting for local variations with geographically weighted regression." *Natural Hazards and Earth System Science* **13**(2): 311–327.

Mason S and Graham N (2002). "Areas beneath the relative operating characteristics (roc) and relative operating levels (rol) curves: Statistical significance and interpretation." *Quarterly Journal of the Royal Meteorological Society* **128**(584): 2145-2166.

Massada AB, Syphard DA, Stewart SI and Radeloff VC (2012). "Wildfire ignition-distribution modelling: a comparative study in the Huron–Manistee national forest, Michigan, USA." *International Journal of Wildland Fire* **22**(2): 174–183.

McArthur A (1967). Fire behavior in Eucalypt forests. . D. o. N. Development. Fosestry and Timber Bureau Leaflet 107, Canberra, ACT, Australia.

McKillup S and Dyar MD (2010). Geostatistics explained: An introductory guide for earth scientists. Cambridge, Cambridge Univ. Press.

Mell WE, Manzello SL, Maranghides A, Butry D and Rehm RG (2010). "The wildland–urban interface fire problem–current approaches and research needs." *International Journal of Wildland Fire* **19**(2): 238-251.

Miranda BR, Sturtevant BR, Stewart SI and Hammer RB (2012). "Spatial and temporal drivers of wildfire occurrence in the context of rural development in northern Wisconsin, USA." *International Journal of Wildland Fire* **21**(2): 141–154.

Mitsopoulos ID and Dimitrakopoulos AP (2007). "Canopy fuel characteristics and potential crown fire behavior in Aleppo pine (Pinus halepensis Mill.) forests." *Annals of Forest Science* **64**(3): 287-299.

Moriondo M, Good P, Durao R, Bindi M, Giannakopoulos C and Corte-Real J (2006). "Potential impact of climate change on fire risk in the Mediterrannean area." *Climate Research* **31**(1): 85–91.

Mozumder P, Helton R and Berrens RP (2009). "Provision of a wildfire risk map: informing residents in the wildland urban interface." *Risk analysis* **29**(11): 1588-1600.

MunichRE (2010). Geo Topics 2009: Natural catastrophes 2009. Analyses, assessments, positions. Topics GEO.

Nemry F and Uihlein A (2008). Environmental Improvement Potentials of Residential Buildings (IMPRO-Building). JRC Scientific and Technical Reports. Spain, JRC

NWCG (2014). Glossary of wildland fire terminology. PMS205. Boise, Idaho, USA, National Wildfire Coordinating Group (NWCG) 1-190.

Oehler F, Oliveira S, Barredo JI, Camia A, SanMiguel-Ayanz J, Pettenella D and Mavsar R (2012). Assessing European wildfire vulnerability. European Geoscience Union General Assembly 2012. Vienna, Austria.

Ohlson DW, Blackwell BA, Hawkes BC and Bonin D (2003). A wildfire risk management system - an evolution of the wildfire threat rating system. 3rd International Wildland Fire Conference and Exhibition. Sydney, Australia.

Oliveira S, Oehler F, SanMiguel-Ayanz J, Camia A and Pereira JMC (2012). "Modeling spatial patterns of fire occurrence in Mediterranean Europe using Multiple Regression and Random Forest." *Forest Ecology and Management* **275**: 117–129.

OregonForestryDepartment (2004). Wildfire Risk Explorer: Identifying and assessment of communitites at risk in Oregon, Draft Version 4.0, Oregon Department of Forestry.

Padilla M and Vega-García C (2011). "On the comparative importance of fire danger rating indices and their integration with spatial and temporal variables for predicting daily human-caused fire occurrences in Spain." *International journal of wildland fire* **20**(1): 46-58.

Papakosta P, Öster J, Scherb A and Straub D (2013). Fire occurrence prediction in the Mediterranean: Application to Southern France. EGU General Assembly. E. G. Union. Vienna. **15**.

Papakosta P, Scherb A, Zwirglmaier K and Straub D (2014). Estimating daily fire risk in the mesoscale by means of a Bayesian network model and a coupled GIS. VII International Conference on Forest Fire Research. D. X. Viegas. Coimbra, Portugal.

Papakosta P and Straub D (2011). Effect of Weather Conditions, Geography and Human Involvement on Wildfire Ignition: A Bayesian Network Model. Applications of Statistics and Probability in Civil Engineering, ICASP11. K. Faber, Nishijima. Zurich, CRC.

Papakosta P and Straub D (2013). A Bayesian network approach to assessing wildfire consequences. Proceedings of the 11th International Conference on Structural Safety & Reliability. G. Deodatis, B. R. Ellingwood and D. M. Frangopol. New York, USA, CRC Press.

Papakosta P and Straub D (2015). "Probabilistic prediction of daily fire occurrence in the Mediterranean with readily available spatio-temporal data." *iforest (submitted)*.

Parisien MA and Moritz MA (2009). "Environmental controls on the distribution of wildfire at multiple spatial scales." *Ecological Monographs* **79**(1): 127–154.

Parsons DJ, Graber DM, Agee JK and Van Wagtendonk JW (1986). "Natural fire management in national parks." *Environmental Management* **10**(1): 21-24.

Paul BK (2011). Environmental Hazards and Disasters: Contexts, Perspectives and Management. Hoboken, John Wiley & Sons.

Pausas JG (1997). "Resprouting of Quercus suber in NE Spain after fire." *Journal of Vegetation Science* **8**(5): 703-706.

Penman TD, Bradstock RA and Price OF (2014). "Reducing wildfire risk to urban developments: Simulation of cost-effective fuel treatment solutions in south eastern Australia." *Environmental Modelling & Software* **52**: 166-175.

Penman TD, Collins L, Price OF, Bradstock RA, Metcalf S and Chong DMO (2013). "Examining the relative effects of fire weather, suppression and fuel treatment on fire behaviour–A simulation study." *Journal of environmental management* **131**: 325-333.

Penman TD, Eriksen C, Blanchi R, Chladil M, Gill A, Haynes K, Leonard J, McLennan J and Bradstock RA (2013). "Defining adequate means of residents to prepare property for protection from wildfire." *International Journal of Disaster Risk Reduction* **6**: 67-77.

Pew KL and Larsen CPS (2001). "GIS analysis of spatial and temporal patterns of human-caused wildfires in the temperate rain forest of Vancouver Island, Canada." *Forest Ecology and Management* **140**(1): 1–18.

Plucinski M (2012). A review of wildfire occurrence research. BushfireCRC, CSIRO Ecosystem Sciences and CSIRO climate Adaptation Flagship.

Plucinski M (2012). "Factors affecting containment area and time of Australian forest fires featuring aerial suppression." *Forest Science* **58**(4): 390-398.

Plucinski M, McCarthy G, Hollis J and Gould J (2012). "The effect of aerial suppression on the containment time of Australian wildfires estimated by fire management personnel." *International Journal of Wildland Fire* **21**(3): 219-229.

Preisler HK, Brillinger DR, Burgan RE and Benoit JW (2004). "Probability based models for estimation of wildfire risk." *International Journal of Wildland Fire*(13): 133–142.

Romero-Calcerrada R, Novillo C, Millington J and Gomez-Jimenez I (2008). "GIS analysis of spatial patterns of human-caused wildfire ignition risk in the SW of Madrid (Central Spain)." *Landscape Ecology* **23**(3): 341-354.

Rothermel RC (1972). A mathematical model for predicting fire spread in wildland fuels. Research paper INT-115, Intermountain Forest and Range Experiment Station, Forest Service, USA.

Rothermel RC (1983). How to predict the spread and intensity of forest and range fires. Ogdon, Utah, USA, Intermountain Forest and Range Experiment Station, Forest Service, Department of Agriculture.

Rothermel RC (1991). Predicting behavior and size of crown fires in the Northern Rocky Mountains. Research Paper INT-438, Forest Service Intermountain Research Station.

Rothermel R and Deeming J (1980). Measuring and interpreting fire behavior for correlation with fire effects. USDA Forest Service General Technical Report INT-93

Russell S and Norvig P (2003). Artificial Intelligence: A Modern Approach, Prentice Hall, Pearson Education International.

Scherb A (2014). Coupling of Bayesian Networks with GIS for wildfire risk assessment and mapping in the Mediterranean. MSc Thesis in Environmental Engineering, Technische Universität München.

Scherb A and Öster J (2013). Canadian Fire Weather Index System for the prediction of wildfire occurrences in South France. Study project, Technische Universität München.

Sebastián-López A, Salvador-Civil R, Gonzalo-Jiménez, J. and SanMiguel-Ayanz J (2008). "Integration of socio-economic variables for modeling long-term fire danger in Southern Europe." *European Journal of Forest Research*(127): 149–163.

Service CF (1984). Tables for the Canadian Forest Fire Weather Index System. Forestry Technical Report, Canadian Forestry Service**:** 73.

Service CS (2010). Construction and housing statistics. Republic of Cyprus, Statistical service.

Service CS (2012). Conventional dwellings enumerated by year of construction (completion). Report table statistics. Republic of Cyprus, Statistical Service.

Schaaf MD, Sandberg DV, Schreuder MD and Riccardi CL (2007). "A conceptual framework for ranking crown fire potential in wildland fuelbeds (This article is one of a selection of papers published in the Special Forum on the Fuel Characteristic Classification System)." *Canadian Journal of Forest Research* **37**(12): 2464-2478.

Scherb A (2014). Coupling of Bayesian Networks with GIS for wildfire risk assessment and mapping in the Mediterranean. Master thesis in Environmental Engineering, Technische Universität München.

Scott JH (1999). "NEXUS: a system for assessing crown fire hazard." *Fire Management Notes*.

Scott JH (2006). Comparison of crown fire modeling systems used in three fire management applications, Rocky Mountain Research Station, Forest Service, Department of Agriculture

Shang BZ, He HS, Crow TR and Shifley SR (2004). "Fuel load reductions and fire risk in central hardwood forests of the United States: a spatial simulation study." *Ecological Modelling* **180**(1): 89-102.

Shepard D (1968). A two-dimensional interpolation function for irregularly-spaced data. Proccedings 23rd ACM National 1968**:** 517–524.

Show SB and Kotok EI (1924). The role of fire in the California pine forests. Department Bulletin No1294. Washington D.C., United States Department of Agriculture.

Song Y, Gong J, Gao S, Wang D, Cui T, Li Y and Wei B (2012). "Susceptibility assessment of earthquake-induced landslides using Bayesian network: A case study in Beichuan, China." *Computers & Geosciences* **42**: 189-199.

Stephens SL and Moghaddas JJ (2005). "Experimental fuel treatment impacts on forest structure, potential fire behavior, and predicted tree mortality in a California mixed conifer forest." *Forest Ecology and Management* **215**(1): 21-36.

Stocks BJ, Alexander ME, Wotton BM, Stefner CN, Flannigan MD, Taylor SW, Lavoie N and Mason JA (2004). "Crown fire behaviour in a northern jack pine-black spruce forest." *Canadian Journal of Forest Research* **34**: 1548-1560.

Straub D (2005). Natural hazards risk assessment using Bayesian networks. Augusti et al. (eds) (Hg.) 2005 – Safety and Reliability of Engineering (Proc. ICOSSAR 05, Rome), Millpress**:** 2535–2542.

Straub D and Der Kiureghian A (2010). "Bayesian Network Enhanced with Structural Reliability Methods: Methodology." *Journal of Engineering Mechanics* **136**(10): 1248–1258.

Syphard AD, Keeley JE, Massada AB, Brennan TJ and Radeloff VC (2012). "Housing arrangement and location determine the likelihood of housing loss due to wildfire." *PloS one* **7**(3): e33954.

Syphard DA, Radeloff VC, Keuler NS, Taylor RS, Hawbaker TJ, Stewart SI and Clayton MK (2008). "Predicting spatial patterns of fire on a southern California landscape." *International Journal of Wildland Fire* **17**(5): 602–613.

Thywissen K (2006). Core terminology of disaster reduction: A comparative glossary. Measuring vulnerability to natural hazards. J. Birkmann. Tokyo, Japan, United Nations University Press**:** 448–496.

Tutsch M, Haider W, Beardmore B, Lertzman K, Cooper AB and Walker RC (2010). "Estimating the consequences of wildfire for wildfire risk assessment, a case study in the southern Gulf Islands, British Columbia, Canada." *Canadian Journal of Forest Research*(40): 2104–2114.

Tymstra C, Bryce RW, Wotton BM and Armitage OB (2010). Development and structure of Prometheus: the Canadian wildland fire growth simulation Model, Northern Forestry Centre. **417**.

UNDRO (1991). Mitigating natural disasters: phenomena, effects and options.: A manual for policy makers and planners. Geneva, (UNDRO, Office of the United Nations Disaster Relief Co-Ordinator).

USDA. (2016). "Fire terminology."   Retrieved 21.02.2016, from http://www.fs.fed.us/nwacfire/home/terminology.html.

Van Wagner CE (1977). "Conditions for the start and spread of crown fire." *Canadian Journal of Forest Research* **7**(1): 23-34.

Van Wagner CE (1987). Development and structure of the Canadian Forest Fire Weather Index System. Forestry Technical Report. Ottawa, Ontario, Canada.

Van Wagner CE (1993). "Prediction of crown fire behavior in two stands of jack pine." *Canadian Journal of Forest Research* **23**(3): 442-449.

Van Wagner CE and Pickett TL (1985). Equations and FORTRAN Program for the Canadian Forest Fire Weather Index System. Forestry Technical Report. Ottawa, Ontario, Canada, Canadian Forestry Service, Government of Canada.

Yassemi S, Dragićević S and Schmidt M (2008). "Design and implementation of an integrated GIS-based cellular automata model to characterize forest fire behaviour." *Ecological Modelling* **210**(1): 71-84.

Van Wagtendonk JW (2006). Fire as a physical process. Fire in California's ecosystems, University of California Press.

Vasilakos C, Kalabokidis K, Hatzopoulos J, Kallos G and Matsinos Y (2007). "Integrating new methods and tools in fire danger rating." *International Journal of Wildland Fire* **16**: 306–316.

Vasilakos C, Kalabokidis K, Hatzopoulos J and Matsinos I (2009). "Identifying wildland fire ignition factors through sensitivity analysis of a neural network." *Natural hazards* **50**(1): 125-143.

Viegas DX, Bovio G, Ferreira A, Nosenzo A and Sol B (1999). "Comparative study of various methods of fire danger evaluation in Southern Europe." *International Journal of Wildland Fire* **9**(4): 235–246.

Vilar L, Woolford DG, Martell DL and Martín MP (2010). "A model for predicting human-caused wildfire occurrence in the region of Madrid, Spain." *International Journal of Wildland Fire* **19**(3): 325-337.

Wotton BM, Martell DL and Logan KA (2003). "Climate change and people-caused forest fire occurrence in Ontario." *Climatic Change* **60**(3): 275–295.

Xanthopoulos G (2008). Parallel lines. Wildfire, International Association of Wildland Fire.

Yang J, He SH, Shifley SR and Gustafson EJ (2007). "Spatial patterns of modern period human-caused fire occurrence in the Missouri Ozark Highlands." *Forest Science* **53**(1).

Yassemi S, Dragićević S and Schmidt M (2008). "Design and implementation of an integrated GIS-based cellular automata model to characterize forest fire behaviour." *Ecological Modelling* **210**(1): 71-84.

Zwirglmaier K (2012). A Bayesian network model for predicting wildfire behavior in Mediterranean regions. MSc Thesis in Environmental Engineering, Technische Universitaet Muenchen.

Zwirglmaier K, Papakosta P and Straub D (2013). Learning a Bayesian network model for predicting wildfire behavior. Proceedings of the 11th International Conference on Structural Safety & Reliability (ICOSSAR). G. Deodatis, B. R. Ellingwood and D. M. Frangopol. New York, USA, CRC Press.